

University of Alberta

**Development of *In Vitro/In Vivo* Correlations Based on the Biopharmaceutics Drug  
Classification System**

By

HAI WEI



A thesis submitted to the Faculty of Graduate Studies and Research in partial fulfillment  
of the requirements for the degree of **DOCTOR OF PHILOSOPHY**

In

Pharmaceutical Sciences

Faculty of Pharmacy and Pharmaceutical Sciences

Edmonton, Alberta

Spring 2007



Library and  
Archives Canada

Bibliothèque et  
Archives Canada

Published Heritage  
Branch

Direction du  
Patrimoine de l'édition

395 Wellington Street  
Ottawa ON K1A 0N4  
Canada

395, rue Wellington  
Ottawa ON K1A 0N4  
Canada

*Your file* *Votre référence*  
*ISBN: 978-0-494-29769-8*  
*Our file* *Notre référence*  
*ISBN: 978-0-494-29769-8*

#### NOTICE:

The author has granted a non-exclusive license allowing Library and Archives Canada to reproduce, publish, archive, preserve, conserve, communicate to the public by telecommunication or on the Internet, loan, distribute and sell theses worldwide, for commercial or non-commercial purposes, in microform, paper, electronic and/or any other formats.

The author retains copyright ownership and moral rights in this thesis. Neither the thesis nor substantial extracts from it may be printed or otherwise reproduced without the author's permission.

#### AVIS:

L'auteur a accordé une licence non exclusive permettant à la Bibliothèque et Archives Canada de reproduire, publier, archiver, sauvegarder, conserver, transmettre au public par télécommunication ou par l'Internet, prêter, distribuer et vendre des thèses partout dans le monde, à des fins commerciales ou autres, sur support microforme, papier, électronique et/ou autres formats.

L'auteur conserve la propriété du droit d'auteur et des droits moraux qui protègent cette thèse. Ni la thèse ni des extraits substantiels de celle-ci ne doivent être imprimés ou autrement reproduits sans son autorisation.

---

In compliance with the Canadian Privacy Act some supporting forms may have been removed from this thesis.

Conformément à la loi canadienne sur la protection de la vie privée, quelques formulaires secondaires ont été enlevés de cette thèse.

While these forms may be included in the document page count, their removal does not represent any loss of content from the thesis.

Bien que ces formulaires aient inclus dans la pagination, il n'y aura aucun contenu manquant.

  
**Canada**

## ABSTRACT

The aim of this study was to develop and evaluate biorelevant *in vitro* methods and to use computer simulations to predict the oral performance of different commercial products based on *in vitro* data. Glyburide was chosen as a model drug. Computer simulations using GastroPlus<sup>TM</sup> were used to assess if *in vitro/in vivo* correlations (IVIVCs) can be established.

Material characterization indicated that all five glyburide Active Pharmaceutical Ingredients (APIs) had similar crystal structures, however, significant differences in surface area, particle size and distribution were observed. Solubility studies demonstrated that the solubility of glyburide was low and pH-dependent. Dissolution tests of the glyburide products were performed in Fasted State Simulated Intestinal Fluid (FaSSIF) using conventional and dynamic pH change protocols. A permeability study using the Caco-2 model showed that glyburide is a highly permeable drug. Diluted FaSSIF medium was suitable to be used as transport medium with the limitation that it interferes with the active transport mechanisms. Computer simulations using the physicochemical data were able to predict the oral absorption of four glyburide products. An IVIVC was established. However, the computer simulations using *in vitro* dissolutions data predicted the oral performance of only two 3.5 mg formulations successfully. The dissolution data obtained from the 5 mg formulations were not predictive.

GastroPlus<sup>TM</sup> is a useful software program for predicting the oral absorption using *in vitro* data. Such methods can assist in the early stages of the drug development process in identifying the potential bioavailability of a drug candidate and this can shorten the time

needed for drug development. Furthermore, software simulations can be used to set API and product specifications. The *in vitro/in silico* methods may be used as a surrogate for bioequivalence studies in the future.

## **DEDICATION**

**This work is dedicated to my beloved Son: Lihua Wei, Mother: Shudong Dong and  
Father: Yongji Wei, whose love and support made this thesis possible.**

## CONTENTS

<b>CHAPTER 1 GENERAL INTRODUCTION</b> .....	1
1. Introduction.....	1
1.1. Background .....	1
1.2. Bioavailability and Bioequivalence .....	1
1.3. Biopharmaceutics and Biopharmaceutics Drug Classification System (BCS).....	3
1.3.1. General Concepts .....	3
1.3.2. Applications of the BCS .....	6
1.4. <i>In Vitro</i> Dissolution Test Development .....	9
1.4.1. Physiology of Gastrointestinal Tract .....	9
1.4.2. <i>In Vitro</i> Dissolution Development .....	11
1.4.2.1. <i>In Vitro</i> Dissolution Apparatuses.....	11
1.4.2.2. Dissolution Media.....	12
1.5. <i>In Vitro /In Vivo</i> Correlation (IVIVC) .....	16
1.5.1. Concepts of IVIVC .....	16
1.5.2. Physiologically-Based Pharmacokinetic Software Models .....	18
1.5.3. Advanced Compartmental Absorption and Transit Model (ACAT) .....	19
1.6. <i>In Vitro</i> Assessment of Gastrointestinal Drug Absorption: Caco-2 Cell Line.....	22
1.6.1. Drug Absorption .....	22
1.6.2. <i>In Vitro</i> Models for Studying Drug Absorption.....	23
1.6.3. Caco-2 Cell Lines .....	25
1.7. Summary of Glyburide Studies.....	27
1.8. Hypotheses and Objectives .....	30
1.9. Format of the Dissertation .....	30
1.10. Reference .....	31
<b>CHAPTER 2 INVESTIGATION OF TRANSPORT MEDIA CONTAINING MICELLES FOR CELL CULTURE PERMEABILITY STUDIES OF POORLY SOLUBLE DRUGS: CASE STUDY GLYBURIDE</b> .....	43
2.1. Introduction.....	43

2.2. Materials and Methods.....	45
2.2.1. Materials .....	45
2.2.2. Preparation of Test Media.....	46
2.2.3. Solubility Study of Glyburide.....	46
2.2.4. MTT Toxicity Study .....	47
2.2.5. Caco-2 Cell Culture and Quality Control .....	48
2.2.6. Media Effect on TEER Values of The Cell Monolayer.....	48
2.2.7. Transport Study.....	49
2.2.8. Competition of Transport Studies.....	49
2.2.9. HPLC Analysis .....	49
2.2.10. Calculation of Apparent Permeability and Statistics .....	50
2.3. Results.....	51
2.3.1. Solubility Study of Glyburide.....	51
2.3.2. MTT Toxicity Studies.....	51
2.3.3. Media Effects on TEER Values of the Cell Monolayers.....	54
2.3.4. Comparison of Transport Studies using HBSS and HQ-FaSSIF.....	55
2.3.5. Impact of (+/-)Verapamil on the Transport Studies.....	56
2.4. Discussion.....	56
2.5. Conclusion .....	59
2.6. References.....	60
<b>CHAPTER 3 PHYSIOCHEMICAL CHARACTERIZATION OF FIVE GLYBURIDE POWDERS: A BCS BASED APPROACH TO PREDICT ORAL ABSORPTION .....</b>	<b>65</b>
3.1. Introduction.....	65
3.2. Materials and Methods.....	66
3.2.1. Materials .....	66
3.2.2. Scanning Electron Microscopy (SEM) .....	67
3.2.3. X-Ray Powder Diffraction (XRPD).....	67
3.2.4. Thermogravimetric Analysis (TGA) .....	67

3.2.5. Differential Scanning Calorimetry (DSC) .....	68
3.2.6. Raman Spectroscopy.....	68
3.2.7. Particle Size Analysis .....	69
3.2.8. Specific Surface Area Measurement.....	69
3.2.9. True Density Measurement.....	70
3.2.10. Dissociation Constant ( $pK_a$ ), Partition Coefficient (logP) and Distribution Coefficient (logD) .....	70
3.2.11. Solubility Determination.....	70
3.2.12. Computer Simulations .....	71
3.2.13. Statistics .....	72
3.3. Results.....	73
3.3.1. Surface Area, True Density, Particle Size and Morphology.....	73
3.3.2. Crystallinity and Form Determination.....	75
3.3.3. Thermal Analysis.....	79
3.3.4. $pK_a$ , LogP and LogD Measurements .....	83
3.3.5. Computer Simulations .....	83
3.4. Discussion.....	86
3.5. Conclusion .....	88
3.6. References.....	90

**CHAPTER 4 BIORELEVANT DISSOLUTION MEDIA AS A PREDICTIVE  
TOOL FOR GLYBURIDE, A CLASS II DRUG.....94**

4.1. Introduction.....	94
4.2. Materials and Methods.....	97
4.2.1. Materials .....	97
4.2.2. Preparation of Dissolution Media .....	98
4.2.3. Solubility of Glyburide in Different Media .....	98
4.2.4. <i>In Vitro</i> Dissolution Studies at pH 6.5 .....	98
4.2.5. Dynamic Dissolution Studies.....	99
4.2.6. Permeability Determination .....	99
4.2.7. HPLC Analysis .....	100
4.2.8. Computer Simulations .....	101



4.2.9. Statistics .....	102
4.3. Results and Discussion .....	103
4.3.1. Solubility of Glyburide in Different Media .....	103
4.3.2. <i>In Vitro</i> Dissolution Studies at pH 6.5 .....	105
4.3.3. Dynamic Dissolution Studies.....	108
4.3.4. Permeability Studies .....	110
4.3.5. Computer Simulations .....	110
4.4. Conclusion .....	114
4.5. References.....	114
<b>CHAPTER 5 A STRATEGY FOR COMPUTER AIDED PREFORMULATION AND REVERSE-ENGINEERING OF PHARMACEUTICAL FORMULATIONS</b> .....	118
5.1. Introduction.....	118
5.2. Materials and Methods.....	120
5.2.1. Materials .....	120
5.2.2. Intrinsic Dissolution and <i>In Vitro</i> Dissolution Tests.....	120
5.2.3. Computer Simulations .....	121
5.2.3.1. Essential Input Data for The Prediction of Drug Absorption .....	121
5.2.3.2. Establishment of an IVIVC Using Physicochemical Data .....	123
5.2.3.3. Establishment of IVIVC Using <i>In Vitro</i> Dissolution Profiles .....	123
5.2.4. Statistics .....	124
5.3. Results and Discussion .....	124
5.3.1. Prediction of Fraction Dose Absorbed.....	124
5.3.2. Establishment of IVIVC Using Physicochemical Data .....	126
5.3.3. Intrinsic Dissolution Test.....	130
5.3.4. Establishment of IVIVC Using <i>In Vitro</i> Dissolution Profiles .....	131
5.3.5. Evaluation of The Computer Aided Drug Development Approach .....	136
5.4 Conclusions.....	141
5.5. References.....	141
<b>CHAPTER 6 APPLICATION OF COMPUTER SIMULATION AND THE USE AND EVALUATION OF INPUT DATA .....</b>	145

6.1. Introduction.....	145
6.2. Results and Discussions.....	146
6.2.1. Particle Size Influence on the Simulations .....	146
6.2.1.1. Influence of Particle Fraction using Physicochemical Data .....	146
6.2.1.2. Computer Simulation Aided Reverse Engineering.....	151
6.2.2. <i>In Vitro</i> Dissolution Data As Input Function For Simulations .....	157
6.2.2.1. Simulations using <i>In Vitro</i> Dissolution Data at Different Agitation Speeds.....	157
6.2.2.2. Reverse Engineering of A Drug Product using <i>In Vitro</i> Dissolution Data.....	161
6.3. References.....	166
<b>CHAPTER 7 SUMMARY AND FUTURE STUDY .....</b>	<b>168</b>
7.1. References.....	172
<b>APPENDIX A PHYSICOCHEMICAL ANALYSIS .....</b>	<b>174</b>
A.1. Introduction.....	174
A.2. Materials and Methods.....	175
A.2.1. Materials.....	175
A.2.2. Dissolution Test .....	176
A.2.3. Isothermal Titration Calorimetry (ITC) and Isothermal Microcalorimetry (IMC).....	176
A.3. Results and Discussion.....	177
A.3.1. IR and NMR of the Glyburide APIs .....	177
A.3.2. Isothermal Titration Calorimetry (ITC) and Isothermal Microcalorimetry (IMC).....	179
A.3.3. <i>In Vitro</i> Dissolution Tests .....	182
A.3.3.1. <i>In Vitro</i> Dissolution Tests of the South Africa Products ST 1 and ST 2.....	182
A.3.3.2. <i>In Vitro</i> Dissolution Tests of Two German Products At Different Agitation Speeds .....	184
A.4. Conclusion .....	185
6.5. References.....	185

<b>APPENDIX B DEMONSTRATION OF THE USE OF GASTROPLUS™</b>	188
B.1. Background of GastroPlus™ (modified from GastroPlus™ Manual, 2006)	188
B.2. Running GastroPlus™ Simulations	189
B.2.1. Compound Tab	190
B.2.2. Physiology Tab	191
B.2.3. Pharmacokinetics Tab	192
B.2.4. Simulation Tab	193
B.2.5. Calculation of Pharmacokinetic Parameters	195
B.2.5.1. Mean and Individual Observed Data	195
B.2.5.2. Comparison of the Simulation Using Different Version Programs	198
B.2.6. Influence of the Absorption Patterns on the Terminal Phase Fitting	200
B.2.5. Calculation of Pharmacokinetic Parameters	195
B.3. Discussion	200
B.3. Conclusion	202
B.3. References	202
<b>APPENDIX C DEMONSTRATION OF KINETICA®</b>	203
C.1. Introduction	203
C.2. Data Sets	206

## LIST OF TABLES

Table 11. Classification of drugs based on BCS <sup>a</sup> .....	5
Table 1.2. <i>In vitro and in vivo</i> correlations (IVIVCs) expectation based on BCS <sup>a</sup> .....	6
Table 1.3. Available dissolution media.....	15
Table 2.1. Comparison of the $P_{app}$ values for the A/A and B/A transport of the drug between the Hank's solution and 2 times diluted high quality FaSSIF (n=3) .....	55
Table 2.2. Transport studies of glyburide in the presence of (+/-) verapamil (50 $\mu$ M) for the A/B and B/A transports using Hank's solution and 2 times diluted high quality FaSSIF (n=3) .....	56
Table 3.1. Pharmacokinetic parameters of different products used for the computer simulations (The mean values of the clinical data obtained from these four products were well described by a two-compartmental model.....	72
Table 3.2. Physicochemical data determined for five glyburide APIs .....	73
Table 3.3. Simulated impact of changes in particle radius and particle size distribution (standard deviation) on the oral performance of glyburide product containing API-4. The measured particle size "mean" and the particle size distribution were theoretically manipulated. The simulated values are listed and the % change compared to the mean value are given in brackets .....	89
Table 4.1. $f_1$ and $f_2$ factors comparing the dissolution profiles between a reference (GR) and a test (GT) formulation at pH 6.5 .....	106
Table 4.2. Comparison of the drug releases (%) at 90 min (n=3) using dynamic and single pH dissolution protocols for a reference (GR) and a test (GT) formulations .....	109
Table 4.3. Comparison of pharmacokinetic parameters of a bioequivalence study between observed and simulated data.....	112
Table 5.1. Essential input data in the compound page for the basic prediction of the fraction dose absorbed using GastroPlus <sup>TM</sup> .....	122
Table 5.2. Pharmacokinetic parameters used for the simulation of the plasma concentration vs. time curve (German reference (GR)).....	123

Table 5.3. Summary of the simulations using physicochemical data as input functions (Observed: $C_{max}$ : 301 ng/mL; $Auc_{0-24}$ : 1359.6 ng/mL*h).....	127
Table 5.4. Summary of the simulations using <i>in vitro</i> dissolution profiles as input functions (Observed: $C_{max}$ : 301 ng/mL; $AUC_{0-24}$ : 1359.6 ng/mL*h).....	132
Table 6.1. Summary of the influence of particle fractions on the simulations using physicochemical data as input functions (German reference (GR) containing API-2: Observed: $C_{max}$ : 301 ng/mL; $Auc_{0-24}$ : 1359.6 ng/mL*h).....	148
Table 6.2. Pharmacokinetic parameters of two South Africa reference products (SR 1 and SR 2) used for the computer simulations (The mean values of the clinical data obtained from these four products were well described by a two-compartmental model).....	153
Table 6.3. Comparison of the predicted and observed $C_{max}$ and AUC for two South African reference products (reference-1 (SR 1) and reference-2 (SR 2))	154
Table 6.4. Summary of the sum of square (SS) for the simulations of two South Africa reference products (SR 1 and SR 2).(SS: Sum of Squares ( $Y_{obs} - Y_{pred}$ ) <sup>2</sup> )....	154
Table 6.5. The simulation summary of the sums of square at different agitation speeds for German reference (GR) and Test (GT) (Sum of Squares ( $Y_{obs} - Y_{pred}$ ) <sup>2</sup> ).....	158
Table 6.6. Comparison of the sums of square between the predicted and observed plasma concentration vs. time curves using experimental or computer optimized dissolution profiles for the South Africa Test 1 (ST 1) and 2 (ST 2) products (Sum of Squares ( $Y_{obs} - Y_{pred}$ ) <sup>2</sup> ).....	162
Table A.1. $f_1$ and $f_2$ factors of the dissolution profiles between different agitation speeds (50, 75 and 100 rpm) of two German products using dynamic pH change in LQ- FaSSIF.....	184
Table B.1. Pharmacokinetic parameters (calculated using Micro Extravascular model fitting in Kinetica <sup>®</sup> 4.4.1) for two individual volunteers (German reference volunteer number 1: GR 1 and German test volunteer number 2: GT 2) .....	196
Table B.2. Simulation results of two individual cases (observed German reference volunteer number 1 (GR 1): $C_{max}$ : 132 ng/mL; $AUC_{0-24}$ : 531 ng/mL*h; German test volunteer number 2 (GT 2): $C_{max}$ : 298 ng/mL; $AUC_{0-24}$ : 3530 ng/mL*h) .....	196

Table B.3. Comparison of pharmacokinetic parameters (mean German reference GR; 15 volunteers; average body weight 65 kg) using the micro extravascular model fitting in Kinetica <sup>®</sup> 3.0 or Kinetica <sup>®</sup> 4.4.1 .....	198
Table B.4. Summary of the simulations using the pharmacokinetic parameters calculated by Kinetica <sup>®</sup> 3.0 and Kinetica <sup>®</sup> 4.4.1 (Mean German reference GR; Observed: C <sub>max</sub> : 301 ng/mL; AUC <sub>0-24</sub> : 1359.6 ng/mL*h) .....	199

## LIST OF FIGURES

Figure 1.1. Factors in GI tract influencing the fraction dose absorbed of the oral dosage forms.....	9
Figure 1.2. Graph of gastrointestinal GI motility .....	11
Figure 1.3. Drug solubilization in micelle and emulsion media .....	15
Figure 1.4. Pathways of drug absorption .....	23
Figure 1.5. Caco-2 model system .....	27
Figure 1.6. Chemical structure of glyburide .....	28
Figure 2.1. Solubility of glyburide powder in different media at different pH (n=3).....	51
Figure 2.2. pH effect on cell toxicity using blank buffers (incubation time 90 min n=6; Blank FaSSIF and FeSSIF are plain buffers without bile salts and lecithin; *: significant difference from control, p<0.05) .....	52
Figure 2.3. Toxicity study of the different chemical grades of biorelevant dissolution media (incubation time 90 min, pH 6.5, n=6; HQ: purer bile salts and lecithin; LQ: crude bile salts and lecithin*: significant difference from control: p<0.05) .....	53
Figure 2.4. Toxicity study of the different concentration of the bile salts and lecithin in HQ-FaSSIF (incubation time 60 min, pH 6.5, n=6) .....	53
Figure 2.5. Time dependent effects on the TEER values of the cell monolayers after incubation in different media (HBSS, HQ-FaSSIF and 2-fold diluted HQ-FaSSIF; apical pH 6.5/basolateral pH 7.4; n=3).....	54
Figure 3.1. Particle appearance of the five glyburide powders using SEM .....	74
Figure 3.2. Comparison of X-ray diffraction spectra of five glyburide APIs.....	76
Figure 3.3. Comparison of the Raman spectra for five glyburide APIs .....	77
Figure 3.4. Comparison of the Raman spectra between crystal and amorphous forms glyburide (A: amorphous glyburide; B: API-2 crystal).....	78
Figure 3.5. TGA spectrum of API-1 .....	80
Figure 3.6. Comparison of five glyburide APIs using DSC .....	81

Figure. 3.7. Glass transition curves of amorphous glyburide obtained at different heating rates .....	82
Figure 3.8. Comparison of the simulated and observed data for German reference (GR) and test (GT) products containing API-2 using physicochemical data as input for the simulations .....	84
Figure 3.9. Comparison of the simulated and observed data for South Africa test 1 (ST 1) and test 2 (ST 2) products containing API-3 and API-4 using physicochemical data as input for the simulation .....	85
Figure 4.1. Solubility of glyburide powders in different media (n=3; Blank-FaSSIF: FaSSIF buffers without bile salts and lecithin; LQ and HQ: LQ and HQ-FaSSIF).....	104
Figure 4.2. Dissolution profiles of two formulations (GR and GT) in different media at pH 6.5 .....	101
Figure 4.3. Dissolution profiles of two formulations (GR and GT) in different media using a pH gradient.....	110
Figure 4.4. Comparison of the simulated and observed data using dynamic dissolution data as input into the simulation software .....	113
Figure 5.1. Comparison of the predicted absorption patterns using logP or the built-in $pK_a$ based solubility model.....	125
Figure 5.2. Comparison of the observed vs. simulated plasma concentration vs. time curves using three different absorption scale factor and ACAT models .....	128
Figure 5.3. Comparison of the predicted absorption pattern between using the concentration gradient and the unidirectional ACAT model.....	129
Figure 5.4. Intrinsic dissolution tests of two glyburide APIs (n=2) .....	130
Figure 5.5. Dissolution profiles of the glyburide tablets in SIF and FaSSIF media at pH 6.5 (n=3) .....	133
Figure 5.6. Dissolution profiles of glyburide tablet in SIF and FaSSIF media using a pH gradient (n=3).....	134
Figure 5.7. Comparison of the simulated and the observed data using dissolution profiles at pH 6.5 and dynamic pH changes as input functions .....	135



Figure 5.8. Comparison of the predicted absorption patterns using physicochemical data and using dissolution profiles at dynamic pH changes .....	140
Figure 6.1. Summary of the influence of particle fractions on the fraction dose absorbed in each compartment using physicochemical data as input functions (German reference (GR) containing API-2 .....	149
Figure 6.2. Summary of the influence of particle fraction on the simulations using physicochemical data as input functions (German reference (GR) containing API-2 .....	150
Figure 6.3. Comparison between simulated and observed plasma time curves for South Africa reference-1 (SR 1). Different particle sizes were chosen to match the observed curves and to try to bring the simulated curves within 10% of the observed values for AUC and $C_{max}$ .....	155
Figure 6.4. Comparison between simulated and observed plasma time curves for South Africa reference-2 (SR 2). Different particle sizes were chosen to match the observed curves and to try to bring the simulated curves within 10% of the observed values for AUC and $C_{max}$ .....	156
Figure 6.5. Comparison of the simulated plasma concentration vs. time curves using <i>in vitro</i> dissolution profiles under dynamic pH changes at different agitation speeds (50, 75 and 100 rpm; German reference product (GR)) .....	159
Figure 6.6. Comparison of the simulated plasma concentration vs. time curves using <i>in vitro</i> dissolution profiles under dynamic pH changes at different agitation speeds (50, 75 and 100 rpm; German test product (GT)).....	160
Figure 6.7. The comparison of the experimental and computer optimized dissolution profiles of two South Africa test products (ST 1 and ST 2) .....	163
Figure 6.8. Comparison of the predicted and observed plasma concentration vs. time curves using experimental dissolution profiles for South Africa Test 1 (ST 1) and 2 (ST 2) products .....	164
Figure 6.9. Comparison of the predicted and observed plasma concentration vs. time curves using computer optimized dissolution profiles for South Africa Test 1 (ST 1) and 2 (ST 2) products.....	165
Figure A.1. IR spectrum of the glyburide API-2 .....	177

Figure A.2. NMR spectrum of the glyburide API-2 .....	178
Figure A.3. ITC of FaSSIF media without glyburide (titrated from pH 5.0 to pH 8.5) .....	180
Figure A.4. ITC of FaSSIF media with 15 mg glyburide (titrated from pH 5.0 to pH 8.5) .....	181
Figure A.5. Comparison of the <i>in vitro</i> dissolution profiles between South African (ST 1 and ST 2) products using a dynamic pH change dissolution protocol in LQ- FaSSIF .....	183
Figure A.6. Comparison of <i>in vitro</i> dissolution profiles of two German products (GR and GT) at different agitation speeds using a dynamic pH change protocol in LQ- FaSSIF (n=3) .....	185
Figure B.1. ACAT model compartments (modified from GastroPlus™ Manual, 2006) .....	189
Figure B.2. Compound Tab showing the physicochemical properties of the drug .....	190
Figure B.3. Physiology Tab .....	191
Figure B.4. Physiology Tab .....	192
Figure B.5. Simulation Tab .....	193
Figure B.6. Simulation output (simulated plasma concentration vs. time curve).....	194
Figure B.7. Simulation output (Fraction dose absorbed in each compartment) .....	194
Figure B.8. Simulation of an individual case (German reference volunteer number 1: GR 1) .....	197
Figure B.9. Simulation of an individual case (German test volunteer number 2: GT 2) .....	197
Figure B.10. Comparison of the simulations between the pharmacokinetic parameters calculated by Kinetica® 3.0 and Kinetica® 3.0 (Mean German reference GR) .....	199
Figure B.11. Comparison of the predicted absorption patterns using physicochemical data and using dissolution profiles at dynamic pH changes (modified from Fig. 5.8, Chapter 5) .....	200
Figure C.1. Individual observed data of 15 volunteers for German reference product ..	204
Figure C.2. Individual observed data of 15 volunteers for German test product .....	204
Figure C.3. Mean observed data for German reference (GR) and test (GT) products ...	205

Figure C.4. Mean observed data for South African test 1 (ST 1) and test 2 (ST 2) products  
.....205

## ABBREVIATIONS

ACAT	Advanced compartmental absorption and transit model
$A_n$	Absorption Number
ANDs	Abbreviated new drug applications
API	Active pharmaceutical ingredient
AUC	Area under the plasma concentration time curve
BA	Bioavailability
BCS	Biopharmaceutics and Biopharmaceutics Drug Classification system
BDM	Biorelevant dissolution medium
BE	Bioequivalence
BL	Blank
$C_{max}$	Maximum plasma concentration after oral doses
Conc.	Substance concentration
Cl	Total body clearance
DMEM	Dulbecco's Modified Eagle's Medium
DMSO	Methy sufoxide
$D_n$	Dissolution Number
$D_0$	Dose Number
DSC	Differential scanning calorimetry
EDTA	Ethylenediaminetetraacetate
FaSSIF	Fasted state simulated intestinal fluid
$F_a$	Fraction dose absorbed
FeSSIF	Fed state simulated intestinal fluid
g	Gram
GI	Gastrointestinal
GR	German reference
GT	German test

h	Hour
HBSS	Hanks' balanced salt solution
HCl	Hydrochloric acid
HEPES	N-(2-Hydroxyethyl)piperazine-N'-(2-ethanesulfonic acid
HQ	High quality
INDs	Investigational new drug applications
IR	Infrared spectroscopy
IVIVC	<i>In vivo</i> and <i>in vitro</i> correlations
LQ	Low quality
LogD	Distribution coefficient
logP	Partition coefficient
M	Molar
MEM	Minimum essential medium
MES	2-(N-Morpholino)ethanesulfonic acid
mg	Milligram
Min	Minute
mL	Milliliter
MMC	Migrating motor complex
MRP	Multidrug resistance protein
MTT	3-(4,5-dimethyl-2-thiazolyl)-2,5-diphenyl-2H tetrazolium bromide
NaOH	Sodium hydroxide
NDAs	New drug applications
NMR	Nuclear magnetic resonance
$P_{app}$	Apparent permeability coefficient
$pK_a$	Dissociation constant
PE	Percent prediction error
SEM	Scanning Electron Microscopy
SGF	Simulated gastric fluid
SIF	Simulated intestinal fluid
SR 1	South African reference 1

SR 2	South African reference 2
ST 1	South African test 1
ST 2	South African test 2
SUPAC-MR	Scale up and post approval changes-modified release dosage forms
TEER	Transepithelial electrical resistance values
TGA	Thermogravimetric analysis
USP	United States Pharmacopoeia
$V_c$	Volume of distribution in central compartment
$\mu\text{g}$	Microgram
$\mu\text{L}$	Microliter
XRPD	X-ray powder diffraction

## CHAPTER 1

### GENERAL INTRODUCTION

#### 1. Introduction

##### 1.1. Background

Over the past decades, the cost for the development of a new drug product has dramatically increased (Grass and Sinko, 2002) and the overall time to commercialize a new drug product has averaged around 15 years (DiMasi *et al.* 2003). The estimated total cost for the development of one successful compound was over \$802 million (DiMasi *et al.* 2003; Adams and Brantner, 2006). The success rate of the new chemical entities (NECs) was less than 20% (Beary *et al.* 1993; PhRMA, 2000). Seventy-five percent of the total drug development costs was due to the failures during the drug development (Abelson, 1993; DiMasi *et al.* 2003). A significant reduction of such expense, without risking the quality and safety of a drug product, can only be realized if sufficient *in vitro* methods exist which are able to predict the *in vivo* performance of drug formulations. Such formulations can improve the success rate of clinical trials and fewer clinical studies would be needed before a drug product is marketed.

##### 1.2. Bioavailability and Bioequivalence

The development and optimization of pharmaceutical formulations combines basic research, manufacturing, clinical testing and marketing of the drug product resulting in a time consuming and costly process. The biopharmaceutical quality and performance of drug products is an important concern of regulatory agencies. The bioavailability (BA) and in some instances bioequivalence (BE) of the orally administered drug products in investigational new drug applications (INDs), new drug applications (NDAs) and abbreviated new drug applications (ANDAs) (FDA, 2003) are critical criteria to assess the quality and performance *in vivo*. Generally, the regulatory approach to the BA and BE

is based on pharmacokinetic key parameters (*in vivo* study) using maximum plasma concentration ( $C_{max}$ ) after dosing and area under the plasma concentration time curve (AUC). According to the Code of Federal Regulation (21 CFR 320.1) in the United States (USA), bioavailability is defined as “ The rate and extent to which the active ingredient or active moiety is absorbed from a drug product and becomes available at the site of action”. Bioequivalence is defined as “ The absence of a significant difference in the rate and extent to which the active ingredient or active moiety in pharmaceutical equivalents or pharmaceutical alternatives becomes available at the site of drug action when administered at the same molar dose under similar conditions in an appropriate designed study”. As mentioned in the statutory definitions of BA/BE above, BA/BE focuses on the drug release from a dosage form and absorption into the systemic circulation (FDA, 2003). BA data for an orally administered formulation provides the estimation of the relative fraction dose absorbed into the systemic circulation. BA data can provide useful pharmacokinetic information such as distribution, elimination, and absorption etc based on the *in vivo* study. Establishing the BA of an oral dosage is a benchmark for comparison with other related formulations like suspensions or intravenous injections. There are two types of bioavailability: Relative (apparent) bioavailability is the availability of a drug product as compared to a recognized standard; Absolute bioavailability is the measurement of the comparison of the respective AUCs after oral and IV administration (Shargel and Yu, 1999). BE is used to compare a reference and a test formulation (FDA, 2003). For drugs which are investigated as IND and NDA, BE studies can be used to compare different formulations at the different stages such as early and late stages of the clinical trial. Furthermore, the BE study is the critical criterion for ANDAs and postapproval changes. Here a BE study has to demonstrate that a generic formulation is bioequivalent to the original reference product (FDA, 2003).

The bioavailability of a drug may be affected by many factors. Formulations are intended to minimize these factors. The goal of formulation design is to compose a dosage form with maximum reproducibility in bioavailability. Generic drugs have the same amount of active ingredients as a brand name formulation. The inactive ingredients in generic drugs may differ from the brand name drugs. These differences in the formulation recipes may affect the drug release and absorption (Kayali, 1994). Although



such products contain the same drug contents, they may not be bioequivalent to the reference.

Generic drugs are one way to keep drug prices low. In the past, different regulatory initiatives in USA have tried to lower the drug costs by changing the regulatory requirements for generics. The Drug Price Competition and Patent Term Restoration Act (Waxman-Hatch Act, 1984, USA) and the Generic Drug Enforcement Act (1992, USA) changed the regulatory requirements and simplified the approval process of new generic drug applications. The approval procedures are now based on the biopharmaceutical equivalence of the products. Many generic drugs that had been proven safe and effective became available (Löbenberg and Amidon, 2000a). Before the Biopharmaceutics Drug Classification System (BCS) was introduced into regulatory framework only *in vivo* studies (BA/BE) were able to provide sufficient information to identify and to evaluate the quality and performance of drug products. This process is time consuming and expensive. Clinical trials are still needed to assess drug safety and efficiency, but dissolution results based on the BCS can be used as a surrogate for BE studies if strong *in vivo* and *in vitro* correlations (IVIVCs) exist. The BCS simplifies the regulatory process and this might result in faster drug approvals and consequently in lower drug prices.

### **1.3. Biopharmaceutics and Biopharmaceutics Drug Classification System (BCS)**

#### **1.3.1. General Concepts**

Biopharmaceutics is the study of the factors influencing the bioavailability of a drug product in man and animals. Modern biopharmaceutics combines the knowledge of physical chemistry, pharmacokinetics, physiology and materials science. It takes into consideration the physical and chemical properties of a drug in a dosage form, and the physiological effects observed after administration (Cheo and Amidon, 2000). The goal of modern biopharmaceutics is to understand and to describe the mechanisms of drug delivery and absorption from a pharmaceutical dosage form into the general circulation system.

Most drugs are orally administered. Conventionally, *in vivo* studies of BA/BE of an oral dosage form are focused on pharmacokinetic parameters, such as AUC and  $C_{\max}$ .

These empirical parameters provide an estimation of the bioavailability in the systemic circulation after oral administration. Little mechanistic information regarding drug absorption in the GI tract can be obtained from pharmacokinetic parameters (Cheo and Amidon, 2000; Löbenberg and Amidon, 2000a). Several different environments and physiological factors have to be considered to trace gastrointestinal (GI) drug absorption. The obviously complex chemistry and physiology involved in this process has to be broken down into its key parameters to gain a mechanistic understanding of the drug absorption process (Löbenberg and Amidon, 2000a). Applying Fick's First Law (Eq. 1.1) to a membrane, the absorption across the mucosal surface can be written as:

$$J_w = P_w * C_w = \frac{dM}{dt} * \frac{1}{A} \quad \text{Eq. 1.1}$$

where  $J_w$  is the mass transport across the gut wall,  $P_w$  can be assumed as the effective permeability,  $C_w$  is the concentration of the drug at the membrane, and  $A$  is the surface area.  $\frac{dM}{dt}$  is the rate of drug across the membrane ( $A$ ) by passive diffusion. Equation 1.1 shows that permeability and the dissolved drug in the gut lumen are the fundamental variables in describing mass transport through a membrane. Dissolution is brought into this equation by the fact that the concentration of poorly soluble drugs is a function of its dissolution behavior.

This mechanistic approach based on permeability and solubility is known as the Biopharmaceutics Drug Classification System (BCS) and was developed by Amidon *et al.* (1995). The rationale behind this classification is, that if two drug products have the same dissolution rate, then both products will have the same drug concentration in the gut lumen, and drug absorption will occur to the same rate and extent (Amidon *et al.* 1995). This will lead to bioequivalence of such products. Accordingly, the BCS classifies the biopharmaceutical property of drugs and drug products into four categories (Table 1.1). Since the year 2000 the BCS has been part of the guidelines of the Food and Drug Administration (FDA) (Löbenberg and Amidon, 2000a).

**Table 1.1.** Classification of drugs based on BCS<sup>a</sup>

Class	Solubility	Permeability
I	High	High
II	Low	High
III	High	Low
IV	Low	Low

<sup>a</sup>Modified from Löbenberg and Amidon (2000a)

The BSC has defined three dimensionless numbers governing drug absorption: Absorption Number ( $An$ ), Dissolution Number ( $Dn$ ) and Dose Number ( $Do$ ).  $An$  can be defined as the ratio of the permeability to the gut radius times the residence time in the small intestine. In other words it can be expressed as the ratio of the residence time to the absorptive time (Eq. 1.2). The Dissolution Number ( $Dn$ ) is the ratio of the residence time in the small intestine and the dissolution time. The equation includes the solubility, diffusivity, density, and the initial particle size (Eq. 1.3). The Dose Number ( $Do$ ) is the ratio of dose concentration to drug solubility (Eq. 1.4). These parameters provide a scientific and mechanistic approach to fundamental processes of drug absorption like membrane permeation, drug dissolution and dose/solubility requirements (Amidon *et al.* 1995).

$$An = \frac{P_{eff}}{R} * t_{res} = \frac{t_{res}}{t_{abs}} \quad \text{Eq. 1.2}$$

$$Dn = t_{res} * 3DC_s / \rho r^2 = t_{res} / t_{diss} \quad \text{Eq. 1.3}$$

$$D_0 = \frac{M_0}{V_0 C_s} \quad \text{Eq. 1.4}$$

where:  $P_{eff}$  = permeability,  $R$  = the gut radius,  $t_{res}$  = mean residence time,  $t_{abs}$  = absorptive time,  $t_{diss}$  = time required for a particle of the drug to dissolve,  $D$  = diffusivity,

$p$  = density,  $r$  = the initial particle radius,  $C_s$  = solubility,  $M_0$  = dose,  $V_0$  = the volume of water taken with the dose (around 250 mL).

### 1.3.2. Applications of the BCS

Since the introduction of the BCS in 1995 (Amidon *et al.* 1995), an increasing impact on the regulatory practice and on regulatory agencies has been shown. Table 1.2 shows the expectation of *in vivo* and *in vitro* correlations (IVIVCs) for the four categories drugs.

**Table 1.2.** *In vitro* and *in vivo* correlations (IVIVCs) expectation based on BCS<sup>a</sup>

Class	IVIV Correlation Expectation
I	IVIVC if dissolution rate is slower than gastric emptying rate, otherwise limited or no correlation
II	IVIVC expected if <i>in vitro</i> dissolution rate is similar to <i>in vivo</i> dissolution rate, unless dose is very high
III	Absorption (permeability) is rate determining and limited or no IVIVC with dissolution rate
IV	Limited or no IVIVC expected

<sup>a</sup>Modified from Amidon *et al.* 1995

Class I drugs such as chloroquine hydrochloride (Verbeeck *et al.* 2005) show that the gastric emptying rate controls the absorption rate if dissolution is rapid enough (Amidon *et al.* 1995). There is limited or no correlation between *in vivo* and *in vitro* dissolution (Amidon *et al.* 1995). Generally, if 85% of the drug is released for the immediate release dosage forms in less than 15 min, then bioequivalence is expected for two drug products (Amidon *et al.* 1995).

Class II drugs such as ibuprofen (Potthast *et al.* 2005) are clearly good candidates for IVIVCs unless their dose is very high (Amidon *et al.* 1995). The dissolution rate and dose numbers of class II drugs are both important factors influencing the rate and extent of drug absorption after oral administration. The *in vivo* dissolution of Class II drugs affects the actual concentration of the active ingredient at the membrane surface of the absorption sites during the GI transit and this is in most cases the absorption limiting factor (Amidon *et al.* 1995). If the applied dissolution media and *in vitro* methods can mimic the *in vivo* dissolution behaviors of a drug product, then the establishment of IVIVC can be expected (Amidon *et al.* 1995; Dressman *et al.* 1998).

Class III drugs such as acetaminophen (Kalantzi *et al.* 2006) show that permeability is the limiting factor in the absorption rate (Amidon *et al.* 1995). There is no or limited IVIVC between *in vivo* performance and *in vitro* dissolution. The *in vitro* behavior of a Class III drug is the same as for a Class I drug. However, the *in vivo* absorption of Class III drugs is governed by the physiological conditions in the GI tract rather than by formulation factors (Amidon *et al.* 1995).

Class IV drugs such as the diuretic acetazolamide (Linderberg *et al.* 2004) can be considered as the worst cases for oral drug delivery (Amidon *et al.* 1995). Both permeability and dissolution are limiting factors in the drug absorption process. No IVIVCs is expected between *in vivo* and *in vitro* dissolution.

In 2000, the guidance for industry entitled “Waiver of *in vivo* bioavailability and bioequivalence studies for immediate release solid oral dosage forms based on a biopharmaceutics classification system” was issued by the FDA (FDA, 2000). A biowaiver for immediate release solid oral dosage can waive the normally required *in vivo* bioavailability and bioequivalence studies if the applied drug product meets three critical requirements of high solubility, high permeability and rapid dissolution. These three requirements play an important role in oral drug absorption because quick absorption is due to high permeability and high solubility associated with quick dissolution. Only such formulations will have an *in vivo* performance independent from dissolution effects. It is expected that 100% of a drug will be dissolved in the stomach before the drug enters the major absorption site in the small intestine. The guidance is only suitable for Class I drugs. The guidance outlines the complete requirements for an

issued biowaiver. The biowaiver can be requested when a test and a reference product are pharmaceutically equivalent. Exceptions to this biowaiver include a narrow therapeutic range or drugs that are absorbed in the oral cavity. The major criteria for the possible use of a biowaiver are: 1) high solubility, which is defined as “the highest dose of a certain drug substance that can dissolve in 250 mL or less of aqueous medium over a physiological pH range of 1-7.5.”; 2) high permeability, which is defined as “the extent of absorption in humans is determined to be 90% or more of an administered dose based on a mass balance determination or in comparison to an intravenous reference dose under the condition of non-considerable instability.”; 3) rapid dissolution, which is defined as “no less than 85% of the labeled amount of the drug substance dissolves within 30 minutes.” (FDA, 2000).

The FDA guidance (FDA, 2000) provides the biowaiver exclusively for BCS Class I drugs. However, the possibility of biowaivers for the other Classes of drugs such as Class III drugs has been extensively discussed (Blume *et al.* 1999; Cheng *et al.* 2004; Kalantzi *et al.* 2006; Yu *et al.* 2002a). The limiting factor in the absorption of Class III drugs is their permeability. If dissolution in Class III products is rapid enough in all the physiological pH conditions, then their behaviors *in vivo* will resemble an oral solution. The BE study of an oral solution can be waived due to the self-evident drug release (FDA, 2003). In order to request a biowaiver for the Class III products, a stricter criterion of *in vitro* dissolution is necessary. Such a criterion might specify that no less than 85% of the labeled amount of drug substance has to be released within 15 minutes compared to the 30 minutes allowed in Class I drugs (Yu *et al.* 2002a). For Class II drugs, the oral absorption is limited by their *in vivo* dissolution (Yu *et al.* 2002a). If the *in vitro* dissolution can be shown to simulate the *in vivo* dissolution, the *in vivo* and *in vitro* correlation (IVIVC) can be expected. However, the difficulty here is to design and validate *in vitro* experiments while simulating the complexity of the physiological conditions in the GI tract (Yu *et al.* 2002a).

## 1.4. *In Vitro* Dissolution Test Development

### 1.4.1. Physiology of Gastrointestinal Tract

The preferred route of drug administration is the oral route. The drug release from an oral dosage form and absorption in the GI tract are influenced by the conditions of the GI tract. It is difficult to comprehensively predict the oral drug release and absorption on the basis of the models available due to complex conditions of the GI tract (Figure 1.1).

There are many factors that can change the drug release and the absorption rate in the GI tract such as the fasted/fed state, pH gradient, intestinal motility and transit, gastric emptying, etc. (Dressman *et al.* 1998; Langguth *et al.* 1994; Lipka *et al.* 1995).

## Factors influencing oral drug uptake

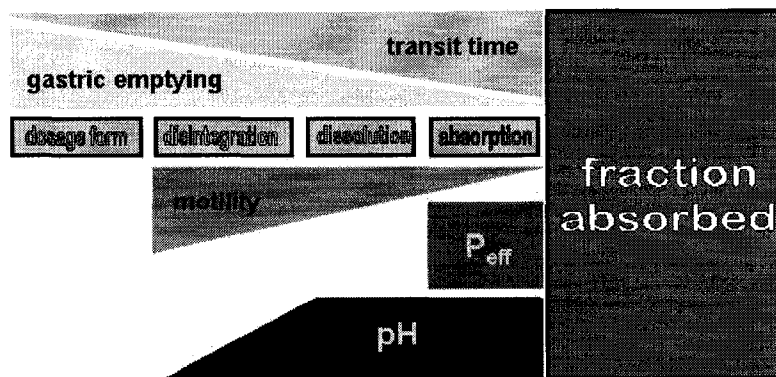


**Figure 1.1.** Factors in GI tract influencing the fraction dose absorbed of the oral dosage forms (Löbenberg and Amidon, 2000a)

For example, there are various fluids secreted by the different sites within the GI tract including hydrochloric acid, bicarbonate, enzymes, bile salts and lecithin (Dressman *et al.* 1998). When one considers the extensive and variable states of the GI tract from fed to fasted conditions, one can understand that the composition of the GI tract can indeed become very complex. The factors influencing the solubility and dissolution of drugs

include pH, buffer capacity, surfactant, food, and the volume of luminal contents (Dressman *et al.* 1998). The variable lumen contents e.g. bile salts, dietary lipids and so forth can increase the solubility of poorly soluble drugs and subsequently enhance the drug dissolution and absorption (Bakatselou *et al.* 1991; Galia *et al.* 1998; Mithani *et al.* 1996). The composition of modern dissolution media must consider these above-mentioned factors in order to obtain a more precise simulation of the GI environment.

The other critical concern of modern dissolution technology is the hydrodynamics in the GI tract. The *in vitro* dissolution methods should be able to simulate the hydrodynamic conditions *in vivo*. There are basically four motility movements in the GI tract and they are referred to jointly as the migrating motor complex (MMC) (Hendrix *et al.* 1987). Figure 1.2 shows the GI motility during fasted and fed state conditions, respectively. Four different phases of cyclic MMC can be clearly observed in fasted state. There is a quiescent phase I where little or no activity is recorded. Only random contractions can be observed. In phase II the contractions start to occur more frequently and more forcefully, until they cumulate in a burst of activity with phase III. Phase III then consists of a peak frequency of contractions. The maximal spikeburst of activity associated with each slow wave appears during phase III. Phase IV happens when the GI motility returns from phase III to phase I. In the fed state there is little or no activity during a prolonged period, especially for the stomach. However, about every two hours, contractions do start to occur, until they cumulate enough to have a burst of activity to clear the contents of the stomach into the intestine. After this a fasted state condition follows (Dressman *et al.* 1998; Zenilman, 1993).



## GI-Motility

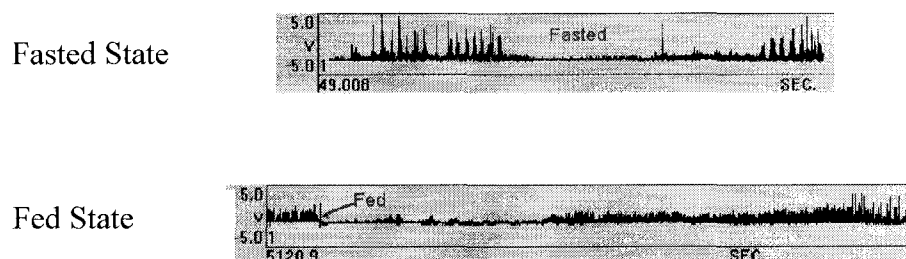


**Figure 1.2.** Graph of gastrointestinal GI motility (provided by Dr. Löbenberg)

The motility of the GI tract controls both the mixing of the luminal contents, and the transit time. The MMC phases may also influence the dissolution rate and therefore the drug absorption. Due to the complexity of the motility of the GI tract there is no single model which can simulate the *in vivo* hydrodynamics, and more work is needed to understand and truly simulate the hydrodynamics in the GI tract.

### 1.4.2. *In Vitro* Dissolution Development

#### 1.4.2.1. *In Vitro* Dissolution Apparatuses

*In vitro* dissolution tests are described in USP chapter <711> “dissolution tests” and chapter <724> “drug release” and they delineate standard methods to assure the batch-to-batch biopharmaceutical quality of oral dosage forms (USP 29, 2006). Drug release tests are routinely used in the pharmaceutical industry for quality control and drug development (Costa and Lobo, 2001). Pharmacopoeias such as the USP, list several different dissolution apparatuses: basket (Apparatus 1), paddle (Apparatus 2), reciprocating cylinder (Apparatus 3) or flow through cell (Apparatus 4). The basket and paddle apparatuses are routinely used because of their easy handling and preparing (Löbenberg *et al.* 2000b). Most dissolution tests are performed using Apparatus 1 and 2 and it is unnecessary to switch to other apparatuses if the results are acceptable (FDA,

1997a). Apparatus 3 is designed for the extended-release products and may not be used for highly soluble immediate release products (Yu *et al.* 2002b). The dissolution performance obtained from Apparatus 1 and 2 might be influenced by the shaft wobble, centering and the distinctive formation of the cone at the bottom of the vessels (Borst *et al.* 1997). Apparatus 3 might avoid these disadvantages and improve IVIVC by mimicking the changes in the GI tract compared to Apparatus 1 and 2 (Borst *et al.* 1997; Yu *et al.* 2002b). However, the tested dosage form must not disintegrate or the test might fail when the test cylinder is moved from one medium to another because too small powder particles with undissolved drug will pass through the screen of the cylinder and stay in the first medium. Apparatus 4 is more suitable for very low soluble drugs. This apparatus can maintain the sink condition during the entire experiment (Sunesen *et al.* 2005). Simulation of the hydrodynamics in the GI tract might be better and closer to reality than in Apparatus 1 and 2 (Perng *et al.* 2003; Qureshi *et al.* 1994). Other apparatuses are available such as Apparatus 5 (paddle over disk), 6 (cylinder) and 7 (reciprocation holder). They are useful for evaluating and testing the transdermal dosage forms (USP 29, 2006). Intrinsic dissolution is an important parameter to characterize the dissolution behavior of a drug powder. Here different physicochemical properties like crystal form, salt, or crystal water content can be evaluated with respect to their influence on the dissolution from a defined surface area (Jinno *et al.* 2000). Intrinsic dissolution is the testing of instantaneous reactions at the solid-liquid surface in different dissolution media using a rotating disk apparatus (Jinno *et al.* 2000). Intrinsic dissolution is described in chapter <1087> of the USP (USP 29, 2006).

#### **1.4.2.2. Dissolution Media**

Various dissolution media are described in the national pharmacopoeias, including simulated intestinal fluid (SIF) and simulated gastric fluid (SGF) (Test Solutions, USP 29, 2006). These media act as buffers that cover the physiological pH range from 1.2 to 6.8 (Löbenberg and Amidon, 2000a). For many poorly soluble drugs, the *in vitro* dissolution in such media will not produce useful information because pH is not the only factor which influences solubility and drug release (Jinno *et al.* 2000). The modifications

of dissolution media such as adding surfactants like sodium lauryl sulfate (SLS), Tween 20 (TW 20) (Amidon *et al.* 1997; Charman *et al.* 1997; Löbenberg and Amidon, 2000a) or using emulsion or organic solvent have been investigated in the past (El-Massik *et al.* 1996). Nevertheless, it still remains an open question whether or not these modified media truly reflect *in vivo* conditions.

The simulation of *in vivo* dissolution in any of the dissolution apparatuses described previously is challenging because each apparatus has its limitations to simulate the physiology and hydrodynamics in the GI tract (Löbenberg *et al.* 2000b). The hydrodynamics within the GI tract can be estimated by comparing *in vivo* data with different duration and agitation conditions of the dissolution test. This enables to define the *in vitro* test conditions to mimic the transition of the drug through the GI tract (Dressman *et al.* 1998). However, to be able to simulate *in vivo* dissolution behavior changing environments are needed. The other critical factor in this issue is how to simulate the *in vivo* conditions using a dissolution medium.

The information obtained from the physiology of the GI tract can be used to develop a suitable dissolution medium in order to provide more meaningful data to evaluate the *in vivo* performance of an oral drug. The knowledge of the composition of the intestinal fluids can assist in the development of suitable biorelevant dissolution media (BDM). For example, sodium taurocholate as a representative bile salt can be used in dissolution media in order to simulate intestinal fluids (Dressman *et al.* 1998).

The goal of modern dissolution media is to mimic the physiological environment of the GI tract. Micelle and emulsion systems are used for such purposes (Löbenberg *et al.* 2000a-b). If a dissolution medium is able to simulate the *in vivo* dissolution process then IVIVCs can be expected. New BDM were developed and published in the 1995 FIP guidance: Fasted state simulated intestinal fluid (FaSSIF) and fed state simulated intestinal fluid (FeSSIF). Both contain bile salts (sodium taurocholate) and lecithin to simulate the physiological environment in the GI tract (Dressman *et al.* 1998). BDMs take the micelle and emulsion characteristics of GI juices into account. If the BDMs provide the best possible simulation of the actual GI environment, such an *in vitro* test will then more suitably reflect the *in vivo* performance of a drug product. Table 1.3 shows different dissolution media and their composition.

Bile salts and lecithin are naturally present in the GI tract. Bile salts can aid the solubilization of the dietary fats in the body (Magee *et al.* 2003). Bile salts usually associate with lecithins, and fatty acids creating mixed micelles in the GI tract after being secreted via the bile duct (Figure 1.3). The formation process and the shapes of the micelles or vesicles formed from bile salts and lecithin are highly sensitive to the environment. For example the formation process is sensitive to the concentration of the bile salts or lecithin and the osmolarity and pH (Leng *et al.* 2003). The micelles and vesicles formed from bile salts and lecithin in different physiological environments can provide the information necessary to simulate the *in vivo* compositions of the intestinal fluids. The resulting biorelevant dissolution media can then simulate the interaction of drugs with the bile salts and food lipids. This is especially important for poorly soluble drugs because such media are able to enhance the solubility of a drug sometimes by a great magnitude such that it has a great impact on the drug absorption and bioavailability of the drug. The micelle system can be used to increase the solubility for many drugs (Efentakis and Dressman, 1998). Yazdaniyan *et al.* (2004) has reported that the solubility of selected model drugs in BDM was higher compared to simple buffers. Simple buffers like USP dissolution media might underestimate the *in vivo* solubilization. If lipids such as long-chain or medium-chain triglyceride associate with bile salts an emulsion system will be formed. Kaukonen *et al.* (2004) has shown that such systems may simulate the interaction between bile salt and lipids *in vivo*. The resulting emulsion system also increased the solubility of poorly soluble drugs dramatically. For example, the solubility of danazol was 142.6 µg/mL in an emulsion system and was only 0.8 µg/mL in plain buffer (Kaukonen *et al.* 2004).

The impact of physiologically adapted dissolution media on the dissolution behavior of Class I and Class II drugs has been previously studied by comparing the dissolution behavior of commercially available products in pharmacopoeia media and in the biorelevant dissolution media (Galia *et al.* 1998). In the case of Class I drugs, there was no significant difference between BDMs and conventional media, which implies that for Class I drugs conventional media are suitable choices. On the other hand, these studies pointed out that BDMs are the preferable dissolution media for certain poorly soluble substances, i.e. glibenclamide, danazol, and ketoconazole, because in comparison to

pharmacopoeial media their ability to improve the amount of dissolved drug was essential (Galia *et al.* 1998; Löbenberg *et al.* 2000a-b).

**Figure 1.3.** Drug solubilization in micelle and emulsion media (Löbenberg and Amidon, 2000a)

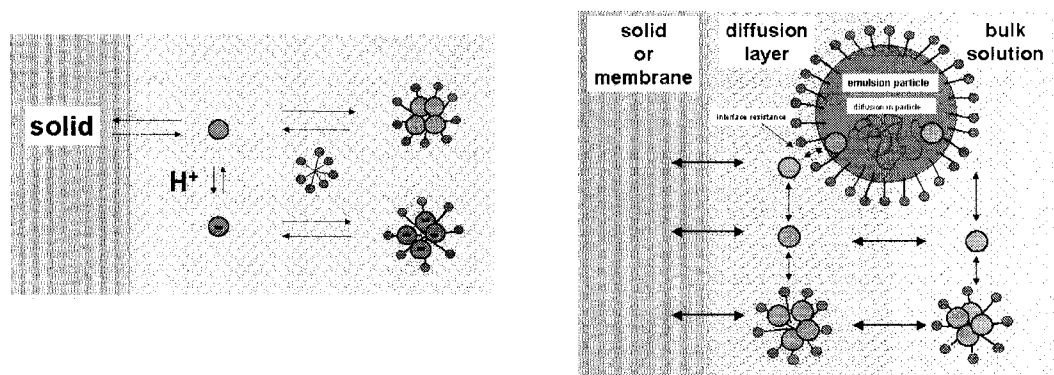


**Table 1.3.** Available dissolution media (Galia *et al.* 1998)

Conventional Media	Pharmacopoeial media	BDMs
Water	Simulated gastric fluid USP 29, 2006 (SGF) Pepsin 3.2 g HCl 7.0 mL NaCl 2.0 g pH 1.2 Water ad. 1000 mL	Fasted state simulated intestinal fluid (FaSSIF) Na taurocholate 1.65 g Lecithin 0.59 g NaOH 0.554 g KH <sub>2</sub> PO <sub>4</sub> 3.9 g KCl 7.7 g pH 6.5 Water ad. 1000 mL
Buffers with various pH values	Simulated intestinal fluid USP 24 (SIF) Pankreatin 10.0 g KH <sub>2</sub> PO <sub>4</sub> 6.8 g NaOH 0.62 g pH 6.8 Water ad. 1000 mL	Fed state simulated intestinal fluid (FeSSIF) Na taurocholate 8.25 g Lecithin 2.95 g CH <sub>3</sub> COOH(1M) 144mL KCl 15.2 g NaOH 4.04 g pH 5.0 Water ad. 1000 mL

## 1.5. *In Vitro* /*In Vivo* Correlation (IVIVC)

### 1.5.1. Concepts of IVIVC

There are two definitions of IVIVC based on the USP and FDA guidelines. USP defines IVIVC as “the establishment of a rational relationship between a biological property, or a parameter derived from a biological property produced by a dosage form, and a physicochemical property of characteristic of the same dosage form (USP 29, 2006)”. FDA defines IVIVC as “A predictive mathematical model describing the relationship between an *in vitro* property of a dosage form (usually the rate and extent of drug dissolution or release) and a relevant *in vivo* response, e.g., plasma drug concentration or amount of drug absorbed” (FDA September 1997). In order to successfully develop IVIVCs, *in vitro* dissolution has to be the rate-limiting step leading to absorption of the drug into systemic circulation (Uppoor, 2001). Emami (2006) has recently reviewed the development and application of the IVIVCs in the pharmaceutical sciences (Emami, 2006).

*In vivo* absorption data that are used to correlate with the *in vitro* dissolution data can be obtained using pharmacokinetic compartment models - (Wagner-Nelson or Loo-Riegelman) or compartment independent models- (DeMons) (Wagner and Nelson, 1964; Yu *et al.* 1997). The Wagner-Nelson method can be used for one-compartment models and the Loo-Riegelman method is suitable for the multi-compartment models. The difference between the numerical deconvolution method (DeMons) and Wagner-Nelson or Loo-Riegelman methods is that DeMons is independent of a compartment model (Grundy *et al.* 1997a-b). The resulting deconvolution data represent the drug input rate of the dosage form such as the fraction dose absorbed for oral dosage forms (USP 29, 2006).

The USP and FDA classified four levels of correlation (level A, B, C and a multiple level C). The ideal correlation is a level A correlation. It is a point-to-point relationship. Normally, these correlations are linear, but non-linear correlations are still acceptable. The level A correlation is the most useful from a regulatory point of view. The method used to develop a level A correlation is as follows: 1) Obtain the *in vivo* input rate of the drug from a dosage form, sometimes referred to as *in vivo* dissolution. 2) Gain a deconvolution of the plasma level data to general percent of drug absorbed for each

formulation using the methods such as Wagner-Nelson and Loo-Riegelman methods. 3) Plot the *in vivo* absorption profile against the *in vitro* dissolution profile to obtain a correlation. There are several advantages of a level A correlation: a) A level A correlation is based on the entire profile, and thus reflects the whole curve. b) It is an ideal quality control parameter. c) The *in vivo* performance of a dosage form can be predicted using *in vitro* dissolution data.

Level B correlations are established between the mean *in vitro* dissolution time (as a single point measure of *in vitro* dissolution or release rate) and either the mean residence time or the mean *in vivo* dissolution time (as a single point measure of the *in vivo* drug input rate). Although level B correlation uses all of the *in vitro* and *in vivo* data, it is not a point-to-point correlation.

Level C correlations are established between a single point measure of dissolution or a release rate (such as mean dissolution time or time for 50% release) and a single point measure of the extent of absorption *in vivo* (such as AUC or  $C_{max}$ ). Similarly, a level C correlation does not reflect the entire plasma concentration vs. time.

Level B and C correlations are single point correlations and may easily fail to reflect the complexity of the *in vivo* processes because two different formulations, which have different dissolution profiles may have the same mean value at a single point measurement (Athanasios *et al.* 1993; Cutler *et al.* 1997). But one big advantage of the Level B and C correlations is that they are easier to be established compared to level A correlations.

Multiple level C uses one or several pharmacokinetic parameters ( $C_{max}$ , AUC) of interest in comparing e.g. the amount of drug released at different time points using dissolution profiles. However, Cutler *et al.* (1997) hypothesized that if one can develop a multiple level C correlation, one also can develop a level A correlation.

The establishment of IVIVCs should be done on the basis of the therapeutic relevance of drug dosage forms. A useful IVIVC that can realistically predict the *in vivo* performance of a drug dosage is related to the therapeutic range as in, for examples,  $C_{max}$ , which is related to a therapeutic drug concentration or AUC, which is related to the extent of absorption (FDA, 2000). There are several factors that may cause a failure in correlation such as a large fluctuation of pharmacokinetic variables that are larger

compared with the therapeutic range or a narrow therapeutic window of certain drug substances (Cutler *et al.* 1997). A predictive IVIVC enables *in vitro* dissolution as a surrogate for biostudies. It can be used to obtain biowaivers and set more meaningful dissolution specifications that predict the *in vivo* performance of a drug product. Based on acceptable IVIVCs, the biowaivers for biostudies may be granted for a manufacturing site, equipment, a manufacturing process, and minor formulation composition changes. IVIVCs can be used to support those drug product changes in SUPAC-MR (scale up and post approval changes-modified release dosage forms) that might need biostudies. However, IVIVCs have many limitations. Before one establishes an IVIVC relationship, certain criteria must be met. Recently, only some drug products have been granted biowaivers (FDA, 1997b). Further investigation in this area is needed.

### **1.5.2. Physiologically-Based Pharmacokinetic Software Models**

Levy *et al.* (1965) reported the development of a relationship between *in vitro* dissolution and *in vivo* bioavailability of aspirin tablets. Some other research groups tried to establish the relationship between *in vitro* dissolution and *in vivo* behaviors of other oral dosage forms in 1970s (Johnson *et al.* 1973; Lindenbaum *et al.* 1973; Wagner *et al.* 1973). Over the past decades, the establishment of IVIVCs has been studied using different drugs, in different dosage forms and applying different models. These models included rat, dog and human. Deconvolution of the plasma concentration vs. time curve using Wagner-Nelson or Loo-Riegelman methods was applied in developing different levels of correlation between *in vitro* dissolution and *in vivo* pharmacokinetic parameters. Commercially available software such as PDx-IVIVC™ (GloboMax®LLC, Slough, Berkshire, UK) provides more convenient ways to develop potential IVIVCs because of its comprehensive models, user-friendly screen and web access (<http://www.globomaxservice.com>). However, today there is still only a limited number of Level A correlations (Grundy *et al.* 1997a-b) found in the literature due to difficulties in development and validation (Dutta *et al.* 2005). This situation has to be improved because Level B (Athanassiou *et al.* 1993) or level C (Balan *et al.* 2000) correlations may not be suitable as surrogates of *in vivo* studies. An alternative method for *in vitro/in vivo*



correlation is based on a convolution technique using *in vitro* data to predict the *in vivo* performance.

The oral absorption can be influenced by many factors such as physicochemical factors (solubility,  $pK_a$ , crystal structure, particle size and size distribution), physiological factors (GI pH, transit time and transport mechanism, permeability) and formulation factors (dosage form) (Agoram *et al.* 2001; Parrott and Lavé 2002). Physiologically-based prediction tools such as computer software are highly desirable because they can integrate the available data and provide useful information during the drug development process of new or generic drugs. Several articles have discussed the physiologically-based pharmacokinetic simulation models for oral dosage forms (Agoram *et al.* 2001; Grass, 1997; Grass and Sinko, 2002; Norris *et al.* 2000; Yokoe *et al.* 2003). The ultimate goal of these physiologically-based pharmacokinetic models is to predict the *in vivo* behavior of certain drugs under specific conditions using computational technology. There are two commercially available programs based on the physiologically-based pharmacokinetic models: iDEA<sup>TM</sup> (*In vitro* determination for the estimation of ADME model) (Grass and Sinko, 2002) and GastroPlus<sup>TM</sup> (Advanced compartmental absorption and transit model, ACAT) (Grass and Sinko, 2002). These two software packages use physiologically based models, which try to account for all known factors influencing the oral drug absorption and to predict the behavior of a xenobiotic's interaction with the body system using mathematical approaches.

### **1.5.3. Advanced Compartmental Absorption and Transit Model (ACAT)**

Traditional quantitative and mechanistic approaches have been developed which consider the entire gastrointestinal tract as a single-compartment (Dressman *et al.* 1984; Ho *et al.* 1983; Oh *et al.* 1993; Sinko *et al.* 1991). For example, a single-tank mixing model using a macroscopic mass balance approach was used to predict the fraction dose absorbed (Oh *et al.* 1993; Sinko *et al.* 1991). The limitations of these models are that they cannot comprehensively consider all the factors such as gastric emptying and small intestinal transit flow, which affect the rate and extent of drug absorption after oral administration.

Yu *et al.* (Yu *et al.* 1996a; 1996b; 1999) developed a compartmental absorption and transit model (CAT) for estimating the fraction dose absorbed based on permeability and solubility parameters. The CAT model describes the drugs transit through the stomach, duodenum, jejunum and ileum, and describes how the drugs are passively absorbed in the duodenum, jejunum, and ileum. According to the CAT model, the human small intestine can be divided into seven series of compartments where drugs transference from one compartment to the next is described by a first-order model (Yu *et al.* 1996b).

The CAT model makes four assumptions: 1. Absorption of drugs from the stomach and colon is negligible. 2. Passive diffusion based absorption across the intestinal membrane of orally administered drugs takes place in the small intestine. 3. Dissolution is instantaneous. 4. When a drug passes through a series of single compartments with linear transfer kinetics, each compartment may have different volumes and flow rates. However, the residence time of the drug in each compartment is the same (Yu *et al.* 1998).

The absorption in each compartment is given by the following equations:

A. Stomach

$$\frac{dM_s}{dt} = -K_s M_s \quad (1.5)$$

B. Small intestine

$$\frac{dM_n}{dt} = K_t M_{n-1} - K_t M_n \quad N=1, 2, \dots, 7. \quad (1.6)$$

C. Colon

$$\frac{dM_c}{dt} = K_t M_n \quad N=7 \quad (1.7)$$

D. The rate of drug absorption from the small intestine

$$\frac{dM_a}{dt} = K_a \sum_{n=1}^7 M_n \quad (1.8)$$

where  $M_s$ ,  $M_c$ ,  $M_n$  and  $M_a$  are the amounts of drug in the stomach, colon, compartments in small intestine and drug absorption from the small intestine;  $t$  is the time;  $K_s$ ,  $K_t$ , and  $K_a$  are the rate constants of gastric emptying, small intestinal transit, and intrinsic absorption, respectively. In Eq. 1.5.2.2, the  $K_s M_s$  replaces the  $K_t M_0$  ( $n=1$ ). From the mass balance, we can derive:

$$M_s + \sum_{n=1}^7 M_n + M_c + M_a = M_0 \quad (1.9)$$

when  $t \rightarrow \infty$ ,  $M_s$  and  $M_n$ 's approach zero, so

$$M_c + M_a = M_0 \quad (1.10)$$

The fraction dose absorbed  $F_a$  can be estimated as:

$$F_a = \frac{M_a}{M_0} = \frac{1}{M_0} \int_0^{\infty} K_a \sum_{n=1}^7 M_n dt \quad (1.11)$$

After combination with Eqs. 1.5.2.1 and 1.5.2.2, the equation of fraction of dose absorbed,  $F_a$ , can be derived as:

$$F_a = 1 - \left(1 + \frac{K_a}{K_t}\right)^{-7} \quad (1.12)$$

There are many limitations using the CAT model. Many factors influencing the oral absorption are not accounted for such as: the dissolution rate, the pH dependence of solubility, the absorption in the stomach or colon and metabolism (GastroPlus™ Manual, 2006). In order to simulate the physiological conditions including all the influencing

factors, an advanced compartmental absorption and transit model (ACAT) based on the original CAT model was developed by Simulation Plus Inc. The current ACAT model divides the small intestine into six compartments, in addition to the stomach, the caecum and the colon compartments. The transit time in each compartment is adapted according to the physiological conditions instead of the equal transit time, which enables to predict the rate and extent of drug absorption (Kuentz *et al.* 2006). The ACAT model tries to include all factors that influence the oral absorption based on the physiological environments. GastroPlus™ was used throughout this entire project.

## **1.6. *In Vitro* Assessment of Gastrointestinal Drug Absorption: Caco-2 Cell Line**

### **1.6.1. Drug Absorption**

Oral drug delivery is the most common route of administration. The extent of absorption of an orally administered drug is influenced by the physicochemical properties of the drug, its formulation and its physiological environment (Hidalgo, 2001; Hillgren *et al.* 1995). The physical and biochemical barriers of the intestinal mucosa strongly influence oral bioavailability such as tight junctions, cell membranes, membrane enzymes and transport mechanisms (Hidalgo, 2001).

There are several mechanisms of the drug transport across the GI membrane. As shown in Figure 1.4, these mechanisms include (Hidalgo, 2001; Löbenberg and Amidon, 2000a): 1) transcellular passive diffusion, 2) paracellular passive diffusion, 3) carrier-mediated transcellular diffusion, 4) vesicular transport. Most oral drugs are absorbed by passive diffusion (Hillgren *et al.* 1995). The paracellular passive diffusion transport is limited due to the tight junctions. Carrier-mediated transport is responsible for the absorption of specific drugs, nutrients and vitamins because many transporters are present in the small intestinal mucosa. Such active transport can substantially enhance the intestinal absorption. The other transporters such as P-glycoprotein and multidrug resistance proteins (MDRs) mediated efflux pumps are able to decrease the uptake of certain drugs by removing them from the cytoplasm by pumping them back into the intestinal lumen. An impact on drug bioavailability was demonstrated by orally co-administering the inhibitors or inducers of such proteins. Leahey *et al.* (1978) reported

that the bioavailability of digoxin (P-glycoprotein substrate) was increased 2-fold when quinidine, a known inhibitor of P-glycoprotein was co-administered. For another example, the bioavailability of talinolol decreased from 55% to 36% when rifampin was orally co-administered due to the induction of P-glycoprotein (Westphal *et al.* 2000).

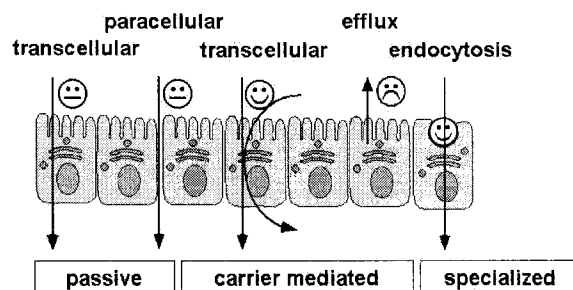


**Figure 1.4.** Pathways of drug absorption (Modified from Löbenberg and Amidon, 2000a)

### 1.6.2. *In Vitro* Models for Studying Drug Absorption

One of the challenges facing the pharmaceutical industry is the development of *in vitro* models that can mimic the absorption process in the intestinal mucus. Suitable *in vitro* models can be used not only to predict intestinal drug absorption but also to understand the absorption mechanisms. It is difficult to develop *in vitro* models that can simulate *in vivo* all physiological characteristics of the intestinal mucosa. Nevertheless a number of *in vitro* models have been developed to provide relatively accurate mimicking of the intestinal mucosa, such as excised gut tissues, isolated enterocytes and membrane vesicles (Hidalgo, 2001; Hillgren *et al.* 1995). The use of everted sacs and intestinal rings can preserve the architectural integrity and determine the absorption across different gastrointestinal segments (Hidalgo, 2001). There are different limitations for each model, the limited viability of these models is one of the common disadvantages. For the intestinal mucosa (stripped or unstripped) mounted into an Ussing chamber (Hidalgo, 2001; Hillgren *et al.* 1995), the complexity of the experimental procedure and

the amount of compound needed in these studies limits the application of this model to the study of the transport mechanisms. Damage of the enterocytes at the edge may lead to falsely high fluxes of the test compounds due to the mounting of the tissue into the Ussing chamber. Isolated brush border membrane vesicles or basolateral membrane vesicles have the limitation not to give any insight of the paracellular transport mechanism because this method studies the uptake of the test compounds into vesicles only. That mimics the transport across cell membranes.

The development of an alternative to tissue models to study *in vitro* intestinal drug absorption was desirable. Cell culture models were investigated. A monolayer of enterocytes has the potential to be the ideal system for studying drug transport across intestinal epithelia (Hidalgo, 2001; Hillgren *et al.* 1995). Isolated enterocytes derived from different disease states can also be used to study the change of uptake induced by disease. The lack of viability and an inability to form a monolayer limits the application of this approach. However such a model might be a suitable tool to study drug uptake in more detail including transepithelial transport or transport polarity. The first alternative such as human adenocarcinoma cell lines that display a number of characteristics of differentiated intestinal epithelial cells (Wilson *et al.* 1990) were developed and became available. There are several cultured cell lines that have been reported such as Caco-2, HT-29, T84, MDCK (Huet *et al.* 1987; Irvine *et al.* 1999; Pinto *et al.* 1983; Zweibaum *et al.* 1985). Caco-2 cells are human colon adenocarcinoma cell lines that differentiate spontaneously under normal culture conditions. They can be used to mimic the intestinal mucosa and to measure drug absorption *in vitro* (Burton *et al.* 1990). HT-29 cells are human colon cancer cells and do not differentiate spontaneously. However, HT-29 can be induced to form enterocyte-like cells that secrete mucus (Huet *et al.* 1987; Pinto *et al.* 1983) and therefore, offer a unique cell culture model for the study of the effect of mucin on drug transport (Hidalgo, 2001; Hillgren *et al.* 1995). T84 cells can differentiate spontaneously in cell culture. Their brush border is not well developed and they do not express microvillous membranes (Meunier *et al.* 1995). Although T84 cells can be used to mimic colonic crypt cells and their morphology, tight junctions and ion transport characteristics (Meunier *et al.* 1995), it is in most cases not a useful model for drug transport. Madin-Darby Canine Kidney (MDCK) cells can be the alternative to Caco-2

cells for the permeability study due to their shorter culture time (Hidalgo, 2001). MDCK cells can differentiate into columnar epithelium and to develop tight junctions (Hidalgo, 2001; Irvine *et al.* 1999). The transepithelial electrical resistance (TEER) values of MDCK monolayer reflect the *in vivo* human TEER values more accurately compared to the Caco-2 model (Hidalgo, 2001).

### 1.6.3. Caco-2 Cell Lines

The Caco-2 cell monolayer model is widely applied and almost universally accepted by pharmaceutical companies and by regulatory agencies as a standard permeability screening model (Shah *et al.* 2006). It has been used since 1989 as an intestinal permeability model (Hidalgo and Borchardt, 1989a). Caco-2 cells spontaneously differentiate on semi-permeable filters (Figure 1.5) to form cell monolayers that are similar to normal intestinal epithelium (Artursson, 1990; Hidalgo *et al.* 1989b; Hilgers *et al.* 1990). The resulting cell monolayers show the features of the intestinal epithelium such as morphology (tight junctions and microvilli) and brush border enzymes (aminopeptidases, esterases, sulfatase and cytochrome P450 enzymes) and transporters (bile acid carrier, large neutral amino acid carrier, PEPT1 carrier and P-glycoprotein) (Hidalgo, 2001; Shah *et al.* 2006). The goal of most *in vitro* Caco-2 experiments is to investigate the relationship between the permeability coefficient of a drug and the extent of its absorption in human intestine. The permeability obtained from the Caco-2 model correlates well with *in vivo* human permeability of many orally administered drugs (Artursson and Karlsson, 1991; Artursson *et al.* 2001; Yamashita *et al.* 2000).

The Caco-2 model can be used to investigate the drug transport via different pathways across the intestinal epithelium. However, the permeability of the paracellular drug transport is 20 to 80-fold lower compared to the human jejunum (Artursson *et al.* 2001). This is due to the difference in the paracellular pathway and the absorptive surface area between Caco-2 monolayers and the human jejunum (Shah *et al.* 2006). The TEER value of Caco-2 monolayers is much higher compared to the human jejunum (Hilgendorf *et al.* 2000). To improve the correlation of the drug transport via paracellular pathways with *in vivo* absorption, several alternative cell models have been developed, such as MDCK or

Caco-2 co-cultured with HT29-MTX. The TEER values of these models are much closer to the small intestine than the Caco-2 model (Hidaglo, 2001). But a further validation of the modified models has to be performed. For the carrier-mediated transport drugs in the Caco-2 model, the permeability of the test drugs is significantly lower compared to the *in vivo* absorption (Hu and Borchardt, 1990; Lennernas *et al.* 1996). Therefore, the Caco-2 model can under- (peptide transporters, etc.) and over- (P-glycoprotein) express the transporters and might lead to a false estimation of the *in vivo* expected absorption (Bohets *et al.* 2001). Overall, the Caco-2 model is a relatively universal *in vitro* model to predict *in vivo* drug absorption. However, a large interlaboratory variability of the permeability measurements has been reported (Artursson and Borchardt, 1997; Shah *et al.* 2006). The permeability of the drug substances obtained from Caco-2 monolayers was correlated with *in vivo* bioavailability data (Fagerholm *et al.* 1996; Rubas *et al.* 1996). The correlation data showed that the same  $P_{app}$  for the same drug could not be obtained between two laboratories. This may be due to the tendency of Caco-2 to alter its phenotype in accordance with the subculture, study conditions and data analysis. It seems that the absolute permeability value is not as important as a comparison with the ranking in order of the permeability values by an individual laboratory as long as in-house reproducibility is achieved.

For many orally administered drugs, the dissolution rate is the limiting factor to the oral absorption. The bridge between *in vitro* dissolution and permeability measurements that allows the prediction of the oral absorption is highly desirable. Ginski and Polli (1999) and Kobayashi *et al.* (2001) reported the development of the dissolution/Caco-2 system. The test drugs were dissolved in dissolution vessels and then the resulting solutions were transferred to the Caco-2 monolayer. The results successfully predicted the oral absorption of the piroxicam, such as  $C_{max}$  and AUC (Ginski and Polli, 1999) and ten other water-soluble drugs (Kobayashi *et al.* 2001). However, more investigation is necessary for the optimization of this system and a universal system is needed that is capable of high throughput.



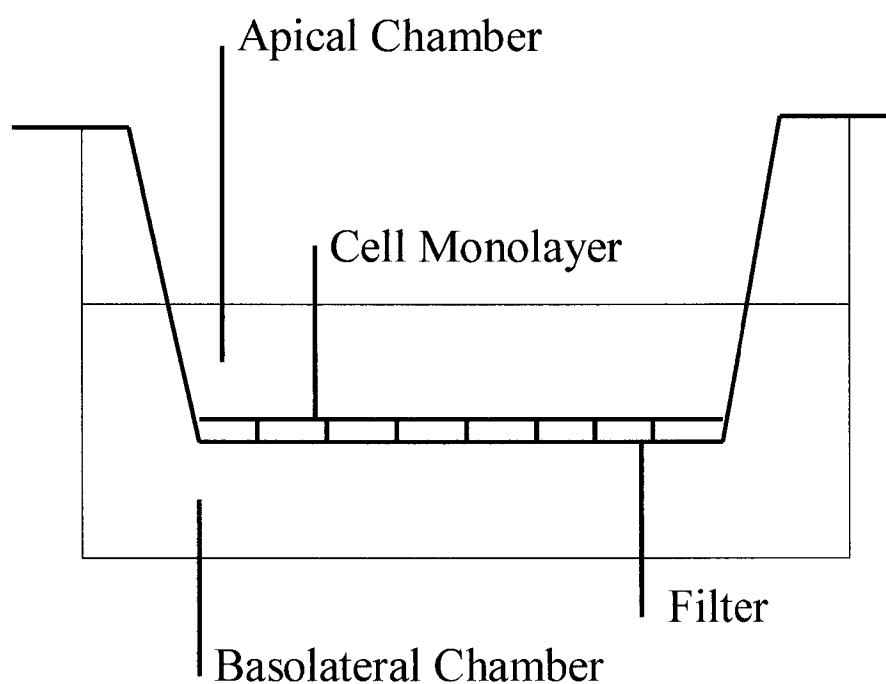


**Fig. 1.5.** Caco-2 model system

### 1.7. Summary of Glyburide Studies

Glyburide (1-[[p-[2-(5-chloro-o-anisamido)-ethyl]phenyl]-sulfo-nyl]-3-cyclohexylurea; also known as glibenclamide, Fig. 1.6) is a second-generation sulfonylurea. It is orally used as a hypoglycemic agent to treat non-insulin dependent (type II) diabetes mellitus (Neuvonen and Kivisto, 1991; Pearson, 1985). Glyburide can stimulate the pancreatic insulin secretion from beta cells of the pancreas after being orally administered (Feldman, 1985; USP 29, 2006). It is a weak acid substance ( $pK_a$  5.3) (The merck index, 1989). The solubility (Wei and Löbenberg, 2006) and the bioavailability studies (USP 29, 2006) indicated that glyburide could be classified as a Class II drugs based on BCS. It has low solubility and high permeability (Wei and Löbenberg, 2006). Glyburide should be administered before a meal based on the therapeutic recommendation (Euglucon N. Rote Liste, 2005; Otoom *et al.* 2001).

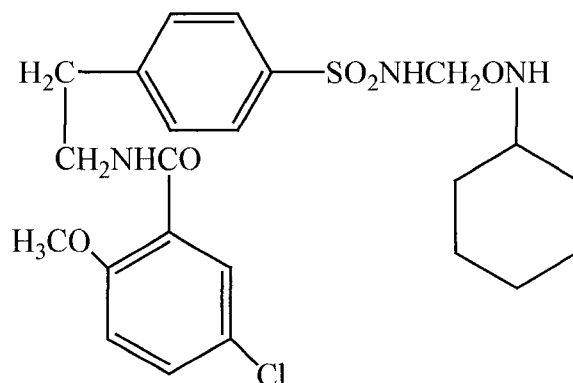


**Figure 1.6.** Chemical structure of glyburide ( $C_{23}H_{30}ClN_3O_5S$ , MW: 494 g/mol)

Glyburide is absorbed throughout the entire gastrointestinal tract. (Brockmeier *et al.* 1985; Neugebauer *et al.* 1985). The biopharmaceutical quality of different glyburide products was investigated by a multinational postmarketing comparative study (Blume *et al.* 1993). The study showed that the products, even for the same brand name products in different countries had remarkable differences in the *in vitro* dissolution behaviors, that resulted in therapeutic differences in bioavailability (Blume *et al.* 1993). The conventional single dose of glyburide is 5 mg per tablet (Shaheen *et al.* 1987). Ganley *et al.* (1984) utilized a water-soluble carrier (polyoxyethylene) to enhance the dissolution of glyburide. A lower dose (3.5 mg) formulation was developed that was bioequivalent to the formulation of 5 mg dose (Shaheen *et al.* 1987). The micronization of the glyburide powder leads to a lower dose of glyburide that has the same therapeutic effect as the conventionally non-micronized powder (5 mg dose) (Shaheen *et al.* 1987). A single dose of glyburide is from 1.5 to 5 mg depending on whether it is micronized or nonmicronized (USP 29, 2006). The protein binding and bioavailability of glyburide is up to 100% and there is no significant first pass metabolism (Pearson, 1985; USP 29, 2006). The nonmicronized and micronized glyburides reach the  $C_{max}$  within 4 and 2-3 hours, respectively. Two primary inactive metabolites are hydroxylated from glyburide to form

4-*trans*-hydroxyglyburide and 3-*cis*-hydroxyglyburide by hepatic oxidative pathways involving the P-450 system (Rydberg *et al.* 1995). The resulting metabolites are excreted in urine (50%) and in feces (50%) via bile.

The material characterizations of solid state forms of glyburide used in this dissertation involve the use of Scanning Electron Microscopy (SEM), X-ray powder diffraction (XRPD), Thermogravimetric analysis (TGA), Differential scanning calorimetry (DSC), Raman spectroscopy, Infrared spectroscopy (IR), Nuclear magnetic resonance (NMR), Isothermal titration calorimetry (ITC), particle size analysis and specific surface area measurement.

SEM can be used to visualize the morphology and particle size and size distribution of APIs (Panagopoulou-Kaplani *et al.* 2000). XRPD can probe the crystalline structure because X-ray wavelengths have the same magnitude as the distance between the atoms or molecules of the crystal forms (Martin, 1993). The spectrum is obtained when X-rays pass through the crystalline form as a ruled grating. TGA shows the weight changes of the APIs with changes in temperature (Martin, 1993). DSC can detect the energy transfer (heat) at the melting point of the APIs when compared to a reference. Raman spectroscopy and IR are complementary techniques of structure investigation and have different detection rules (Anderson, 2000). Both of them measure the vibrational energies of molecules (Anderson, 2000). An IR signal signifies a change in dipole movement of the molecule and is the asymmetric stretch. Raman spectroscopy is used to detect the Raman effect, which is the change in polarizability of the molecule and is symmetric stretch. The above techniques can be used to detect or identify the solid state structure or character of the APIs such as polymorphism and amorphous forms. The amorphous forms or polymorphic APIs can be detected within the detection limits of the methods (Salekigerhardt *et al.* 1994). Material characterization of a drug substances is one of the essential steps for the preformulation. The obtained information can be used to assure a constant performance of a product.

## 1.8. Hypothesis and Objectives

### Hypothesis:

Biorelevant dissolution methods and permeability measurement combined with computer simulations are able to predict the oral absorption characteristics of Class II drugs

### Objectives

- To determine the permeability of the selected drugs in the Caco-2 model using BDMs and Hank's solution as transport media
- To investigate the physicochemical properties of the different batches of glyburide powders using material characterization methods
- To investigate the influence of the chemical grades of the bile salts and lecithin used in the BDMs on the solubility and to compare with using USP dissolution media
- To develop a biorelevant dissolution method, which can mimic the physiological environment in the GI tract
- To study the *in vitro* dissolution behaviors of the glyburide tablets using BDMs and USP dissolution media
- To predict the oral absorption of the glyburide formulations using the *in vitro* data as input function into the ACAT model

## 1.9. Format of the Dissertation

The dissertation is the mixed format according to the thesis handbook. Chapter 1 is the general background and methods covering the whole dissertation. Chapter 2 (submitted to Journal of Pharmacy & Pharmaceutical Sciences, 2006), 3 (submitted to Pharmaceutical Research, 2006), 4 (European Journal of Pharmaceutics Sciences, 19, 45-52, 2006) and 5 (submitted to Molecular Pharmaceutics, 2006) are the publications that have been published or submitted. Chapters 6, Appendix A, Appendix B and Appendix C contain the unpublished research that is important to the whole dissertation. Chapter 7 is the

general discussion, conclusions and proposed future research related to the field of this dissertation.

### 1.10. References

Abelson, P. H. Improvements in health care. *Science*. 260, 11, 1993.

Adams, C. P. and Brantner, V.V. Estimating the cost of new drug development: is it really 802 million dollars? *Health Aff. (Millwood)*. 25 (2), 420-428, 2006.

Amidon, G. L., Lennernas, H., Shah, V. P. and Crison, C. R. A theoretical basis for a biopharmaceutic drug classification: the correlation of *in vitro* drug product dissolution and *in vivo* bioavailability. *Pharm. Res.* 12, 413-20, 1995.

Amidon, G. L., Choe S. Y., Vieira, M. and Oh, D. M. Solubility, intrinsic dissolution and solubilization: influence on absorption, in: G.L. Amidon, G. L., Robinson, J. R. and Williams, R. L. (Eds.), Scientific Foundations for regulating Drug Product Quality, *AAPS Press, Alexandria*, 99-113, 1997.

Agoram, B., Walter, S. and Bolger, B. M. Predicting the impact of physiological and biochemical processes on oral drug bioavailability. *Adv. Drug. Del. Rev.* 50, S41-S67, 2001.

Anderson, L. G. Raman spectroscopy.  
<http://carbon.cudenver.edu/public/chemistry/classes/chem4538/raman.htm>. 2000.

Artursson, P. Epithelial transport of drugs in cell culture. I: A model for studying the passive diffusion of drugs over intestinal absorptive (Caco-2) cells. *J. Pharm. Sci.* 79 (6), 476-482, 1990.

Artursson, P. and Karlsson, J. Correlation between oral drug absorption in and apparent drug permeability coefficients in human intestinal epithelial Caco-2 cells. *Biochem Biophys. Res. Commun.* 175, 880-885, 1991.

Artursson, P. and Borchardt, R. T. Intestinal drug absorption and metabolism in cell cultures: Caco-2 and beyond. *Pharm. Res.* 14 (12), 1655-1658, 1997.

Artursson, P., Palm, K. and Luthman, K. Caco-2 monolayers in experimental and theoretical predictions of drug transport. *Adv. Drug Deliv. Rev.* 46 (1-3), 27-43, 2001.

Athanassiou, G. C., Rekkas, D. M. and Choulis N. H. Correlation of in vitro dissolution data with in vivo plasma concentrations, for three, orally administered, formulations of sulphamethoxazole-trimethoprim, by statistical moments analysis. *Int. J. Pharm.* 90, 51-58, 1993.

Bakatselou, V., Oppenheim, R. C. and Dressman, J. B. Solubilization and wetting effects of bile salts on the dissolution of steroids. *Pharm. Res.* 8, 1461-1469, 1991.

Balan, G., Timmins, P., Greene, D. S. and Marathe, P. H. In-vitro In-vivo correlation models for glibenclamide after administration of metformin/glibenclamide tablets to healthy human volunteers. *J. Pharm. Pharmacol.* 52, 831-838, 2000.

Beary, J. F., Eaton, C. R. and Wierenga D. E. Basic research and the cost of health care. *Science.* 262, 1358, 1993.

Borst, I., Ugwu, S. and Beckett, A. H. New and extended application for USP drug release apparatus 3. *Dissolut. Technol.* 1-6, 1997.

Blume, H., Ali, S. L. and Siewert, M. Pharmaceutical quality of glibenclamide products: a multinational postmarket comparative study. *Drug. Dev. Ind. Pharm.* 19, 2713-2741, 1993.

Blume, H. H. and Schug, B. S. The biopharmaceutics classification system (BCS): Class III drugs-better candidates for BA/BE waiver? *Eur. J. Pharm. Sci.* 9, 117-121, 1999.

Brockmeier, D., Grigoleit, H. G. and Leonhardt, H. Absorption of glibenclamide from different sites of the gastro-intestinal tract. *Eur. J. Clin. Pharmaco.* 29 (2), 193-197, 1985.

Burton, P. S., Conradi, R. A. and Hilgers, A. R. Caco-2 cell monolayers as a model for drug transport cross the intestinal mucus. *Pharm. Res.* 7, 902-910, 1990.

Charman, W. N., Porter, C. J. H., Mithani, S. D. and Dressman J. B. Physiochemical and physiological mechanisms for the effects of food on drug absorption: the role of lipids and pH. *J. Pharm. Sci.* 86, 268-282, 1997.

Cheng, C. L., Yu, L. X., Lee, H. L., Yang, C. Y., Lue, C. S. and Chou, C. H. Biowaiver extension potential to BCS Class III high solubility-low permeability drugs: bridging evidence for metformin immediate-release tablet. *Eur. J. Pharm. Sci.* 22, 297-304, 2004.

Cheo, S. Y. and Amidon, G. L. Modern biopharmaceutics (CD). 2000.

Costa, P. and Lobo, J. M. S. Modeling and comparison of dissolution profiles. *Eur. J. Pharm. Sci.* 13, 123-133, 2001.

Cuttler, D. J., Beyssac, E. and Aiache, J. M. Level B and C in vivo/in vitro correlations: statistical considerations. *Int. J. Pharm.* 158, 185-193, 1997.

DiMasi, J. A., Hansen, R. W. and Grabowski, H. G. The price of innovation: new estimates of drug development costs. *J. Health Econ.* 22 (2), 151-185, 2003.

Dressman, J. B., Amidon, G. L., Reppas, C. and Shan, V. P. Dissolution testing as a prognostic tool for oral drug absorption: immediate release dosage forms. *Pharm. Res.* 15 (1), 11-21, 1998.

Dutta, S., Qiu, Y., Samara, E., Cao, G. and Granneman, G. R. Once-a-day extended-release dosage form of divalproex sodium III: development and validation of a level A in vitro-in vivo correlation (IVIVC). *J. Pharm. Sci.* 94 (9), 1949-1956, 2005.

Efentakis, M. and Dressman, J. B. Gastric juice as a dissolution medium: surface tension and pH. *Eur. J. Drug Metabol. Pharmacokinet.* 23, 97-102, 1998.

El-Massik, M. A., Darwish, I. A., Hassan, E. E. and El-Khordagui, L. K. Development of a dissolution medium for glibenclamide. *Int. J. Pharm.* 140, 69-76, 1996.

Emami, J. In vitro-in vivo correlation: from theory to applications. *J. Pharm. Pharm. Sci.* 9 (2), 169-189, 2006.

Euglucon N. Rote Liste. BPI. Frankfurt/Main, 2005

Fagerholm, U., Johansson, M. and Lennernas, H. Comparison between permeability coefficients in rat and human jejunum. *Pharm. Res.* 13, 1336-1342, 1996.

Feldman, J. M. Glyburide: a second-generation sulfonyurea hypoglycemic agent. *Pharmacotherapy.* 5, 43-62, 1985.

FDA, Guidance for industry: Dissolution testing of immediate release solid oral dosage forms. U.S. Department of Health, Food and Drug Administration, Center for Drug Evaluation and Research (CDER) BP, August, 1997.

FDA, Guidance for industry: SUPAC-MR: modified release oral dosage forms; scale up and postapproval changes: chemistry, manufacturing, and controls; *in vitro* dissolution testing and *in vivo* bioequivalence documentation. U.S. Department of Health, Food and Drug Administration, Center for Drug Evaluation and Research (CDER) BP, September, 1997.

FDA, Guidance for industry, Waiver of *in vivo* bioavailability and bioequivalence studies for immediate release solid oral dosage forms based on a biopharmaceutics classification system. CDER. August 2000.

FDA, Guidance for industry: Bioavailability and bioequivalence studies for orally administered drug products- general considerations. U.S. Department of Health, Food and Drug Administration, Center for Drug Evaluation and Research (CDER) BP, March 2003.

Galia, E., Nicolaidis, E., Horter, D., Löbenberg, R., Dressman, J. B. and Reppas, C. Evaluation of various dissolution media for predicting *in vivo* performance of class I and class II drugs. *Pharm. Res.* 15, 698-705, 1998.

Ganley, J. A., McEwen, J., Colvert, R. T. and Barker, C. J. The effect of *in vivo* dispersion and gastric emptying on glibenclamide absorption from a novel, rapidly dissolving capsule formulation. *J. Pharm. Pharmacol.* 36, 734-739, 1984.

GastroPlus Manual, version 5.1. Simulation Plus Inc. Lancaster. USA. 2006.



Ginski, M. J. and Polli, J. E. Prediction of dissolution-absorption relationships from a dissolution/Caco-2 system. *Int. J. Pharm.* 177, 117-125, 1999.

Grass, M. G. and Sinko, P. J. Physiologically-based pharmacokinetic simulation modeling. *Adv. Drug. Del. Rev.* 54, 433-451, 2002.

Grundy, J. S., Anderson, K. E., Rogers, J. A. and Foster, R. T. Studies on dissolution testing of the nifedipine gastrointestinal therapeutic system. I. Description of a two-phase in vitro dissolution test. *J. Controlled Release.* 48, 1-8, 1997a.

Grundy, J. S., Anderson, K. E., Rogers, J. A. and Foster, R. T. Studies on dissolution testing of the nifedipine gastrointestinal therapeutic system. II. Improved in vitro-in vivo correlation using a two-phase dissolution test. *J. Controlled Release.* 48, 9-17, 1997b.

Hendrix, T. R., Castell, D. O. and Wood, J. D. Alimentary tract motility: Stomach, small intestine, colon and biliary tract, Unit 10B in: undergraduate teaching series (American Gastroenterological Association), Milner-Fenwick Inc., Maryland, USA, 1987.

Hidalgo, I. J. and Borchardt, R. T. Transport of bile acids in a human intestinal epithelial cell line, Caco-2. *Biochim. Biophys. Acta*, 1035, 97-103, 1989a.

Hidalgo, I. J., Raub, T. J. and Borchardt, R. T. Characterization of the human colon carcinoma cell line Caco-2 as a model system for intestinal epithelial permeability. *Gastroenterology.* 96 (3), 736-749, 1989b.

Hidalgo, I. J. Assessing the absorption of new pharmaceuticals. *Curr. Top. Med. Chem.* 1, 385-401, 2001.

Hilgendorf, C., Spahn-Langguth, H., Regardh, C. G., Lipka, E., Amidon, G. L. and Langguth, P. Caco-2 versus Caco-2/HT29-MTX co-cultured cell lines: permeabilities via diffusion, inside- and outside-directed carrier-mediated transport. *J. Pharm. Sci.* 89 (1), 63-75, 2000.

Hilgers, A. R., Conradi, R. A. and Burton, P. S. Caco-2 cell monolayers as a model for drug transport across the intestinal mucosa. *Pharm. Res.* 7 (9), 902-910, 1990.

Hillgren, K. M., Kato, A. and Borchardt, R. T. In vitro systems for studying intestinal drug absorption. *Med. Res. Rev.* 15 (2), 83-109, 1995.

Ho, N. F. H., Park, J. Y., No, P. F. and Higuchi, W. I. Advanced quantitative and mechanistic approaches in interfacing gastrointestinal drug absorption studies in animals and humans. In: Crouthanel, W. and Sarapu, A. C. (Eds.), *Animal Models for Oral Drug Delivery in Man: In situ and in vivo approaches.* American Pharmaceutical Association, Washington, DC, 27-106, 1983.

Hu, M. and Borchardt, R. T. Mechanism of L- $\alpha$ -methyldopa transport through a monolayer of polarized human intestinal epithelial cells (Caco-2). *Pharm. Res.* 7 (12), 1313-1319, 1990.

Huet, C., Sahuquillo-Merino, C., Coudrier, E. and Louvard, D. Absorptive and mucus-secreting subclones isolated from a multipotent intestinal cell line (HT-29) provide new models for cell polarity and terminal differentiation. *J. Cell Biol.* 105, 345-357, 1987.

Irvine, J. D., Takahashi, L., Lockhart, K., Cheong, J. and Tolan J. W. MDCK (Madin-Darby Canine Kidney) cells: a tool for membrane permeability screening. *J. Pharm. Sci.* 88 (1), 28-33, 1999.

Jinno, J., Oh, D. M., Crison, J. R. and Amidon, G. L. Dissolution of ionizable water-insoluble drugs: the combined effect of pH and surfactant, *J. Pharm. Sci.* 89 (2), 268-274, 2000.

Johnson, B. F., Greer, H., McCreie, J., Bye, C. and Fowle, A. Rate of dissolution of digoxin tablets as a predictor of absorption. *Lancet.* 1 (7818), 1473-1474, 1973.

Kalantzi, L., Reppas, C., Dressman, J. B., Amidon, G. L., Junginger, H. E., Midha, K. K., Shah, V. P., Stavchansky, S. A. and Barends, D. M. Commentary: biowaiver monographs for immediate release solid oral dosage forms: acetaminophen (paracetamol). *J. Pharm. Sci.* 95 (1), 4-14, 2006.

Kaukonen, A. M., Boyd, B. J., Porter, C. J. H. and Charman, W. N. Drug solubilization behavior during in vitro digestion of simple triglyceride lipid solution formulations. *Pharm. Res.* 21 (2), 245-253, 2004.

Kayali, A. Bioequivalency evaluation by comparison of *in vitro* dissolution and *in vivo* absorption using reference equations, *Eur. J. Drug. Metabol. Pharmacokinet.* 3, 271-277, 1994.

Kobayashi, M., Sada, N., Sugawara, M., Iseki, K. and Miyazaki, K. Development of a new system for prediction of drug absorption that takes into account drug dissolution and pH change in the gastro-intestinal tract. *Int. J. Pharm.* 221, 87-94, 2001.

Kuentz, M., Nick, S., Parrot, N. and Röthlisberger, D. A strategy for preclinical formulation development using GastroPlus™ as pharmacokinetic simulation tool and a statistical screening design applied to a dog study. *Eur. J. Pharm. Sci.* 27, 91-99, 2006.

Langguth, P., Lee, K. M., Spahn-Lannguth, H. and Amidon, G. L. Variable gastric emptying and discontinuities in drug absorption profiles: dependence of rates and extent of cimetidine absorption on motility phase and pH. *Biopharm. Drug. Dispos.* 15, 719-746, 1994.

Leahey, E. B. Jr., Reiffel, J. A., Drusin, R. E., Heissenbuttel, R. H., Lovejoy, W. P. and Bigger, J. T. Jr. Interaction between quinidine and digoxin. *JAMA.* 240, 533-534, 1978.

Leng, J., Egelhaaf, S. U. and Cates, M. E. Kinetics of the micelle-to-vesicle transition: aqueous lecithin-bile salt mixtures. *Biophysical J.* 85, 1624-1646, 2003.

Lennernas, H., Palm, K., Fagerholm, U. and Autursson, P. Comparison between active and passive drug transport in human intestinal epithelial (Caco-2) cells: *in vitro* and human jejunum *in vivo*. *Int. J. Pharm.* 127 (1), 103-107, 1996.

Levy, G., Leonards, J. R. and Procknal, J. A. Development of *in vitro* dissolution tests which correlate quantitatively with dissolution rate-limited drug absorption in man. *J. Pharm. Sci.* 54, 1719-1722, 1965.

Lindenbaum, J., Buttler, V. P., Morphy, J. E. and Cresswell, R. M. Correlation of digoxin tablet dissolution-rate with biological availability. *Lancet.* 1, 1215-1217, 1973.

Lindenberg, M., Kopp, S. and Dressman, J. B. Classification of orally administered drugs on the world health organization model list of essential medicines according to the biopharmaceutics classification system. *Eur. J. Pharm. Biopharm.* 8, 265-278, 2004.

Lipka, E., Lee, I. D., Langguth, P., Spahn-Langguth, H., Mutschler, E. and Amidon, G. L. Celiprolol double-peak occurrence and gastric motility: non-linear mixed effects modeling of bioavailability data obtained in dogs. *J. Pharmacokinet. Biopharmacokinet.* 23, 267-286, 1995.

Löbenberg, R. and Amidon, G. L. Modern bioavailability, bioequivalence and biopharmaceutics classification system. New scientific approaches to international regulatory standards. *Eur. J. Pharm. Biopharm.* 50, 3-12, 2000a.

Löbenberg, R., Kramer, J., Shah, V. P., Amidon, G. L. and Dressnan, J. B. Dissolution testing as prognostic tool for oral drug absorption: Dissolution behavior of glibenclamide. *Pharm. Res.* 17 (4), 439-444, 2000b.

Magee, G. A., French, J., Gibbon, B. and Luscombe, C. Bile salt/lecithin mixed micelles optimized for the solubilization of a poorly soluble steroid molecule using statistical experimental design. *Drug Dev. Indus. Pharm.* 29 (4), 441-450, 2003.

Martin A. Physical pharmacy. 4<sup>th</sup> edition, Williams & Wilkins, Baltimore, Maryland, USA, 1993.

Meunier, V., Bourrie, M., Berger, Y. and Fabre, G. The human intestinal epithelial cell line Caco-2; pharmacological and pharmacokinetic applications. *Cell Bio. Toxi.* 11, 187-194, 1995.

Mithani, S. D., Bakatselou, V., TenHoor, C. N. and Dressman, J. B. Estimation of the increase in solubility of drugs as a function of bile salt concentration. *Pharm. Res.* 13, 163-167, 1996.

Neugebauer, G., Betzien, G., Hrstka, V., Kaufmann, B., Möllendorff, V. E. and Abshagen, U. Absolute bioavailability and bioequivalence of glibenclimide (Semi-Euglucon<sup>®</sup>N). *Int. J. Clin. Pharmacol. Therapy and Toxicology.* 23 (9), 453-460, 1985.

Neuvonen, P. J. and Kivisto, K. T. The effects of magnesium hydroxide on the absorption and efficacy of two glibenclamide preparations. *Br. J. Clin. Pharmac.* 32, 215-220, 1991.

- Norris, D.A., Leesman, G. D., Sinko, P. J. and Grass, G. M. Development of predictive pharmacokinetic simulation models for drug discovery. *J. Control. Release.* 65, 55-62, 2000.
- Oh, D. M., Curl, R. L. and Amidon, G. L. Estimating the fraction dose absorbed from suspensions of poorly soluble compounds in humans: a mathematical model. *Pharm. Res.* 10,264–270, 1993.
- Otoom, S., Hasan, M. and Najib, N. The bioavailability of glyburide (glibenclamide) under fasting and feeding conditions: a comparative study. *Int. J. Pharm. Med.* 15, 117-120, 2001.
- Panagopoulou-Kaplani, A. and Malamataris, S. Preparation and characterization of a new insoluble polymorphic form of glibenclamide. *Int. J. Pharm.* 195, 239-246, 2000.
- Parrott, N. and Lavé, T. Predicting of intestinal absorption: comparative assessment of GASTROPLUS™ and IDEA™. *Eur. J. Pharm. Sci.* 17, 51-61, 2002.
- Pearson, J. G. Pharmacokinetics of glyburide. *Am. J. Med.* 79 (suppl. 3B), 67-71, 1985.
- Perng, C.Y., Kearney, A. S., Palepu, N. R., Smith, B. R. and Azzarano, L. M. Assessment of oral bioavailability enhancing approaches for SB-247083 using flow-through cell dissolution testing as one of the screens. *Int. J. Pharm.* 250, 147-156, 2003.
- PhRMA. Why do drugs cost so much: PhRMA, Washington DC, 1-22, 2000.
- Pinto, M., Robin-Leon, S. and Appay, M. D. Enterocyte-like differentiation and polarization of the human colon carcinoma cell line Caco-2 in culture. *Bio. Cell.* 47, 323-330, 1983.
- Potthast, H., Dressman, J. B., Junginger, H. E., Midha, K. K., Oeser, H., Shah, V. P., Vogelpoel, H. and Barends, D. M. Commentary: biowaiver monographs for immediate release solid oral dosage forms: ibuprofen. *J. Pharm. Sci.* 94 (10), 2121-2131, 2005.

Qureshi, S. A., Caille, G., Brien, R., Piccirilli, G., Yu, V. and McGilveray, I. J. Application of flow-through dissolution method for the evaluation of oral formulations of nifedipine. *Drug Dev. Ind. Pharm.* 20, 1869-1882, 1994.

Rubas, W., Cromwell, M. E., Shahrokh, Z., Vilagran, J., Nguyen, T. N., Wellton, M., Nguyen, T. H. and Mrshy, R. J. Flux measurements across Caco-2 monolayers may predict transport in human large intestinal tissue. *J. Pharm. Sci.* 85, 165-169, 1996.

Rydberg, T., Jönsson, A. and Melander, A. Comparison of the kinetics of glyburide and its active metabolites in humans. *J. Clin. Pharm. Thera.* 20, 283-295, 1995.

Salekigerhardt, A., Ahlneck, C. and Zografi, G. Assessment of disorder in crystalline solids. *Int. J. Pharm.* 101 (3), 237-247, 1994.

Shah, P., Jogani, V., Bagchi, T. and Misra, A. Role of Caco-2 cell monolayers in prediction of intestinal drug absorption. *Biotechnol. Prog.* 22, 186-198, 2006.

Shaheen, O., Othman, S., Jalal, I., Awidi, A. and Al-Turk, W. Comparison of pharmacokinetics and pharmacodynamics of a conventional and a new rapidly dissolving glibenclamide preparation. *Int. J. Pharm.* 38, 123-131, 1987.

Shargel, L. and Yu, A. B. C. Applied biopharmaceutics and pharmacokinetics. 4 edition. McGraw-Hill/Appleton & Lange. 1999

Sinko, P. J., Leesman, G. D. and Amidon, G. L. Predicting fraction dose absorbed in humans using a macroscopic mass balance approach. *Pharm. Res.* 8, 979-988, 1991.

Sunesen, V. H., Pedersen, B. L., Kristensen, H. G. and Müllertz, A. In vivo in vitro correlations for a poorly soluble drug, danazol, using the flow-through dissolution method with biorelevant dissolution media. *Eur. J. Pharm. Sci.* 24, 305-313, 2005.

The Merck Index. 11<sup>th</sup> editon, Merck & Co., Inc, Rahway, New Jersey, USA, 1989.

Verbeeck, R. K., Junginger, H. E., Midha, K. K., Shah, V. P. and Barends, D. M. Commentary: biowaiver monographs for immediate release solid oral dosage forms based on biopharmaceutics classification system (BCS) literature data: chloroquine phosphate,

chloroquine sulfate, and chloroquine hydrochloride. *J. Pharm. Sci.* 94 (7), 1389-1395, 2005.

Uppoor, V. R. S. Regulatory perspectives on *in vitro* (dissolution)/*in vivo* (bioavailability) correlations. *J. Controlled Release.* 72, 127-132, 2001.

United States Pharmacopeia, USP 29, U. S. Pharmacopeial convention Inc. Rockville, 2006.

Wagner, J. G. and Nelson, E. Kinetic analysis of blood levels and urinary excretion in absorptive phase after single doses of drug. *J. Pharm. Sci.* 53 (11), 1392-1403, 1964.

Wagner, J. G., Christensen, M., Sakmar, E., Blair, D., Yates, J. D., Willis, P. W., Sedman, A. J. and Stoll, R. G. Equivalence lack in digoxin plasma levels. *JAMA.* 224 (2), 199-204, 1973.

Wei, H. and Löbenberg, R. Biorelevant dissolution media as a predictive tool for glyburide a class II drug. *Eur. J. Pharm. Sci.* 29, 45-52, 2006.

Westphal, K., Weinbrenner, A. and Zschiesche, M. Induction of P-glycoprotein by rifampin increases intestinal secretion of talinolol in human being: a new type of drug/drug interaction. *Clin Pharmacol Ther.* 68, 345-355, 2000.

Wilson, G. Cell culture techniques for the study of drug transport. *Eur. J. Drug. Metabol. Pharm.* 15, 159, 1990.

Yamashita, S., Furubayashi, T., Kataoka, M., Sakane, T., Sezaki, H. and Tokuda, H. Optimized conditions for prediction of intestinal drug permeability using Caco-2 cells. *Eur. J. Pharm. Sci.* 10 (3), 195-204, 2000.

Yazdaniyan, M., Briggs, K., Jankovsky, C. and Hawi, A. The “high solubility” definition of the current FDA guidance on biopharmaceutical classification system may be too strict for acidic drugs. *Pharm. Res.* 21 (2), 293-299, 2004.

Yokoe, J., Iwasaki, N., Haruta, S., Kadano, K., Ogawara, K., Higaki, K. and Kimura, T. Analysis and prediction of absorption behavior of colon-targeted prodrug in rats by GI-transit-absorption model. *J. Controlled. Release.* 86, 305-313, 2003.

Yu, L. X., Lipka, E., Crison, J. R. and Amidon, G. L. Transport approaches to the biopharmaceutical design of oral drug delivery systems: prediction of intestinal absorption. *Adv. Drug Del. Rev.* 19, 359-376, 1996a.

Yu, L. X., Crison, J. R. and Amidon, G. L. Compartmental transit and dispersion model analysis of small intestinal transit flow in humans. *Int. J. Pharm.* 140, 111-118 1996b.

Yu, L. X. and Amidon G. L. Characterization of small intestinal transit time distribution in humans. *Int. J. Pharm.* 171, 157-163, 1998.

Yu, L. X. and Amidon G. L. A Compartmental absorption and transit model for estimating oral drug absorption. *Int. J. Pharm.* 186, 119-125, 1999.

Yu, L. X., Amidon, G. L., Poli, J. E., Zhao, H., Mehta, M. U., Conner, D. P., Shah, V. P., Lesko, L. J., Chen, M. L., Lee, V. H. L. and Hussain, A. S. Biopharmaceutics classification system: the scientific basis for biowaiver extensions. *Pharm. Res.* 19 (7), 921-925, 2002a.

Yu, L. X., Wang, J. T. and Hussain, A. S. Evaluation of USP apparatus 3 for dissolution testing of immediate-release products. *AAPS PharmSci.* 4 (1), 1-5, 2002b.

Yu, Z., Hwang, S. S. and Gupta, S. K. DeMonS – A new deconvolution method for estimation drug absorbed at different time intervals and/or drug disposition model parameters using a monotonic cubic spine. *Biopharm. Drug Dispos.* 18 (6), 475-487, 1997.

Zenilman, M. E. Origin and control of gastrointestinal motility. *Sur. Clin. North Am.* 73 (6), 1081-1099, 1993.

Zweibaum, A., Pinto, M. and Chevalier, G. Enterocytic differentiation of a subpopulation of the human colon tumor cell line HT-29 selected for growth in sugar-free medium and its inhibition by glucose. *J. Cell Physiol.* 122, 21-29 1985.



## CHAPTER 2

### INVESTIGATION OF TRANSPORT MEDIA CONTAINING MICELLES FOR CELL CULTURE PERMEABILITY STUDIES OF POORLY SOLUBLE DRUGS: CASE STUDY GLYBURIDE

#### 2.1. Introduction

The prediction of the oral absorption of a drug is extremely important in the pharmaceutical industry at an early stage in the drug development process (Obata *et al.* 2004; Patel and Forbes, 2006). Although there are several different processes involved in oral drug absorption, solubility and permeability of a drug candidate are the two fundamental parameters that define oral absorption (Amidon *et al.* 1995). A mechanistic approach using these two fundamental parameters in oral drug absorption was developed by Amidon *et al.* (1995) and is known as the Biopharmaceutics Drug Classification System (BCS).

Solubility is one of the key variables in governing the rate and extent of oral drug absorption. In order to simulate the *in vivo* solubility of a drug in the intestinal fluids, the development of suitable media reflecting the physiological conditions is a critical issue, especially for the poorly soluble drugs. There are various media described in the national pharmacopoeias that are used for drug release testing. Most of them are either the plain buffers simulating the pH conditions in GI tract or the solutions containing the surfactant to increase the solubility of poorly soluble substances (Löbenberg and Amidon, 2000a). However, artificial media might not reflect the *in vivo* conditions truly. New biorelevant dissolution media (BDM) were developed and published in the 1995 FIP Dissolution Guidance: Fasted state simulated intestinal fluid (FaSSIF) and fed state simulated intestinal fluid (FeSSIF). They contain bile salts (sodium taurocholate) and lecithin to simulate the physiological environment in the GI tract (Dressman *et al.* 1998). *In vitro* dissolution tests using BDMs showed that BDMs were the better media choice to

simulate *in vivo* dissolution (Dressman and Reppas, 2000; Løbenberg *et al.* 2000b). However, the chemical grades of the bile salts and lecithin in BDMs have influence on the simulation of the physiological environments in the GI tract. Wei and Løbenberg (2006) and Vertzoni *et al.* (2004) reported that the BDMs consisting of low quality chemical grade (crude) bile salts and lecithin simulated the physiological environments much better compared to the BDMs consisting of high quality chemical grade (high purity) bile salts and lecithin.

Intestinal permeability is another critical factor in determining the rate and extent of absorption and bioavailability of a potential drug candidate (Ingels *et al.* 2004). Several *in vitro* and *in situ* experimental methods such as the use of cultured epithelial cell lines and rat intestinal perfusion have been developed to predict intestinal drug permeability (Artursson and Karlsson, 1990a; Lennernas, 1998, Polentarutti *et al.* 1999). Since the early 1990s, the Caco-2 cell model has been introduced as a means of determining the intestinal permeability of drug compounds (Hidalgo *et al.* 1989; Jung *et al.* 2006; LeCluyse *et al.* 1997). Caco-2 originated from a human colon carcinoma (Yamashita *et al.* 2000). The monolayer formed by Caco-2 cells shows the features of absorptive intestinal cells such as a microvilli structure, passive, carrier-mediated, paracellular transport system and efflux by P-glycoprotein (Artursson and Borchardt, 1997; Artursson *et al.* 2001; Blais *et al.* 1987; Hidalgo *et al.* 1989; Yamashita *et al.* 2000). Permeability measurements are taken using the routine transport media of the Hanks' balanced salt solution (HBSS) with 25 mM glucose (Yamashita *et al.* 2000). The salt solutions are buffered using N-(2-Hydroxyethyl)piperazine-N'-(2-ethanesulfonic acid (HEPES) or 2-(N-Morpholino)ethanesulfonic acid (MES) at pH 7.4 or 6.5. The pH conditions are assumed to mimic the intestinal pH gradient between the intestinal lumen and interstitial fluid in the villi of the small intestine (Yamashita *et al.* 2000). For drugs having low aqueous solubility co-solvents with no more than 1% DMSO can be added into HBSS to increase the solubility (Ingels *et al.* 2002). These transport media can maintain the cells healthy and the ionic equilibrium at the cell membrane during the permeability experiment (Ingels *et al.* 2002). However, these media do not reflect the real physiological conditions in the GI tract due to the lack of micelle solubilization. The BDMs described previously can simulate such physiological environments much better

(Wei and Löbenberg, 2006). Ingels *et al.* (2002, 2004) had reported that the FaSSIF can potentially be used as transport media in Caco-2 monolayers. FaSSIF showed an inhibition of P-glycoprotein efflux. FeSSIF had significant toxic effects on the Caco-2 monolayer. Patel and Forbes (2006) modified both BDMs to develop more compatible transport media for the Caco-2 model by changing the ratio of the bile salts and lecithin, pH and osmolality of the BDMs; however, the modified media were not suitable for rat intestinal perfusion experiments.

The aim of this study was to investigate the impact of the chemical grade of ingredients used in BDMs on the Caco-2 model when the BDMs were used as transport media. The performance of BDMs was compared with HBSS. Three drugs were selected: (+/-) metoprolol, a passive transcellular transport marker (Lennernas, 1997); (+/-) verapamil, a P-glycoprotein inhibitor (Zastre *et al.* 2004) and glyburide as a poorly soluble test drug. In this study, the permeability classification of glyburide based on the biopharmaceutics drug classification system (BCS) was investigated. The resulting permeability classification of glyburide can be used potentially for regulatory applications such as biowaivers (Potthast *et al.* 2005).

## **2.2. Materials and Methods**

### **2.2.1. Materials**

(+/-) metoprolol, lucifer yellow, sodium taurocholate crude (catalog number: T-0750; low quality: LQ) and 97% pure (catalog number: T-4009; high quality: HQ), and 3-(4,5-dimethyl-2-thiazolyl)-2,5-diphenyl-2H tetrazolium bromide (MTT) were purchased from Sigma-Aldrich (St. Louis, Missouri, USA). (+/-) verapamil and egg-lecithin 60% (catalog number: 102146; low quality: LQ) was ordered from ICN Biomedicals Inc (Aurora, Ohio, USA). Egg-phosphatidylcholine, Lipoid E PC 99.1% pure (high quality: HQ) was a gift from Lipoid GmbH (Ludwigshafen, Germany). Potassium dihydrogen phosphate, potassium chloride, sodium chloride, sodium hydroxide, phosphoric acid and hydrochloric acid were purchased from BDH Inc (Toronto, Ontario, Canada).

Dulbecco's modified eagle's medium (DMEM), L-glutamine, trypsin-EDTA, HEPES, L-glutamine and minimum essential medium (MEM) nonessential amino acids were purchased from the GIBCO BRL Co. (Carlsbad, California, USA). Fetal bovine serum (FBS), HBSS and MES were obtained from Sigma (St. Louis, Missouri, USA). Rat collagen was a gift from Dr. Robert Campenot (Department of Cell biology, University of Alberta, Canada). PBS contains 140 mM NaCl, 260 mM KCl, 8.1 mM Na<sub>2</sub>HPO<sub>4</sub>, 1.47 mM KH<sub>2</sub>PO<sub>4</sub>, PH 7.2. The biorelevant dissolution media (BDM) and Hank's solution with 10 mM MES or HEPES were adjusted to pH 6.5 or 7.4 using 0.1 N HCl or 0.2 N NaOH, respectively. The resulting solutions were used as transport media in the permeability study. Transwell<sup>®</sup> inserts (24.5 mm, pore size 0.4 μm, 4.7 cm<sup>2</sup>, Corning Costar (Acton, Massachusetts, USA) were used to grow Caco-2 cell monolayer on them and to perform transport experiments. Cell culture flasks (75 cm<sup>2</sup>) were used to grow cells prior to seeding them on the Transwell<sup>®</sup> inserts. Both were obtained from Corning Costar (Acton, Massachusetts, USA).

### **2.2.2. Preparation of Test Media**

Fasted state simulated intestinal fluids (FaSSIF) and fed state simulated intestinal fluids (FeSSIF) were made from two chemical grades (LQ and HQ) of sodium taurocholate and lecithin. The FaSSIF and FeSSIF contained 3 and 15 mM of sodium taurocholate and 0.75 and 3.75 mM of lecithin, respectively (Galia *et al.* 1998). Blank FaSSIF and FeSSIF (BL-FaSSIF and BL-FeSSIF) had the same composition and pH as FaSSIF and FeSSIF but did not contain lecithin or sodium taurocholate.

### **2.2.3. Solubility Study of Glyburide**

The solubility study of glyburide in HBSS, HQ-FaSSIF and 2-fold diluted HQ-FaSSIF at pH 6.5 and 7.4 were studied. The protocol of the solubility study and sample analysis was described in Chapter 3 and 4 (Wei and Löbenberg, 2006; Chapter 3; Chapter 4).

..

#### 2.2.4. MTT Toxicity Study

Caco-2 cells were purchased from ATCC (Rockville, Maryland, USA). Caco-2 cells were maintained at 37°C in an atmosphere of 5% CO<sub>2</sub> and 90% relative humidity in Dulbecco's Modified Eagle's Medium (DMEM) with 4.5 g/L glucose, 10% (v/v) fetal bovine serum, 1% (v/v) glutamine, 1% Minimum Essential Medium (MEM) nonessential amino acids and 10 mM HEPES. Cells were grown in 75 cm<sup>2</sup> flasks and were passaged every 5 days at a split ratio of 1:4 and confluence was reached within 6-7 days after each passage.

The exponentially growing cells were trypsinized, centrifuged and suspended in growth medium and diluted to 1 x 10<sup>4</sup> cells/mL. The cells were seeded into 96-well plates at 1000 cells/well and incubated in 37°C, 5% CO<sub>2</sub> for one week. The growth medium was changed every 48 hours. On the day of the experiment, the growth media was removed. The test media (pH 5.0, 6.5 or 7.4) included BL-FaSSIF, BL-FeSSIF, LQ-FaSSIF, LQ-FeSSIF, HQ-FaSSIF, HQ-FeSSIF and 2, 4, 8-fold diluted HQ-FaSSIF. The test medium (200 µL) was added into each well. Control wells were filled with 200 µL of DMEM growth medium. The plates were incubated at different time intervals (15, 30, 60 and 90 min) at 37°C in humidified atmosphere containing 95% air and 5% CO<sub>2</sub>. MTT was dissolved in PBS at 5 mg/mL, filtered through a 0.45 µm membrane filter as stock solution. Before the experiment, the stock solution was diluted to 1:10 in pre-warmed DMEM medium. After the Caco-2 cells in each well were exposed to the test media at different time intervals (60 or 90 min), the test media was removed. Diluted MTT solution (250 µL) was added to each well. The plates were incubated at 37°C for 4 hours. The MTT solution was then removed from the wells and 150 µL of dimethyl sulfoxide (DMSO) was added to each well. The plates were on a shaker for 15 min to dissolve the formazan crystals in DMSO and then read immediately at 570 nm on a scanning multiwell spectrophotometer (PowerWave X 340, Bio-Tek Instruments Inc. Analysis software: KCJUNIOR Version 1.11, Pennsylvania, USA).

### **2.2.5. Caco-2 Cell Culture and Quality Control**

The passage number for the cells used in the experiments was between 38 and 45. The membranes of Transwell<sup>®</sup> inserts were coated using rat collagen (0.5 mL of rat collagen (1:4 dilution)). The collagen solution was added to the apical chamber and the insert was left uncovered in the laminar flow hood until dry. The cells (50,000 cells/cm<sup>2</sup>) in growth medium were seeded in each apical chamber of the Transwell<sup>®</sup> insert. Growth medium (3.0 mL) was transferred to the basolateral side. The media in both apical and basolateral sides were changed every 48 hours.

The integrity and permeability of the cell monolayer was determined by electrical resistance measurements (VOHM, World Precision Inc., Sarasota, Florida, USA). The transepithelial electrical resistance values (TEER) obtained in the absence of cells were considered as background measurements (around 100  $\Omega$  cm<sup>2</sup>). The transport experiment took place based on the TEER of the monolayer when it reached 400  $\Omega$  cm<sup>2</sup> or higher. This is typically the case following 18 to 23 days after seeding the cells on the Transwell<sup>®</sup> inserts. Before and after each experiment, the TEER values were measured in all inserts and the integrity of the cell monolayer was confirmed. Lucifer yellow (100 $\mu$ M) was used as a paracellular quality control marker, its apparent permeability coefficient ( $P_{app}$ ) should be less than  $2 \times 10^{-7}$  cm/s. Lucifer yellow was measured by 485 nm excitation and 530 nm emission using a spectrofluorometer (model: FLUOROMAX, SPEX Industries Inc., Edison, New Jersey, USA). In order to fulfill the “sink condition” for the transport study; that is, the drug is absorbed instantaneously while it dissolves (Gennaro *et al.* 2000), the cumulative amount in the receiver chamber should be less than 10% of the loading amount at the last sampling time, which is described by the calculation equation of permeability (Artursson, 1990b).

### **2.2.6. Media Effect on TEER Values of The Cell Monolayer**

The different media (HBSS, HQ-FaSSIF and 2-fold diluted HQ-FaSSIF, pH 6.5) were added to the apical sides, and HBSS (pH 7.4) was added to the basolateral sides. After

different incubation time intervals (0, 15, 30, 60 and 90 min), the TEER values were measured. The obtained values were compared to initial measurements (100%).

### **2.2.7. Transport Study**

The transport studies were started by washing the cell monolayers twice using test media and then pre-incubating them for 15 min at 37<sup>0</sup>C in an atmosphere of 95% humidity. For all the transport experiments, the receiver compartments were at pH 7.4. For the apical to basolateral (A/B) direction, 1.5 mL of test medium containing the test drug was placed in the apical compartment. For basolateral to apical direction (B/A), 3 mL of test media containing the test drug was placed in the basolateral compartment. Samples (100 µL) were withdrawn from the receiver compartments at predetermined time intervals, and replaced with fresh medium. The concentrations of the test compounds (+/-) metoprolol or (+/-) verapamil were 100 µM. The concentrations of glyburide were 8 and 25 µM at pH 6.5 and 7.4, respectively.

### **2.2.8. Competition of Transport Studies**

The interaction of glyburide with P-glycoprotein was investigated using 50 µM (+/-) verapamil in the apical compartment. Both transport directions were studied. The experimental conditions and procedures were the same as described above.

### **2.2.9. HPLC Analysis**

Sample analysis was achieved by HPLC. The HPLC system consisted of an automatic sample injector (SIL-9A, Shimadzu, Kyoto, Japan), a pump (LC-60, Shimadzu, Kyoto, Japan), a UV detector (SPD-6AV, Shimadzu, Kyoto, Japan) and an analytical column LiChospher 60 Rp-select B (5µm, Merck Darmstadt, Germany) with a guard column. The samples were centrifuged at 12, 000 rpm for 15 min using an Eppendorf centrifuge (Model 5415, Brinkmann, Filderstadt, Germany). Supernatant (30 µL) was directly injected into the HPLC system. Samples were stable for the duration of the analysis. An

integrator (C-R3A, Shimadzu, Kyoto, Japan) was used for peak integration. The mobile phase for both glyburide and (+/-) verapamil consisted of a mixture of the acetonitrile and (25 mM, pH 4.5) sodium dihydrogen phosphate buffer (45:55). Glyburide and (+/-) verapamil were detected at a wavelength of 230 nm and the retention time was 5.5 and 8 min, respectively. The mobile phase for (+/-) metoprolol consisted of a mixture of the acetonitrile and (25 mM, pH 4.5) sodium dihydrogen phosphate buffer (25:75) and detected at a wavelength of 222 nm with a retention time of 5 min.

### 2.2.10. Calculation of Apparent Permeability and Statistics

The apparent permeability coefficient ( $P_{app}$ ) was calculated using the following Eq. 2.1 (Yamashita *et al.* 2000)

$$P_{app} = \frac{V}{A * C_0} \times \frac{dc}{dt} (cm / s) \quad (2.1)$$

where:

$dc/dt$ : the permeability rate (mM/s), is the initial slope of a plot of the cumulative receiver concentration versus time ,

V: the volume of the receiver chamber (mL),

A: the surface area of the monolayer (cm<sup>2</sup>), which is 4.7 cm<sup>2</sup> for the transwell insert in this experiment, and

C<sub>0</sub>: initial concentration (mM) in donor compartment.

In all cases, significance of differences between experiments was calculated by Student's t test using two-tailed distributions and two-sample equal variance (Microsoft Excel, Version 2000, Microsoft Inc. Seattle, Washington, USA). Statistical significance was calculated at the 95% (p <0.05) confidence level.



## 2.3. Results

### 2.3.1. Solubility Study of Glyburide

The solubility study of glyburide in HBSS, HQ-FaSSIF and 2-fold diluted HQ-FaSSIF at pH 6.5 and 7.4 is shown in Fig. 2.1. The solubility of glyburide is pH dependent due to its weak acid (El-Massik *et al.* 1996). HQ-FaSSIF showed the highest solubility followed by 2-fold diluted HQ-FaSSIF, and finally by HBSS.

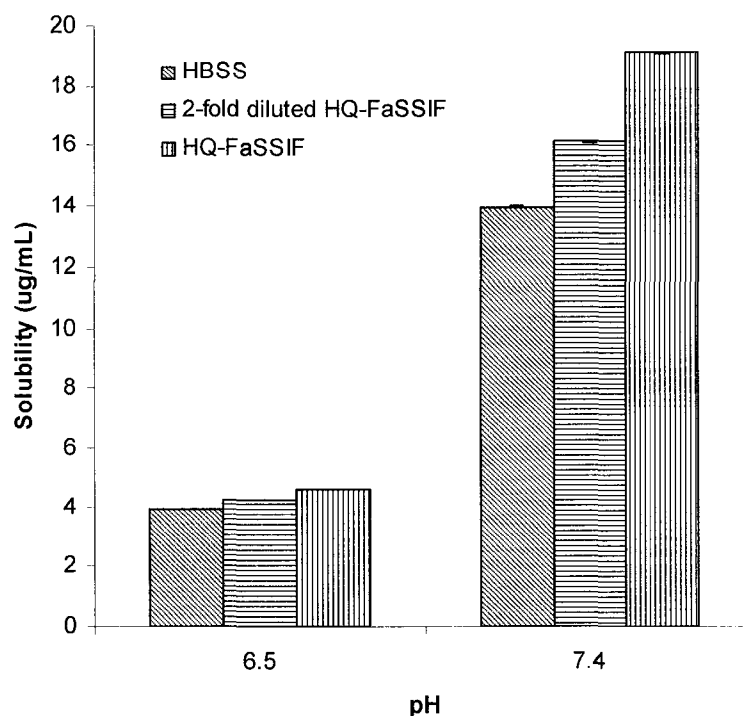


**Figure 2.1.** Solubility of glyburide powder in different media at different pH (n=3)

### 2.3.2. MTT Toxicity Studies

MTT is a tetrazolium salt. The mitochondrial dehydrogenase in living cells can break down the MTT and the resulting dark blue compound can be detected by a spectrophotometer (Mosmann *et al.* 1983, Tada *et al.* 1986). Fig. 2.2, 2.3 and 2.4 show a summary of the toxicity studies using BDMs. The percentages of the absorbance of each test compared to the control cells that were treated by normal growth medium are shown in the figures. Fig. 2.2 shows that the absorbance for the cells exposed to BL-FaSSIF and

BL-FeSSIF at pH 5.0 as assessed by MTT were significantly lower ( $64.12 \pm 5.51\%$  and  $6.02 \pm 0.53\%$ ,  $p < 0.05$ ) compared to the control. There was no significant toxicity at pH 6.5 and 7.4 for both buffers ( $p > 0.05$ ). The toxicity of the chemical grades of the bile salts and lecithin are shown in Fig. 2.3. The absorbance of cells exposed to the LQ-BDMs and HQ-FeSSIF at pH 6.5 were significantly lower ( $p < 0.05$ ) compared to the control. There was no significant difference in MTT conversion when the cells were treated by HQ-FaSSIF ( $94.92 \pm 18.21\%$ ). Fig. 2.4 shows there are no significant differences ( $p > 0.05$ ) in the toxicity of three different concentrations of HQ-FaSSIF that were tested as 2, 4 and 8-fold dilutions.

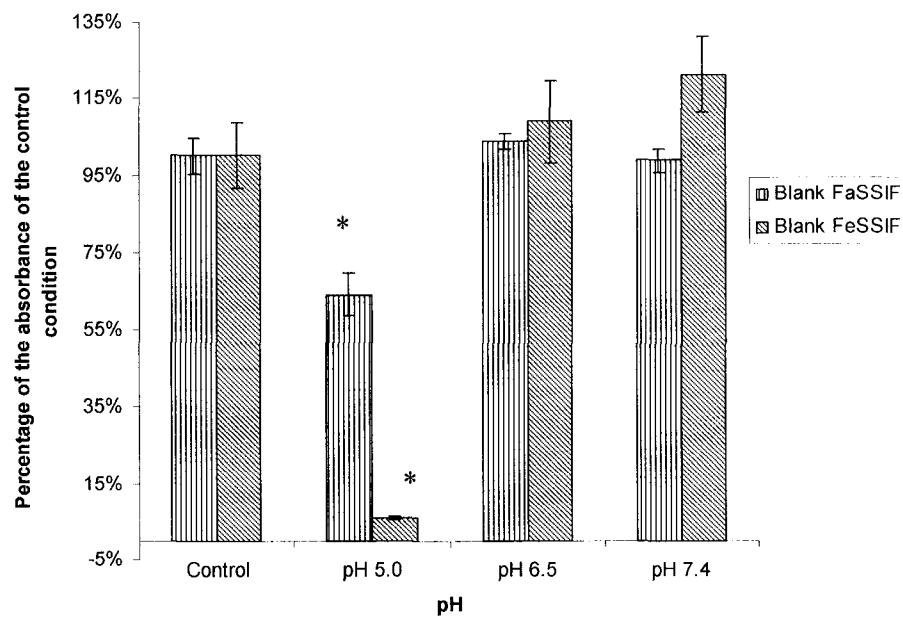


**Figure 2.2.** pH effect on cell toxicity study using blank buffers (incubation time 90 min;  $n=6$ ; Blank FaSSIF and FeSSIF are plain buffers without bile salts and lecithin; \*: significant difference from control,  $p < 0.05$ )

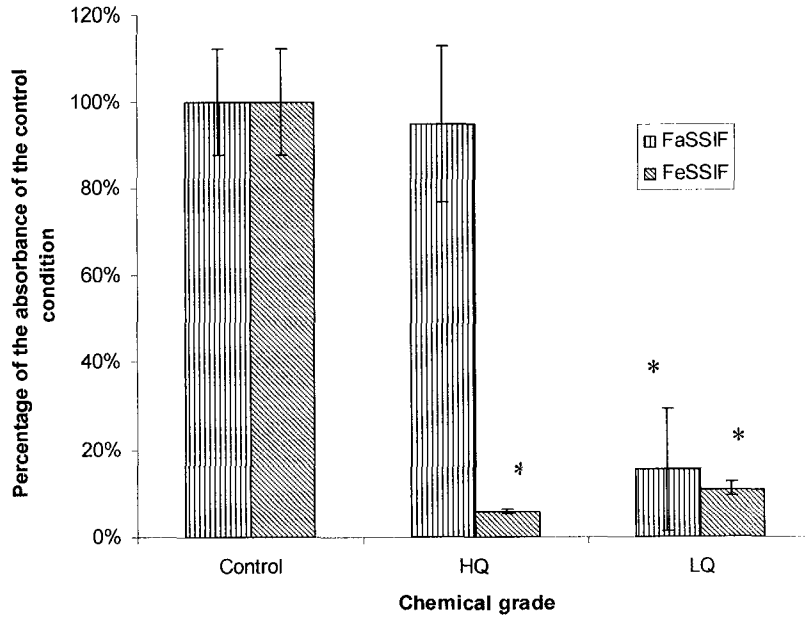


**Figure 2.3.** Toxicity study of the different chemical grades of BDM (incubation time 90 min; pH 6.5, n=6; HQ: purer bile salts and lecithin; LQ: crude bile salts and lecithin; \*: significant difference from control:  $p < 0.05$ )

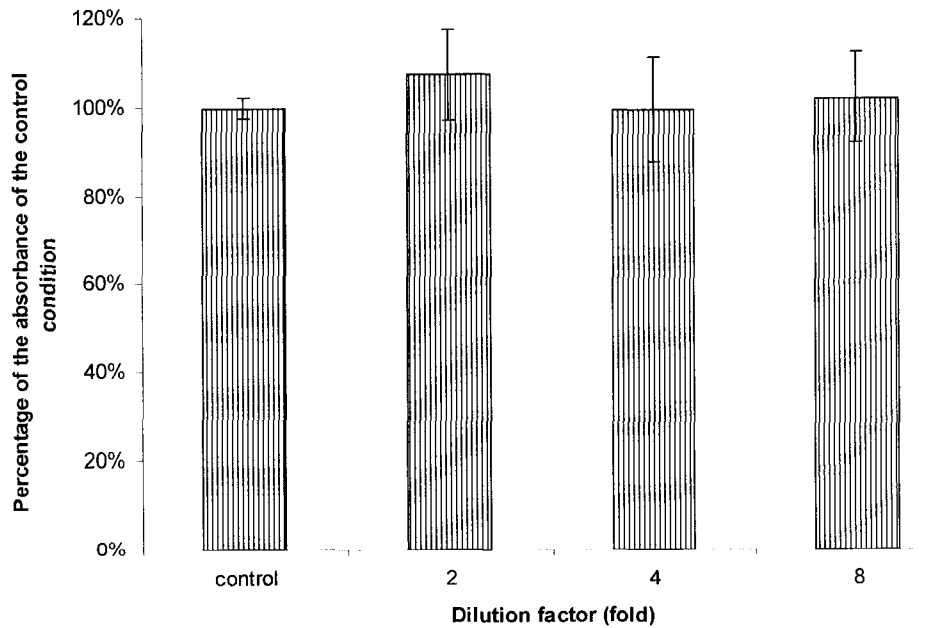


**Figure 2.4.** Toxicity study of the different concentration of the bile salts and lecithin in HQ-FaSSIF (incubation time 60 min; pH 6.5, n=6)

### 2.3.3. Media Effects on TEER Values of the Cell Monolayers

The effects of different media on the TEER values of the cell monolayer are given in Fig. 2.5 as the percentage of the initial values (100%). The TEER values slightly decreased to 95.33% and 93.83% (compared to initial values 100%) after 90 min incubation with HBSS and 2-fold diluted HQ-FaSSIF. The TEER values after 90 min incubation for both media still met the requirement for the TEER values as described previously. However, the TEER values dropped to 80.92% after 90 min incubation with undiluted HQ-FaSSIF and was below the required TEER value defined for transport studies.

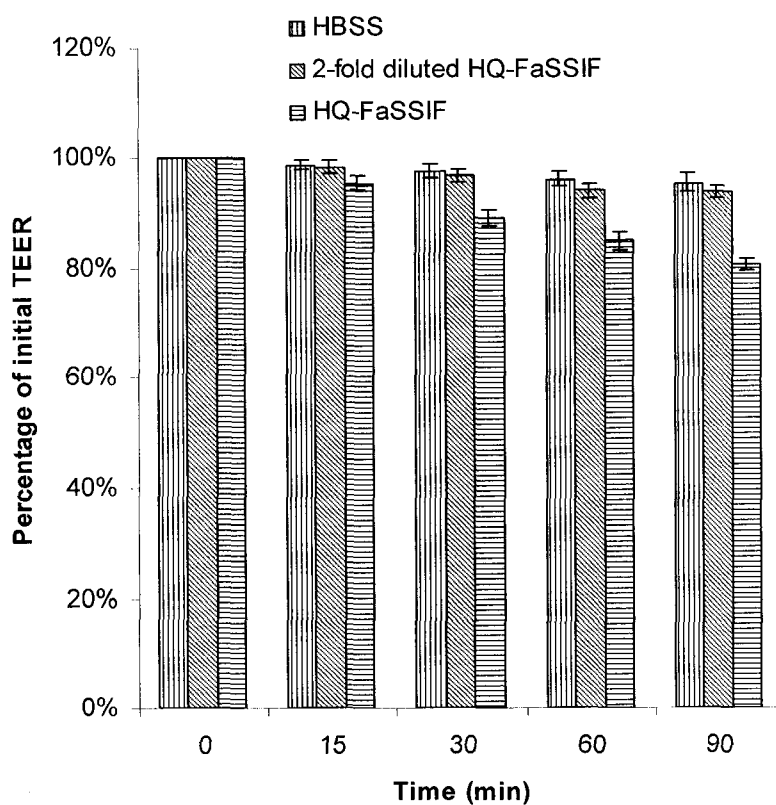


**Figure 2.5.** Time dependent effects on the TEER values of the cell monolayers after incubation in different media (HBSS, HQ-FaSSIF and 2-fold diluted HQ-FaSSIF; apical pH 6.5/basolateral pH 7.4; n=3)

### 2.3.4. Comparison of Transport Studies using HBSS and HQ-FaSSIF

Table 2.1 shows the comparison of the transport studies between Hank's solution and 2-fold diluted HQ-FaSSIF. The tests were performed under both pH conditions (pH 7.4 both sides and pH gradient pH 6.5/7.4). For (+/-) metoprolol and glyburide, there were no significant differences between HBSS and 2-fold diluted HQ-FaSSIF under both pH conditions. The  $P_{app}$  values of (+/-) metoprolol and glyburide under different experiment conditions (both pH conditions and bi-directional) were within the same range ( $10^{-5}$  cm/s). The ratios ( $P_{ratio}$ ) between  $P_{app}$  (B/A) and  $P_{app}$  (A/B) were around 1. For (+/-) verapamil, the  $P_{app}$  values of direction (A/B) were similar under all the experiment conditions. However, the  $P_{app}$  values of direction (B/A) were different between HBSS and 2-fold diluted HQ-FaSSIF. The  $P_{app}$  values of direction (B/A) decreased using 2-fold diluted HQ-FaSSIF. The  $P_{ratio}$ s were  $3.34 \pm 0.24$  (donor pH 7.4) and  $2.51 \pm 0.33$  (donor pH 6.5) using HBSS as transport medium and dropped to  $1.16 \pm 0.08$  and  $1.16 \pm 0.20$  using 2-fold diluted HQ-FaSSIF.

**Table 2.1.** Comparison of the  $P_{app}$  values for the A/B and B/A transport of the drug between the Hank's solution and 2-fold diluted high quality FaSSIF (n=3)

Compounds	Hank's solution			2-fold diluted HQ-FaSSIF		
	$P_{app}(\times 10^{-5}$ cm/s)		$P_{ratio}$	$P_{app}(\times 10^{-5}$ cm/s)		$P_{ratio}$
	A/B	B/A		A/B	B/A	
<b>pH 7.4 (donor side)</b>						
(+/-) metoprolol	1.804±0.153	1.734±0.159	0.96	2.012±0.120	2.130±0.030	1.06
(+/-) verapamil	1.044±0.019	3.482±0.253*	3.34	1.154±0.042	1.344±0.132*	1.16
Glyburide	1.287±0.016	1.458±0.144	1.13	1.419±0.019	1.301±0.078	0.92
<b>pH 6.5 (donor side)</b>						
(+/-) metoprolol	1.578±0.169	1.423±0.105	0.90	1.624±0.132	1.555±0.120	0.96
(+/-) verapamil	1.137±0.113	2.854±0.259*	2.51	1.257±0.122	1.453±0.104*	1.16
Glyburide	1.580±0.094	1.491±0.154	0.94	1.568±0.126	1.203±0.112	0.77

$P_{ratio}$ :  $P_{app}$  (B/A)/  $P_{app}$  (A/B); In all experiments, the medium in receiver side was pH 7.4

### 2.3.5. Impact of (+/-)Verapamil on the Transport Studies

Transport studies using glyburide were also performed in the presence of the P-glycoprotein substrate, (+/-) verapamil. A summary of these studies is shown in Table 2.2. The transport study conditions were the same. Both directions were tested. The obtained  $P_{app}$  values were similar to the values obtained without (+/-) verapamil. There were no significant decrease or increase for the obtained  $P_{app}$  values. The  $P_{app}$  values were all at the order of  $10^{-5}$  cm/s.

**Table 2.2.** Transport studies of glyburide in the presence of (+/-) verapamil (50  $\mu$ M) for the A/B and B/A transports using the Hank's solution and 2-fold diluted high quality FaSSIF (n=3)

Compounds	Hank's solution			2-fold diluted HQ-FaSSIF		
	$P_{app}(x10^{-5}$ cm/s)			$P_{app}(x10^{-5}$ cm/s)		
	A/B	B/A	$P_{ratio}$	A/B	B/A	$P_{ratio}$
<b>pH 7.4 (donor side)</b>						
Glyburide	1.289±0.045	1.215±0.110	0.94	1.210±0.054	1.187±0.042	0.98
<b>pH 6.5 (donor side)</b>						
Glyburide	1.456±0.125	1.373±0.161	0.94	1.458±0.086	1.542±0.141	1.06

$P_{ratio}$ :  $P_{app}$  (B/A)/  $P_{app}$  (A/B); In all experiments, the medium in receiver side was pH 7.4

### 2.4. Discussion

There are many factors that can influence oral drug absorption in the GI tract such as pH, transit time and composition of the intestinal fluids (Galia *et al.* 1998; Dressman *et al.* 1998). BDMs might be used to simulate the physiological conditions in the GI tract to provide more biorelevant information during the *in vitro* assessment of drug candidates.

The two major components, bile salts and lecithin, are used in BDMs to improve wetting and solubilization of lipophilic drugs. This is due to micelle solubilization (Jinno *et al.* 2000). This is the most important reason in applying BDMs for Caco-2 model as transport media instead of co-solvent such as DMSO that is not biorelevant conditions. Solubility study of glyburide has shown (Fig. 2.1) the improvement of the solubilization by HQ-FaSSIF and 2-fold diluted HQ-FaSSIF compared to HBSS.

The pH in the small intestine shows a pH gradient along the intestines, which influence the ionization of a compound. The permeability across the GI membrane decreases when the ionized fraction of a compound increases (Kuentz *et al.* 2006). The average pH for the fasted state is around 6.5 while for the fed state pH is 5.0 in intestinal lumen (Dressman *et al.* 1998; Gray and Dressman, 1996). Biorelevant dissolution media such as FaSSIF and FeSSIF that reflect the physiological conditions have a pH 6.5 and 5.0, respectively (Galia *et al.* 1998). The MTT studies showed that a significant toxic effect exists on the cells at pH 5.0 (Fig. 2.2). It indicated that pH 5.0 might be an irritant pH value applied to the Caco-2 cells. This is in accordance with reports of Patel and Forbes (2006). The modified FeSSIF at pH 6.0 was better tolerated by Caco-2 monolayers compared to pH 5.0. In order to truly reflect the physiological conditions, Yamashita *et al.* (2000) had suggested to use a pH gradient between the apical and basolateral sides (pH 6.5/7.4). This may reflect better the *in vivo* conditions between the intestinal lumen and interstitial fluid in the villi of the small intestine. The applied experimental conditions can reflect the impact of pH gradient on the permeability of the ionizable compounds that can be described by pH partition hypothesis (Youdim *et al.* 2003). The results in Fig. 2.3 indicated that the LQ-BDMs had significant toxic effects on the Caco-2 cells. This might be due to unknown impurities in the low chemical grade bile salts and lecithin used (Wei and Löbenberg, 2006). The HQ-FaSSIF showed no significant toxic effect on the Caco-2 cells; however, HQ-FeSSIF damaged the Caco-2 cells significantly. These results are in accordance with Ingels *et al.* (2002) and Patel and Forbes (2006) who have previously reported that FeSSIF is not suitable for Caco-2 cells due to the high concentration of bile salts (sodium taurocholate, NaTC). They showed that bile salts (NaTC) have a concentration dependent toxic effect on Caco-2 monolayers (Ingels *et al.* 2002). One way to reduce the toxicity is to increase the ratio of the lecithin (Narain *et al.* 1999). Patel and

Forbes (2006) modified the FeSSIF by using the ratio of bile: lecithin 2:1 instead of 4:1. The modified FeSSIF was more compatible with the Caco-2 monolayer than with the original FeSSIF. Another method used was to co-culture Caco-2 cell with other cell lines such as Ht29GlucH, which could produce mucous layer as a protective barrier (Meaney *et al.* 1999). In the present study, the potential application of HQ-FaSSIF as a transport medium was investigated. In order to verify the toxicity of the HQ-FaSSIF, HQ-FaSSIF was diluted using a blank FaSSIF buffer. This reduced the concentration of NaTC. The results shown in Fig. 2.4 indicated that no significant toxic effects were observed in any of the four dilutions. Neither was a significant toxic effect observed at the pH 7.4 (data not shown). The transepithelial electrical resistance values (TEER) can be used to monitor the maturation, integrity and maintenance of the Caco-2 monolayers' tight junctions (Ranaldi *et al.* 2003). The TEER of the cell monolayer was reduced by up to 20% (Fig. 2.5) after incubation with HQ-FaSSIF for 90 min and was below the acceptable range to perform permeability studies. The TEER values of Caco-2 monolayers were maintained within the required range for both HBSS and 2-fold diluted HQ-FaSSIF under the same conditions as for HQ-FaSSIF. This indicated that 2-fold diluted HQ-FaSSIF was more compatible with the Caco-2 model than with the original HQ-FaSSIF. Ingels *et al.* (2002) reported that undiluted HQ-FaSSIF was compatible with Caco-2 monolayers for at least 2 hours. The discrepancies in results between present and previous studies might be due to the different batches of NaTC and lecithin that were used (Wei and Löbenberg, 2006). The comparative results obtained in the transport studies of (+/-) metoprolol and glyburide summarized in Table 2.1 indicated that 2-fold diluted HQ-FaSSIF might be suitable as a transport medium for the Caco-2 model. The  $P_{ratio}$  of verapamil obtained from HBSS was close to 3. If the  $P_{ratio}$  is above 2, then active drug transport through the cell membrane is involved and efflux mechanism by P-glycoprotein have to be considered and tested (Faassen *et al.* 2003; Karlsson *et al.* 1993). This result confirms that (+/-) verapamil is the P-glycoprotein substrate in the Caco-2 model. However, the  $P_{ratio}$  of (+/-) verapamil obtained from 2-fold diluted HQ-FaSSIF decreased to around 1.0 due to the inhibition of NaTC on the P-glycoprotein transporter previously reported by Ingels *et al.* (2002, 2004). The results showed that different batches of NaTC had the same inhibition effect on the P-glycoprotein. Due to the



inhibition of NaTC on the efflux modulated by P-glycoprotein, FaSSIF might not be suitable for mechanistic studies of drug transport through Caco-2 cell monolayer. (Ingels *et al.* 2002 and 2004).

As mentioned previously, several groups reported that glyburide was a P-glycoprotein substrate using the molecular biological methods (Golstein *et al.* 1999; Payen *et al.* 2001). In order to investigate the transport mechanism of glyburide using the Caco-2 model, the P-glycoprotein competitor (+/-) verapamil was added to the apical compartment during the transport studies (Zastre *et al.* 2004). (+/-) verapamil as a competitor might inhibit the efflux of glyburide caused by P-glycoprotein due to the high affinity of (+/-) verapamil for P-glycoprotein (Pachot *et al.* 2003). The transport studies summarized in Table 2.1 and 2.2 showed that the  $P_{ratio}$  of the glyburide in all experiments with or without (+/-) verapamil were similar and were approximately 1. The results do not confirm that the glyburide was a P-glycoprotein substrate in this study. Further investigations of the transport mechanisms of glyburide are necessary. The resulting  $P_{app}$  of glyburide under all the experiment conditions in this study was at the order of  $10^{-5}$  cm/s. It indicates that glyburide can be considered as a high permeability drug that was confirmed by the up to 100% bioavailability (Faassen *et al.* 2003; Vogelpoel *et al.* 2004). Due to the high permeability and low aqueous solubility of glyburide (El-Massik *et al.* 1996) glyburide can be classified into the Class II drug category based on the biopharmaceutics drug classification system (BCS) (Amidon *et al.* 1995). The information of glyburide's classification can assist formulation scientists in product development. Furthermore, this information can be used by regulatory agencies to decide on the application of biowaivers.

## 2.5. Conclusion

The toxicity study showed that the low chemical grade of bile salts and lecithin had significant toxic effects on the Caco-2 cells. This might be due to unknown impurities in these chemicals. Both chemical grades of FeSSIF damaged the Caco-2 cells dramatically and this can be linked to the high concentration of NaTC. HQ-FaSSIF showed no significant toxic effects on the cell lines. Further monitoring of the TEER of Caco-2

monolayers indicated that 2-fold diluted HQ-FaSSIF was compatible with the cell monolayers compared to undiluted HQ-FaSSIF. Comparison of the transport studies of (+/-) metoprolol, glyburide and (+/-) verapamil using classic HBSS and 2-fold diluted HQ-FaSSIF showed similar results, especially for the apical to basolateral direction. The inhibition of the efflux mediated by P-glycoprotein was confirmed in the presence of the P-glycoprotein substrate, (+/-) verapamil. 2-fold diluted HQ-FaSSIF might be suitable as a transport medium for compounds that do not have an active transport mechanism. The active transport of glyburide by efflux mediated by P-glycoprotein could not be confirmed using either media. However, the obtained  $P_{app}$  combined with previously published solubility of glyburide can help to classify glyburide as a Class II drug.

## 2.6. References

Amidon, G. L., Lennernas, H., Shah, V. P. and Crison, J. R. A theoretical basis for a biopharmaceutical drug classification: the correlation of in vitro drug product dissolution and in vivo bioavailability. *Pharm. Res.* 12 413-420, 1995.

Artursson, P. and Karlsson, J. Correlation between oral drug absorption in humans and apparent drug permeability coefficients in human intestinal epithelial (Caco-2) cells. *Biochem. Biophys. Res. Comm.* 175 (3), 880-885, 1990a.

Artursson, P. Epithelial transport of drugs in cell culture I: A model for studying the passive diffusion of drugs over intestinal absorptive (Caco-2) cells. *J. Pharm. Sci.* 79, 476-482, 1990b.

Artursson, P. and Borchardt, R. T. Intestinal drug absorption and metabolism in cell cultures: Caco-2 and beyond. *Pharm. Res.* 14, 1655-1658, 1997.

Artursson, P., Palm, K. and Luthman, K. Caco-2 monolayers in experimental and theoretical predictions of drug transport. *Adv. Drug Deli. Rev.* 46, 27-43, 2001.

Blais, A., Bissonnette, P. and Berteloot, A. Common characteristics for  $\text{Na}^+$ -dependent sugar transport in Caco-2 cells and human fetal colon. *J. Membrane Biol.* 99, 113-125, 1987.

- Dressman, J. B., Amidon, G. L., Reppas, C. and Shan, V. P. Dissolution testing as a prognostic tool for oral drug absorption: immediate release dosage forms. *Pharm. Res.* 15(1), 11-21, 1998.
- Dressman, J. B. and Reppas, C. In vitro-in vivo correlation for lipophilic, poorly water-soluble drugs. *Eur. J. Pharm. Sci.* 11, 873-880, 2000.
- El-Massik, M. A., Darwish, I. A., Hassan, E. E. and El-Khordagui, L. K. Development of a dissolution medium for glibenclamide. *Int. J. Pharm.* 140, 69-76, 1996.
- Faassen, F., Vogel, G., Spanings, H. and Vromans, H. Caco-2 permeability, P-glycoprotein transport ratios and brain penetration of heterocyclic drugs. *Int. J. Pharm.* 263, 113-122, 2003.
- Galia, E., Nicolaidis, E., Hörter, D., Löbenberg, R., Reppas, C. and Dressman J. B. Evaluation of various dissolution media for predicting in vivo performance of class I and II drugs. *Pharm. Res.* 15 (5), 698-705, 1998.
- Gray, V. and Dressman, J. B. Simulated intestinal fluid, TS-change to pH 6.8. *Pharmacop. Forum.* 22, 1943-1945, 1996.
- Golstein, P. E., Boom, A., Geffel, J. V. and Jacobs, P. P-glycoprotein inhibition by glibenclamide and related compounds. *Eur. J. Physiol.* 437, 652-660, 1999.
- Gennaro, A. R., Marderosian, A.H.D., Hanson, G. R., Medwick, T., Popovich, N. G., Schnaare, R. J., Schartz, J. B. and White, H. S. Remington: the science and practice of pharmacy, Chapter 35: dissolution. Twentieth edition, Lippincott Williams & Wilkins, Baltimore, Maryland, USA, 2000.
- Hidalgo, I., Raub, T. and Borchardt, R. Characterization of human colon carcinoma cell line (Caco-2) as a model system for intestinal epithelial permeability. *Gastroenterology.* 96, 736-749, 1989.
- Ingels, F., Deferme, S., Destexhe, E., Oth, M., Mooter, G. V. D. and Augustijns, P. Simulated intestinal fluid as transport medium in the Caco-2 cell culture model. *Int. J. Pharm.* 232, 183-192, 2002.

Ingels, F., Beck, B., Oth, M. and Augustijns, P. Effect of simulated intestinal fluid on drug permeability estimation across Caco-2 monolayers. *Int. J. Pharm.* 274, 221-232, 2004.

Jinno, J., Oh, D. M., Crison, J. R. and Amidon, G. L. Dissolution of ionizable water-insoluble drugs: the combined effect of pH and surfactant. *J. Pharm. Sci.* 89 (2), 268-275, 2000.

Jung, S. J., Choi, S. O., Um, S. Y., Kim, J., Choo, H. Y. P., Choi, S. Y. and Chung, S. Y. Prediction of the permeability of drugs through study on quantitative structure-permeability relationship. *J. Pharmaceu. Biomed. Anal.* 41 (2), 469-475, 2006.

Karlsson, J., Kuo, S. M., Ziemniak, J. and Artursson, P. Transport of celiprolol across human intestinal epithelial (Caco-2) cells: mediation of secretion by multiple transporters including P-glycoprotein. *Br. J. Pharmacol.* 110, 1009-1016, 1993.

Kuentz, M., Nick, S., Parrott, N. and Röthlisberger, D. A strategy for preclinical formulation development using GastroPlus™ as pharmacokinetic simulation tool and a statistical screening design applied to a dog study. *Eur. J. Pharm. Sci.* 27, 91-99, 2006.

LeCluyse, E. L. and Sutton, S. C. In vitro models for selection of development candidates. Permeability studies to define mechanisms of absorption enhancement. *Adv. Drug Deliv.* 23, 163-183, 1997.

Lennernas, H. Human jejunal effective permeability and its correlation with preclinical drug absorption models. *J. Pharm. Pharmacol.* 49, 627-638, 1997.

Lennernas, H. Human intestinal permeability. *J. Pharm. Sci.* 87, 403-410, 1998.

Löbenberg, R. and Amidon, G. L. Modern bioavailability, bioequivalence and biopharmaceutics classification system. New scientific approaches to international regulatory standards. *Eur. J. Pharm. Biopharm.* 50, 3-12, 2000a.

Löbenberg, R., Krämer, J., Shah, V. P., Amidon, G. L. and Dressman, J. B. Dissolution testing as prognostic tool for oral drug absorption: dissolution behavior of glibenclamide. *Pharm. Res.* 17(4), 439-444, 2000b.

Meaney, C. and O'Driscoll, C. Mucus as a barrier to the permeability of hydrophilic and lipophilic compounds in the absence and presence of sodium taurocholate micellar systems using cell culture models. *Eur. J. Pharm. Sci.* 8, 167-175, 1999.

Mosmann, T. Rapid colorimetric assay for cellular growth and survival: application to proliferation and cytotoxicity assays. *J. Immunol. Methods.* 65, 55-63, 1983.

Narrain, P. K., DeMaria, E. J. and Heuman, D. M. Cholesterol enhances membrane-damaging properties of model bile by increasing the intervesicular-intermixed micellar concentration of hydrophobic bile salts. *J. Surg. Res.* 84 (1), 112-119, 1999.

Obata, K., Sugano, K., Machida, M. and Aso, Y. Biopharmaceutics classification by high throughput solubility assay and PAMPA. *Drug. Dev. Ind. Pharm.* 30, 181-185, 2004.

Pachot, J. I., Botham, R. P. and Haegele, K. D. Experimental estimation of the role of P-glycoprotein in the pharmacokinetic behavior of telithromycin, a novel ketolide, in comparison with roxithromycin and other macrolides using the Caco-2 cell model. *J. Pharm. Pharmaceut. Sci.* 6 (1), 1-12, 2003.

Patel, N. and Forbes, B. Use of simulated intestinal fluids with Caco-2 cells and rat ileum. *Drug. Dev. Ind. Pharm.* 32, 151-161, 2006.

Payen, L., Delugin, L., Courtois, A., Trinquart, Y., Guillouzo, A. and Fardel, A. The sulphonylurea glibenclamide inhibits multidrug resistance protein (MRP 1) activity in human lung cancer cells. *Br. J. Pharmacol.* 132, 778-784, 2001.

Polentarutti, B. I., Peterson, A. L., Sjoberg, A. K., Anderberg, E. K. I., Utter, L. M. and Ungell, A. L. B. Evaluation of viability of excised rat intestinal segments in the Ussing chamber: investigation of morphology, electrical parameters, and permeability characteristics. *Pharm. Res.* 16, 446-454, 1999.

Potthast, H., Dressman, J. B., Junginger, H. E., Midha, K. K., Oeser, H., Shah, V. P., Vogelpoel, H. and Barends D. M. Commentary: biowaiver monographs for immediate release solid oral dosage forms: ibuprofen. *J. Pharm. Sci.* 94 (10), 2121-2131, 2005.

Ranaldi, G., Consalvo, R., Sambuy, Y. and Scarino, M. L. Permeability characteristics of parental and clonal human intestinal Caco-2 cell lines differentiated in serum-supplemented and serum-free media. *Toxi. In Vitro.* 17, 761-767, 2003.

Tada, H., Shiho, O., Kuroshima, K. I., Koyama, M. K. and Tsukamoto, K. An improved colorimetric assay for interleukin 2. *J. Immunol. Methods.* 93, 157-165, 1986.

Vertzoni, M., Fotaki, N., Kostewicz, E., Stippler, E., Leuner, C., Nicolaidis, E. and Dressman, J. B., Reppas, C. Dissolution media simulating the intraluminal composition of the small intestine: physiological issues and practical aspects. *J. Pharm. Pharmacol.* 56, 453-462, 2004.

Vogelpoel, H., Welink, J., Amidon, G. L., Junginger, H. E., Midha, K. K., Möller, H., Olling, M., Shah, V. P. and Barends, D. M. Biowaiver monographs for immediate release solid oral dosage forms based on biopharmaceutics classification system (BCS) literature data: verapamil hydrochloride, propranolol hydrochloride and atenolol (Commentary). *J. Pharm. Sci.* 93 (8), 1945-1956, 2004.

Wei, H. and Löbenberg, R. Biorelevant dissolution media as a predictive tool for glyburide a class II drug. *Eur. J. Pharm. Sci.* 29, 45-52, 2006.

Yamashita, Y., Furubayashi, T., Kataoka, M., Sakane, T., Sezaki, H. and Tokuda, H. Optimized conditions for prediction of intestinal drug permeability using Caco-2 cells. *Eur. J. Pharm. Sci.* 10, 195-204, 2000.

Youdim, K. A., Avdeef, A. and Abbott, N. J. In vitro trans-monolayer permeability calculations: often forgotten assumptions. *DDT.* 8 (21), 997-1003, 2003.

Zastre, J., Jackson, J. and Burt, H. Evidence for modulation of P-glycoprotein-mediated efflux by methoxypolyethylene glycol-block-polycaprolactone amphiphilic diblock copolymers. *Pharm. Res.* 21, 1489-1497, 2004.

## CHAPTER 3

### PHYSIOCHEMICAL CHARACTERIZATION OF FIVE GLYBURIDE POWDERS: A BCS BASED APPROACH TO PREDICT ORAL ABSORPTION

#### 3.1. Introduction

Glyburide (also known as glibenclamide) is a second-generation sulfonylurea. It is used orally as a hypoglycemic agent to treat non-insulin dependent (type II) diabetes mellitus (Neuvonen and Kivisto, 1991; Pearson, 1985). Glyburide controls sugar levels by stimulating insulin secretion in the pancreas and increases tissue sensitivity to insulin (Davis and Granner, 1996). Due to its low aqueous solubility (Löbenberg *et al.* 2000a), high bioavailability of up to 100% (Löbenberg *et al.* 2000a; Neuvonen and Kivisto, 1991), and high permeability (Vogelpoel *et al.* 2004), glyburide can be classified as a Class II drug based on the Biopharmaceutics Drug Classification System (BCS) (Löbenberg and Amidon, 2000b).

As with Class II drugs in general, glyburide's *in vivo* dissolution behaviour could be the limiting/controlling factor for absorption and bioavailability (Galia *et al.* 1998). Glyburide's solubility in gastrointestinal fluids and the changing pH in the gastrointestinal tract impacts on its *in vivo* dissolution (Patterson *et al.* 2005). Clinical studies using glyburide indicate a variability in bioavailability (USP DI, 1999) and previous studies have demonstrated that the oral absorption of glyburide is formulation-dependent (Neugebauer *et al.* 1985). The dissolution behavior of different formulations has been correlated to oral absorption characteristics and bioavailability of such products during a multinational postmarket comparative study (Blume *et al.* 1993). Many scientific approaches have been applied for the enhancement of the solubility of glyburide and to optimize its *in vivo* dissolution and bioavailability (Panagopoulou-Kaplani and Malamataris, 2000). These approaches include addition of surfactants (Singh, 1986), complex formation with cyclodextrins (Esclusa-Díaz *et al.* 1994), preparation of solid dispersion systems (Tashtoush *et al.* 2004; Valleri *et al.* 2004),

micronisation (Rupp *et al.* 1984), and crystalline-form conversion (Hassan *et al.* 1997). Processes such as spray-drying, milling and crystallization from different solvents have resulted in significant differences in the solid state properties with regard to the solubility of glyburide (Arnqvist *et al.* 1983; Hassan *et al.* 1997). The solubility of amorphous glyburide increases significantly compared to crystalline forms of the drug (Timmins *et al.* 2006).

*In vitro* and *in vivo* correlations (IVIVCs) are highly desirable for the prediction of *in vivo* performance of a dosage form (Vogelpoel *et al.* 2004). Such approaches can either be used in formulation development or retrospectively to reverse-engineer generic drugs. One way to predict the oral absorption of a drug involves the use of a mathematical model called Advanced Compartmental Absorption and Transit model (ACAT). It is commercially available under the name GastroPlus™.

The objective of this study was to investigate the solid-state (powder) properties of five pharmaceutical grades of glyburide. These five powders were either used or considered for use to produce commercial products by different manufacturers. As previously mentioned, the solid-state properties have significant influence on the bioavailability of glyburide products. This manuscript describes how an *in silico* (computer simulation) method can be used to predict the oral performance of glyburide using powder properties and other *in vitro* data as input functions into the software. The simulations were compared with clinical data that were provided from manufacturers of some glyburide formulations.

## **3.2. Materials and Methods**

### **3.2.1. Materials**

Five glyburide active pharmaceutical ingredients (APIs) were obtained from several sources: two from a German manufacturer (API-1: Lot 094; API-2: Lot 149, Hoechst AG, Frankfurt, Germany), two from South Africa (API-3: Lot IK2; API-4: Lot IK1, Comment: API-3 was milled from API-4) and API-5 (USP grade raw material: Lot RR302528/0, Fundação para o Remédio Popular (FURP), São Paulo State, Brazil).



Sodium taurocholate (crude: catalog number: T-0750) was purchased from Sigma-Aldrich (St. Louis, Missouri, USA). Egg-lecithin 60% (catalog number: 102146) was purchased from ICN Biomedicals Inc (Aurora, Ohio, USA). Potassium dihydrogen phosphate, potassium chloride, sodium chloride, sodium hydroxide, phosphoric acid and hydrochloric acid (analytical grade) were purchased from BDH (BDH Inc. Toronto, Ontario, Canada).

### **3.2.2. Scanning Electron Microscopy (SEM)**

Samples were evaluated using a JEOL JSM5900-LV scanning electron microscope (SEM, JEOL LTD., Tokyo, Japan). Analysis was carried out in low vacuum mode at 20 Pa using a voltage of 15 kV. The APIs were uniformly spread on the surface of insulated double sided carbon tape. No sputter coating was required. Micrographs were acquired at 500x magnification.

### **3.2.3. X-Ray Powder Diffraction (XRPD)**

XRPD patterns were measured using a Scintag XDS-2000 spectrometer (Thermo ARL, Ecublens, Switzerland). The instrumental conditions were as follows: Si (Li) Peltier - cooled solid state detector;  $\text{CuK}_\alpha$  source at a generator power of 45 kV and 40 mA; divergent beam (2 mm and 4 mm) and receiving beam slits (0.5 mm and 0.2 mm); scan range set from  $2\text{-}40^\circ 2\theta$  with a step size of  $0.02^\circ$  and a count time of 2 seconds. The APIs were uniformly dispersed on a quartz disk.

### **3.2.4. Thermogravimetric Analysis (TGA)**

A Perkin Elmer Diamond Thermogravimetric/Differential Thermal Analyzer (TG/DTA, Perkin Elmer Instruments, Wellesley, Massachusetts, USA) using a heating rate of  $10^\circ\text{C}/\text{min}$  from  $30^\circ\text{C}$  to  $315^\circ\text{C}$  under nitrogen at  $100\text{ mL}/\text{min}$  was used. The instrument balance was verified using a 20 mg standard weight and indium and tin were used for temperature calibration.

### 3.2.5. Differential Scanning Calorimetry (DSC)

The thermal behaviour was investigated using a TA robotic differential scanning calorimeter (Q 1000, TA Instrument Inc., New Castle, Delaware, USA). DSC analyses (sample: 5 mg, n=2) were carried out in aluminum pans under nitrogen at a flow rate of 50 mL/min. The temperature and heat flow were calibrated with indium and tin. The samples were analyzed from 30°C to 185°C using a heating rate of 10°C/min. The amorphous form of glyburide was prepared by DSC following the modified melting and quench cooling method (Panagopoulou-Kaplani and Malamataris, 2000; Patterson *et al.* 2005). Samples (5 mg) were heated in aluminium pans at 10°C/min to 185°C (complete melt) and then cooled to room temperature at 10°C/min.

The glass transition of the amorphous form was measured by reheating the amorphous melt using three heating rates (20, 50 and 100°C/min). The furnace temperature was cooled to 30°C between each successive heating cycle past the compound's glass transition temperature. A similar method was applied to all glyburide lots to ensure the absence of amorphous content, which could drastically affect the dissolution of the API.

### 3.2.6. Raman Spectroscopy

A Bruker RFS 100/S FT-Raman spectrometer (Bruker Optics Inc., Billerica, Massachusetts, USA) was used along with BrukerQuant 2 software for spectral analysis. The laser power was set to 250 mW with a scan range from 3500-0  $\text{cm}^{-1}$ , a scan resolution of 4  $\text{cm}^{-1}$ , an aperture setting of 3.5 and a scan number of 64 -256. Raman spectra for both the surface of intact and ground glyburide tablets were recorded by averaging three measurements. The surface of the tablets were analyzed by spectrally averaging three different positions on the tablet's surface, the powders were re-packed and re-analyzed 3 times in 2-mm diameter metal sample holders to ensure reproducibility of the results and minimize the effects of sample inhomogeneity. Spectral processing using first derivative and vector normalization was applied to the spectra prior to analysis.

### 3.2.7. Particle Size Analysis

The particle size and particle distribution of the glyburide APIs were analyzed by a particle size analyzer (COULTER<sup>®</sup> LS 230 Particle Size Analyzer, Coulter Corporation, Fullerton, California, USA).

Suspensions of the glyburide APIs were prepared in a solvent (0.1% w/v) solution consisting of lecithin in 2,2,4-trimethylpentane. The particles were well-dispersed and no significant agglomerates were present in the solution. Continuous agitation at 50 rpm was applied during measurements and the particle size distribution data were presented as arithmetic means based on size, 10% (D10), 25% (D25), 50% (D50), 75% (D75) and 90% (D90) of the particle volume undersize. The percentage volume undersize is the percentage of the total volume of particles in the distribution profile below a specific particle size.

### 3.2.8. Specific Surface Area Measurement

Measurement of the specific surface area of solids was performed with a Quantachrome Autosorb-1 surface area and pore size analyzer (Quantachrome Instruments, Boynton Beach, Florida, USA). The instrument was connected via the lower back panel to nitrogen and helium lines (both regulated at 10 psi). The vacuum gauges were set to 10 and 100 millitorr, respectively. The cold trap, which was filled with liquid nitrogen during operation, was maintained at 77° K to trap impurities from the gas lines. The instrument was calibrated using standard powders obtained from Quantachrome for multipoint BET (Brunauer, Emmett and Teller equation) analysis. The surface area of the standard reference was 2.17 m<sup>2</sup>/g with a 95% reproducibility limit of 0.19 m<sup>2</sup>/g (Quantachrome catalogue No. 20007: lot No. 3101, Quantachrome Instruments, Boynton Beach, Florida, USA).

### **3.2.9. Density Measurement**

The densities of the glyburide APIs were measured with a Quantachrome Ultracycrometer 1000 (Quantachrome Instruments, Boynton Beach, Florida, USA) under helium at 18 psi and the samples were stored in desiccators overnight. Duplicate measurements were performed at 23.7°C using a flow purge of 30 min.

### **3.2.10. Dissociation Constant ( $pK_a$ ), Partition Coefficient ( $\log P$ ) and Distribution Coefficient ( $\log D$ )**

The  $pK_a$ ,  $\log P$  and  $\log D$  of glyburide APIs were measured by spectrophotometric titrations using a Sirius flagship instrument for  $pK_a$  and  $\log P$  using pH-metric technology (GL $pK_a$ ) in combination with a D-Pas detector (Sirius Analytical Instruments Ltd., East Sussex, UK). Data acquisition was achieved with Refinement Pro software V1.104 (Sirius Analytical Instruments Ltd., East Sussex, UK). UV absorbance measurements were performed using a fiber optic probe and photodiode array detector (Sirius Analytical Instruments Ltd, East Sussex, UK) equipped with a deuterium lamp. Titrations using different concentrations of KOH or HCl were performed in aqueous media containing 0.15M KCl under argon 60 mL/min, at 25°C.

### **3.2.11. Solubility Determination**

Twenty milligrams (excess) API-2 were added to 10 mL of FaSSIF (fasted state simulated intestinal fluid containing 3mM sodium taurocholate and 0.75 mM lecithin (Galia *et al.* 1998) at pH 1.7, 5.0, 6.5, 7.4 and stirred overnight (12 h) at 37±0.5°C in a water bath. The pH of each sample was checked during the experiment and the resulting solution was then filtered through a 0.22  $\mu$ m Millex-GP membrane filter (Millipore, Bedford, Massachusetts, USA). The filter membrane was checked for glyburide adsorption (known concentrations of the samples were checked by HPLC before and after filtration) and solubility was determined by HPLC analysis.

### 3.2.12. Computer Simulations

The *in vitro* data were applied to previously used simulation protocols (Wei and Löbenberg, 2006) accordingly adapted. GastroPlus™ (version 5.1, Simulations Plus Inc., Lancaster, California, USA) was used to estimate absorption and pharmacokinetics of the five APIs. The program requires insertion of the relevant physicochemical, physiological and pharmacokinetic input data in specific spread sheets provided in the software program. These data include properties such as the physical and chemical characteristics of the APIs, gastrointestinal permeability and the relevant dose information. Bulk density, solubility, pKa, LogD, particle size and particle distribution were obtained from the material characterization described above. The human permeability ( $P_{eff}$ ) of glyburide was estimated as  $3.5 \times 10^{-4}$  cm/s (Wei and Löbenberg, 2006). The solubility-pH profiles of glyburide were obtained as previously described (Wei and Löbenberg, 2006) and the diffusion coefficient of glyburide was estimated using GastroPlus™. The same dose as administered in the clinical studies was used for the simulations.

The immediately release dosage form model was selected in GastroPlus™. The physicochemical data including pKa, logD, solubility, particle size distribution and the drug dose were used by the software to calculate the drug concentration in each compartment. Pharmacokinetic data were obtained from clinical studies performed on products containing the relevant glyburide APIs (Blume *et al.* 1993; Kanfer, 2003). German reference (GR, 15 volunteers) and test (GT, 15 volunteers) products (dose 3.5 mg) contain API-2 and South Africa test 1 (ST 1, 31 volunteers) and 2 (ST 2, 28 volunteers) products (dose 5 mg) from South Africa contain API-3 and API-4. Pharmacokinetic parameters of the clinically observed mean data such as volume of distribution, clearance and micro-rate constants (Table 3.1) were obtained using the Kinetica software package (version 3.0, InnaPharse Corporation, Philadelphia, Pennsylvania, USA) and were entered into the pharmacokinetic spreadsheet in GastroPlus™.

In the “Physiological Data” input spreadsheet, the human fasted state model was chosen and the default values for transit time and pH were selected for each

compartment. The recommended absorption scale factor model (logD model) was chosen to account for absorption.

**Table 3.1.** Pharmacokinetic parameters of different products used for the computer simulations. The mean values of the clinical data obtained from these four products were well described by a two-compartmental model (Rydberg *et al.* 1997).

	C <sub>max</sub> (ng/mL)	AUC <sub>0-n</sub> <sup>*</sup> (ng/mL*h)	Clearance (L/h)	V <sub>c</sub> (L)	K <sub>12</sub> (h <sup>-1</sup> )	K <sub>21</sub> (h <sup>-1</sup> )
GR (API-2)	301	1359.6	2.47	1.83	0.409	0.100
GT (API-2)	221	1441.3	1.64	6.18	0.161	0.069
ST 1 (API-3)	196	1067.0	3.91	9.69	0.151	0.043
ST 2 (API-4)	95	563.8	7.40	2.31	0.406	0.235

n<sup>\*</sup>: GR: 24 h; GT: 24 h; ST 1: 30 h; ST 2: 36 h

### 3.2.13. Statistics

Percent Prediction Error (%PE) was calculated according to the FDA Guidance for industry using Eq. 3.1 (FDA, 1997) below.

$$\%PE = \frac{Observed - Predicted}{Observed} \times 100 \quad (3.1)$$

Linear regression analysis for the observed vs. simulated data using a 95% confident interval was performed using Excel (Microsoft Inc. Seattle, Washington, USA).

In all cases, significance of differences between experiments was calculated by Student's t test using two-tailed distributions and two-sample equal variance (Microsoft Excel, Version 2000, Microsoft Inc. Seattle, Washington, USA). Statistical significance was calculated at the 95% (p < 0.05) confidence level.

### 3.3. Results

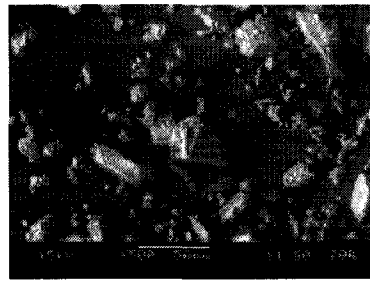
#### 3.3.1. Surface Area, Density, Particle Size and Morphology

The SEM micrographs were used to determine the particle size and morphology of the five glyburide APIs (Fig. 3.1). All five APIs consisted of irregularly shaped particles. However, each glyburide API had different particle sizes and size distributions which might be due to the different manufacturing or milling processes (Chikhalia *et al.* 2006). API-1 had the largest particle size and widest particle size distribution (Table 3.2). API-1 was the least cohesive powder due to its larger particle size. The particle size and size distributions of API-2 and API-5 were similar, but more of the larger particles existed in API-5 samples. The particle size and size distributions of API-3 and API-4 were smaller compared to the other three APIs. API-3 had smaller and more uniform particles compared to API-4. This was confirmed by the processing information obtained from the supplier who stated that API-3 was made by milling API-4.

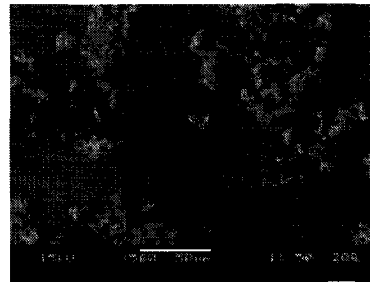
The physicochemical parameters of the five glyburide APIs including specific surface area, density and particle size and particle size distribution are given in Table 3.2. API-1 contained the biggest particles and had the widest size distribution followed by API-5, API-2, API-4 and API-3. The surface area of API-1 was the smallest followed by API-5, API-2, API-4 and API-3 which confirms the visual observation using SEM data. Particle size, surface area and SEM data confirmed that API-3 was produced by milling API-4.

**Table 3.2.** Physicochemical data determined for five glyburide APIs

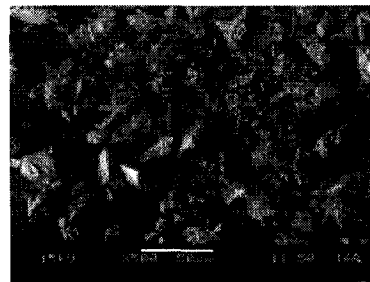
	density (n=2, g/mL)	Surface area (m <sup>2</sup> /g)	Mean particle size and SD (μM)	D10 (μM)	D25 (μM)	D50 (μM)	D75 (μM)	D90 (μM)
API-1	1.35	0.45	22.65±25.39	0.96	2.82	11.73	36.66	61.77
API-2	1.38	1.67	12.55±12.87	1.31	3.47	8.41	17.47	29.69
API-3	1.35	3.96	4.25±3.97	0.76	1.49	2.94	5.57	9.75
API-4	1.35	3.48	5.18±5.19	0.88	1.84	3.63	6.61	11.35
API-5	1.36	1.53	15.10±16.80	1.15	3.20	8.71	20.95	39.12



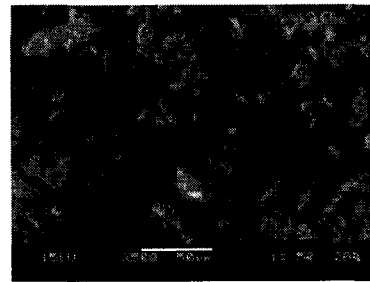
API-1



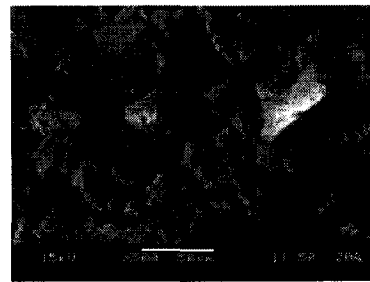
API-3



API-2



API-4



API-5

**Figure 3.1.** Particle appearance of the five glyburide powders using SEM



### 3.3.2. Crystallinity and Form Determination

XRPD was used to determine the extent of crystallinity and the identity of crystalline forms present in the five APIs (Fig. 3.2) (Panagopoulou-Kaplani and Malamataris, 2000). The XRPD results showed no distinguishable differences in the diffraction patterns between the different APIs. There were no detectable amounts of amorphous drug in the API samples. This indicated that all five APIs consisted of the same crystalline form. However, XRPD might not be sensitive enough to detect small quantities of different crystal forms or small amounts of amorphous drug. Typically the detection limit of this method for the detection of amorphous forms requires at least 10% amorphous content (Salekigerhardt *et al.* 1994).

Raman spectroscopy can be used to investigate both chemical and physical characteristics of solid-state materials. Szép *et al.* (2005) reported that the characteristic bands of commonly used excipients such as lactose monohydrate and corn starch are below  $1500\text{ cm}^{-1}$ . In order to avoid any overlap with excipients, the measured range,  $1650$  to  $1500\text{ cm}^{-1}$ , a range associated primarily with carbon-carbon double bonds and phenyl ring stretching and breathing, was selected. The acquired whole Raman spectra of the five APIs were almost identical (Fig. 3.3) and the spectra for the API in the tablets were almost identical to the API raw material spectra. However, all the above spectra were remarkably different from the spectra of the amorphous forms produced, where a shift to the high wave number was observed (Fig. 3.4). These results indicated that all the APIs were constitutionally similar, which is in agreement with the results from XPRD.

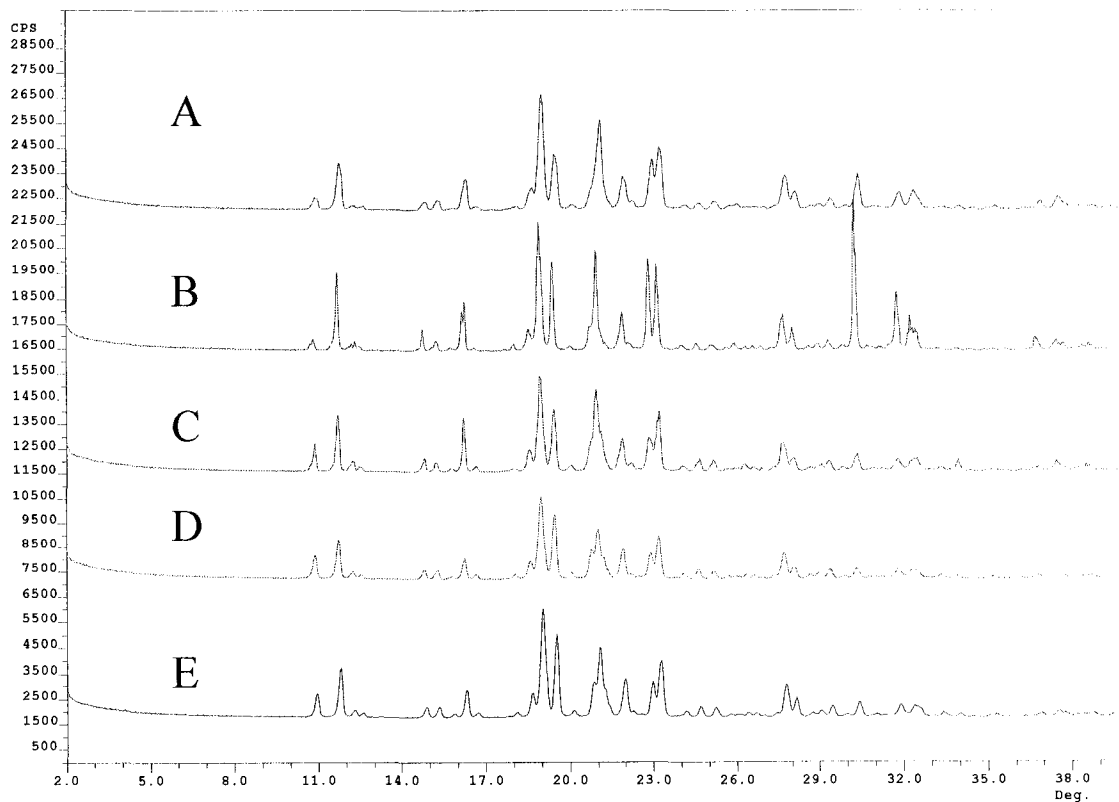


**Figure 3.2.** Comparison of X-ray diffraction spectra of five glyburide APIs (A: API-2; B:API-1; C:API-5; D:API-3; E:API-4)

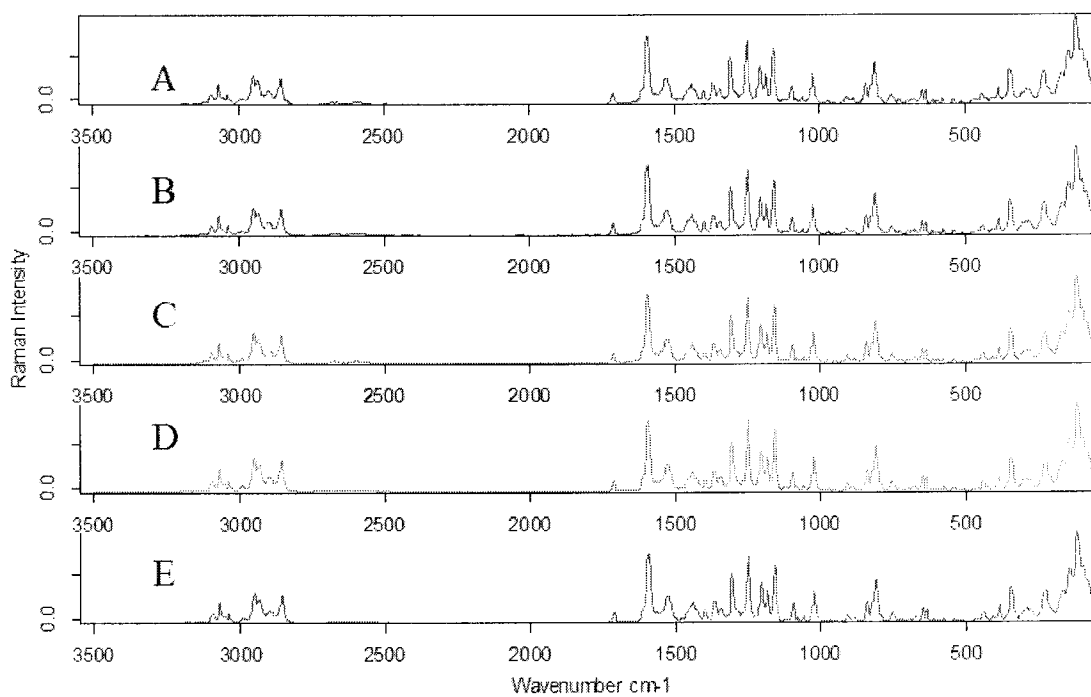


**Figure 3.3.** Comparison of the Raman spectra for five glyburide APIs (A: API-4; B: API-3; C: API-5; D: API-1; E: API-2)

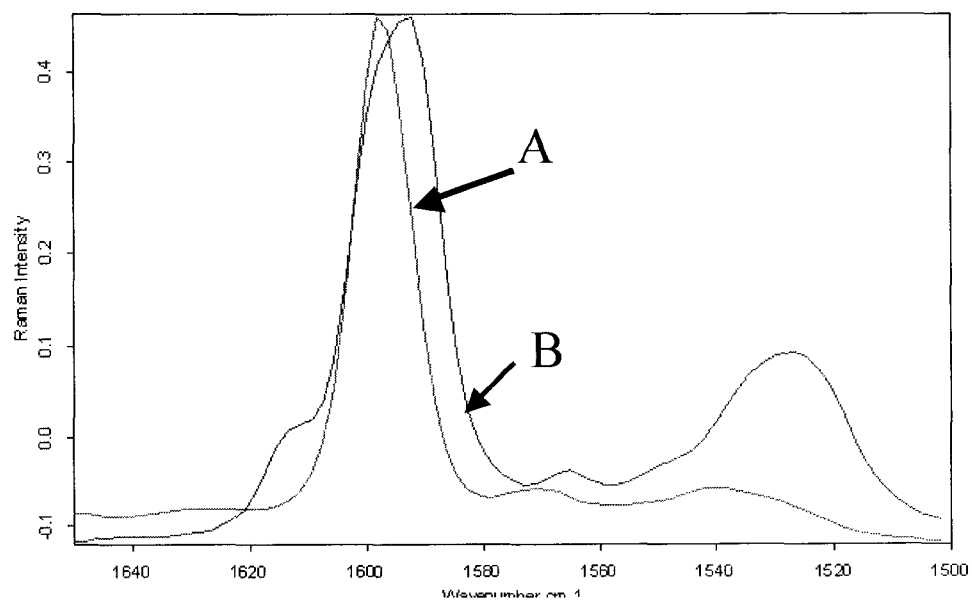


**Figure 3.4** Comparison of the Raman spectra between crystal and amorphous glyburide forms (A: amorphous glyburide; B: API-2 crystal)

### 3.3.3. Thermal Analysis

Considering instrument variability, the acquired TGA spectra (Fig. 3.5) from all five APIs were similar. One common thermal property of all five APIs was that they degraded above the melting point (175°C). The onset of the degradation temperature range was from 195 to 200°C. The weight loss from 30°C to melting point (175°C) was negligible and probably due to the low volatile content and non-hygroscopic nature of glyburide.

The entire range (30°C - 185°C) of the DSC curves (data not shown) for all five APIs showed only one single sharp endothermic peak at 175°C, corresponding to its melting point. There were no glass transition (T<sub>g</sub>) or recrystallisation exothermic peaks in the DSC curves which confirmed that no amorphous forms were present in the APIs (Chikhaliya *et al.* 2006). The DSC curves (range from 160°C to 185°C) of the APIs are shown in Fig. 3.6. The enthalpy ( $\Delta H$ ) of all five APIs was determined as: API-1 (90 J/g), API-2 (99 J/g), API-3 (102 J/g), API-4 (98 J/g), and API-5 (92 J/g). Although API-1 had the lowest enthalpy, no amorphous content was detected by any of these methods described in this study. The lower enthalpy may simply be due to greater crystalline defects relative to the other glyburide batches. The endothermic peak of the crystalline API corresponding to its melting point will broaden with the reduction of enthalpy if the amorphous drug or other impurities are present (Valleri *et al.* 2004). The endothermic peak of API-3 was the sharpest. The endothermic peaks of API-1 and API-5 were broader compared to the others but the difference can be considered minor. The amorphous form of glyburide API was produced by a modified Melting and Quench Cooling method (Panagopoulou-Kaplani and Malamataris, 2000; Patterson *et al.* 2005). Detection of the amorphous form can be achieved by applying high ramp temperature rates to the samples (<http://pslc.ws/macrog//dsc.htm>). In this study, ramp rates (20, 50 and 100<sup>0</sup>C/min) were applied for each heating and cooling cycle. The glass transition temperature of the amorphous form obtained from the Melting and Quench Cooling method using this cycle temperature program was determined to be approximately 60°C. The glass transition curve of the amorphous form was sharper when the ramp rate was increased, especially at 100°C/min (Fig. 3.7). The same temperature program was applied to the five APIs. No

glass transition curves were detected even at the highest ramp rate. This indicates that the APIs did not contain any detectable or appreciable amounts of amorphous material.

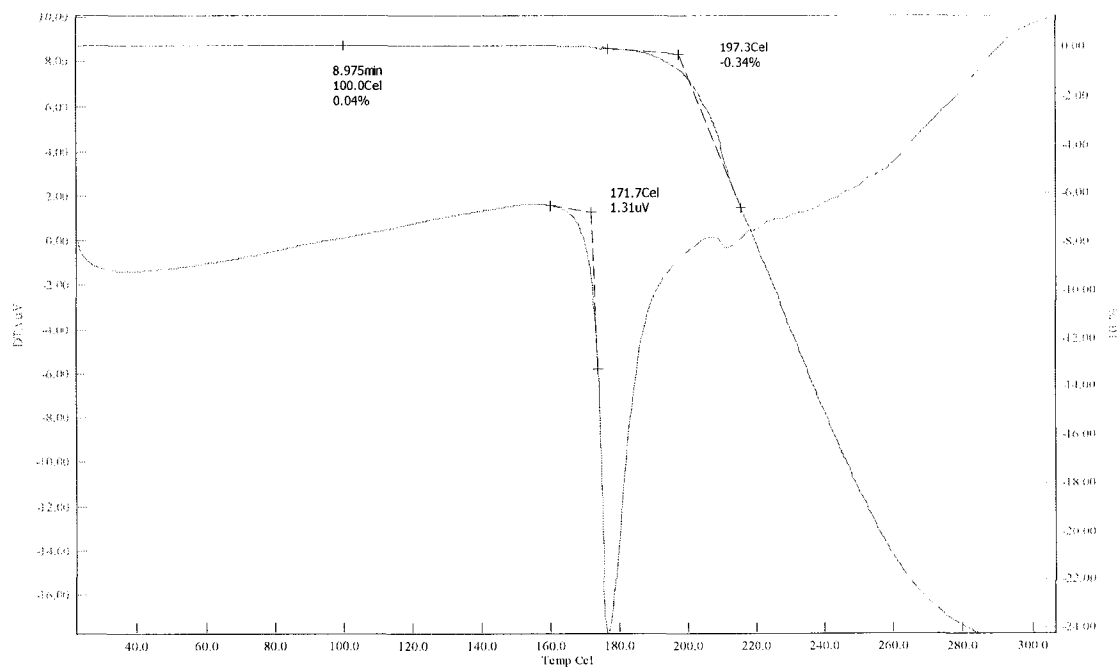


**Figure 3.5.** TGA spectrum of API-1

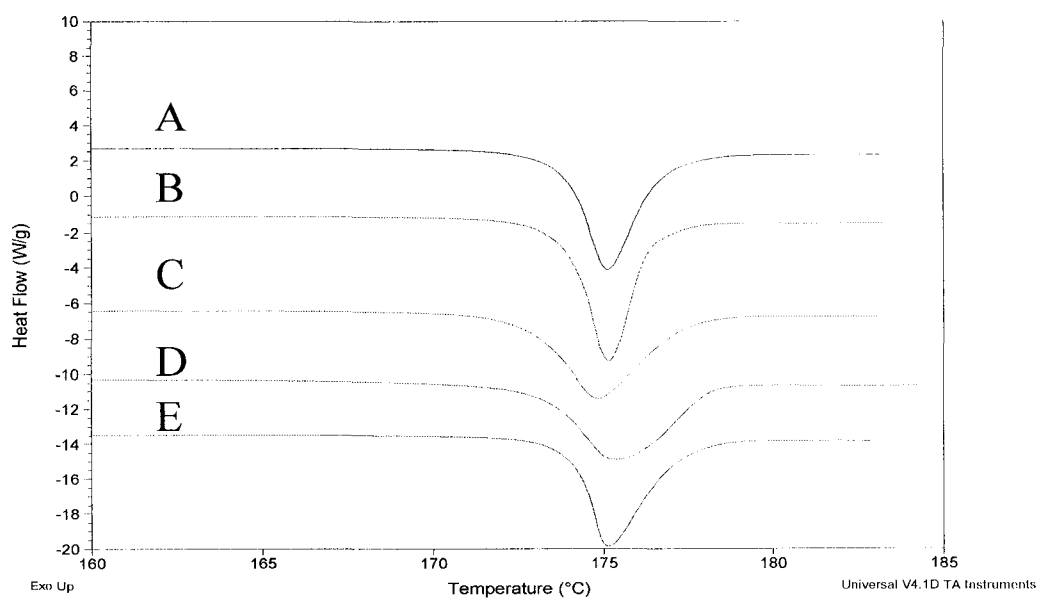


**Figure 3.6.** Comparison of five glyburide APIs using DSC (A: API-4; B: API-3; C: API-5; D: API-1; E: API-2)

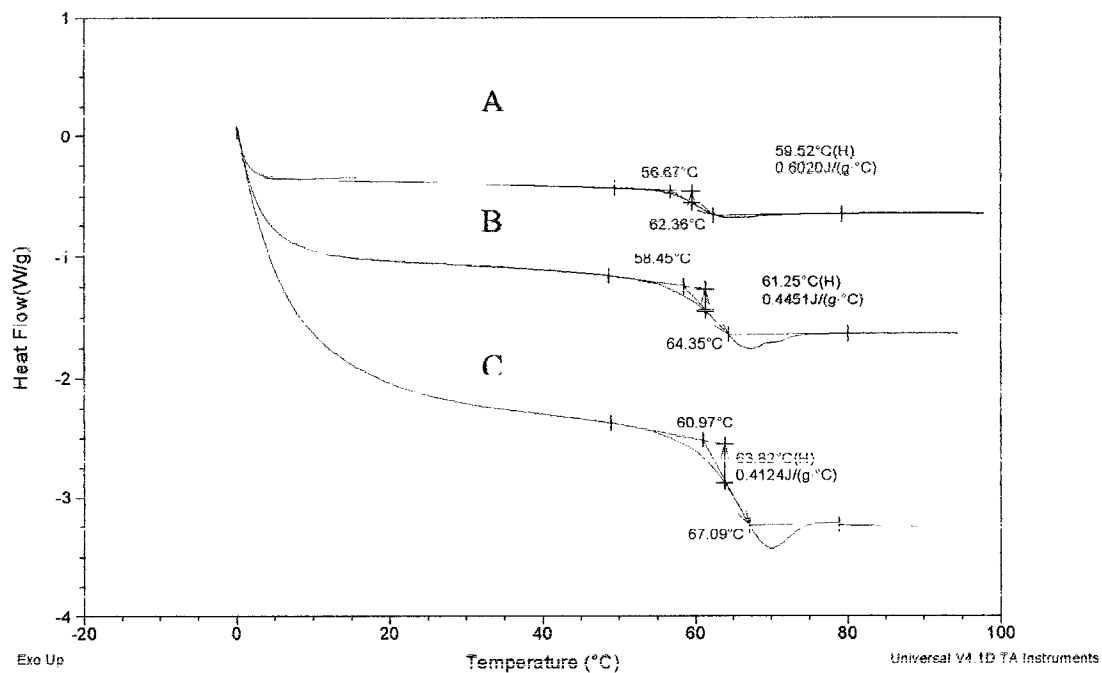


**Figure. 3.7.** Glass transition curves of amorphous glyburide obtained at different heating rates (A. 20<sup>0</sup>C/min; B. 50<sup>0</sup>C/min; C. 100<sup>0</sup>C/min)



### 3.3.4. pK<sub>a</sub>, LogP and LogD Measurements

The experimental pK<sub>a</sub> and logP of the glyburide APIs were 5.1 and 4.5, respectively. This is in agreement with data reported in literature (pK<sub>a</sub> 5.3) (The merck index, 1989). The logD profile was derived from the pK<sub>a</sub> and logP data.

### 3.3.5. Computer Simulations

The predicted plasma time curves were compared with the *in vivo* data obtained from the mean drug concentrations in plasma data following administration of the relevant products to healthy volunteers (Blume *et al.* 1993; Kanfer, 2003). Fig. 3.8 shows the observed and predicted data for API-2. API-2 from this manufacturer was used in a *in vivo* bioequivalence study between GR and GT products. The simulation of the GR product predicts C<sub>max</sub>, T<sub>max</sub> and AUC<sub>0-24</sub> within prediction errors of 1.9%, 20% and 9.4%, respectively. Raman spectroscopy was used to compare the drug powders in this product with the test product (data not shown). The results suggested that the API in both products were similar. Based on this assumption the oral performance of the GT product was simulated using its clinically observed PK data and the physicochemical input data of API-2. The simulation predicts C<sub>max</sub>, T<sub>max</sub> and AUC<sub>0-24</sub> within prediction errors of 9.4%, 15% and 6.4%, respectively. The differences between both products seem to be formulation dependent e.g. use of different excipients which might cause different pharmacokinetic profiles after *in vivo* studies. Fig. 3.9 shows simulations of product ST 1 and ST 2 containing API-3 and API-4, respectively. As mentioned previously, API-3 was milled from API-4. API-3 had a smaller particle size and particle size distribution. Bioavailability studies on these two products were performed in different sets of subjects. This might explain the differences in the observed profiles. However, the absorption patterns calculated by the ACAT model were found to be similar for both products. The simulations for API-3 and API-4 predict C<sub>max</sub>, T<sub>max</sub> and AUC within prediction errors of 0.8% and 4.6%, 4.0% and 20%, 2.3% and 15.2%, respectively. The simulation results using only the *in vitro* data as input functions showed that the *in silico* model was suitable to predict the oral absorption of the four glyburide products.

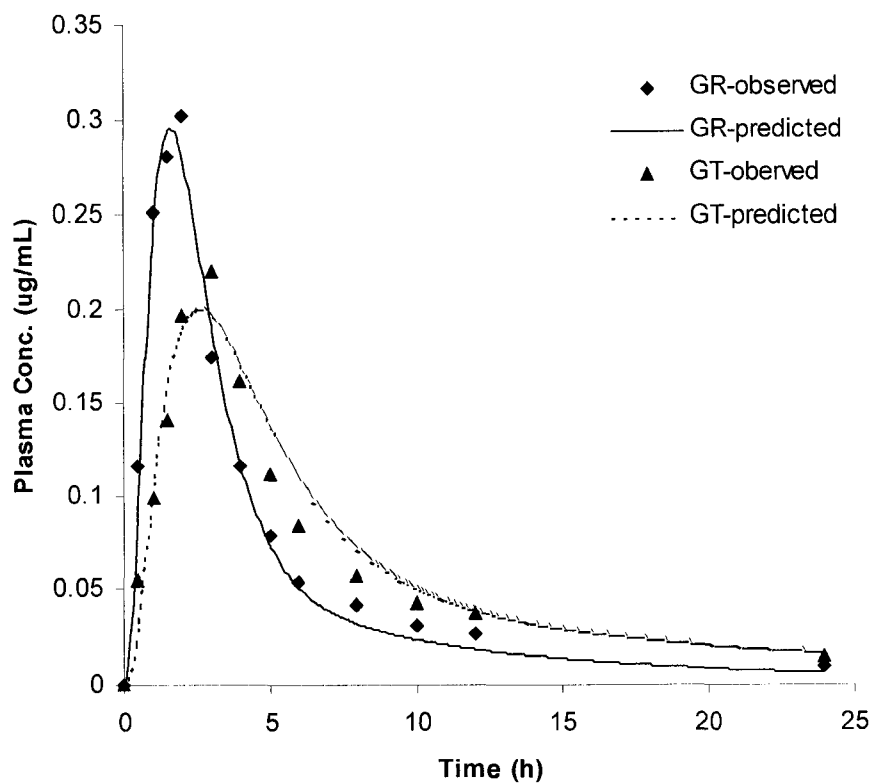


**Figure 3.8.** Comparison of the simulated and observed data for German reference (GR) and test (GT) products containing API-2 using physicochemical data as input for the simulation

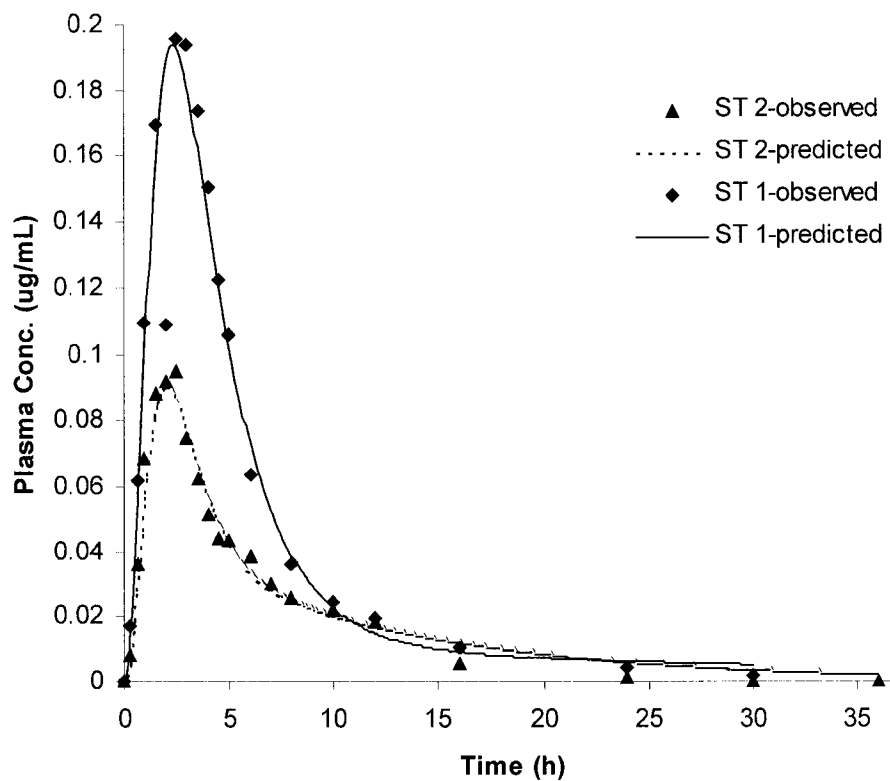


**Figure 3.9.** Comparison of the simulated and observed data for South Africa test 1 (ST 1) and test 2 (ST 2) products containing API-3 and API-4, respectively using physicochemical data as input for the simulation.

### 3.4. Discussion

Glyburide is absorbed throughout the entire gastrointestinal tract (Brockmeier *et al.* 1985); therefore, it is a good model drug for simulation using the ACAT model. Literature describes different crystal and amorphous forms of glyburide. Chikhalia *et al.* (2006) discussed that the milling processes could activate the surface of drug particles by energy transfer and form a peripheral disordered layer that had amorphous characteristics. APIs containing amorphous forms and peripheral disordered layers might have greater weight loss than pure crystals when the temperature is increased. Such effects can be detected by sublimation of the amorphous layer and will change the TGA thermogram. API-3 which was milled from API-4 showed the same thermal property in the TGA analysis compared to API-4. The results of XPRD, DSC and Raman spectroscopy indicated that no differences in the composition existed between the five investigated APIs. The possibility of polymorphism can be eliminated based on the material characterizations. Panagopoulou-Kaplani and Malamataris (2000) reported crystal form conversions during the production and storage of glyburide in tablets. The solubility of such recrystallized API had changed significantly. The results obtained in the present study derived from Raman spectra showed there were no significant crystal conversions during the production and storage of the products investigated.

The material characterizations using SEM, particle size and size distribution analysis further showed that significant differences between the APIs were detected only for the particle size and particle size distribution. A reduced particle size of an API can improve the solubility and intrinsic dissolution rate, therefore an influence on the drug's bioavailability may be expected (Atkinson *et al.* 1962). Pharmaceutical preparations which used micronized glyburide showed better absorption, less variability and required a lower dose compared to non-micronized glyburide (Suleiman and Najib, 1989). Timmins *et al.* (2006) showed that controlled particle size distribution can significantly influence the reproducibility of a product's bioavailability (Cordes and Müller, 1996). Balan *et al.* (2000) optimized glyburide formulations as shown by comparing the bioavailability of different formulations that contained different particle sizes of glyburide. They showed that a controlled particle size and size distribution reduced the variability in

bioavailability. Table 3.3 shows an example of the possible impact on drug absorption when the particle size or particle size distribution of the product containing API-4 is changed. In the first case, the particle size was theoretically decreased (down to 25%) or increased (up to 400%) while size distribution was kept constant. In the second case, the particle size distribution was theoretically decreased (down to 25%) or increased (up to 400%) while the mean particle size was kept constant. The theoretical predicted impact on  $C_{max}$ , AUC and  $T_{max}$  are shown in table 3.3. The influence of the particle size and size distribution on the AUC and  $C_{max}$  are similar. Particle size has, as expected, a more pronounced influence on  $T_{max}$  compared to an increase in particle size distribution. Such simulations may be used by formulation scientists to set particle size and particle size distribution specifications for APIs and allow predictions to be made when an API's particle size or particle size distribution may cause an unacceptable deviation from the observed plasma concentrations vs. time. In early drug development, such simulations can be used to estimate plasma concentration levels and can help to define which formulation approach could be used to develop a suitable drug product. This can shorten the time needed for the drug development process because biowaivers may be justified on the basis of simulation studies (Balan *et al.* 2000; Cordes and Müller, 1996). Another application of such simulations might be the optimization of an existing dosage form or the pre-selection of a dosage form for a drug under development. Here the formulation scientist can use the pre-defined dosage form models of the software to improve drug plasma concentration vs. time curves. Examples are gastric drug release from a floating dosage form or simulation of the passage through the gastrointestinal tract of a dispersed vs. an integral dosage form. However, it has to be pointed out that such simulations have to assume that the dosage form does not impact the pharmacokinetic parameters. The last example for the application of predictive simulations is reverse engineering of drug products. If the physicochemical data for API-1 was used in the simulations the resulting plasma concentration vs. time curve would be significantly different from the other APIs. It was previously demonstrated by the impact on drug absorption when the particle size or particle size distribution was theoretically changed (Table 3.3). Products made with API-1 probably do not meet current bioequivalence criteria. Formulation scientists can input the physicochemical data of the API they intend to use and predetermine if it has an

appropriate particle size and size distribution. This can assist in defining further manufacturing processes such as the necessity of milling.

### **3.5. Conclusions**

The material characterizations of the five glyburide APIs showed the absence of crystalline differences between the APIs studied. However, the five APIs showed differences in surface area, particle size and size distribution. Such differences might influence the dissolution and bioavailability of glyburide. Particle size, being a key parameter for drug dissolution, was used in the ACAT model to predict the oral performance of different glyburide products. A basic *in vitro/in vivo* relationship between the API particle size and clinically observed plasma versus time profiles was established for three APIs. The information obtained by such *in silico* models can be valuable for formulation scientists to set meaningful API specifications, develop new drug products or to reverse engineer generic versions of existing drug products. Bioequivalence studies may justifiably be waived based on computer simulations.

**Table 3.4.** Simulated impact of changes in particle radius and particle size distribution (standard deviation) on the oral performance of a glyburide product containing API-4. The measured particle size “mean” and the particle size distribution were theoretically manipulated. The simulated values are listed and the % change compared to the mean value are given in brackets

<b>Particle Radius (<math>\mu\text{M}</math>)</b>	<b>0.65<math>\pm</math>2.6</b>	<b>1.3<math>\pm</math>2.6</b>	<b>2.6<math>\pm</math>2.6 (mean)</b>	<b>5.2<math>\pm</math>2.6</b>	<b>10.4<math>\pm</math>2.6</b>
AUC <sub>0-36</sub>	650.1 (+0.1%)	649.9 (+0%)	649.2	646.2 (-0.5%)	622.5 (-4.1%)
C <sub>max</sub>	0.097 (+7.8%)	0.095 (+5.6%)	0.090	0.079 (-12.2%)	0.057 (-36.7%)
T <sub>max</sub>	1.8 (-10%)	1.9 (-5.0%)	2.0	2.4 (+20%)	3.5 (+75%)
<b>Standard Deviation (SD <math>\pm\mu\text{M}</math>)</b>	<b>2.6<math>\pm</math>0.7</b>	<b>2.6<math>\pm</math>1.3</b>	<b>2.6<math>\pm</math>2.6 (mean)</b>	<b>2.6<math>\pm</math>5.2</b>	<b>2.6<math>\pm</math>10.4</b>
AUC <sub>0-36</sub>	650.2 (+0.2%)	650.1 (+0.1%)	649.2	643.4 (-0.9%)	612.9 (-5.6%)
C <sub>max</sub>	0.101 (+12.2%)	0.098 (+8.9%)	0.090	0.077 (-14.4%)	0.061 (-32.2%)
T <sub>max</sub>	1.9 (-5%)	1.9 (-5%)	2.0	2.16 (+8%)	2.4 (+20%)

AUC: ng/mL\*h; C<sub>max</sub>: ng/mL; T<sub>max</sub>: h

### 3.6. References

Arnqvist, H. J., Karlberg, B. E. and Melander, A. Pharmacokinetics and effects of glibenclamide in two formulations, HB 419 and HB 420, in type 2 diabetes. *Annals Clin. Res.* 15 (Suppl. 37), 21-25, 1983.

Atkinson, R. M., Bedord, C., Child, K. J. and Tomich, E. J. Effect of particle size on blood griseofulvin levels in man. *Nature.* 193, 588-589, 1962.

Balan, G., Timmins, P., Greene, D.S. and Marathe, P. H. In-vitro In-vivo correlation models for glibenclamide after administration of metformin/glibenclamide tablets to healthy human volunteers. *J. Pharm. Pharmacol.* 52, 831-838, 2000.

Blume, H., Ali, S. L. and Siewert, M. Pharmaceutical quality of glibenclamide products: a multinational postmarket comparative study. *Drug. Dev. Ind. Pharm.* 19, 2713-2741, 1993.

Brockmeier, D., Grigoleit, H. G. and Leonhardt, H. Absorption of glibenclamide from different sites of the gastro-intestinal tract. *Eur. J. Clin. Pharmco.* 29 (2), 193-197, 1985.

Chikhalia, V., Forbes, R. T., Storey, R. A. and Ticehurst, M. The effect of crystal morphology and mill type on milling induced crystal disorder. *Eur. J. Pharm. Sci.* 27, 19-26, 2006.

Cordes, D. and Müller, B. W. Deactivation of amorphous glibenclamide during dissolution. *Eur. J. Pharm. Sci.* 4, 187, 1996.

Davis, S. N. and Granner, D. K. Insulin, oral hypoglycemic agents and the pharmacology of endocrine pancreas. In *The Pharmacological Basis of Therapeutics*, 9<sup>th</sup> Ed.; Gilman, A.G., Ed.; McGraw-Hill: New York, 1487-1518, 1996.

Esclusa-Díaz, M. T., Torres-Labandeira, J. J., Kata, M. and Vila-Jato, J. L. Inclusion complexation of glibenclamide with 2-hydroxypropyl- $\beta$ -cyclodextrin in solution and in solid state. *Eur. J. Pharm. Sci.* 1 (6), 291-296, 1994.



Galia, E., Nicolaides, E., Hörter, D., Löbenberg, R., Reppas, C. and Dressman, J. B. Evaluation of various dissolution media for predicting in vivo performance of class I and II drugs. *Pharm. Res.* 15 (5), 698-705, 1998.

FDA, Guidance for industry: Extended release oral dosage forms: development, evaluation and application of in vitro/in vivo correlations. U.S. Department of Health Food and Drug Administration Center for Drug Evaluation and Research. 1997.

Hassan, M. A., Sheikh Salem, M., Sallam, E. and Al-Hindawi, M. K. Preparation and characterization of a new polymorphic form and a solvate of glibenclamide. *Acta Pharmaceutica Hungarica.* 67 (2-3), 81-88, 1997.

<http://pslc.ws/cacrog//dsc.htm>, Polymer Science Learning Center, Department of Polymer Science, The University of Southern Mississippi

Kanfer, I. Personal communication, Faculty of Pharmacy, Rhodes University, South Africa, 2003.

Löbenberg, R., Krämer, J., Shah, V. P., Amidon, G. L. and Dressman, J. B. Dissolution testing as prognostic tool for oral drug absorption: dissolution behavior of glibenclamide. *Pharm. Res.* 17 (4), 439-444, 2000a.

Löbenberg, R. and Amidon, G. L. Modern bioavailability, bioequivalence and biopharmaceutics classification system. New scientific approaches to international regulatory standards. *Eur. J. Pharm. Biopharm.* 50, 3-12, 2000b.

Neuvonen, P. J. and Kivisto, K. T. The effects of magnesium hydroxide on the absorption and efficacy of two glibenclamide preparations. *Br. J. Clin. Pharmacol.* 32, 215-220, 1991.

Neugebauer, G., Betzien, G., Hrstka, V., Kaufmann, B., Möllendorff, E. V. and Abshagen, U. Absolute bioavailability and bioequivalence of glibenclamide (Semi-Euglucon<sup>®</sup>N). *Int. J. Clin. Pharmacol. Therapy and Toxicology.* 23 (9), 453-460, 1985.

Panagopoulou-Kaplani, A. and Malamataris, S. Preparation and characterization of a new insoluble polymorphic form of glibenclamide. *Int. J. Pharm.* 195, 239-246, 2000.

- Patterson, J. E., James, M. B., Forster, A. H., Lancaster, R. W., Butler, J. M. and Rades, T. The influence of thermal and mechanical preparative techniques on the amorphous state of four poorly soluble compounds. *J. Pharm. Sci.* 94 (9), 1998-2012, 2005.
- Pearson, J. G. Pharmacokinetics of glyburide. *Am. J. Med.* 79 (suppl. 3B), 67-71, 1985.
- Rupp, W., Badian, M., Heptner, W. and Malerczyk, V. Bioavailability and in vitro liberation of glibenclamide from a new dosage form. *Biopharm. Pharmacokinet. Eur. Congr.* 2<sup>nd</sup> 1, 413-420, 1984.
- Rydberg, T., Jönsson, A., Karlsson, M. and Meldander, A. Concentration-effect relations of glibenclamide and its active metabolites in man: modeling of pharmacokinetics and pharmacodynamics. *Br. J. Clin. Pharmacol.* 43, 373-381, 1997.
- Salekigerhardt, A., Ahlneck, C. and Zografí, G. Assessment of disorder in crystalline solids. *Int. J. Pharm.* 101 (3), 237-247, 1994.
- Singh, J. Effect of sodium lauryl sulfate and Tween<sup>®</sup> 80 on the therapeutic efficacy of glibenclamide tablet formulation in terms of BSL lowering in rabbits and diabetic human volunteers. *Drug Dev. Ind. Pharm.* 12, 851-866, 1986.
- Suleiman, M. S. and Najib, N. M. Isolation and physicochemical characterization of solid forms of glibenclamide. *Int. J. Pharm.* 50 (2), 103-109, 1989.
- Szép, A., Marosi, G. Y., Bálint, M. and Bódis, M. Micro-Raman spectroscopy of solid pharmaceuticals. Proceeding of the 8<sup>th</sup> polymers for advanced technologies international symposium, Budapest, Hungary, 9,13-16, 2005.
- Tashtoush, B., Al-qashi, Z. S. and Najib, N. M. In vitro and in vivo evaluation of glibenclamide in solid dispersion systems. *Drug Dev. Ind. Pharm.* 30 (6), 601-607, 2004.
- The Merck Index. 11<sup>th</sup> editon, Merck & Co., Inc, Rahway, New Jersey, USA, 1989.
- Timmins, P., Marathe, P. H., Cave, G., Arnold, M. E., Dennis, A. B. and Greene, D. S. Development of a glyburide-metformin fixed combination tablet with optimized glyburide particle size. *Drug Dev. Ind. Pharm.* 66, 25-35, 2006.

United States Pharmacopeia, USP DI. *Drug Information for Health Care Professionals*. Vol I, U. S. Pharmacopeial convention Inc. Rockville, MD, 1999.

Valleri, M., Mura, P., Maestrelli, F., Cirri, M. and Ballerini, R. Development and evaluation of glyburide fast dissolving tablets using solid dispersion technique. *Drug Dev. Ind. Pharm.* 30 (5), 525-534, 2004.

Vogelpoel, H., Welink, J., Amidon, G. L., Junginger, H. E., Midha, K. K., Möller, H., Olling, M., Shah, V. P. and Barends, D. M. Biowaiver monographs for immediate release solid oral dosage forms based on biopharmaceutics classification system (BCS) literature data: verapamil hydrochloride, propranolol hydrochloride and atenolol (Commentary). *J. Pharm. Sci.* 93 (8), 1945-1956, 2004.

Wei, H. and Löbenberg, R. Biorelevant dissolution media as a predictive tool for glyburide a class II drug. *Eur. J. Pharm. Sci.* 29, 45-52, 2006.

## CHAPTER 4

### BIORELEVANT DISSOLUTION MEDIA AS A PREDICTIVE TOOL FOR GLYBURIDE A CLASS II DRUG

#### 4.1. Introduction

Oral dosage forms are the most common formulations because of their convenient administration and their economy of manufacture (Grass, 1997). In order to successfully develop an oral product, the formulation scientists have to investigate the physicochemical properties of all potential drug candidates. These properties include but are not limited to solubility, bulk density,  $pK_a$ , crystallinity, osmolality, pH, X-ray diffraction, IR spectra, density, particle size and surface area. High throughput *in vitro* technologies are commonly used for such screenings (Parrot and Lavé, 2002). These methodologies are optimized to characterize one characteristic at a time. The disadvantage of such specialized tests is that they use artificial test conditions, which might not reflect the drugs behaviour in a biological environment. This is especially important for poorly soluble drugs. The *in vivo* performance and bioavailability of drugs must be studied in patients in order to ensure efficacy and safety. Due to the time consuming procedure and the high costs of clinical studies, *in vitro* and *in vivo* correlations (IVIVCs) are highly desirable to predict the *in vivo* performance of dosage forms (Vogelpoel *et al.* 2004). Therefore, the development of more universal *in vitro* methods that can be used to estimate the *in vivo* performance of a potential drug product in an early stage of the development process is highly desirable.

A mechanistic approach to the oral drug absorption was developed by Amidon *et al.* (1995) and is known as the Biopharmaceutics Drug Classification System (BCS). It defined two fundamental parameters: solubility and permeability. Both are the key variables in governing the rate and extent of oral drug absorption. Based on the theory of the BCS and the physiology of the gastrointestinal (GI) tract, a mathematical model was developed called the Compartmental Absorption and Transit model (CAT) (Yu *et al.*

1996a). The CAT model can be used to predict the oral absorption of drugs. Compared to traditional models, such as the Single-Tank mixing model (Sinko *et al.* 1991) or the macroscopic mass balance (Oh *et al.* 1993), the CAT model adopted the physiological GI conditions much better (Yu *et al.* 1996b). However, the CAT model does not consider any absorption in the stomach or the colon. A new model called Advanced Compartmental Absorption and Transit model (ACAT) was developed by Simulations Plus Inc. and is available under the name GastroPlus™. The ACAT model includes more physicochemical and physiological factors, and accounts for the absorption in the stomach and colon (GastroPlus™ Manual, 2006).

In order to predict the oral drug absorption the software requires certain input parameters. Such parameters should reflect the *in vivo* conditions and include solubility and permeability. For poorly soluble drugs, the dissolution might be directly influenced by the solubility of the drug substances in the intestinal juices. If the permeability of a poorly soluble drug is high, its *in vivo* dissolution behaviour might be the limiting/controlling factor of drug absorption (Galia *et al.* 1998). Therefore, for computer simulations it is important to develop *in vitro* dissolution methods that can simulate the *in vivo* dissolution behaviour.

*In vitro* dissolution tests are standard methods accepted by regulatory agencies to assess the biopharmaceutical quality of drug products (Löbenberg *et al.* 2000a). Drug release tests are routinely used in the pharmaceutical industry for quality control and drug development (Costa and Lobo, 2001). Pharmacopoeias like the USP list several different dissolution apparatuses such as the basket, paddle, reciprocating cylinder or flow through cell. The basket and paddle apparatus is routinely used because of its easy handling (Löbenberg *et al.* 2000a). The simulation of the *in vivo* dissolution in such an apparatus is challenging because it may only simulate one condition at a time. For example, it may only simulate the gastric environment separately from the others. However, to be able to simulate the *in vivo* dissolution behaviour changing environments are needed. The development of suitable dissolution media with changing environmental conditions is a critical issue, especially for the poorly soluble drugs. There are various dissolution media described in the national pharmacopoeias including simulated intestinal fluid (SIF) and simulated gastric fluid (SGF) (USP 29, 2006). These media are buffers that cover the

physiological pH range from 1.2 to 6.8 (Löbenberg *et al.* 2000a). For many poorly soluble drugs, the *in vitro* dissolution in such media will not produce useful information because pH is not the only factor which influences solubility and drug release (Jinno *et al.* 2000). The modifications evident in dissolution media such as adding surfactants (Löbenberg and Amidon, 2000b) or using emulsion or organic solvent were investigated in the past (El-Massik *et al.* 1996). But these modified media might not truly reflect the *in vivo* conditions. In order to improve *in vitro/in vivo* conditions, the dissolution media should mimic the physiological environment of the GI tract (Galia *et al.* 1998). New biorelevant dissolution media (BDM) were developed and published in the 1995 FIP guidance: Fasted state simulated intestinal fluid (FaSSIF) and fed state simulated intestinal fluid (FeSSIF). They contain bile salts (sodium taurocholate) and lecithin to simulate the physiological environment in the GI tract (Dressman *et al.* 1998). The advantage of using these media is that they might simulate the *in vivo* dissolution. The *in vitro* dissolution can then be used to predict the oral drug absorption (Löbenberg *et al.* 2000a).

Glyburide is a second-generation sulfonylurea. It is orally used as a hypoglycemic agent to treat non-insulin dependent (type II) diabetes mellitus (Neuvonen and Kivisto, 1991; Pearson, 1985). The aqueous solubility of the glyburide is low, and highly pH dependent in the physiological range due to its  $pK_a$  of 5.3 (Löbenberg *et al.* 2000a). Previous studies have demonstrated that the oral absorption of the glyburide is formulation dependent (Neugebauer *et al.* 1985). Blume *et al.* (1993) had shown that the dissolution behaviours of different formulations play an important role in the oral performance and the bioavailability of this drug.

In this study two commercial glyburide formulations were investigated. Since the glyburide should be administered before a meal to obtain sufficient pharmacokinetic profiles, only the fasted state medium FaSSIF was investigated (Euglucon N. Rote Liste, 2005; Otoom *et al.* 2001;). The research presented in this chapter focuses on the dissolution behaviour of glyburide formulations in the FaSSIF of different chemical purities. The dissolution behaviours in other media including simulated intestinal fluid and the blank-FaSSIF without bile salts and lethicin were also studied as controls. The obtained *in vitro* dissolution profiles were used as input function, in GastroPlus<sup>TM</sup> to

predict the oral absorption. The establishment of *in vivo/in vitro* correlations (IVIVCs) is discussed.

## **4.2. Material and Methods**

### **4.2.1. Materials**

Sodium taurocholate crude (catalog number: T-0750; low quality: LQ) and 97% pure (catalog number: T-4009; high quality: HQ) were purchased from Sigma-Aldrich (St. Louis, Missouri, USA). Egg-lecithin 60% (catalog number: 102146; low quality: LQ) was purchased from ICN (Aurora, Ohio, USA). Egg-phyphatidylcholine, Lipoid E PC 99.1% pure (high quality: HQ) was a gift from Lipoid GmbH (Ludwigshafen, Germany). Potassium dihydrogen phosphate, potassium chloride, sodium chloride, sodium hydroxide, phosphoric acid and hydrochloride acid (analytical grade) were purchased from BDH Inc (Toronto, Ontario, Canada).

Two 3.5 mg glyburide tablets were used as follows: Euglucon N<sup>®</sup> 3.5 mg tablets as reference product (GR) (Lot# 01N400, Boehringer Mannheim/Hoechs, Germany) and Glukovital<sup>®</sup> 3.5 mg tablet as test product (GT) (Lot#09601, Dr. August Wolff Arzneimittel, Bielefeld, Germany).

Dulbecco's modified eagle's medium (DMEM), L-glutamine, transferrin, trypsin-EDTA, HEPES were purchased from the GIBCO BRL Co (Carlsbad, California, USA). Fetal bovine serum (FBS), sodium pyruvate and Hank's solution were obtained from Sigma (St. Louis, Missouri, USA). PBS contains 140 mM NaCl, 260 mM KCl, 8.1 mM Na<sub>2</sub>HPO<sub>4</sub>, 1.47 mM KH<sub>2</sub>PO<sub>4</sub>, PH 7.2. The pH of Hank's solution with 10 mM MES or HEPES was adjusted to pH 6.5 or 7.4 using 0.1 N HCl or 0.2 N NaOH, respectively. The resulting solution was used as a transport medium in the permeability study. Transwell<sup>®</sup> inserts (24.5 mm, pore size 0.4 μm, 4.7 cm<sup>2</sup>, Corning Costar) were used for the Caco-2 cell monolayer culture and transport experiments. Cell culture flasks (75 cm<sup>2</sup>) were used for the normal cell culture experiments. Both were obtained from Corning Costar (Acton, Massachusetts, USA).

#### **4.2.2. Preparation of Dissolution Media**

The composition of the simulated intestinal fluid (SIF) was the same as USP 29, 2006 without pancreatin. Fasted state simulating intestinal fluid (FaSSIF) was made from two chemical grades (LQ and HQ) of sodium taurocholate and lecithin. The FaSSIF contains 3mM sodium taurocholate and 0.75 mM lecithin (Galia *et al.* 1998). The blank of FaSSIF (BL-FaSSIF) had the same composition as FaSSIF but did not contain lecithin or sodium taurocholate.

#### **4.2.3. Solubility of Glyburide in Different Media**

Twenty milligrams (excess) Glyburide powder (Lot#N326, Hoechst AG, Frankfurt, Germany) was added into 10 mL of different dissolution media (two chemical grades of FaSSIF, SIF and BL-FaSSIF) at pH 1.7, 5.0, 6.5, 7.4 values and stirred overnight (12 h) at  $37\pm 0.5^{\circ}\text{C}$  water bath. The pH of each sample was checked during the period of the experiment. The resulting solution was then filtered through a 0.22  $\mu\text{m}$  Millipore membrane filter. The filter membrane was checked for adsorption and no adsorption was detected.

#### **4.2.4. *In Vitro* Dissolution Studies at pH 6.5**

A USP dissolution apparatus II (DT 6 Erweka, Heusenstamm, Germany) was used for all dissolution studies. The dissolution test was carried out at  $37\pm 0.5^{\circ}\text{C}$  in 900 mL dissolution media at 75 rpm. The samples were withdrawn using a 10 mL syringe (BD, Becton, Dickinson and Company, Franklin Lakes, New Jersey, USA) assembled with the steel tube and 10  $\mu\text{m}$  filter (lot # 31119B, Varian, Palo Alto, California, USA). At each sampling time, 5 mL sample was withdrawn and 5 mL blank medium (preheated at  $37\pm 0.5^{\circ}\text{C}$ ) was added back into vessels.



#### 4.2.5. Dynamic Dissolution Studies

The dissolution apparatus and conditions were the same as previously described. The pH of the dissolution media was changed during the experiment. Five pH values were selected, pH 6.0, 6.5, 7.0, 7.5 and 5.0 corresponding to the physiological environment in the duodenum, jejunum, ileum and colon, respectively. The pH change was adapted to the pH changes used by GastroPlus™ software. Samples were taken at 30, 90, 150, 210 and 270 min. At the end of each time interval, the pH was changed using concentrated sodium hydroxide or phosphoric acid. A pH meter (Digital 109, Corning, Acton, Massachusetts, USA) was used to monitor the adjustment to the desired pH value.

#### 4.2.6. Permeability Determination

Caco-2 cells (passages 36-45, ATCC, Rockville, MD, USA) were maintained at 37°C in Dulbecco's Modified Eagle's Medium with 4.5 g/L glucose, 1mM sodium pyruvate, 10% (v/v) fetal bovine serum, 10 µg/mL human transferrin, and 4.8 mg/mL HEPES, in an atmosphere of 5% CO<sub>2</sub> and 90% relative humidity. The cells (50,000 cells/cm<sup>2</sup>) in medium were seeded in each apical chamber of Transwell® insert. Medium (3 mL) was transferred in the basal receiving side.

The integrity and permeability of the cell monolayer was determined by electrical resistance measurements (VOHM, World Precision Inc., Sarasota, Florida, USA). The transepithelial electrical resistance values obtained in the absence of cells was considered as background measurements. The transport experiment was started based on the TEER of the monolayer when it reached 400 Ω cm<sup>2</sup> or higher. This is typically the case after 18 to 23 days after seeding cells on the transwell inserts. Lucifer yellow was used as a paracellular quality control marker, its effective permeability coefficient ( $P_{eff}$ ) should be less than  $2 \times 10^{-7}$  cm/s. Lucifer yellow was measured by 485 nm excitation and 530 nm emission using a spectrofluorometer (model: FLUOROMAX, SPEX Industries Inc., Edison, New Jersey, USA). Glyburide (20 µM) was dissolved in the transport medium (1.5 mL) and was carefully added to the apical surface. Blank transport medium (3 mL) was added to basolateral receiving side. The cells were incubated at 37°C in an

atmosphere of 95% humidity; the concentration of the glyburide in both chambers was analyzed by HPLC at predetermined time intervals. In order to maintain the sink condition, the inserts were moved to the pre-prepared wells that contained fresh transport medium at predetermined time intervals. After each experiment, the TEER values were measured in all inserts and the integrity of the cell monolayer was confirmed.

The apparent permeability coefficient ( $P_{app}$ ) was calculated using Eq. 4.1

where:

$$P_{app} = \frac{V}{A * C_0} \times \frac{dc}{dt} (cm / s) \quad (4.1)$$

$dc/dt$ : the permeability rate (mM/s), is the initial slope of a plot of the cumulative receiver concentration versus time,

V: the volume of the receiver chamber (mL),

A: the surface area of the monolayer (cm<sup>2</sup>), which is 4.7 cm<sup>2</sup> for the transwell insert in this experiment, and

C<sub>0</sub>: initial concentration (mM) in donor compartment.

#### 4.2.7. HPLC Analysis

Sample analysis was achieved by HPLC. The HPLC system consisted of an automatic sample injector (SIL-9A, Shimadzu, Kyoto, Japan), a pump (LC-60, Shimadzu, Kyoto, Japan), a UV detector (SPD-6AV, Shimadzu, Kyoto, Japan) and an analytical column LiChoCART 125-4 LiChospher 60 Rp-select B (5µm, Merk Darmstadt, Germany) with a guard column. The samples were centrifuged at 12, 000 rpm for 15 min using an Eppendorf centrifuge (Model 5415, Brinkmann, Filderstadt, Germany). Supernatant (30 µL) was directly injected into the HPLC system. The mobile phase consisted of a mixture of the acetonitrile and (25 mM, pH 4.5) sodium dihydrogen phosphate buffer. The percentage of the acetonitrile in the mobile phase was between 42 and 45% based on the separation of the impurities in the sample matrices. The drug, glyburide was detected at a wavelength of 230 nm and the retention time was between 5 to 8 min depending on the organic ratio in the mobile phase. Samples were stable during the analytical time. An

integrator (C-R3A, Shimadzu, Kyoto, Japan) was used for peak integration. Analysis of the dissolution and cell culture samples used the same HPLC conditions.

#### 4.2.8. Computer Simulations

GastroPlus™ (version 4.0.0005, Simulations Plus Inc., Lancaster, California, USA) was used to simulate the absorption and pharmacokinetics of the reference (GR) and test (GT) formulations. The program has three input pages: compound, physiology, and pharmacokinetics. In the compound page, basic data of the drug's physical and chemical properties such as bulk density, solubility, dose,  $pK_a$  and particle radius are entered. The values used in this study were taken from the manufacturer's certificate of analysis, literature or estimated using computer software (Reynolds *et al.* 1993; Budavari *et al.* 1996). The human permeability ( $P_{app}$ ) of glyburide was estimated using Caco-2 data (see section 4.2.8). The solubility-pH profiles of glyburide were obtained as described in the previous section. The log P of glyburide was calculated by the KowWin online-software available on the internet (Syracuse, 2004). The diffusion coefficient of glyburide was estimated by GastroPlus™.

The *in vitro* dissolution profiles of glyburide tablets were used as input functions into GastroPlus™ using the “tabulated *in vitro* data” function. The drug release profiles were used by the software to calculate the drug concentration in each compartment. The estimated human permeability data were computed using the human fasted log D absorption model to account for permeability. The *in silico* gut (GastroPlus™) then calculates the fraction dose absorbed based on the ACAT model using drug concentration, permeability, surface area and transit time in each compartment. Pharmacokinetic parameters e.g. volume of distribution, clearance and micro constants can be added to the software in the pharmacokinetic page, which enables the software to calculate plasma concentration-time curves.

In the physiology page, the default values for transit time were selected for each compartment.

The clinical data for both formulations were obtained from a bioequivalence study and all data were made available to us (Blume *et al.* 1989). The pharmacokinetic data were

calculated using the software Kinetica 2000 (InnaPhase Corporation, Philadelphia, Pennsylvania, USA). The Micro Extravascular fitting model was selected to calculate pharmacokinetic parameters. The mean values of the clinical data from 15 healthy volunteers for both formulations were well fit with a two-compartmental model (Rydberg *et al.* 1997). The pharmacokinetic parameters, such as clearance, volume of distribution,  $K_{12}$ ,  $K_{21}$ , etc were used for the simulations using GastroPlus™.

#### 4.2.9. Statistics

Release profiles comparison: the difference factor ( $f_1$  Eq. 4.2) and similarity factor, ( $f_2$  Eq. 4.3) were used to compare the drug release profiles according to the following equations are as below (Costa and Lobo, 2001):

$$f_1 = \frac{\sum_{j=1}^n |R_j - T_j|}{\sum_{j=1}^n R_j} \times 100 \quad (4.2)$$

$$f_2 = 50 \times \log \left\{ \left[ 1 + (1/n) \sum_{j=1}^n |R_j - T_j|^2 \right]^{-0.5} \times 100 \right\} \quad (4.3)$$

Where  $n$  is the sample number;  $R_j$  and  $T_j$  are the percentages of the reference and test drug release, respectively, at different time intervals  $j$ . The  $f_1$  value increases proportionally due to the dissimilarity between the two dissolution profiles. If  $f_2$  of two dissolution drug release profiles is between 50 and 100, then these two drug release profiles are similar. A value under 50 indicates differences between the release profiles (Costa and Lobo, 2001).

Percent prediction error (%PE) was calculated using the Eq.4.4 (FDA, 1997).

$$\%PE = \frac{Observed - Predicted}{Observed} \times 100 \quad (4.4)$$

Linear Regression: The linear regression for the observed and simulated data was performed using MS Office Excel (2000). The 95% confident interval was applied for analysis of linear regression.

In all cases, significance of differences between experiments was calculated by Student's t test using two-tailed distributions and two-sample equal variance (Microsoft Excel, Version 2000, Microsoft Inc. Seattle, Washington, USA). Statistical significance was calculated at the 95% ( $p < 0.05$ ) confidence level.

### **4.3. Results and Discussion**

#### **4.3.1. Solubility of Glyburide in Different Media**

Glyburide ( $pK_a$  5.3) is a weak acid with poor aqueous solubility (El-Massik *et al.* 1996). The solubility of glyburide powder was measured in four different media including BL-FaSSIF, SIF, HQ-FaSSIF and LQ-FaSSIF at different pH values (pH 1.7, 5.0, 6.0, 6.5, 7.0, and 7.4) and the results are presented in Fig. 4.1. The pH of each sample did not change throughout the experimental period. The results showed that the solubility of the glyburide was highest in the LQ-FaSSIF (43.21  $\mu\text{g/mL}$ ) at pH 7.4, and decreased from the high quality HQ-FaSSIF, SIF down to BL-FaSSIF. The solubility in all media decreased from a high pH to a low pH due to the drug's  $pK_a$  of 5.3. As a weak acid, glyburide has a higher solubility in a basic aqueous environment. However, it can be considered as a poorly soluble drug considering the entire physiological pH range. The results showed that glyburide had higher solubility in FaSSIF compared to BL-FaSSIF or SIF ( $p < 0.05$ ). FaSSIF contains lecithin and bile salts (sodium taurocholate). The concentrations of bile salts and lecithin in FaSSIF are adapted to physiological conditions (Dressman *et al.* 1998). Bile salts and lecithin can increase the wetting process for the lipophilic drugs and solubilize the drug into the micelles formed by bile salts and lecithin. Therefore, pH and micelles impact the solubility of glyburide. This is in accordance with results reported by Jinno *et al.* (2000) for piroxicam. The solubility data obtained in this study showed that the micelles formed by LQ bile salt and LQ lecithin were able to solubilize glyburide better compared to the chemically purer HQ bile salt and HQ lecithin ( $p < 0.05$ ). The difference between HQ- and LQ-FaSSIF is the chemical grade of the bile salt and lecithin used to prepare the media. LQ-media contain other components like glycocholic, cholic, deoxycholic and other bile acids from crude ox bile to a higher extent while the HQ-media contain 97% pure sodium taurocholate. The different composition of

media impacts the solubility of glyburide. Woodford (Woodford, 1969) reported that the addition of 1-monoolein to a taurocholate micelle system increased the solubility of cholesterol. He concluded that a three-component micelle system (monoolein-taurocholate-cholesterol) formed different micelles compared to the pure taurocholate-cholesterol system. The improved solubility of glyburide in LQ-media might be due to similar effects caused by the presence of the other bile components. BL-FaSSIF and SIF are plain buffers. They mainly influence the solubility of glyburide by means of pH. Such media might not reflect the physiological environment of GI tract due to the lack of micelle solubilization.

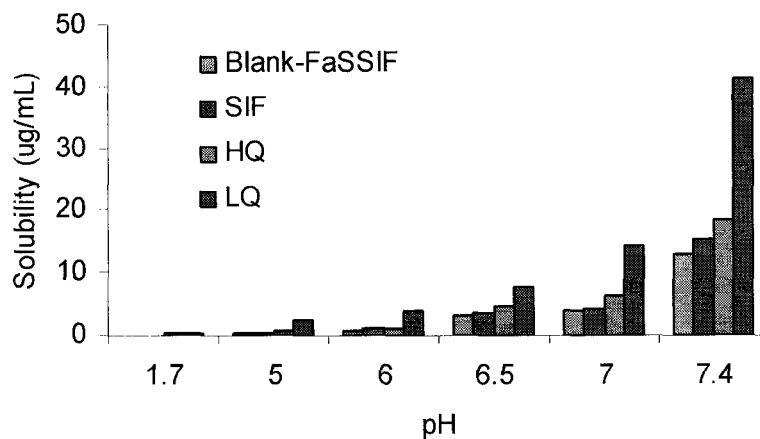


**Figure 4.1.** Solubility of glyburide powders in different media (n=3, Blank-FaSSIF: FaSSIF buffers without bile salts and lecithin; LQ and HQ: LQ and HQ-FaSSIF )

### 4.3.2. *In Vitro* Dissolution Studies at pH 6.5

The common limiting factor for oral absorption of Class II drug substances is their lack of dissolution due to limited solubility (Galia *et al.* 1998). For such drugs solubility might be the major factor influencing their dissolution behaviour. In order to establish meaningful IVIVCs, the *in vitro* dissolution tests have to simulate the *in vivo* dissolution behaviours or need at least a relationship, which can be established using a scaling factor (Löbenberg *et al.* 2000a). Fig. 4.2 shows the dissolution of the reference (GR) and test (GT) formulations in four different media at pH 6.5. The drug release of the GT formulation in pH 6.5 media was slower compared to the GR formulation during the first 30 minutes. This was observed in all four dissolution media. Both formulations had the highest release in LQ-FaSSIF. The graph shows that the drug release of the reference (GR) and test (GT) formulations in LQ-FaSSIF was over 60% and 40%, respectively within 90 min. In the other three media, the drug releases were below 40% within 90 min, which is due to limited drug solubility in these media as confirmed by results of a solubility study (Fig. 4.1). Table 4.1 shows the values of two comparison factors:  $f_1$  is the difference factor and  $f_2$  is the similarity factor. Both can be used to assess dissolution profiles between formulations. The  $f_1$  and  $f_2$  factors were equal to 79.6 and 30.1, respectively, when the dissolution tests were performed in LQ-FaSSIF. A higher  $f_1$  value corresponds to dissimilarity while a  $f_2$  value below 50 indicates differences between two dissolution profiles (Costa and Lobo, 2001). The  $f_1$  obtained from LQ-FaSSIF is the highest among the four media and the  $f_2$  factors obtained from LQ-FaSSIF is the lowest compared to the other three media. This indicates that the LQ-FaSSIF differentiated formulation differences better compared to the other media. The  $f_2$  factors of dissolution profiles in SIF and BL-FaSSIF were 47.8 and 42 while the  $f_1$  factors were 51.9 and 67.9, respectively. Although in these media the  $f_1$  and  $f_2$  factors showed differences in the dissolution profiles, the values of the  $f_2$  factors were close to the critical value of 50, which divides between similarity and dissimilarity (Costa and Lobo, 2001). In contrast, the comparison of the formulations in HQ-FaSSIF produced an  $f_1$  value of 10.5 and an  $f_2$  factor of 61.2. In this medium the dissolution profiles would be considered similar. The results above show that LQ-FaSSIF can best differentiate between the dissolution

behaviours of both formulations. This might be due to different interactions between the formulation components and the components of the dissolution media. Vertzoni *et al.* (2004) showed that the LQ-FaSSIF had a substantial impact on the dissolution profiles of two highly lipophilic drugs. The study showed that the *in vitro* dissolution in LQ-FaSSIF is more suitable to describe the *in vivo* dissolution performance of those two drug products. In an earlier study, Löbenberg *et al.* (2000a) reported that the drug releases of two glyburide formulations in a HQ-FaSSIF were able to differentiate between dissolution behaviours of two formulations. However, in the present study HQ-FaSSIF exhibited the lowest discriminative power between the two tested formulations. The different results might be due to the different batches of lecithin and sodium taurocholate used to prepare the media and the volume used for the tests (Sznitowska *et al.* 2002). Leng *et al.* (2003) investigated the formation of vesicles and micelles using bile salts and lecithin. They identified different stages of the vesicle formation. Different vesicle shapes and mono and multi laminar vesicles can be formed. This was shown to be highly sensitive to environmental and physicochemical factors of the used bile salts and lecithin. This effect might also explain the discriminative power of certain biorelevant media. The drug and excipients of pharmaceutical formulations might interact differently with media and either support or destruct the formation of certain vesicles and might solubilize the drug differently compared to other vesicles. However, this has to be investigated more. The characterization and investigation of the effect of vesicle structure on the dissolution behaviour can help to further standardize biorelevant media.

**Table 4.1.**  $f_1$  and  $f_2$  factors comparing the dissolution profiles between a reference (GR) and a test (GT) formulation at pH 6.5

	LQ-FaSSIF	HQ-FaSSIF	SIF	BL-FaSSIF
$f_1$	79.6	10.5	51.9	67.9
$f_2$	30.1	61.2	47.8	42



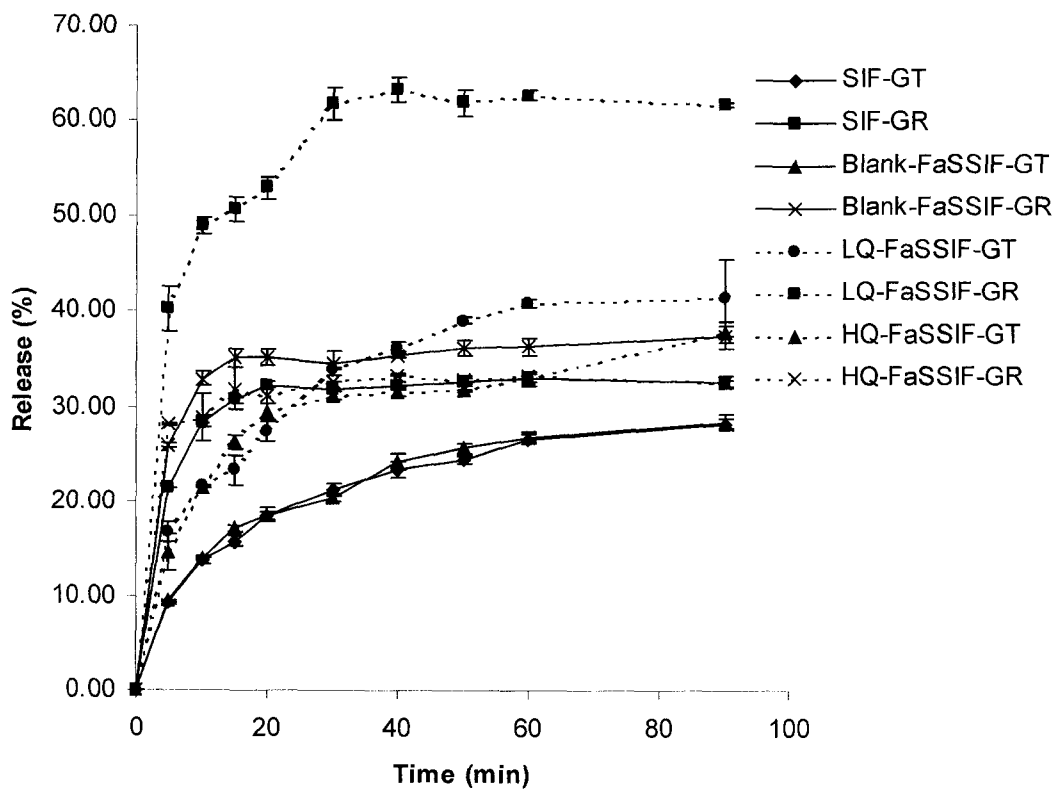


**Figure 4.2.** Dissolution profiles of two formulations (GR and GT) in different media at pH 6.5 (n=3)

### 4.3.3. Dynamic Dissolution Studies

The dynamic dissolution test of the two formulations was performed following the pH profile used by the ACAT model as discussed earlier. Fig. 4.3 shows the drug release under changing pH values in different dissolution media. The drug release of the test (GT) formulation was slower than that of the reference (GR) formulation. This was observed in all media. Compared to the single pH (Fig. 4.2) the drug release for both formulations was slower in all media within the first 30 minutes. However, after four hours the drug release was higher in all media. This can be attributed to the solubility of glyburide at different pH values. The drug release increased when the pH increased. When the pH was changed to 7.5, the drug release reached a plateau for both formulations in all media. When the pH of the media was changed from 7.5 to 5.0, the drug concentration in LQ-FaSSIF did not change and stayed on the plateau for 1 hour. These results showed that the micelles formed kept the glyburide in solution without precipitation despite the unfavorable pH. The LQ lecithin and LQ bile salts enhanced either the stability of the micelles or increased in drug solubilization. However, in HQ-FaSSIF, the drug concentration for GR and GT dropped slightly from 83% to 79% and 78% to 71 %, respectively. A t-test indicated that there are no statistically significant differences between the drug release changes ( $p > 0.05$ ). However, the observed decrease might be due to a precipitation of some glyburide due to the pH change and the unfavorable pH condition. A more pronounced precipitation was observed in the SIF and BL-FaSSIF. The concentrations dropped from above 75% to under 12% for both formulations. This can be explained by the nature of SIF and BL-FaSSIF, which are plain buffers.

Comparing the 90 minutes drug release values of the fixed pH experiment and the dynamic dissolution experiment (Table 4.2) reveals that the pH change had an impact on the solubilization capacity of the HQ-FaSSIF. At 90 minutes the pH of dissolution media in both experiments was the same. While the drug release in the two buffers (SIF and BL-FaSSIF) and the LQ-FaSSIF was nearly the same for each formulation and media, a significant increase in drug release was observed in the HQ-FaSSIF ( $p < 0.05$ ). At all other pH values the HQ-FaSSIF had lower drug concentrations compared to the LQ-FaSSIF.

This observation supports the earlier discussed formation of different types of vesicles and the impact of environmental factors on this process. However, such effects have to be studied in greater detail.

**Table 4.2.** Comparison of drug release (%) at 90 min (n=3) using dynamic and single pH dissolution protocols for a reference (GR) and a test (GT) formulations

	Reference formulation		Test formulation	
	Single pH 6.5	Dynamic pH	Single pH 6.5	Dynamic pH
LQ-FaSSIF	61.73±0.18	63.75±0.86	41.53±4.00	44.02±5.48
HQ-FaSSIF*	32.58±0.28	77.75±2.53	38.01±1.12	54.99±0.07
SIF	27.0±0.60	34.74±0.65	28.30±0.58	26.11±1.01
BL-FaSSIF	37.45±1.10	33.91±0.58	28.40±0.82	26.43±1.02

\*: t-Tests indicated that there is significant difference in the drug release between the single pH and dynamic pH dissolution tests ( $p < 0.05$ ).

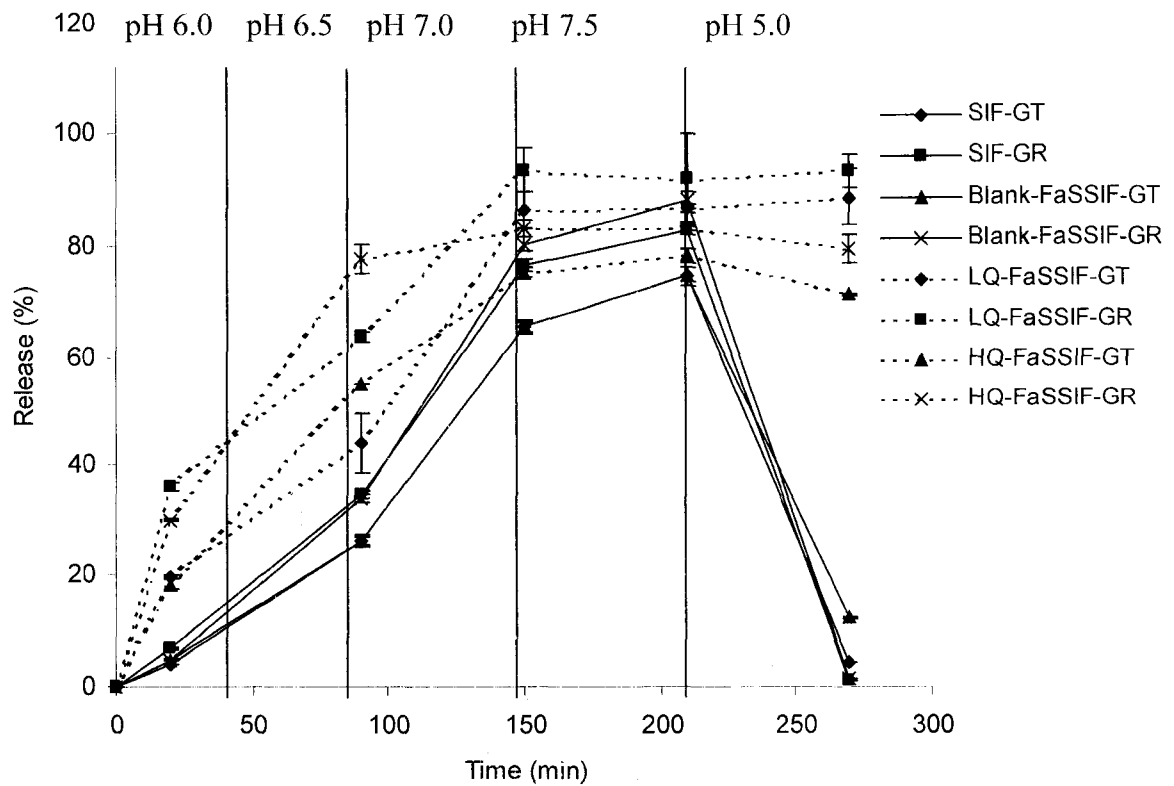


**Figure 4.3.** Dissolution profiles of two formulations (GR and GT) in different media using a pH gradient (n=3)

#### 4.3.4. Permeability Studies

The human permeability ( $P_{\text{eff}}$ ) of the glyburide was estimated by GastroPlus™ as  $3.5 \times 10^{-4}$  cm/s, using *in vitro* Caco-2 data. Vogelpoel *et al.* (2004) suggested that, if the human permeability ( $P_{\text{eff}}$ ) of a drug is above  $2 \times 10^{-4}$  cm/s or the bioavailability is over 90%, this drug can be considered as a highly permeable drug. Literature shows that glyburide's bioavailability can be up to 100% depending on the formulation (Neugebauer *et al.* 1985). Therefore, glyburide can be classified as a highly permeable drug as confirmed using the Caco-2 model. Based on the BCS (Amidon *et al.* 1995), glyburide is a typical Class II drug, which has high permeability and low aqueous solubility.

#### 4.3.5. Computer Simulations

The computer simulations using the GastroPlus™ were performed by using dissolution profiles and pH-solubility profiles as major input functions. All the physical and chemical properties of the glyburide described previously were kept the same. The human permeability ( $P_{\text{eff}}$ ) of the glyburide was estimated as  $3.5 \times 10^{-4}$  cm/s. A parameter sensitivity analyses using GastroPlus™ showed that the predicted  $C_{\text{max}}$  and AUC will not be significantly influenced between a permeability of  $2 \times 10^{-4}$  cm/s and  $10 \times 10^{-4}$  cm/s. This confirms that glyburide is a typical Class II drug and dissolution, not permeability, is the limiting factor in oral absorption (Löbenberg and Amidon, 2000b). Using the single pH dissolution profiles, the simulated plasma concentration profiles did not match the clinical data. The predicted  $C_{\text{max}}$  and AUC were half and 1/3 of observed data, respectively (Table 4.3). The prediction errors of the  $C_{\text{max}}$  and AUC were  $\pm 38$ , 63, 59 and 67% for the reference (GR) and test (GT) formulations, respectively. The *in vitro* dissolutions at fixed pH condition were not able to simulate the *in vivo* plasma levels. Therefore, the *in vivo* dissolution seems to be different.

Using the dynamic pH dissolution profiles as input function for the simulations showed that only the dissolution profiles obtained from LQ-FaSSIF were able to predict the clinically observed data (Fig. 4.4). LQ-FaSSIF might be more physiologically relevant compared to other media. The prediction errors of  $C_{\text{max}}$  and AUC were  $\pm 7$ ,  $\pm 14$ ,  $\pm 4$  and

$\pm 0.7\%$  for the reference and test formulations, respectively (Table 4.3). The dynamic dissolution profiles obtained from LQ-FaSSIF showed the best simulation results compared to the results obtained from the other dissolution media (Table 4.3). The prediction errors of the AUC and  $C_{\max}$  obtained from the other three media such as HQ-FaSSIF, BL-FaSSIF and SIF are much higher (up to  $\pm 28\%$ ) compared to LQ-FaSSIF. The goodness of fit (linear regression) for the simulation obtained from LQ-FaSSIF, regression coefficient for the reference and test formulations were 0.94 and 0.93 respectively. The simulation results clearly showed that an *in vitro/in vivo* relationship between the dynamic dissolution in LQ-FaSSIF and the *in vivo* plasma curves exists. The *in vitro* dissolution following the dynamic pH profiles seems to mimic the *in vivo* dissolution. The USP 29 (Chapter 1088) describes different levels of IVIVC. A level A correlation is a point to point correlation and the strongest correlation possible (USP 29, 2006). The *in vitro* dissolution properties can serve as a surrogate for *in vivo* performance. Results of this study in the different media showed that LQ-media successfully predicted the oral performance of the two formulations. Applied *in vitro* dissolutions seem to predict the *in vivo* dissolution as required for a level A correlation.

**Table 4.3.** Comparison of pharmacokinetic parameters of a bioequivalence study between observed and simulated data (observed reference (GR):  $C_{\max}$ : 301 ng/mL;  $AUC_{0-24}$ : 1359.6 ng/mL\*h; observed test (GT):  $C_{\max}$ : 221 ng/mL;  $AUC_{0-24}$ : 1441.3 ng/mL\*h)

Media	Simulated				Prediction Error (%)			
	GR		GT		GR		GT	
	$C_{\max}$	AUC	$C_{\max}$	AUC	$C_{\max}$	AUC	$C_{\max}$	AUC
a.	187	499	917	477	38	63	59	67
b.	385	1180	89	1230	28	13	14	15
c.	355	1100	190	1240	18	19	14	14
d.	384	1010	202	1270	28	26	8	12
e.	318	1170	230	1452	7	14	4	0.7

a: single pH 6.5; b: BL-FaSSIF; c: SIF; d: HQ-FaSSIF; e: LQ-FaSSIF  
 $C_{\max}$ : ng/mL; AUC: ng/mL\*h

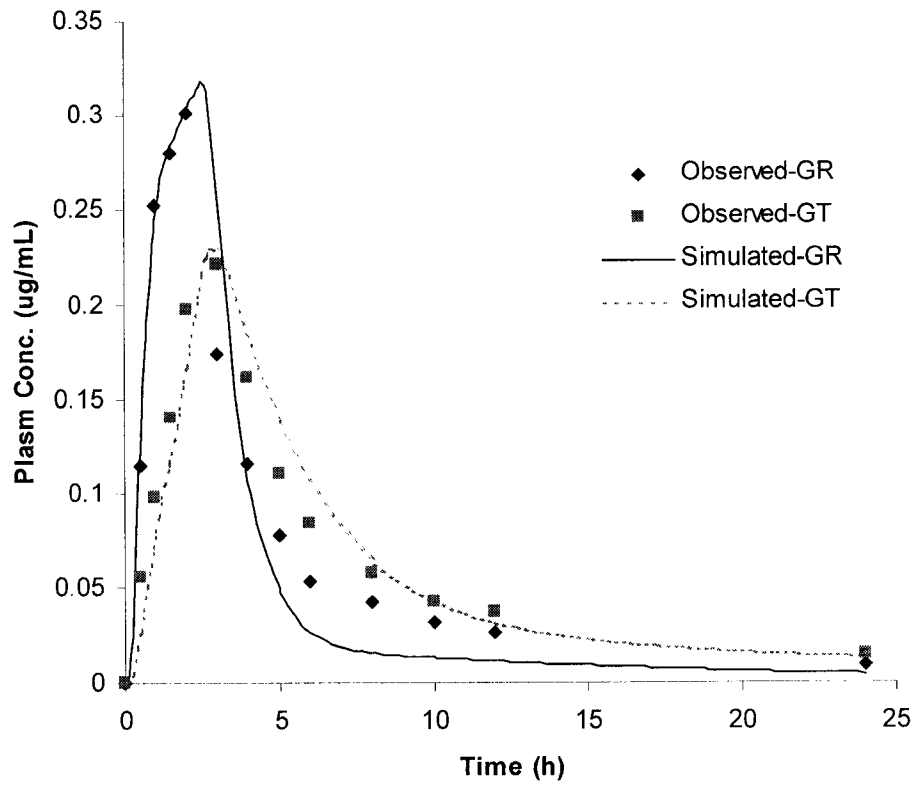


**Figure 4.4.** Comparison of the simulated and observed data using dynamic dissolution data as input into the simulation software.

#### 4.4. Conclusions

Biorelevant dissolution media (BDMs) are a complex mixture of bile salts and lecithin. This study showed that environmental changes which *in vivo* dynamically happen in the gastrointestinal tract have an impact on the solubilization of glyburide, as indicated by the LQ- and HQ-media. These effects have to be studied in more detail. Computer simulations using the ACAT model showed that the LQ-FaSSIF data were best able to predict plasma levels of two investigated glyburide formulations if a pH gradient was applied. The used *in vitro* and *in silico* methods were able to predict the oral performance of two glyburide formulations. An *in vitro/in vivo* correlation (IVIVC) could be established.

#### 4.5. References

- Amidon, G. L., Lennernas, H., Shah, V. P. and Crison, J. R. A theoretical basis for a biopharmaceutic drug classification: the correlation of *in vitro* drug product dissolution and *in vivo* bioavailability. *Pharm. Res.* 12, 413-420, 1995.
- Blume, H., Ali, S. L. and Siewert, M. Pharmaceutical quality of glibenclamide products: a multinational postmarket comparative study. *Drug Dev. Ind. Pharm.* 19, 2713-2741, 1993.
- Blume, H. and Mutschler, E. *Bioäquivalenz*, Govi-Verlag, Eschborn, 1989.
- Budavari, S. and O'Neil, M. J. *The Merck Index*. Chapman & Hall, 1996.
- Costa, P. and Lobo, J. M. S. Modeling and comparison of dissolution profiles. *Eur. J. Pharm. Sci.* 13, 123-133, 2001.
- Dressman, J. B., Amidon, G. L., Reppas, C. and Shan, V. P. Dissolution testing as a prognostic tool for oral drug absorption: immediate release dosage forms. *Pharm. Res.* 15(1), 11-21, 1998.



El-Massik, M. A., Darwish, I. A., Hassan, E. E. and El-Khordagui, L. K. Development of a dissolution medium for glibenclamide. *Int. J. Pharm.* 140, 69-76, 1996.

Euglucon N. Rote Liste. BPI. Frankfurt/Main, 2005.

FDA, Guidance for industry: Extended release oral dosage forms: development, evaluation and application of in vitro/in vivo correlations. U.S. Department of Health Food and Drug Administration Center for Drug Evaluation and Research, 1997.

Galia, E., Nicolaidis, E., Hörter, D., Löbenberg, R., Reppas, C. and Dressman J. B. Evaluation of various dissolution media for predicting in vivo performance of class I and II drugs. *Pharm. Res.* 15 (5), 698-705, 1998.

GastroPlus™ Manual, Simulation Plus Inc. Lancaster, California, USA, 2004.

Grass, M. G. Simulation models to predict oral drug absorption from in vitro data. *Adv. Drug Del. Rev.* 23, 199-219, 1997.

Jinno, J., Oh, D. M., Crison, J. R. and Amidon, G. L. Dissolution of ionizable water-insoluble drugs: the combined effect of pH and surfactant. *J. Pharm. Sci.* 89 (2), 268-275, 2000.

Leng, J., Egelhaaf, S. U. and Cates, M. E. Kinetics of the micelle-to-vesicle transition: aqueous lecithin-bile salt mixtures. *Biophys. J.* 85, 1624-1646, 2003.

Löbenberg, R., Krämer, J., Shah, V. P., Amidon, G. L. and Dressman, J. B. Dissolution testing as prognostic tool for oral drug absorption: dissolution behaviour of glibenclamide. *Pharm. Res.* 17(4), 439-444, 2000a.

Löbenberg, R. and Amidon, G. L. Modern bioavailability, bioequivalence and biopharmaceutics classification system. New scientific approaches to international regulatory standards. *Eur. J. Pharm. Biopharm.* 50, 3-12, 2000b.

Neugebauer, G., Betzien, G., Hrstka, V., Kaufmann, B., Möllendorff, V. E. and Abshagen, U. Absolute bioavailability and bioequivalence of glibenclimide (Semi-Euglucon®N). *Int. J. Clin. Pharmacol. Therapy and Toxicology.* 23 (9), 453-460, 1985.

Neuvonen, P. J. and Kivisto, K. T. The effects of magnesium hydroxide on the absorption and efficacy of two glibenclamide preparations. *Br. J. Clin. Pharmacol.* 32, 215-220, 1991.

Oh, D. M., Curl, R. L. and Amidon, G. L. Estimating the fraction dose absorbed from suspensions of poorly soluble compounds in humans: a mathematical model. *Pharm. Res.* 10, 264-270, 1993.

Otoom, S., Hassan, M. and Najib, N. The bioavailability of glyburide (glibenclamide) under fasting and feeding conditions: a comparative study. *Int. J. Pharm. Med.* 15, 117-120, 2001.

Parrott, N. and Lavé, T. Predicting of intestinal absorption: comparative assessment of GASTROPLUS™ and IDEA™. *Eur. J. Pharm. Sci.* 17, 51-61, 2002.

Pearson, J. G. Pharmacokinetics of glyburide. *Am. J. Med.* 79 (suppl. 3B), 67-71, 1985.

Reynolds, J. E. F. Martindale. *The Extra Pharmacopeia*. Vol. 30. The pharmaceutical Press, London, 1993.

Rydberg, T., Jönsson, A., Karlsson, M. and Meldander, A. Concentration-effect relations of glibenclamide and its active metabolites in man: modeling of pharmacokinetics and pharmacodynamics. *Br. J. Clin. Pharmacol.* 43, 373-381, 1997.

Sinko, P. J., Leesman, G. D. and Amidon, G. L. Predicting fraction dose absorbed in humans using a macroscopic mass balance approach. *Pharm. Res.* 8, 979-988, 1991.

Syracuse Research Corporation. Interactive LogKow (KowWin) Demo, [http://www.syrres.com/esc/est\\_kowdemo.htm](http://www.syrres.com/esc/est_kowdemo.htm). 1999-2004.

Sznitowska, M., Dabrowska, E. A. and Janicki, S. Solubilizing potential of submicron emulsions and aqueous dispersions of lecithin. *Int. J. Pharm.* 246, 203-206, 2002.

United States Pharmacopeia, USP 29, 2006. U. S. Pharmacopeial Convention Inc. Rockville, MD.

Vertzoni, M., Fotaki, N., Kostewicz, E., Stippler, E., Leuner, C., Nicolaidis, E., Dressman, J. B. and Reppas, C. Dissolution media simulating the intraluminal composition of the small intestine: physiological issues and practical aspects. *J. Pharm. Pharmacol.* 56, 453-462, 2004.

Vogelpoel, H., Welink, J., Amidon, G. L., Junginger, H. E., Midha, K. K., Möller, H., Olling, M., Shah, V. P. and Barends, D. M. Biowaiver monographs for immediate release solid oral dosage forms based on biopharmaceutics classification system (BCS) literature data: verapamil hydrochloride, propranolol hydrochloride and atenolol (Commentary). *J. Pharm. Sci.* 93 (8), 1945-1956, 2004.

Woodford, F. P. Enlargement of taurocholate micelles by added cholesterol and monoolein: self-diffusion measurements. *J. Lip. Res.* 10, 539-545, 1969.

Yu, L. X., Lipka, E., Crison, J. R. and Amidon, G. L. Transport approaches to the biopharmaceutical design of oral drug delivery systems: prediction of intestinal absorption. *Adv. Drug. Deliv. Rev.* 19, 359-376, 1996a.

Yu, L. X., Crison, J. R. and Amidon, G. L. Compartmental transit and dispersion model analysis of small intestinal transit flow in humans. *Int. J. Pharm.* 140, 111-118, 1996b.

## CHAPTER 5

### A STRATEGY FOR COMPUTER AIDED PREFORMULATION AND REVERSE-ENGINEERING OF PHARMACEUTICAL FORMULATIONS

#### 5.1. Introduction

Many science fields, especially physics and chemistry, have achieved the move from experimental sciences to mostly predictive sciences over the past decades. The life sciences are still experimental and widely nonpredictive sciences due to the complexity of the biological environments (Wishart, 2005). Today, due to the advances in computer processing and high throughput technologies in drug screening, *in silico* methods in pharmaceuticals are rapidly advancing.

Classically, a potential active drug candidate from synthesis or extraction was evaluated by either animal models or *in vitro* surrogates (Grass, 1997; Grass and Sinko, 2002). The selection process of the lead drug substances has significant impact on the success rate of the drug development process. The advanced technologies in combinatorial chemistry and high throughput screening provide a way to identify and screen the thousands of the compounds for a particular target (Grass and Sinko, 2002); however, the success rate of new drug candidates is still low (DiMasi, 1995). It has been reported that the reason for the failure in drug development was mostly related to poor pharmacokinetic properties of the drugs (Grass and Sinko, 2002; Prentis *et al.* 1988). High throughput technologies for an oral drug candidate can generate *in vitro* data such as solubility,  $pK_a$ , crystal structure, particle size and size distribution. Predictive models, which can process such data with respect to their possible oral absorption properties are highly desired (Argoram *et al.* 2001; Parrott and Lavé, 2002). Oral dosage forms are the most common formulations because of their convenient administration and their economic way of manufacturing (Grass, 1997). The oral absorption of a drug is influenced by several major factors such as the physicochemical properties of the drugs, the formulation of the drug products and the physiological environment in the gastrointestinal tract (Parrott and Lavé, 2002). To be

able to predict the oral absorption, the models have to consider the complexity of *in vivo* absorption, not only the properties of the drugs and drug products, but also the physiological conditions. Therefore, a physiologically-based predictive model could provide a rationally scientific approach to the prediction of the oral absorption. Several articles have discussed the physiologically-based pharmacokinetics simulation models for oral dosage forms (Argoram *et al.* 2001; Grass, 1997; Grass and Sinko, 2002; Norris *et al.* 2000; Yokoe *et al.* 2003). Pharmaceutical scientists tried to use a mathematical approach to describe and integrate all processes involved in the oral absorption in the GI tract. The ultimate goal of these physiologically-based pharmacokinetic models is to predict the *in vivo* behaviors of certain drugs under specific conditions using computational technology.

GastroPlus™ is a commercially available program using the Advanced Compartmental Absorption and Transit model (ACAT). The ACAT model is based on the principles of the Biopharmaceutics Drug Classification System (BCS) and the physiology of the gastrointestinal (GI) tract. The ACAT model divides the gastrointestinal tract into several compartments including stomach, small intestine and colon. The model tries to account for all the factors governing oral absorption such as  $pK_a$ , dissolution, pH-gradient in the GI tract, and transit time (GastroPlus™ Manual, 2006).

The purpose of this study was to investigate the applications of GastroPlus™ that are potentially utilized during the drug development process. Glyburide (also known as glibenclamide) was chosen as the model drug. GastroPlus™ was used to predict the oral absorption of a glyburide's Active Pharmaceutical Ingredient (API) using physicochemical powder properties followed by the simulation of a commercial glyburide product using *in vitro* dissolution data. In this chapter different steps and options are described on how to use the GastroPlus™ program and how it can be used in formulation development for a specific case.

## 5.2. Materials and Methods

### 5.2.1. Materials

Sodium taurocholate crude (catalog number: T-0750; low quality: LQ) was purchased from Sigma-Aldrich (St. Louis, Missouri, USA). Egg-lecithin 60% (catalog number: 102146; low quality: LQ) was purchased from ICN (Aurora, Ohio, USA). Potassium dihydrogen phosphate, potassium chloride, sodium chloride, sodium hydroxide, phosphoric acid and hydrochloride acid (analytical grade) were purchased from BDH (BDH Inc. Toronto, Ontario, Canada). Pharmaceutical grades of crystalline glyburide APIs were the gifts from different manufacturers. API-2: Lot 149, Hoechst AG, Frankfurt, Germany; API-5: USP grade raw material: Lot RR302528/0, Fundação para o Remédio Popular (FURP), São Paulo State, Brazil. Euglucon N<sup>®</sup> 3.5 mg tablets (GR) (Lot# 01N400, Boehringer Mannheim/Hoechs, Germany) were used in the dissolution tests. The composition of the simulated intestinal fluid (SIF) was the same as USP 29 without pancreatin. The FaSSIF contains 3 mM sodium taurocholate and 0.75 mM lecithin (Galia *et al.* 1998).

### 5.2.2. Intrinsic Dissolution and *In Vitro* Dissolution Tests

The intrinsic dissolution apparatus was modified from the design described by Jinno *et al.* (2000) A 0.5 cm<sup>2</sup> surface area compacted tablet was prepared by compressing 200 mg glyburide powder at 1000 psi pressure for 5 min using a hydraulic press (ENERPAG P142, GlobePharma, New Brunswick, New Jersey, USA). The distance of the bottom of the beaker to the die face was 1.5 inches. Dissolution tests were performed at 100 rpm. The volume of the dissolution medium at 37°C (FaSSIF, pH 6.5) was 150 mL. The sampling intervals were 1, 5, 10, 15, 20, 25, 30, 40, 50, and 60 min. At each sampling interval, 3 mL sample was withdrawn and 3 mL pre-warmed blank medium was replaced. Sample analysis was previously described in Chapter 4. The *in vitro* dissolution tests of the glyburide tablets at pH 6.5 or dynamic pH gradient were performed using SIF and FaSSIF as previously described in Chapter 4.

### **5.2.3. Computer Simulations**

#### **5.2.3.1. Essential Input Data for the Prediction of Drug Absorption**

GastroPlus™ (version 5.1, Simulations Plus Inc., Lancaster, California, USA) was used to simulate the absorption of glyburide powder. The essential input data are listed in Table 5.1. These data were used as input functions into the compound page of the software to obtain the first simulation of the fraction dose absorbed.

In the physiology page, physiological fasted condition (human) was selected. The recommended absorption scale factor model “logD” was selected. The related physiological parameters such as transit time, pH, length, radius and volume for each compartment were automatically set as default. The default concentration gradient ACAT model was used.

In the second simulation,  $pK_a$  and logD instead of logP were defined in the built-in  $pK_a$  based solubility model. The other parameters were kept constant.

**Table 5.1.** Essential input data in the compound page for the basic prediction of the fraction dose absorbed using GastroPlus™

**First stage for absorption prediction**

Essential input data for a prediction

Drug	Dose (mg)	Dosage form	Solubility (mg/mL, pH 7.4)	Particle radius ( $\mu\text{m}$ )	Particle density (g/mL)	Diffusion coefficient ( $\text{cm}^2/\text{s}$ $\times 10^{-5}$ )	logP	Perme ability ( $\text{cm}/\text{sx}$ $10^{-4}$ )
Glyburide	3.5	Immediate release	0.043	6.28	1.38	0.5878	4.5	3.5

Data obtained from material characterizations



### 5.2.3.2. Establishment of an IVIVC Using Physicochemical Data

In order to establish an IVIVC, pharmacokinetic data have to be put into the software's pharmacokinetic parameter page. The *in vivo* data were obtained from a clinical study (Blume and Mutchler, 1989). The pharmacokinetic data of the glyburide product were calculated (Table 5.2) using Kinetica<sup>®</sup> 3.0 (InnaPhase Corporation, Philadelphia, Pennsylvania, USA). The Micro Extravascular Model Fitting mode was selected to calculate pharmacokinetic parameters.

The pH-solubility profile of glyburide was determined (Chapter 4; Wei and Löbenberg, 2006a) and used as input instead of the built-in pK<sub>a</sub> based solubility model. The essential input data and default models were kept as described in the previous section. Three absorption scale factor models (logD, Opt logD and theoretical) and two ACAT models (concentration gradient and unidirectional) were tested individually in order to find the optimized model settings for the simulation of the observed plasma concentration vs. time curve.

**Table 5.2.** Pharmacokinetic parameters used for the simulation of the plasma concentration vs. time curve (German reference (GR))

C <sub>max</sub> (ng/mL)	AUC <sub>0-24</sub> (ng/mL*h)	Clearance (L/h)	V <sub>c</sub> (L)	K <sub>12</sub> (h <sup>-1</sup> )	K <sub>21</sub> (h <sup>-1</sup> )
301	1359.6	2.47	1.83	0.409	0.100

### 5.2.3.3. Establishment of IVIVC Using *In Vitro* Dissolution Profiles

The above optimized model settings were used for the simulation. The dissolution profiles were loaded into the control release formulation input spreadsheet of the software and the corresponding pH-solubility profiles were used as described earlier.

## 5.2.4. Statistics

Percent Prediction Error (%PE) was calculated using the Eq.5.1 (FDA, 1997).

$$\%PE = \frac{Observed - Predicted}{Observed} \times 100 \quad (5.1)$$

Least square analysis: the least square analysis (Sum of Squares: SS) was performed using the Eq.5.2. The least SS indicate minimal difference between observed and predicted data (Brocks, 2002).

$$SS = \sum_1^n (Y_{obs} - Y_{pred})^2 \quad (5.2)$$

Release Profiles Comparison: The similarity factor, ( $f_2$  Eq. 5.3) was used to compare the drug release profiles according to the following equation (Costa and Lobo, 2001):

$$f_2 = 50 \times \log \left\{ \left[ 1 + (1/n) \sum_{j=1}^n |R_j - T_j|^2 \right]^{-0.5} \times 100 \right\} \quad (5.3)$$

where  $n$  is the sample number;  $R_j$  and  $T_j$  are the percentages of the reference and test drug release, respectively, at different time intervals  $j$ . If  $f_2$  of two dissolution drug release profiles is between 50 and 100, then these two drug release profiles are similar. A value under 50 indicates differences between the release profiles (Costa and Lobo, 2001).

## 5.3. Results and Discussion

### 5.3.1. Prediction of Fraction Dose Absorbed

The prediction of the oral absorption using essential input data only results in the calculation of the fraction dose absorbed in each compartment. No pharmacokinetic parameters are necessary (GastroPlus™ Manual, 2006). Fig. 5.1 shows the prediction of the fraction dose absorbed. The absorption patterns were different when using logP (experimental measurement or computer estimation) or the built-in  $pK_a$  based solubility models. The fraction dose absorbed using logP was higher in the duodenum (15.3%), jejunum 1 (33.4%) and jejunum 2 (19.7%) compared with the built-in  $pK_a$  based solubility model. Fraction dose absorbed was 1.2% in the duodenum, 13.1% in the

jejunum 1 and 13.3% in the jejunum 2 using the built-in  $pK_a$  based solubility model. The fraction dose absorbed using the built-in  $pK_a$  based solubility model was higher in the last four compartments (ileum 2: 9.3%, ileum 3: 7%, caecum: 25.8% and colon: 14.3%) compared with the logP absorption pattern (ileum 2: 6.5%, ileum 3: 3.8%, caecum: 7.9% and colon: 1.8%). The total fractions dose absorbed of logP and the built-in  $pK_a$  based solubility model were 99.8% and 95.7%, respectively.

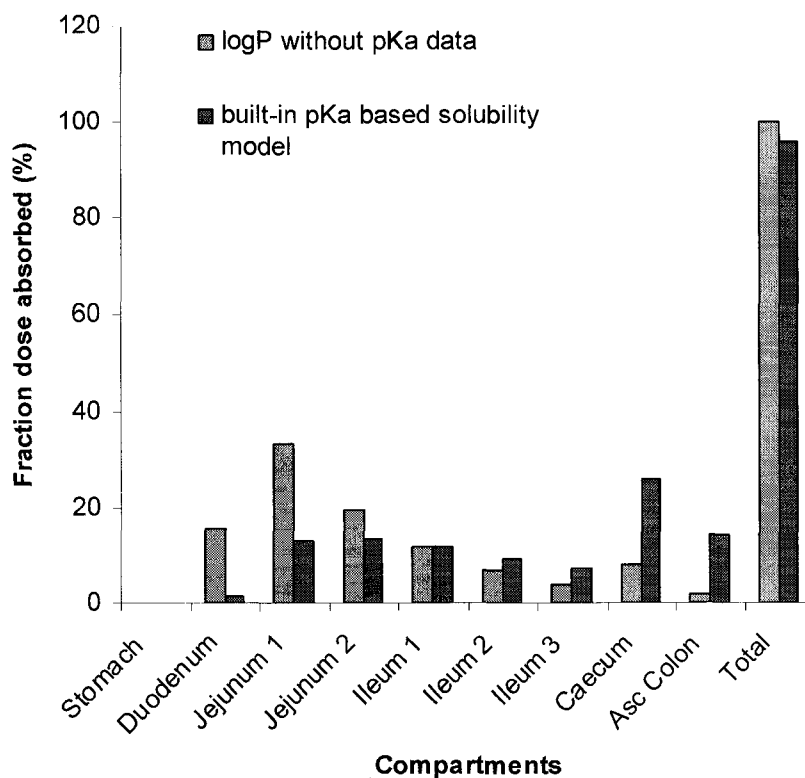


**Figure 5.1.** Comparison of the predicted absorption patterns using logP or the built-in  $pK_a$  based solubility model

### 5.3.2. Establishment of IVIVC Using Physicochemical Data

To further predict the observed plasma concentration vs. time curve, the pharmacokinetic parameters in Table 5.2. were used in the software. An experimental pH-solubility profile was determined and used in the simulations instead of the built-in  $pK_a$  based solubility model (GastroPlus<sup>TM</sup> Manual, 2006). Fig. 5.2 shows the simulated profiles vs. observed data using three absorption scale factor models and two different ACAT models available in the GastroPlus<sup>TM</sup>. The predicted plasma concentration vs. time curves did not match the observed curve well when the concentration gradient ACAT model was used with any of the three different absorption scale factor models. The predicted  $C_{max}$  and AUC were underestimated. The prediction errors of  $C_{max}$  and AUC were up to 36 and 9%, respectively (Table 5.3). The sums of squares of three absorption scale factor models (logD: 0.050; Opt logD: 0.046; Theoretical: 0.045) were similar. This indicates that the three absorption scale factor models result only in minor difference for the simulation of glyburide's performance. Therefore, the logD absorption scale factor model was selected for all further simulations as default.

When the unidirectional ACAT model was applied instead of the default concentration gradient ACAT model the simulated plasma concentration vs. time curve match the observed curve closely (Fig. 5.2). The predicted  $C_{max}$  and AUC were close to observed data. The prediction errors of  $C_{max}$  and AUC were 5 and 4 %, respectively (Table 5.3). The sum of squares (0.004) was much lower than that obtained using the default concentration gradient ACAT model (0.050). A comparison of the absorption patterns between the concentration gradient and unidirectional ACAT models is shown in Fig. 5.3. The fractions dose absorbed using unidirectional ACAT model were higher in the duodenum (5.8%), jejunum 1 (22.7%) and jejunum 2 (18.1%) compared to the concentration gradient ACAT model. The fractions dose absorbed were 1.2%, 13.1% and 13.3% in duodenum, jejunum 1 and jejunum 2, respectively, when using the concentration gradient ACAT model. The total fraction dose absorbed of the default concentration gradient and unidirectional ACAT models were 96.8% and 95.7%, respectively. Comparison of the absorption patterns and the simulated plasma

concentration vs. time curves indicates that absorption patterns have an impact on the oral performance of a drug product.

**Table 5.3.** Summary of the simulations using physicochemical data as input functions (Observed:  $C_{\max}$ : 301 ng/mL;  $AUC_{0-24}$ : 1359.6 ng/mL\*h)

	Simulated		Prediction Error (%)		
	$C_{\max}$	AUC	$C_{\max}$	AUC	SS
A-logD	197	1254.8	35	8	0.050
A-Opt logD	194	1239.9	36	9	0.046
A-theoretical	193	1232.8	36	9	0.045
B-logD	286	1298.8	5	4	0.004

A: pH-solubility profiles; ACAT model: concentration gradient. B: pH-solubility profiles; ACAT model: unidirectional. SS: Sum of Squares ( $Y_{\text{obs}} - Y_{\text{pred}}$ )<sup>2</sup>

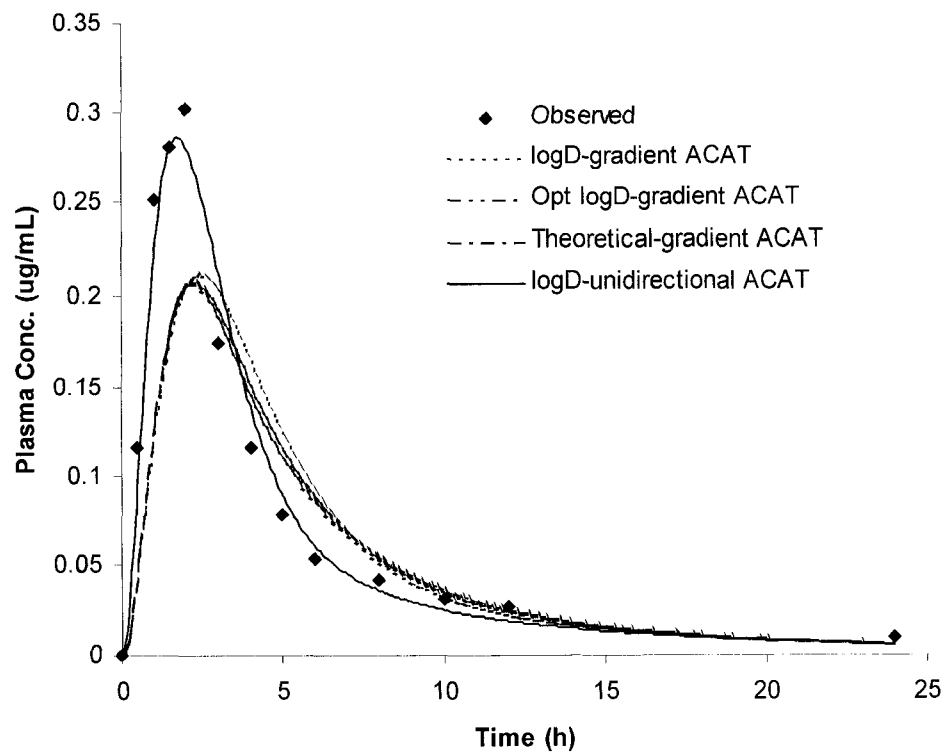


**Figure 5.2.** Comparison of the observed vs. simulated plasma concentration vs. time curves using three different absorption scale factor and ACAT models (Opt: optimize)

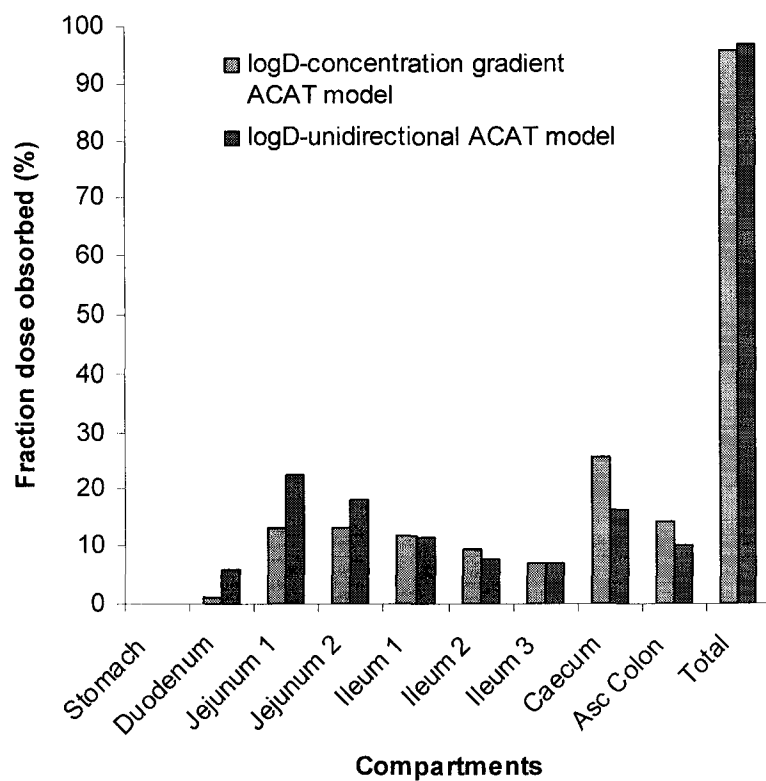


**Figure 5.3.** Comparison of the predicted absorption pattern between using the concentration gradient and the unidirectional ACAT model

### 5.3.3. Intrinsic Dissolution Test

The intrinsic dissolutions of two glyburide APIs were investigated in the FaSSIF at pH 6.5. Fig. 5.4 shows the amount of drug dissolved per unit area ( $\mu\text{g}/\text{cm}^2$ ) vs.time (min) profiles of two glyburide APIs. These two intrinsic dissolution profiles show the significantly different trends compared to each other. The similarity factor ( $f_2$ ) was 12, which was much lower than the critical value 50. The intrinsic dissolution rates of these APIs (API-2 and API-5) were 1.84 and 0.14  $\text{mg}/\text{cm}^2/\text{min}$ , respectively.

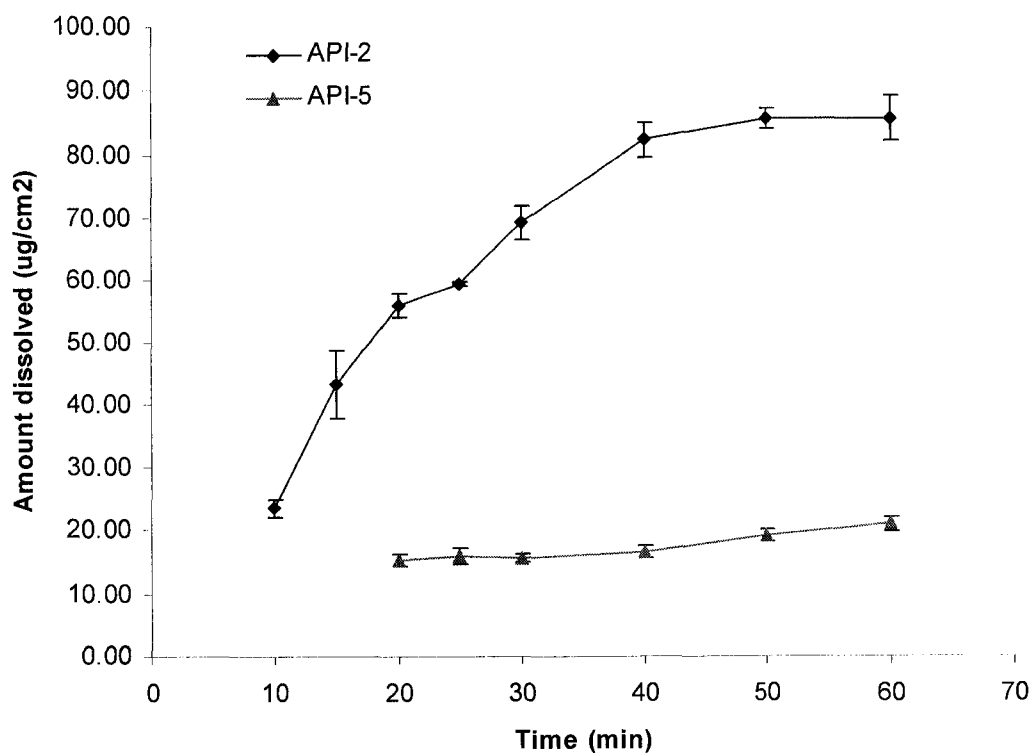


**Figure 5.4.** Intrinsic dissolution tests of two glyburide APIs (n=2)



#### 5.3.4. Establishment of IVIVC Using *In Vitro* Dissolution Profiles

The *in vitro* dissolution profiles of a commercial glyburide product in SIF and FaSSIF are shown in Fig. 5.5 and 5.6. The major difference between both dissolution methods is that the first was performed at a constant pH of 6.5 while the latter was performed with pH changes over time. The dynamic pH changes simulate the physiological environment in GI tract. The resulting dissolution profiles were used as input functions into GastroPlus™. For the *in vitro* dissolution obtained at a single pH 6.5, the predicted  $C_{\max}$  obtained from the FaSSIF was the same as the observed  $C_{\max}$  (prediction error of  $C_{\max}$ : 0%), but the simulated plasma concentration vs. time curve did not match the observed curves (Fig. 5.7). The prediction error of the AUC using FaSSIF obtained at a single pH 6.5 was 36%. The prediction errors of  $C_{\max}$  and AUC using SIF obtained at single pH 6.5 were 59 and 67%, respectively (Table 5.4). The sums of squares for using FaSSIF and SIF were 0.030 and 0.123, respectively. The simulations using the dynamic dissolution protocol obtained from FaSSIF and SIF gave much better fits (Fig. 5.7). The prediction errors of  $C_{\max}$  and AUC in FaSSIF were 19% and 6%, respectively (Table 5.4). The sum of squares using the dynamic dissolution data was the lowest (0.019) compared to other dissolution profiles such as the dissolution profiles obtained at a single pH 6.5 or obtained from SIF.

**Table 5.4.** Summary of the simulations using *in vitro* dissolution profiles as input functions (Observed:  $C_{\max}$ : 301 ng/mL;  $AUC_{0-24}$ : 1359.6 ng/mL\*h)

	Simulated		Prediction Error (%)		
	$C_{\max}$	AUC	$C_{\max}$	AUC	SS
A: FaSSIF	301	864.8	0	36	0.030
A: SIF	123	444.9	59	67	0.123
B: FaSSIF	359	1280.2	19	6	0.019
B: SIF	371	1116.0	23	18	0.061

A: *in vitro* dissolution at pH 6.5; B: *in vitro* dissolution using dynamic pH changes;  
 ACAT model: unidirectional; Absorption scale factor model: logD; SS: Sum of Squares  
 $(Y_{\text{obs}} - Y_{\text{pred}})^2$

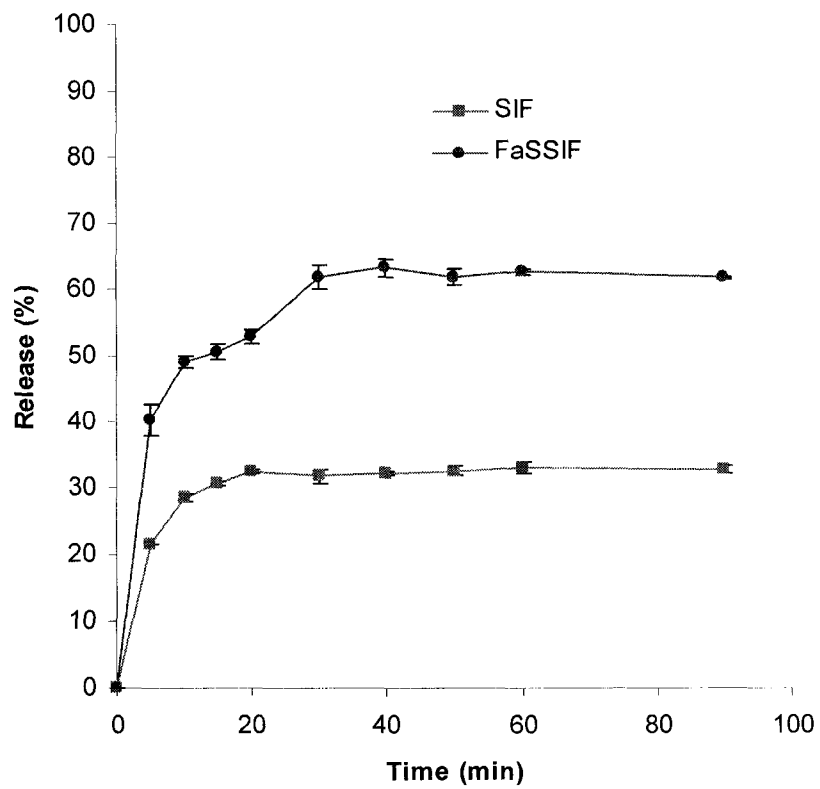


**Figure 5.5.** Dissolution profiles of the glyburide tablets in SIF and FaSSIF media at pH 6.5 (n=3)

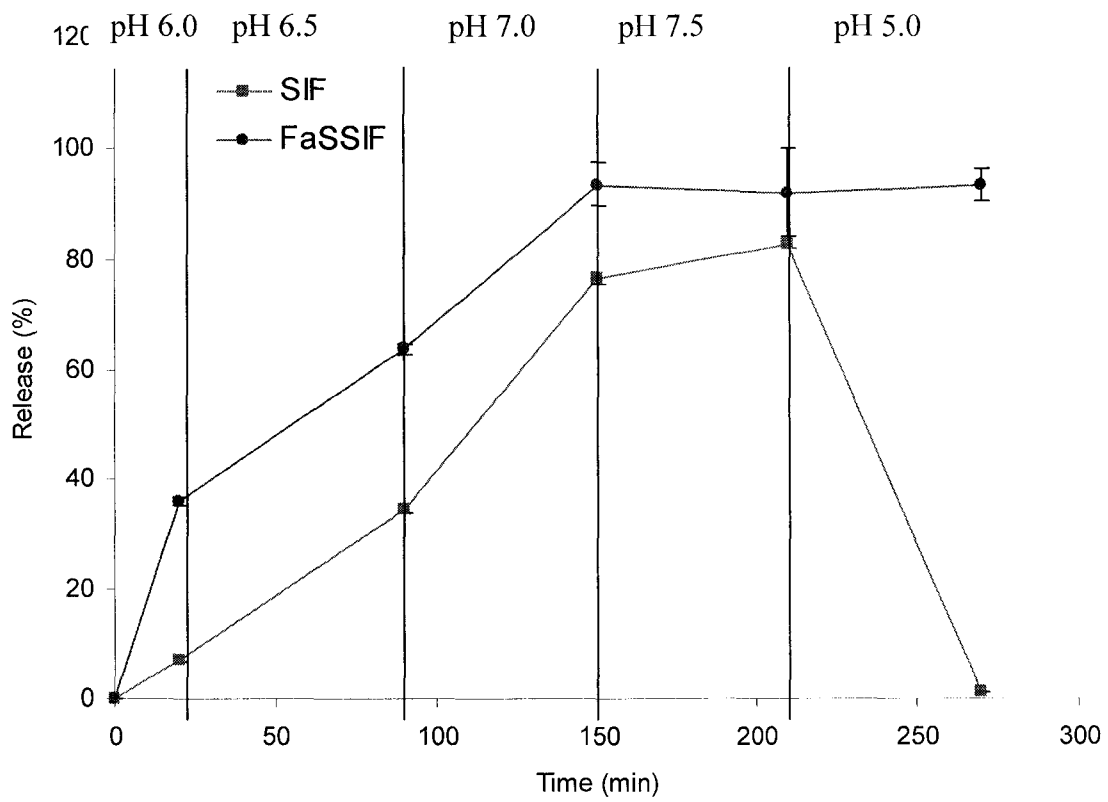


**Figure 5.6.** Dissolution profiles of glyburide tablet in SIF and FaSSIF media using a pH gradient (n=3)

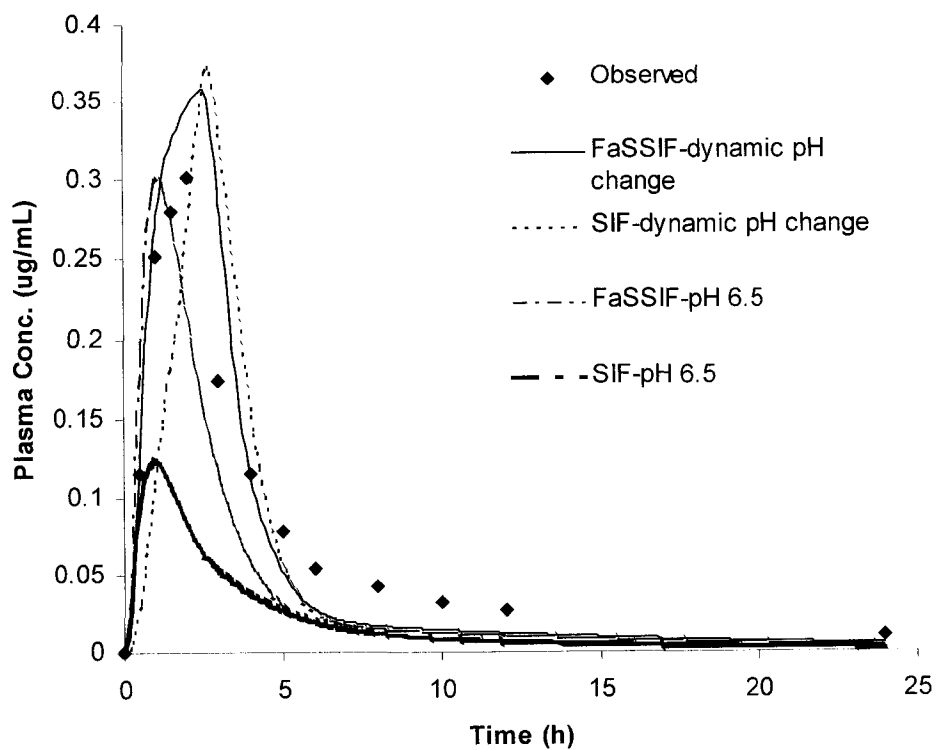


**Figure 5.7.** Comparison of the simulated and the observed data using dissolution profiles at pH 6.5 and dynamic pH changes as input functions

### 5.3.5. Evaluation of the Computer Aided Drug Development Approach

GastroPlus™ can provide a very simple prediction of the fraction dose absorbed ( $F_a$ ) based on essentially physicochemical data only. This is especially attractive for the neutral compounds due to the use of logP only. For glyburide, as a weak acid drug, the estimation of the predicted absorption was presumably closer to reality using the built-in  $pK_a$  based solubility model instead of the log P model. Although the fraction dose absorbed using only logP was slightly higher than that obtained using the built-in  $pK_a$  based solubility model, this difference might not have a significant influence on the estimation of oral absorption at this early stage. However, the different absorption patterns in each compartment using log P or the built-in  $pK_a$  based solubility models might be of more interest to formulation scientists. This information for example, can be used to assess the drug release at different segments of the GI tract from an immediate release tablet. Optimal drug release might assure optimized drug absorption. At this time point, it is not known whether the absorption patterns might have an influence on the pharmacokinetics or not. It can only be speculated that a different absorption pattern might result in different plasma concentration vs. time curves *in vivo* (GastroPlus™ Manual, 2006). The predicted fraction dose absorbed in each compartment using APIs' physicochemical data provides useful information of the intrinsic absorption properties of the APIs at an early stage. For example, the predicted absorption pattern indicates the major absorption sites of the drug within the GI tract. The information can be used by formulation scientists to design suitable formulations that match the predicted absorption properties in the different gut segments.

For formulation development it is essential to investigate intrinsic dissolution properties of different APIs that are supplied by different manufacturers or produced by different processes. Fig. 5.4 shows the intrinsic dissolution of two APIs from different suppliers. Physicochemical characterization of the two APIs showed that both are very similar in respect to particle size, surface area and crystal form (Wei *et al.* 2006b). Computer simulations resulted in similar estimates of the fraction dose absorbed. However, the intrinsic dissolution data reveal that API-5 has poor dissolution properties that might have clinically relevant consequences. Different techniques used for particle

size reduction such as micronization or milling might be responsible for the differences in the intrinsic dissolution rates (Charoenchaitrakool *et al.* 2000; Tong *et al.* 2001).

Computer simulations using the ACAT model and physicochemical input data would not be able to differentiate between these two APIs. It demonstrates the importance of dissolution testing as performance test (Wei *et al.* 2006b).

Another important factor that should be considered is the pH-solubility profile of a drug in biorelevant media. Such media contain bile salts and lecithin in physiological concentrations. The micelle solubilization combined with the pH effect can simulate *in vitro* the *in vivo* solubility (Yazdanian *et al.* 2004). Input data that reflect the *in vivo* situation truly improve the prediction power (Vertzoni *et al.* 2004). In the case of glyburide, the theoretical estimation using the built-in pK<sub>a</sub> based solubility model showed only minor differences compared to the experimental data (data not shown). However, this might be different for other drugs as shown by Kaukonen *et al.* (2004) using micelle solubilization for drugs. For example, the solubility of danazol was 142.6 µg/mL in the emulsion system and was only 0.8 µg/mL in plain buffer (Kaukonen *et al.* 2004).

GastroPlus<sup>TM</sup> can simulate the observed plasma concentration vs. time curve based on the input pharmacokinetic parameters. If pharmacokinetic data are available for a drug through e.g. a phase I study, such data can be used to establish the first correlation between the simulated and observed data. The establishment of an IVIVC involves the optimization of the input functions and the selection of the related physiologically-based models. The software offers the selection of three related physiologically-based absorption scale factor models (GastroPlus<sup>TM</sup> Manual, 2006). The theoretical absorption scale factor model uses the ratio of the volume of a cylindrical compartment to its available surface area for absorption. LogD absorption scale factor model is the default model that considers the influence of the drugs' logD at different pH in GI tract on the effective permeability. Optimized logD absorption scale factor model is modified from logD absorption scale factor model by slight equation changes and therefore, is more amendable to nonlinear optimization of the absorption scale factor fitting (GastroPlus<sup>TM</sup> Manual, 2006). The simulation results in Fig. 5.2 indicated that all three models gave similar simulation results for glyburide and therefore the use of the default model seems to be most appropriate. A different situation was given when the two ACAT models were

compared. If the default concentration gradient ACAT model was used, the predicted  $C_{\max}$  values were underestimated by up to 36% (Table 5.3). This model considers drug transport across the membrane of the gut enterocytes in either direction (apical to basolateral or basolateral to apical membranes) depending on the concentration gradient. However, literature shows that the oral absorption of glyburide is rapid and complete (Neugebauer *et al.* 1985; Brockmeier *et al.* 1985). The absorption of glyburide takes place throughout the entire GI tract (Brockmeier *et al.* 1985). Up to 100% of the oral dose can be bioavailable depending on the formulation. Therefore, the second ACAT (unidirectional) model, which assumes that all drugs are absorbed instantly into the blood was tested. Using this model the prediction errors of  $C_{\max}$  and AUC were only 5 and 4%, respectively. However, both models show different absorption patterns throughout the gut. It is not clear what consequences such differences have. More drugs and their absorption patterns have to be investigated using both models. For glyburide, a basic IVIVC was established using physicochemical data obtained from *in vitro* measurements.

The previous prediction of the oral absorption and the establishment of an IVIVC were based on the physicochemical data. These simulations considered particle dissolution but not the dissolution behavior of the dosage form. It is well established that formulation factors such as solid dispersions (Valleri *et al.* 2004) or adding surfactant can influence the dissolution of Class II drugs (El-Massik *et al.* 1996) and furthermore influence the *in vivo* absorption (Blume *et al.* 1993). In order to correlate the *in vitro* dissolution to the *in vivo* absorption, conventionally the *in vivo* absorption data are derived by the deconvolution methods such as pharmacokinetic compartment models - (e.g. Wagner-Nelson or Loo-Riegelman) or compartment independent models- (e.g. DeMons) (USP 29, 2006; Wagner *et al.* 1964; Yu *et al.* 1997). The resulting percent *in vivo* fraction dose absorbed vs. time profiles are correlated to the percent *in vitro* released vs. time profiles and the IVIVC can be established (Dutta *et al.* 2005; Grundy *et al.* 1997ab). For the ACAT model, it is able to utilize drug release profiles to calculate the amount of absorbed drug in each compartment and therefore calculate the plasma concentration vs. time profiles based on the input pharmacokinetic parameters of the drugs. The critical key here is to develop *in vitro* dissolution methods that can simulate the *in vivo* dissolution behavior of a drug product. Fig. 5.5 shows an *in vitro* dissolution test using the USP



paddle apparatus. The dissolutions were performed using FaSSIF or SIF at a single pH of 6.5 (Wei *et al.* 2006a). The drug release in FaSSIF was increased compared to SIF. However, in the human GI tract a pH gradient exists (Löbenberg and Amidon, 2000). Fig. 5.6 shows the dissolution behaviors of the glyburide tablets obtained from such a dynamic pH change that simulates the pH gradient in the GI tract using FaSSIF and SIF (Wei and Löbenberg, 2006a). As shown in the graph glyburide precipitates when the pH is changed from 7.5 to 5.0 in SIF while no precipitation occurs in FaSSIF. This is due to micelle solubilization caused by bile salts and lecithin that keeps the drug in solution. Fig. 5.7 shows the simulations when the obtained drug release profiles are used as input functions into the software. The single pH conditions do not predict the clinically observed data. However, the dynamic pH change conditions simulated the observed data well. Table 5.4 summarizes the prediction errors and the sum of squares for the simulations. The “best” simulation was obtained using FaSSIF and dynamic pH change conditions. An IVIVC was established using dissolution data and computer simulations. Such an IVIVC can be characterized as level A correlation according to the USP definition (USP 29, 2006).

As discussed earlier, the calculations used by GastroPlus™ potentially enables formulation scientists to obtain absorption pattern data (Fig. 5.1, 5.3 and 5.8). The information given by such a pattern may be used to assess, develop or optimize formulations and their drug release requirements in the different segments of the GI tract. This might be used to distinguish between a “good formulation” and a “poor formulation”. Comparison of the absorption patterns between the physicochemical data based IVIVC and the dissolution based IVIVC shows that both patterns are relatively similar. The simulated plasma concentration vs. time curves match the observed curves well for both cases. It can be concluded that the proposed *in vitro* dissolution method reflects the *in vivo* performance of the drug accurately, and the ACAT model theoretically describes the absorption procedure appropriately based on the physicochemical data or *in vitro* dissolutions. However, more examples need to be studied between the interaction of the absorption pattern and pharmacokinetics. This might help to establish the predictable relationships between absorption patterns, plasma concentration vs. time curve and drug release profiles.

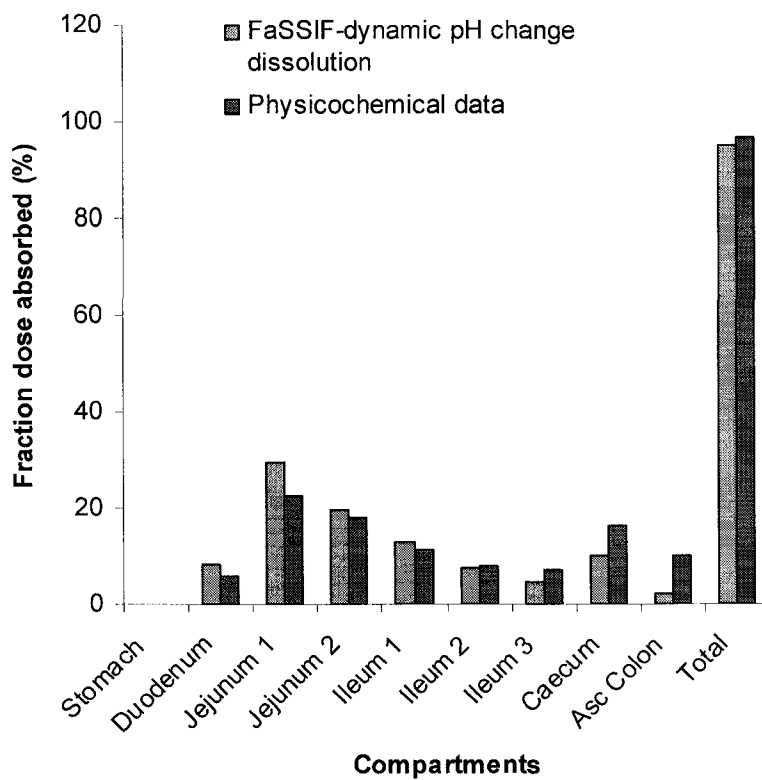


**Figure 5.8.** Comparison of the predicted absorption patterns using physicochemical data and using dissolution profiles at dynamic pH changes

## 5.4. Conclusions

GastroPlus™ is a useful tool for predicting the oral drug absorption. The predicted fraction dose absorbed based on essentially physicochemical data can give a good estimation and guidance for the formulation design of drug candidates at an early stage in the drug development process. The established IVIVCs based on the physicochemical data of API or *in vitro* dissolution profiles of the drug products can provide useful information for the design of new formulations. The interaction between the absorption patterns and pharmacokinetics might give a more comprehensive approach to the development and optimization of the formulation. In both cases, the successful prediction of oral absorption can potentially shorten the time length of drug development at the early stages or facilitate the reverse engineering for generic products.

## 5.5. References

- Agoram, B., Walter, S. and Bolger, B. M. Predicting the impact of physiological and biochemical processes on oral drug bioavailability. *Adv. Drug. Del. Rev.* 50, S41-S67, 2001.
- Blume, H. and Mutschler, E. *Bioäquivalenz*, Govi-Verlag, Eschborn, 1989.
- Blume, H., Ali, S. L. and Siewert, M. Pharmaceutical quality of glibenclamide products: a multinational postmarket comparative study. *Drug Dev. Ind. Pharm.* 19, 2713-2741, 1993.
- Brockmeier, D., Grigoleit, H. G. and Leonhardt, H. Absorption of glibenclamide from different sites of the gastro-intestinal tract. *Eur. J. Clin. Pharmacol.* 29 (2), 193-197, 1985.
- Brocks, D. Advanced pharmacokinetics (Pharm 615 class notes), Faculty of Pharmacy and Pharmaceutical Sciences, University of Alberta, Edmonton, Alberta, Canada, 2002.

Charoenchaitrakool, M., Dehghani, F. and Foster N. R. Micronization by rapid expansion of supercritical solutions to enhance the dissolution rates of poorly water-soluble pharmaceuticals. *Ind. Eng. Chem. Res.* 39, 4794-4802, 2000.

Costa, P. and Lobo, J. M. S. Modeling and comparison of dissolution profiles. *Eur. J. Pharm. Sci.* 13, 123-133, 2001.

DiMasi, J. A. Success rates for new drugs entering clinical testing in the United States. *Clin. Pharmacol. Ther.* 58, 1-14, 1995.

Dutta, S., Qiu, Y., Samara, E., Cao, G. and Granneman, G. R. Once-a-day extended-release dosage form of divalproex sodiumIII: development and validation of a level A in vitro-in vivo correlation (IVIVC). *J. Pharm. Sci.* 94 (9), 1949-1957, 2005.

El-Massik, M. A., Darwish, I. A., Hassan, E. E. and El-Khordagui, L. K. Development of a dissolution medium for glibenclamide. *Int. J. Pharm.* 140, 69-76, 1996.

FDA, Guidance for industry: Extended release oral dosage forms: development, evaluation and application of in vitro/in vivo correlations. U.S. Department of Health Food and Drug Administration Center for Drug Evaluation and Research. 1997.

Galia, E., Nicolaidis, E., Hörter, D., Löbenberg, R., Reppas, C. and Dressman, J. B. Evaluation of various dissolution media for predicting in vivo performance of class I and II drugs. *Pharm. Res.* 15 (5), 698-705, 1998.

GastroPlus Manual, version 5.1. Simulation Plus Inc. Lancaster, California, USA, 2006.

Grass, M. G. Simulation models to predict oral drug absorption from in vitro data. *Adv. Drug Del. Rev.* 23, 199-219, 1997.

Grass, M. G. and Sinko, P. J. Physiologically-based pharmacokinetic simulation modeling. *Adv. Drug. Del. Rev.* 54, 433-451, 2002.

Grundy, J. S., Anderson, K. E., Rogers, J. A. and Foster R. T. Studies on dissolution testing of the nifedipine gastrointestinal therapeutic system. I. Description of a two-phase in vitro dissolution test. *J. Controlled Release.* 48, 1-8, 1997a.

Grundy, J. S., Anderson, K. E., Rogers J. A. and Foster R. T. Studies on dissolution testing of the nifedipine gastrointestinal therapeutic system. II. Improved in vitro-in vivo correlation using a two-phase dissolution test. *J. Controlled Release*. 48, 9-17, 1997b.

Jinno, J., Oh, D. M., Crison, J. R. and Amidon, G. L. Dissolution of ionizable water-insoluble drugs: the combined effect of pH and surfactant. *J. Pharm. Sci.* 89 (2), 268-275, 2000.

Kaukonen, A. M., Boyd, B. J., Porter, C. J. H. and Charman, W. N. Drug solubilization behavior during in vitro digestion of simple triglyceride lipid solution formulations. *Pharm. Res.* 21 (2), 245-253, 2004.

Löbenberg, R. and Amidon, G. L. Modern bioavailability, bioequivalence and biopharmaceutics classification system. New scientific approaches to international regulatory standards. *Eur. J. Pharm. Biopharm.* 50, 3-12, 2000.

Neugebauer, G., Betzien, G., Hrstka, V., Kaufmann, B., Möllendorff V. E. And Abshagen, U. Absolute bioavailability and bioequivalence of glibenclimide (Semi-Euglucon<sup>®</sup>N). *Int. J. Clin. Pharmacol. Therapy and Toxicology*. 23 (9), 453-460, 1985.

Norris, D. A., Leesman, G. D., Sinko, P. J. and Grass, G. M. Development of predictive pharmacokinetic simulation models for drug discovery. *J. Control. Release*. 65, 55-62, 2000.

Parrott, N. and Lavé, T. Predicting of intestinal absorption: comparative assessment of GASTROPLUS<sup>™</sup> and IDEA<sup>™</sup>. *Eur. J. Pharm. Sci.* 17, 51-61, 2002.

Prentis, R. A., Lis, Y. and Walker, S. R. Pharmaceutical innovation by the seven UK-owned pharmaceutical companies (1964-1985). *Br. J. Clin. Pharmacol.* 25, 387-396, 1988.

Tong, H. Y., Shekunov, B. Y., York, P. and Chow, A. H. L. Characterization of two polymorphs of salmeterol xinafoate crystallized from supercritical fluids. *Pharm Res.* 18 (6), 852-858, 2001.

United States Pharmacopeia, Chapter in vitro and in vivo evaluation of dosage forms. U. S. Pharmacopeial convention Inc. Rockville, USP 29, 2006.

Valleri, M., Mura, P., Maestrelli, F., Cirri, M. and Ballerini, R. Development and evaluation of glyburide fast dissolving tablets using solid dispersion technique. *Drug Dev. Ind. Pharm.* 30 (5), 525-534, 2004.

Vertzoni, M., Fotaki, N., Kostewicz, E., Stippler, E., Leuner, C., Nicolaidis, E., Dressman, J. B. and Reppas, C. Dissolution media simulating the intraluminal composition of the small intestine: physiological issues and practical aspects. *J. Pharm. Pharmacol.* 56, 453-462, 2004.

Wagner, J. G. and Nelson, E. Kinetic analysis of blood levels and urinary excretion in absorptive phase after single doses of drug. *J. Pharm. Sci.* 53 (11), 1392-1403, 1964.

Wei, H. and Löbenberg, R. Biorelevant dissolution media as a predictive tool for glyburide a class II drug. *Eur. J. Pharm. Sci.* 29, 45-52, 2006a.

Wei, H., Dalton, C., Di Maso, M., Kanfer, I. and Löbenberg, R. Physicochemical characterization of five glyburide powders: A BCS based approach to predict oral absorption. *Pharm. Res.* submitted, 2006.

Wishart, B. Bioinformatics in drug development and assessment. *Drug. Metab. Rev.* 37, 279-210, 2005.

Yazdaniyan, M., Briggs, K., Jankovsky, C. and Hawi, A. The “high solubility” definition of the current FDA guidance on biopharmaceutical classification system may be too strict for acidic drugs. *Pharm. Res.* 21 (2), 293-299, 2004.

Yokoe, J., Iwasaki, N., Haruta, S., Kadano, K., Ogawara, K., Higaki, K. and Kimura, T. Analysis and prediction of absorption behavior of colon-targeted prodrug in rats by GI-transit-absorption model. *J. Control. Release.* 86, 305-313, 2003

Yu, Z., Hwang, S. S. and Gupta S. K. DeMonS – A new deconvolution method for estimating drug absorbed at different time intervals and/or drug disposition model parameters using a monotonic cubic spline. *Biopharm. Drug Dispos.* 18 (6), 475-487, 1997.

## CHAPTER 6

### APPLICATION OF COMPUTER SIMULATIONS AND THEIR USE AND EVALUATION OF INPUT DATA

#### 6.1. Introduction

GastroPlus™ is a useful software program for predicting the oral absorption of drugs. Previous chapters 3, 4 and 5 have shown the prediction of the oral absorption and the establishment of an IVIVC based on the physicochemical data of glyburide APIs or *in vitro* dissolution profiles of glyburide products as input functions into GastroPlus™. The methods and application of GastroPlus™ have been described in previous chapters. In this chapter, the utilization and evaluation of the input data were investigated in more detail. The influence of the particle size and distribution on the simulation was studied. The computer aid reverse engineering for the API selection and the optimization of formulation is demonstrated in this chapter. The resulting simulations gave more comprehensive understanding of GastroPlus™ and the related ACAT model. Due to the irregularly observed individual plasma concentration vs. time curves, the simulations were based on pharmacokinetic parameters calculated from the mean observed data the same as the previous chapters. However, the *in vitro* dissolution profiles obtained from different agitation speeds were used as input functions that potentially simulated the different hydrodynamic properties in the GI tract (Appendix A). The resulting predicted plasma concentration vs. time curves were compared to each other in an effort to identify suitable agitation speeds. The materials and methods have been described in Chapters 3, 4, 5 and Appendix A.

## 6.2. Results and Discussion

### 6.2.1. Particle Size Influence on the Simulations

#### 6.2.1.1. Influence of Particle Fraction using Physicochemical Data

A reduced particle size of an API can improve the solubility and intrinsic dissolution rate; therefore, an influence on a drug's bioavailability is expected if dissolution is the rate limiting factor (Atkinson *et al.* 1962). For example, pharmaceutical preparations that use micronized glyburide as API showed better absorption and less variability and required a lower dose compared to non-micronized glyburide (Suleiman and Najib, 1989). The particle size analysis of the APIs can provide information on particle size and particle size distribution as presented in Chapter 3. The API powder is normally polydisperse (Martin, 1993). In order to compare two batches of API powders the statistical average or mean diameters as the basis for comparison are calculated based on Edmundson equation (Eq. 6.1, Martin, 1993).

$$d_{mean} = \left( \frac{\sum nd^{p+f}}{\sum nd^f} \right) \quad \text{Eq. 6.1}$$

where,  $n$  is the number of particles in a size range;  $d$  is the equivalent diameter;  $p$  is an index related to the size of individual particle such as the particle length, surface or volume;  $f$  is the frequency index that the frequency of a particle in a certain size range occurs.

However, it is important to compare two batches of API powders with not only their average or mean diameters, but also their particle size distribution. The particle size distribution can be obtained by plotting the number, or weight of particles within a specific range against the size range. The applied particle analysis method (Chapter 3) gave the mean diameters of different batches of APIs and the particle size distributions expressed as the percentage volume undersize. Fig. 6.1 shows the predicted fraction dose absorbed in each compartment (ACAT model) when the particle fraction of an API (API-2) was changed. The fraction dose absorbed decreased in the duodenum, jejunum 1 and jejunum 2 when the particle size increased. On the other hand, the fraction dose absorbed in the colon increased when the particle size increased. The total fraction dose absorbed



decreased following the increase in particle size. Fig. 6.2 and Table 6.1 show a summary of the simulations of the German reference products (GR) containing API-2. The simulations using D50 (8.4  $\mu\text{m}$ ) values or Dmean (12.6  $\mu\text{m}$ ) values give the best prediction. The sum of the squares is only 0.04 for both D50 and Dmean and is much smaller than that for the other fractions. The predicted errors of  $C_{\text{max}}$  and AUC for both cases (D50 and Dmean) are relatively small and the simulated plasma concentration vs. time curves match the observed curve better compared to the other particle fractions.

The simulated impact of the theoretical changes in particle size and particle size distribution on the oral performance has been demonstrated in Chapter 3. The interaction between absorption pattern and the pharmacokinetics of an API or a product were discussed in detail (Chapter 5). In this chapter, the impact of the particle size and size distribution using experimental data on the simulation of the oral absorption and performance was investigated. Such information can assist formulation scientists to estimate the suitable particle size and size distribution before any further manufacturing processes are performed such as in the selection of appropriate milling processes; or whether milling is necessary at all. In this presented case, the expected particle sizes are the D50 or Dmean. This result confirms that controlled particle size distribution can significantly influence the reproducibility of a product's bioavailability (Timmins *et al.* 2006). Formulation scientists can select suitable processes such as screening or milling to obtain the expected particle size and size distribution based on the data of particle analysis. Also the absorption patterns of different particle sizes can assist formulation scientists to estimate the drug release at different segments of the GI tract that assures optimal drug absorption. Therefore, specifications for the particle size and size distribution can be set based on the experimental data and computer simulation. This might help to decide on the formulation development and manufacturing processes.

**Table 6.1.** Summary of the influence of particle fractions on the simulations using physicochemical data as input functions (German reference (GR) containing API-2: Observed:  $C_{\max}$ : 301 ng/mL;  $AUC_{0-24}$ : 1359.6 ng/mL\*h)

	Simulated		Prediction Error (%)		
	$C_{\max}$	AUC	$C_{\max}$	AUC	*SS
D10	376	1334.2	25	2	0.020
D25	360	1329.8	20	2	0.013
D50	321	1316.1	7	3	0.004
D75	246	1269.7	18	7	0.019
D90	164	1147.8	46	16	0.088
Dmean	286	1298.8	5	4	0.004

10% (D10: 1.31  $\mu\text{m}$ ), 25% (D25: 3.47  $\mu\text{m}$ ), 50% (D50: 8.41  $\mu\text{m}$ ), 75% (D75: 17.47  $\mu\text{m}$ ) and 90% (D90: 29.69  $\mu\text{m}$ ) of the particle volume undersize and Dmean: 12.55  $\mu\text{m}$ ). SS: Sum of Squares  $(Y_{\text{obs}} - Y_{\text{pred}})^2$

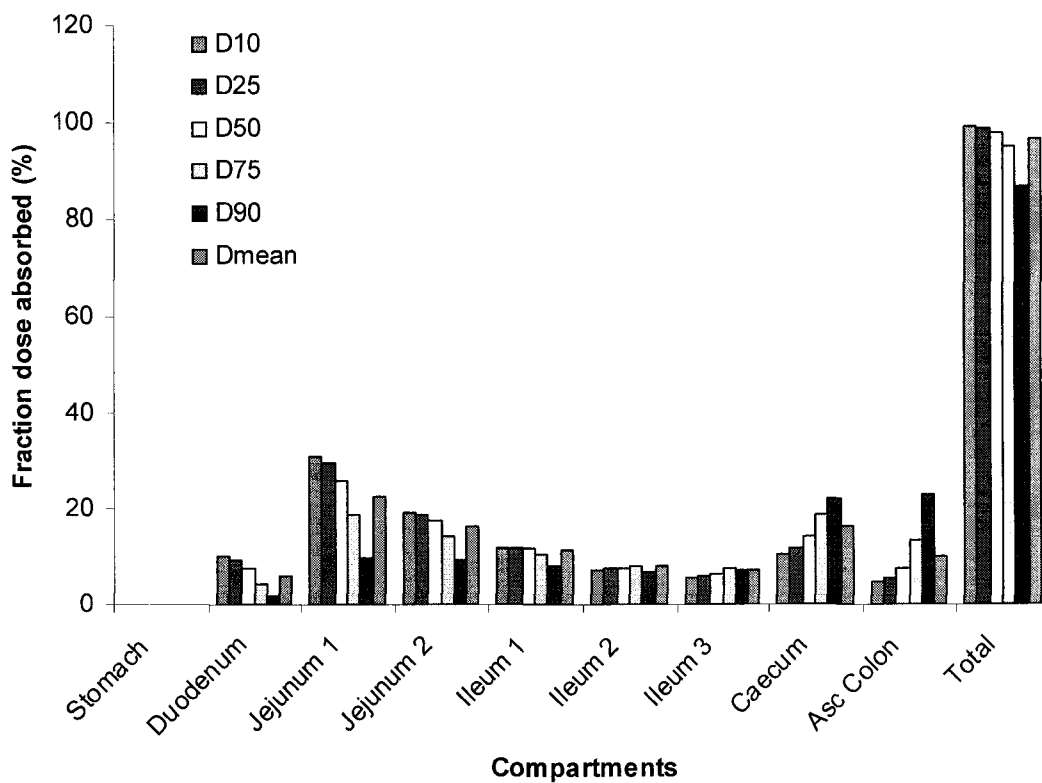


**Figure 6.1.** Summary of the influence of particle fractions on the fraction dose absorbed in each compartment using physicochemical data as input functions (German reference (GR) containing API-2; 10% (D10: 1.31  $\mu\text{m}$ ), 25% (D25: 3.47  $\mu\text{m}$ ), 50% (D50: 8.41  $\mu\text{m}$ ), 75% (D75: 17.47  $\mu\text{m}$ ) and 90% (D90: 29.69  $\mu\text{m}$ ) of the particle volume undersize and Dmean: 12.55  $\mu\text{m}$ ).

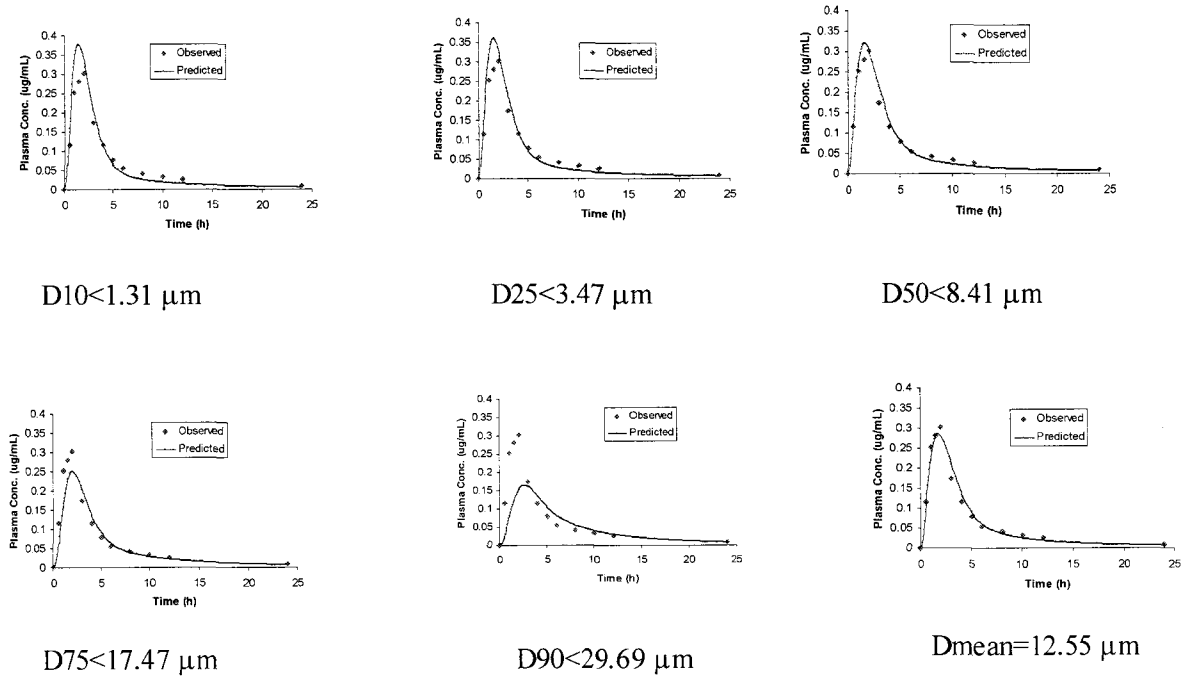


**Figure 6.2.** Summary of the influence of particle fraction on the simulations using physicochemical data as input functions (German reference (GR) containing API-2)

### 6.2.1.2. Computer Simulation Aided Reverse Engineering

The information available from the South Africa studies showed that there were two bioequivalence studies. Two glyburide reference products (5 mg dose; Lot #8017495, SR 1; Lot #8010886, SR 2) were used as references and two test products were manufactured. No other information other than the dose of the reference products was known, however, they were assumed to be bioequivalent. A test formulation (ST 1) containing API-3 (Chapter 3) that was milled from API-4 was manufactured and a bioequivalence (BE) study was performed. The BE study failed and showed too high plasma concentration levels of the test product. Then a second formulation (ST 2) containing API-4 was developed and a BE study was performed. The BE study failed again. During the development of the first generic product, the manufacturer selected a milling process presumably based on the empirical expertise. There were no other scientific approaches to this issue as to whether the milling process was necessary or not. The *in vitro* dissolution profiles of the generic test and the reference products were matched (the data was provided by manufacture). For the second generic formulation, the manufacturer developed the product based on the empirical expertise again without the measurement of the particle size of the API powders. They assumed that the milled API had smaller particle size than the un-milled. Actually, the two APIs have quite similar particle sizes (Chapter 3). The failed BE studies might have been avoided if a particle analysis was performed with computer simulation together.

If GastroPlus™ had been available, then no further milling processes would have been needed based on the computer simulations. For example, the computer simulation using the particle size as a major variable would have revealed that the particle size of API-3 and 4 was already too small. A computer-based estimation can be achieved by the valuable function of GastroPlus™ called computer optimization process. The software can be used to simulate the observed plasma concentration vs. time curves as described in Chapter 3. The calculated pharmacokinetic parameters of both South Africa reference products (SR 1 and SR 2) are summarized in Table 6.2. All the physicochemical parameters are the same as those in Chapter 3 except for the particle sizes and the pharmacokinetic parameters. First, an empirically chosen particle radius (8.0 μm) for

both reference products was used as input function to perform the simulation. The simulated plasma concentration vs. time curves relatively match the observed curves (Fig. 6.3 and 6.4). The prediction errors of AUC and  $C_{max}$  are around 10%: SR 1: +14.3% and -0.9%; SR 2: -10.5% and +8.6%, respectively (Table 6.3). Second, the computer optimization processes for the particle radius based on the input empirical particle radius and the resulting simulations were performed. The goal of the optimization process was to estimate the theoretical particle sizes that can potentially give better fits of the simulations compared to the empirical particle sizes. The computer estimated the particle radius of the reference-1 (SR 1) and 2 (SR 2) as 4.6 and 3.4  $\mu\text{m}$ , respectively, after the optimization process. The simulated plasma concentration vs. time curves using the computer estimated particle radius match the observed well for reference-2 (SR 2) product. The sum of squares for SR 2 between predicted and observed values using the computer estimated particle radius (3.4  $\mu\text{m}$ ) was 0.0002 (Table 6.4). For reference-1 (SR 1), the predicted plasma concentration vs. time curve using computer estimated particle radius did not match the observed curve very well.  $C_{max}$  was over estimated by up to 33.1% (Table 6.3). The prediction errors of  $C_{max}$  for both products were +33.1% and +4.5%. The prediction errors of AUC were -0.5% and +9.1%. The sums of squares for the simulations of both products using computer estimated particle radius (4.6  $\mu\text{m}$  and 3.4  $\mu\text{m}$ ) were 0.0103 and 0.0002 (Table 6.4). The simulation results indicated that the computer estimated particle radius was suitable for SR 2 (3.4  $\mu\text{m}$ ) and the empirical estimated particle radius (8.0  $\mu\text{m}$ ) will fit for SR 1.

It was assumed that both reference products used the same particle sizes and both product batches used in the clinical tests were bioequivalent to each other. Simulations were performed to match the FDA requirement of the prediction errors for both studies by changing the particle sizes empirically. The FDA guideline requires that simulations can predict the oral performance within 10% for AUC and  $C_{max}$  (FDA September, 1997). Based on the data obtained from the API characterization in Chapter 3, a no larger than 8.0  $\mu\text{m}$  particle radius might be the best guess to make both studies acceptable to FDA requirements. As shown in Tables 6.3 and 6.4 particle radius (8.0  $\mu\text{m}$ ) results in better prediction values for reference 1 (SR 1). A further optimization by changing the empirical particle radius was performed. Based on the information generated by the

simulations a particle size of 6-8  $\mu\text{m}$  might be the most appropriate to make both generic products (ST 1 and ST 2) bioequivalent to the reference products. The particle size of 6.0-8.0  $\mu\text{m}$  gave relatively better prediction errors of the AUC and  $C_{\text{max}}$  and a small sum of squares for both reference products (Table 6.3 and 6.4). As mentioned previously, the particle radius of API-3 and API-4 in both products (ST 1 and ST 2) were 2.1 and 2.6  $\mu\text{m}$ , respectively, and were too small to result in a bioequivalent product based on the computer simulation. The presented *in silico* approach demonstrates how computer simulations can assist formulation scientists in their work. Selections of particle size and size distribution can be based on simulation results rather than on empirical guesses. This study shows how generic drug development can benefit from computer simulations. Both failed studies could have been avoided if computer simulations had been used. The present study clearly demonstrates that time and money could have been saved using computer simulations and at the end of the development process a generic product would have been on the market. However, it has to be demonstrated that computer simulations can predict oral performance of other drugs with the same precision as shown for glyburide.

**Table 6.2.** Pharmacokinetic parameters of two South Africa reference products (SR 1 and SR 2) used for the computer simulations (The mean values of the clinical data obtained from these four products were well described by a two-compartmental model (Rydberg *et al.* 1997)

	$C_{\text{max}}$ (ng/mL)	AUC <sub>0-n</sub> * (ng/mL*h)	Clearance (L/h)	$V_c$ (L)	$K_{12}(\text{h}^{-1})$	$K_{21}(\text{h}^{-1})$
SR 1 (Lot #8017495)	142.6	940.9	4.77	13.30	0.143	0.059
SR 2 (Lot #8010886)	66.9	493.3	9.01	36.06	0.298	0.282

\* n : SR 1: 30 h; SR 2: 36 h.

**Table 6.3.** Comparison of the predicted and observed  $C_{max}$  and AUC for two South African reference products (reference-1 (SR 1) and reference-2 (SR 2))

	Simulated				Prediction Error (%)			
	SR 1		SR 2		SR 1		SR 2	
	* $C_{max}$	*AUC	$C_{max}$	AUC	$C_{max}$	AUC	$C_{max}$	AUC
a.	142.6	940.9	66.9	493.3				
b.	182.9	935.5	66.6	538.0	+28.3	-0.6	-0.4	+9.0
c.	176.7	934.5	64.4	537.5	+23.9	-0.7	-3.7	+9.0
d.	170.1	933.1	62.2	536.8	+27.5	-0.8	-7.0	+8.8
e.	163.0	931.4	59.9	535.9	+14.3	-0.9	-10.5	+8.6
f.	189.9	936.1	69.9	538.5	+33.1	-0.5	+4.5	+9.1

a: Observed; b, c, d, e: Empirical estimated particle radius (5, 6, 7, 8  $\mu\text{m}$ ); f: Computer estimated particle radius (SR 1: 4.6  $\mu\text{m}$ ; SR 2: 3.4  $\mu\text{m}$ )

\* $C_{max}$ : ng/mL; AUC<sub>0-n</sub>: ng/mL\*h

**Table 6.4.** Summary of the sum of squares (SS) for the simulations of two South Africa reference products (SR 1 and SR 2). (SS: Sum of Squares ( $Y_{obs} - Y_{pred}$ )<sup>2</sup>)

	Computer estimated (SR 1:4.6 $\mu\text{m}$ ; SR 2: 3.4 $\mu\text{m}$ )	Empirical estimated (5 $\mu\text{m}$ )	Empirical estimated (6 $\mu\text{m}$ )	Empirical estimated (7 $\mu\text{m}$ )	Empirical estimated (8 $\mu\text{m}$ )
SR 1	0.0103	0.0073	0.0052	0.0046	0.0055
SR 2	0.0002	0.0002	0.0006	0.0011	0.0019



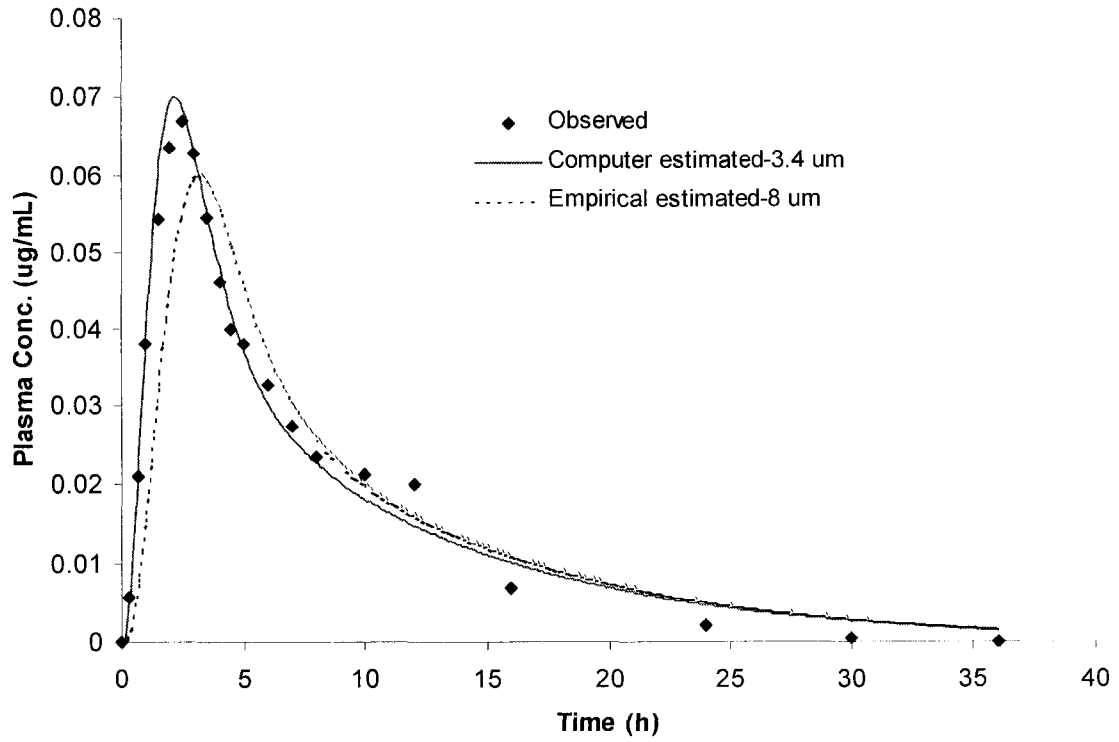


**Figure 6.3.** Comparison between simulated and observed plasma time curves for South Africa reference-1 (SR 1). Different particle sizes were chosen to match the observed curves and to try to bring the simulated curves within 10% of the observed values for AUC and  $C_{max}$ .

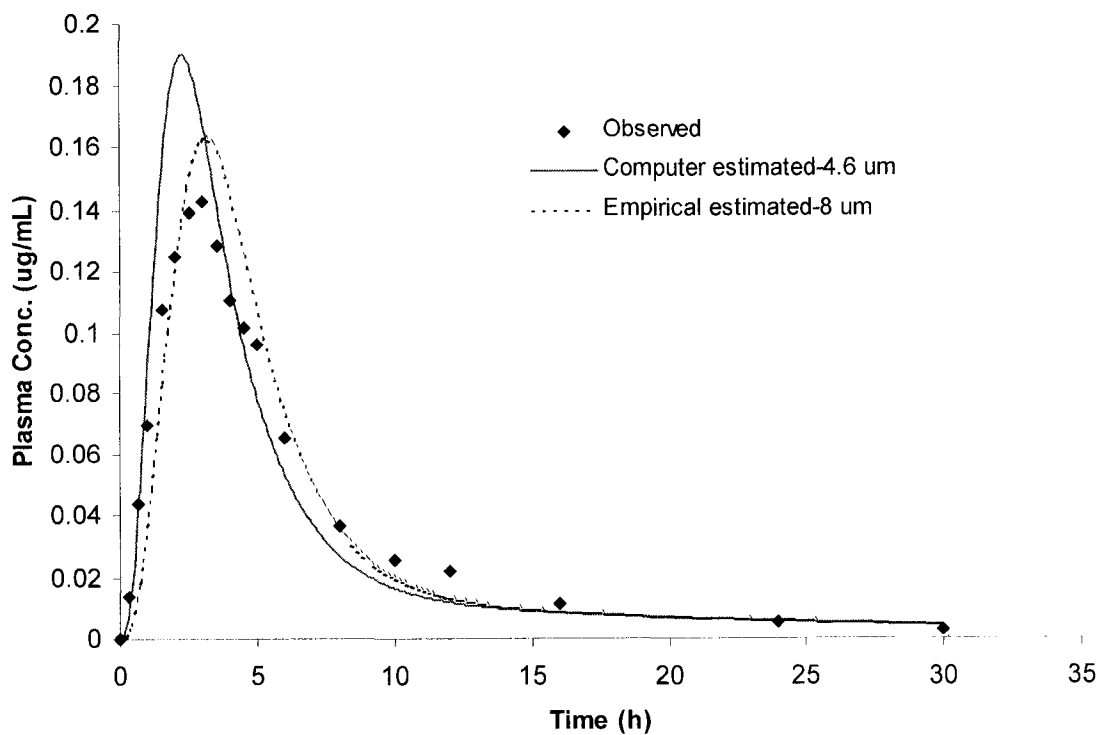


**Figure 6.4.** Comparison between simulated and observed plasma time curves for South Africa reference-1 (SR 2). Different particle sizes were chosen to match the observed curves and to try to bring the simulated curves within 10% of the observed values for AUC and  $C_{max}$

## 6.2.2. *In Vitro* Dissolution Data as Input Function for Simulations

### 6.2.2.1. Simulations using *In Vitro* Dissolution Data at Different Agitation Speeds

Clinical studies of glyburide reported a large variability in bioavailability due to the individual physiological conditions (USP DI, 1999). The clinical studies of two German products (GR and GT) were obtained from 15 volunteers. The large standard deviations (standard deviation: SD) of the plasma concentration at each time point are shown in Fig. 6.5 and 6.6. The dots represent the mean value of the 15 volunteers and the error bars show the variability. Many research groups have reported that the hydrodynamic property (agitation force) is an important factor in simulating biorelevant dissolution conditions of dosage forms. Literature shows that drug releases is different at different agitation speeds (Kamba *et al.* 2003). The goal of a modified dissolution test is to simulate the hydrodynamics in the GI tract caused by motility (Kamba *et al.* 2003; Qureshi *et al.* 2004; Rostami-Hokjegan *et al.* 2002; Wu *et al.* 2004). The dissolution tests of the two German glyburide tablets have been performed at different agitation speeds in LQ-FaSSIF as described in Appendix A. Previous simulations were able to predict/simulate the mean values of the plasma concentration vs. time curves of the *in vivo* study. However, individually the 15 volunteers exhibited a huge variability of plasma concentrations at each time point. To be able to match the observed plasma concentration vs. time curves with computer simulations it was necessary to obtain correct pharmacokinetic parameters from the compartmental model fitting described in Chapters 3, 4 and 5. However, this was not always possible for many of the individual volunteers. In this present study we therefore focus on the mean observed values. The dissolution profiles generated with the different agitation speeds were used to simulate the mean plasma concentration vs. time curves (Fig. 6.5 and 6.6). The sums of squares are summarized in Table 6.5. The sums of the squares at 75 and 100 rpm are relatively lower for both products compared to that at 50 rpm. In Appendix A, the comparison of the dissolution profiles at different agitation speeds showed that there was no significant difference between 75 and 100 rpm. Only the dissolution profiles obtained from 50 rpm showed a slight difference from the other two agitation speeds. The simulation results such as the sum of squares confirmed this conclusion. The sums of squares of 75 and 100

rpm are similar but lower than that at 50 rpm for both products and gave better fits on the observed mean data. The FDA guidance recommends that dissolution test for immediate release dosage form should be performed at 50/75 rpm using apparatus II (FDA, August 1997). Therefore, 75 rpm was selected to perform the dissolution tests for predicting the mean value in this case. In order to find a universal agitation speed for predicting the mean value, more agitation speeds should be tested.

**Table 6.5.** The simulation summary of the sums of squares at different agitation speeds for German reference (GR) and Test (GT) (Sum of Squares  $(Y_{obs} - Y_{pred})^2$ )

	50 rpm	75 rpm	100 rpm
GR	0.027	0.019	0.015
GT	0.015	0.008	0.010

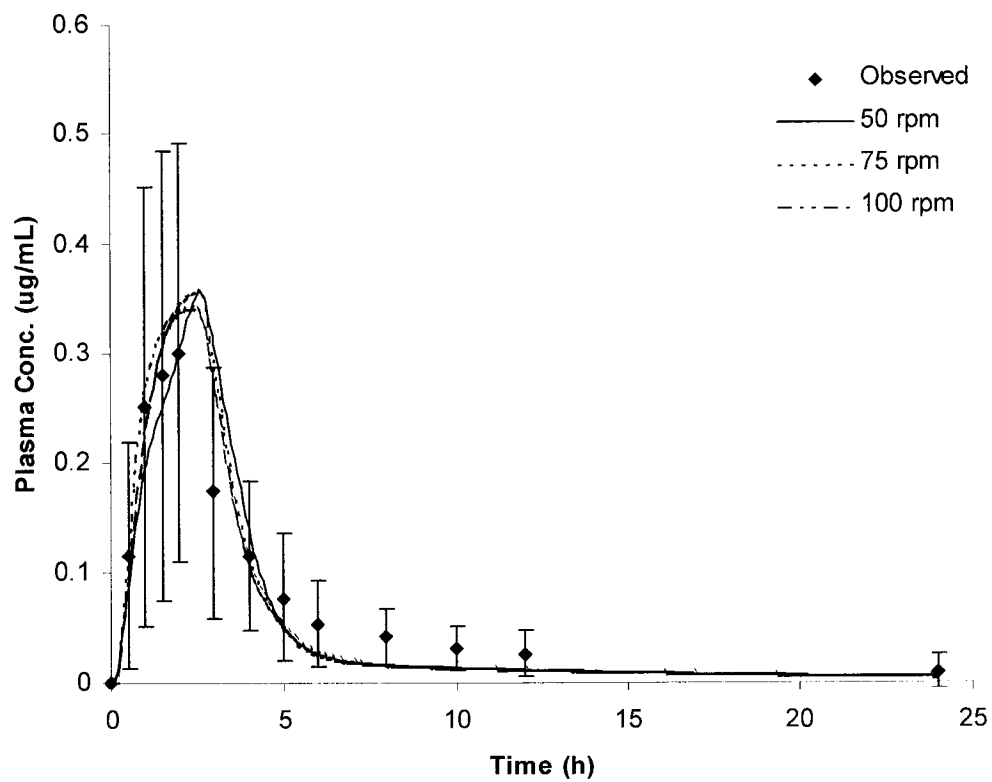


**Figure 6.5.** Comparison of the simulated plasma concentration vs. time curves using *in vitro* dissolution profiles under dynamic pH changes at different agitation speeds (50, 75 and 100 rpm; German reference product (GR))

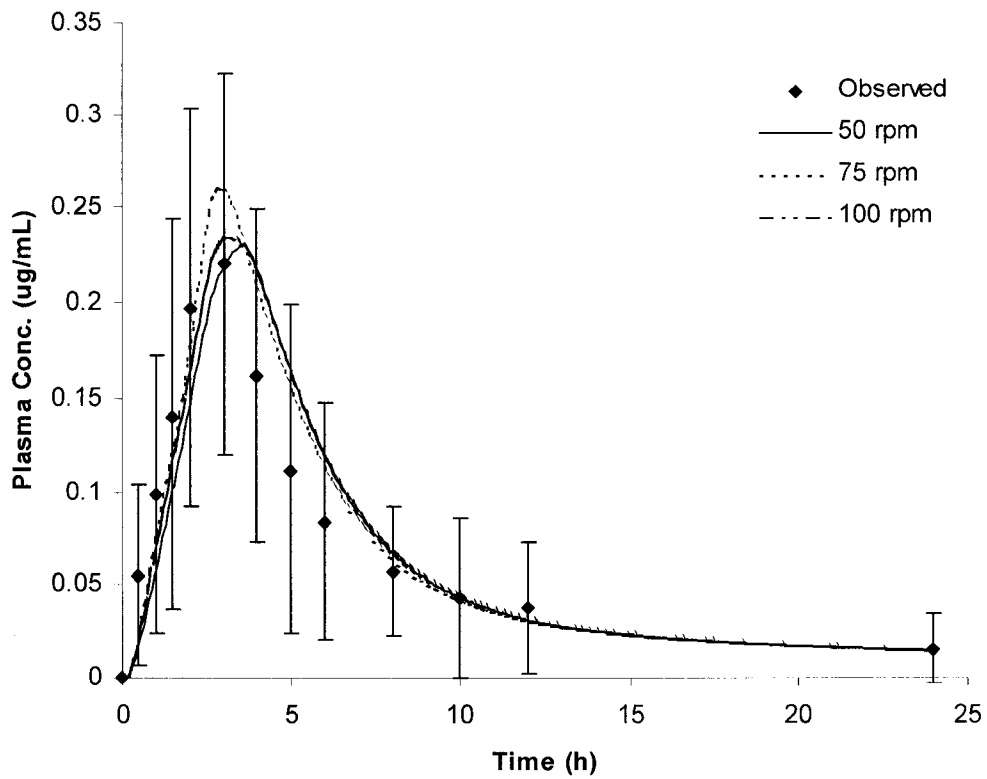


**Figure 6.6** Comparison of the simulated plasma concentration vs. time curves using *in vitro* dissolution profiles under dynamic pH changes at different agitation speeds (50, 75 and 100 rpm; German test product (GT))

### 6.2.2.2. Reverse Engineering of a Drug Product using *In Vitro* Dissolution Data

The goal of predictive *in vitro* dissolution testing is to simulate *in vitro* the *in vivo* dissolution behavior. As described in previous chapters, biorelevant dissolution media (BDMs), especially low quality (LQ) media can sufficiently simulate the physiological composition of intestinal fluids in the human GI tract. The previous results (Chapter 4) showed that LQ-FaSSIF can differentiate between clinically relevant formulation factors of two German glyburide products (GR and GT, 3.5 mg dose) using their dissolution behaviors. However, the same protocol applied to South Africa glyburide products (SR 1 and ST 1; SR 2 and ST 2; 5 mg dose) was not able to differentiate between reference and generic products (data provided by manufacturer). The dissolution behaviors of both products were almost identical but the drug releases were quite low at only up to 47% of the labeled drug dose (Fig. 6.7). The simulated plasma concentration vs. time curves did not match the observed curves when the dissolution profiles were used as input functions (Fig 6.8). Fig. 6.7 shows the computer optimized dissolution profiles for both test products. The estimated drug releases of the two test products using computer optimization should be more than 90%. The predicted plasma concentration vs. time curves using the computer optimized profiles as input functions matched the observed curves well (Fig. 6.9). The sums of squares (Table 6.6) confirmed the results.

Literature shows that the development of a level A correlation (IVIVC) is classically based on the deconvolution of *in vivo* data and convolution of *in vitro* dissolution data (Eddington *et al.* 2000; Mahayni *et al.* 2000; Rekhi *et al.* 1997). The established IVIVC can be used to predict the oral absorption using *in vitro* dissolution profiles based on internal and external predictability (Mahayni *et al.* 2000). But these studies did not use IVIVC information for optimization of formulations. The GastroPlus™ (ACAT model) can change this situation. For example, the results of this study indicate that the dissolution obtained from LQ-FaSSIF can not reflect the *in vivo* dissolution universally. However, the computer optimized dissolution profiles can be used as target for the formulation scientist. They can develop and optimize a suitable formulation based on the target dissolution profile obtained from computer optimization. The information provided here can shorten the time of drug development and save money. The results show that

further modification of the dissolution methods using BDMs is necessary. A universal biorelevant dissolution protocol is therefore highly desired. If a universal *in vitro* dissolution method can be developed, then product specifications can be set based on the *in vitro* dissolution criteria simulated using software models.

**Table 6.6.** Comparison of the sums of squares between the predicted and observed plasma concentration vs. time curves using experimental or computer optimized dissolution profiles for the South Africa Test 1 (ST 1) and 2 (ST 2) products (Sum of Squares  $(Y_{\text{obs}} - Y_{\text{pred}})^2$ )

	Experimental dissolution	Computer optimized dissolution
ST 2	0.081	0.005
ST 1	0.025	0.000



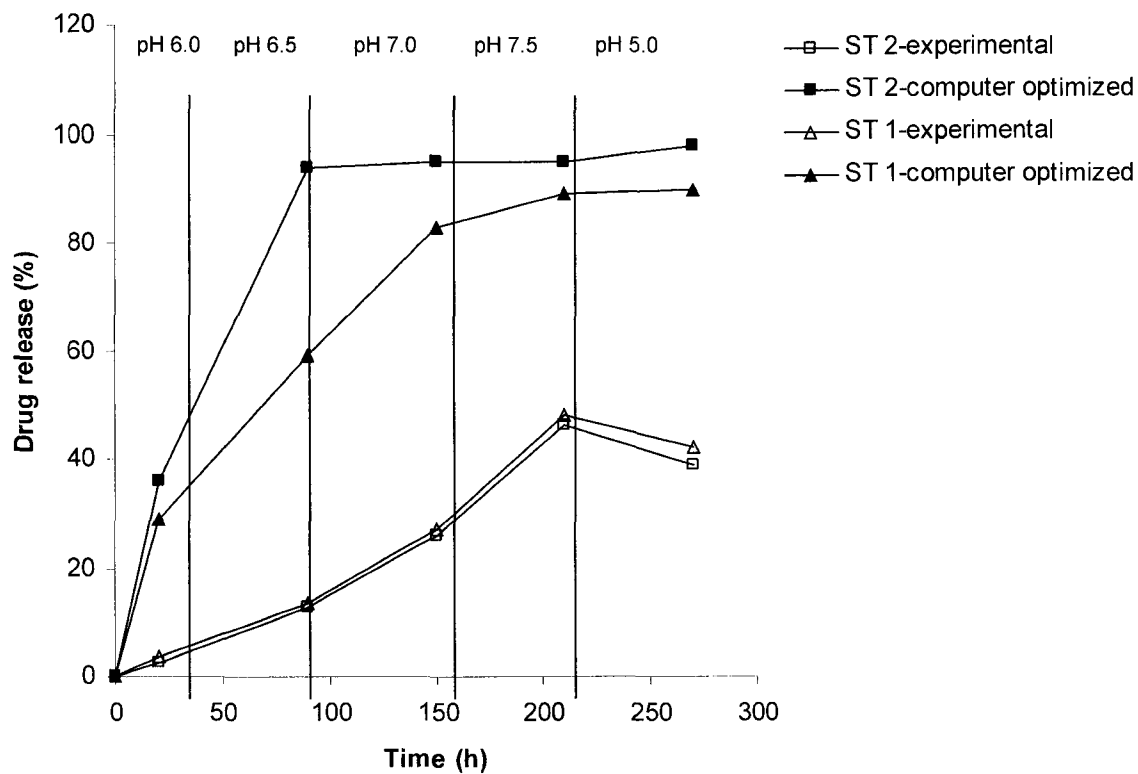


**Figure 6.7.** The comparison of the experimental and computer optimized dissolution profiles of two South Africa test products (ST 1 and ST 2)

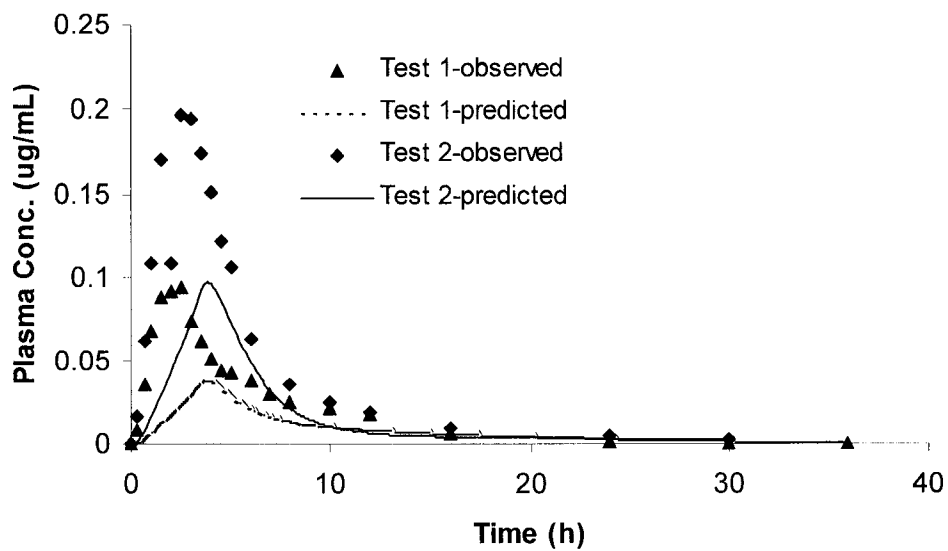


**Figure 6.8.** Comparison of the predicted and observed plasma concentration vs. time curves using experimental dissolution profiles for South Africa Test 1 (ST 1) and 2 (ST 2) products

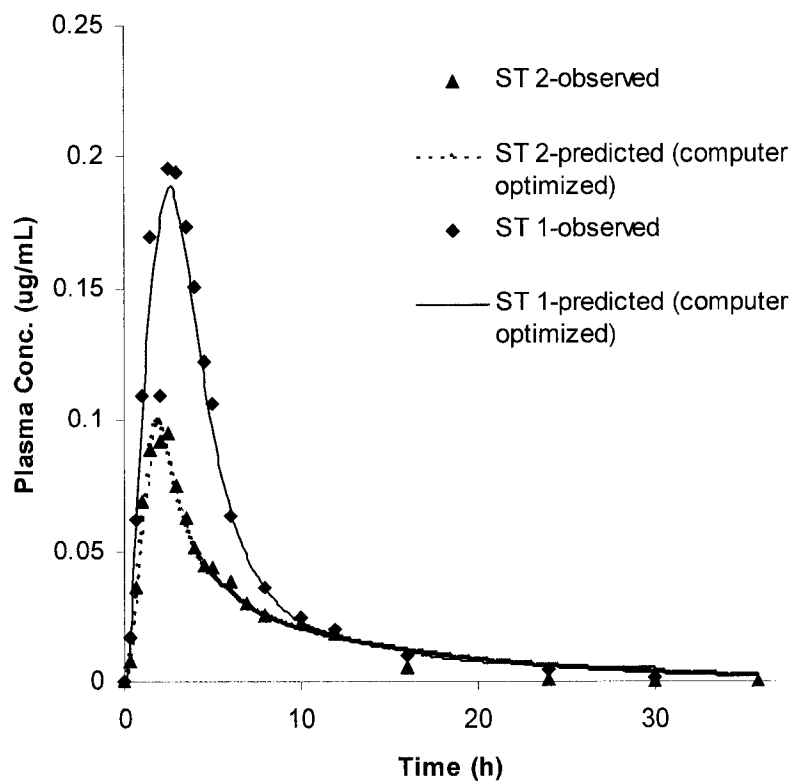


**Figure 6.9.** Comparison of the predicted and observed plasma concentration vs. time curves using computer optimized dissolution profiles for South Africa Test 1 (ST 1) and 2 (ST 2) products

### 6.3. References

Atkinson, R. M., Bedord, C., Child, K. J. and Tomich, E. J. Effect of particle size on blood griseofulvin levels in man. *Nature*. 193, 588-589, 1962.

Eddington, N. D., Rekhi, G. S., Lesko, L. J. and Augsburger, L. L. Scale-up effects on dissolution and bioavailability of propranolol hydrochloride and metoprolol tartrate tablet formulations. *AAPS Pharm. Sci. Tech.* 1 (2), E14, 2000.

FDA, Guidance for industry: Dissolution testing of immediate release solid oral dosage forms. U.S. Department of Health, Food and Drug Administration, Center for Drug Evaluation and Research (CDER) BP, August, 1997.

FDA, Guidance for industry: Extended release oral dosage forms: development, evaluation, and application of in vitro/in vivo correlation. U.S. Department of Health, Food and Drug Administration, Center for Drug Evaluation and Research (CDER) BP, September, 1997.

Kamba, M., Seta, Y., Takeda, N., Hamaura, T., Kusai, A., Nakane, H. and Nishimura, K. Measurement of agitation force in dissolution test and mechanical destructive force in disintegration test. *Int. J. Pharm.* 250, 99-109, 2003.

Mahayni, H., Rekhi, G. S., Uppoor, R. S., Marroum, P., Hussain, A. S., Augsburger, L. L. and Eddington, N. D. Evaluation of "external" predictability of an in vitro-in vivo correlation for an extended-release formulation containing metoprolol tartrate. *J. Pharm. Sci.* 89 (10), 1354-1361, 2000.

Martin A. Physical pharmacy. 4<sup>th</sup> edition, Williams & Wilkins, Baltimore, Maryland, USA, 1993.

Qureshi, S. A. Choice of rotation speed (rpm) for bio-relevant drug dissolution testing using a crescent-shaped spindle. *Eur. J. Pharm. Sci.* 23, 271-275, 2004.

Rekhi, G. S., Eddington, N. D., Fossler, M. J., Schwartz, P. and Lesko, L. J. Evaluation in vitro release rate and in vivo absorption characteristics of four metoprolol tartrate immediate-release tablet formulations. *Pharm. Develop. Tech.* 2 (1), 11-24, 1997.

Rostami-Hodjegan, A., Shiran, M. R., Tucker, G. T., Conway, B. R., Irwin, W. J., Shaw, L. R. and Grattan, T. J. A new rapidly absorbed paracetamol tablet containing sodium bicarbonate. II. Dissolution studies and in vitro/in vivo correlation. *Drug Dev. Ind. Pharm.* 28 (5), 533-543, 2002.

Rydberg, T., Jönsson, A., Karlsson, M. and Meldander, A. Concentration-effect relations of glibenclamide and its active metabolites in man: modeling of pharmacokinetics and pharmacodynamics. *Br. J. Clin. Pharmacol.* 43, 373-381, 1997.

Suleiman, M. S. and Najib, N. M. Isolation and physicochemical characterization of solid forms of glibenclamide. *Int. J. Pharm.* 50 (2), 103-109, 1989.

Timmins, P., Marathe, P. H., Cave, G., Arnold, M. E., Dennis, A. B. and Greene, D. S. Development of a glyburide-metformin fixed combination tablet with optimized glyburide particle size. *Drug Dev. Ind. Pharm.* 66, 25-35, 2006.

United States Pharmacopeia, USP DI. *Drug Information for Health Care Professionals*. Vol I, U. S. Pharmacopeial convention Inc. Rockville, MD, 1999.

Wu, Y., Kildsig, D. O. and Ghaly, E. S. Effect of hydrodynamic environment on tablets dissolution rate. *Pharm. Dev. Tech.* 9 (1), 25-37, 2004.

## CHAPTER 7

### SUMMARY AND CONCLUSION

Many major industries have moved away from experimental testing of a large amount of candidates to predictive evaluation using computer simulations to both design and test new products (Grass *et al.* 2002; Wishart, 2005). The drug development in the pharmaceutical industry depends still on a “build-and test” method that screens large amounts of chemical candidates. The current drug development process needs years of screening and evaluation and potentially faces high failure rates at the end. The advanced combinatorial chemistry and high throughput screening only enhance the “build and test” speed. This situation is due to the complexity of the physiological environment of the human body. Prentis *et al.* (1988) noticed that the high failure rate in drug development was due to the poor pharmacokinetic properties and efficacy of the chosen drug candidates. Bioavailability was the major limiting factor in the drug development process. Therefore, the prediction of the pharmacokinetic parameters, using physiologically-based models, will be a desirable progress that can significantly change the situation. The importance of such simulations is not only for the pharmaceutical industry but also for the regulatory agencies to evaluate a drug product and to decide on necessary *in vivo* studies.

The definition of the physiologically-based pharmacokinetic simulation model is “a representation of the operation or features of one process or system through the use of another.” (Grass and Sinko, 2002). Pharmacokinetic simulations predict the behavior of molecules in humans (or animals) under specific conditions prospectively based on the historical data. Theoretically, the physiologically-based pharmacokinetic simulation models can include all the pharmaceutical dosage forms. In this study, we focused on orally administered glyburide and its dosage forms.

Conventionally, animal models such as rat, dog, etc. are used to investigate certain pharmacokinetic parameters of the drugs before they are tested in humans. However, there is no reliable relationship between animal bioavailability and human bioavailability

for these species (Lin, 1995). Therefore, the prediction of human bioavailability based on the interpretation of animal bioavailability should be used with caution. A physiologically-based pharmacokinetic simulation model potentially provides a more reliable way than an animal model, which can identify and optimize parameters of dosage forms for human use independently.

Amidon and his colleagues developed the Biopharmaceutics Drug Classification System (BCS) based on two fundamental parameters: aqueous drug solubility and gastrointestinal permeability. Both control the rate and extent of oral drug absorption (Amidon *et al.* 1995). The objective of BCS is to predict the oral absorption and *in vivo* performance of a drug product based on the measurements of permeability and solubility. An Advanced Compartmental Absorption and Transit model (ACAT) was developed based on the theory of BCS (GastroPlus™ Manual, 2006). It uses a mathematical approach, which considers all physicochemical and physiological processes including pH, permeability, dissolution, solubility, transit time and metabolism. In this study, *in vitro* solubility/dissolution and permeability data were used as major input functions into the software to predict the oral absorption of four products. *In vivo* and *in vitro* correlations (IVIVCs) for these products were established.

The hypothesis was that biorelevant dissolution methods and permeability measurements combined with computer simulations are able to predict the oral performance of drug products. In order to test the hypothesis, several objectives had to be achieved. Therefore, a series experiments were designed:

- 1) The permeability of glyburide using the Caco-2 cell monolayer was determined and showed that glyburide is a highly permeable drug. A toxicity study of BDMs that potentially simulated the physiological conditions was performed. The Caco-2 cell model can tolerate two times diluted high quality FaSSIF (HQ-FaSSIF). The comparison of BDMs and Hank's solution as transport media showed that two times diluted HQ-FaSSIF might be used as transport media in the Caco-2 model with the limitation of its interaction with active transport mechanisms such as the efflux mediated by P-glycoprotein.

- 2) Material characterization involved X-ray powder diffraction (XRPD), thermogravimetric analysis (TGA), differential scanning calorimetry (DSC), raman

spectroscopy, nuclear magnetic resonance (NMR), particle size and particle size distribution, specific surface area and true density measurements, as well as dissociation constant (pKa), partition coefficient (logP) and distribution coefficient (logD). Material characterizations of five different glyburide powders used to produce different reference and generic glyburide tablets indicated that all of them had similar crystal structures, however, significant differences in surface area, particle size and particle size distribution were observed. No polymorphism was detected that might influence the bioavailability.

3) Solubility studies in different media such as USP dissolution media and BDMs demonstrated that the solubility of glyburide was pH-dependent and the drug can be considered as a low soluble drug. Combination with the permeability study, glyburide can be classified as a Class II drug whose *in vivo* dissolution is the limiting factor for the oral absorption (Galia *et al.* 1998). BDM improve the solubility of glyburide due to the micelle solubilization.

4) Two German products (3.5 mg dose): reference (GR) and test (GT) and two South African products (5 mg dose): ST 1 and ST 2 were tested. The physicochemical properties of the APIs used to produce these products were obtained from material characterization as mentioned previously. Bioequivalent studies of these products were available to us.

5) Different media were evaluated to mimic the *in vivo* dissolution such as conventional buffers and BDMs. The *in vitro* dissolution tests were performed at a single pH or using a dynamic pH gradient protocol.

6) The chemical grade of bile salts and lecithin was investigated. Dissolution tests performed in LQ-FaSSIF were able to differentiate between two German products. The dissolution tests of the products performed in LQ-FaSSIF using a dynamic pH change showed the most predictive power when compared to other media or compared to the situation when a single pH was used.

7) The *in vitro* data were used for computer simulations. The results were compared with the actual clinical data to establish IVIVC. Computer simulations using the data obtained from the material characterization were able to predict the oral absorption of four glyburide formulations (two 3.5 mg and two 5.0 mg dose). An *in vitro/in vivo* correlation (IVIVC) was established. The established IVIVC can be used to evaluate the



particle size and size distribution of the API powders. The API specification can be potentially set based on the experimental and theoretical data of the particle size and size distribution. However, the computer simulations using *in vitro* dissolutions data predicted the oral performance of only two 3.5 mg formulations successfully. The dissolution data from the 5 mg formulations was not predictive. After applying the computer optimization based on the established IVIVC, the theoretical dissolution profiles for both 5.0 mg formulations can be used as targets to reverse engineer a suitable formulation. The hypothesis of this study was partially proven.

During the past years, several multi-functional physiologically-based models have been developed and are commercially available to predict the oral absorption and to establish the IVIVC such as: iDEA<sup>TM</sup> (*In vitro* determination for the estimation of ADME model) and GastroPlus<sup>TM</sup> (Advanced compartmental absorption and transit model, ACAT). Compared to other physiologically-based models that simulate specific *in vivo* conditions such as the simulation of the precipitation of poorly soluble drugs in the GI tract (Willmann *et al.* 2003) and gastrointestinal flow (Kostewicz *et al.* 2004), both GastroPlus<sup>TM</sup> and iDEA<sup>TM</sup> use more comprehensive absorption models which try to include more physicochemical and physiological conditions in the GI tract.

Conventionally the prediction of the oral absorption and the establishment of an IVIVC for an orally administered product were achieved by establishing a relationship between the *in vivo* and *in vitro* data using convolution and deconvolution methods (Polli *et al.* 1997). The method is only suitable for specific cases as well as the physiologically-based models that simulate specific *in vivo* conditions each time (Polli *et al.* 1997). In this study, GastroPlus<sup>TM</sup> and the ACAT model were tested. The rationale behind the hypothesis was if *in vitro* biorelevant method can simulate the *in vivo* performance of a drug an IVIVC is expected. For Class II drugs, biorelevant dissolution methods are critical due to their limited dissolution (Galia *et al.* 1998). In order to prove the hypothesis based on the present study, some specific investigations were performed. For example, the influence of the inconsistency of bile salts and lecithin on the dissolution results was shown in Chapter 4 and Appendix A. In the future, standardization of BDMs ingredients has to be achieved to obtain more reliable results (Vertzoni *et al.* 2004). The BDM compositions need to be optimized to improve the reflection of the physiological

conditions (Patel *et al.* 2006). This will lead to a more universal test protocol (Chapter 6). The different dissolution apparatuses might be tested such as apparatus IV to investigate if they are able to simulate the hydrodynamics in the GI tract more closely compared to apparatus II, which was used in this study (Sunesen *et al.* 2005). Examples that seem to be feasible were shown for danazol products using apparatus IV and BDMs (Sunesen *et al.* 2005). The developed dynamic pH change dissolution protocol in Chapters 4 and Appendix A has partially proved this application. Furthermore, the developed *in vitro/in silico* methods should be tested using more drugs and this might lead to the development of a universal *in vitro/in silico* method. Such a universal *in vitro/in silico* method can be used to set API or product specifications. Such methods can assist in the early stage of the drug development process in identifying the potential bioavailability or pharmacokinetics properties of a drug candidate. In post market studies, computer simulations can be used for product optimization or computer aided reverse engineering of generic products. In both cases, the information obtained by simulations can shorten the time length of the drug development process and can save money. The ultimate goal is that an *in vitro/in silico* method may be used as a surrogate for bioequivalence studies in the future.

## 7.1. References

- Amidon, G. L., Lennernas, H., Shah, V. P. and Crison, C. R. A theoretical basis for a biopharmaceutic drug classification: the correlation of *in vitro* drug product dissolution and *in vivo* bioavailability. *Pharm. Res.* 12, 413-20, 1995.
- Galia, E., Nicolaidis, E., Horter, D., Löbenberg, R., Dressman, J. B. and Reppas, C. Evaluation of various dissolution media for predicting *in vivo* performance of class I and class II drugs. *Pharm. Res.* 15, 698-705, 1998.
- GastroPlus™ Manual, version 5.1. Simulation Plus Inc. Lancaster, California, USA. 2006
- Grass, M. G. and Sinko, P. J. Physiologically-based pharmacokinetic simulation modeling. *Adv. Drug. Del. Rev.* 54, 433-451, 2002.

- Kostewicz, E. S., Wunderlich, M., Brauns, U. Becker, R., Bock, T. and Dressman, J. B. Predicting the precipitation of poorly soluble weak bases upon entry in the small intestine. *J. Pharm. Pharmacol.* 56, 43-51, 2004.
- Lin, J. H. Species similarities and differences in pharmacokinetics. *Drug. Metab. Dispos.* 23, 1008-1019, 1995.
- Patel, N. and Forbes, B. Use of simulated intestinal fluids with Caco-2 cells and rat ileum. *Drug. Dev. Ind. Pharm.* 32, 151-161, 2006.
- Prentis, R. A., Lis, Y. and Walker, S. R. Pharmaceutical innovation by the seven UK-owned pharmaceutical companies (1964-1985). *Br. J. Clin. Pharmacol.* 15, 387-396, 1988.
- Polli, J. E., Rekhi, S., Augsburger, L. L. and Shah, V. P. Methods to compare dissolution profiles and a rationale for wide dissolution specifications for metoprolol tartrate tablets. *J. Pharm. Sci.* 86 (6), 690-700, 1997.
- Sunesen, V. H., Pedersen, B. L., Kristensen, H. G. and Mullertz, A. In vivo in vitro correlations for a poorly soluble drug, danazol, using the flow-through dissolution method with biorelevant dissolution media. *Eur. J. Pharm. Sci.* 24 (4), 305-313, 2005.
- Vertzoni, M., Fotaki, N., Kostewicz, E., Stippler, E., Leuner, C., Nicolaidis, E., Dressman, J. B. and Reppas, C. Dissolution media simulating the intraluminal composition of the small intestine: physiological issues and practical aspects. *J. Pharm. Pharmacol.* 56, 453-462, 2004.
- Willmann, S., Schmitt, W., Keldenich, J. and Dressman, J. B. A physiologic model for simulating gastrointestinal flow and drug absorption in rats. *Pharm. Res.* 20 (110), 1766-1771, 2003.
- Wishart, B. Bioinformatics in drug development and assessment. *Drug. Metab. Rev.* 37, 279-210, 2005.

## APPENDIX A

### PHYSICOCHEMICAL ANALYSIS

#### A.1. Introduction

There are several aspects related to this project that have not previously been mentioned. These are 1) nuclear magnetic resonance (NMR) and infrared spectroscopy (IR) analysis of the APIs, 2) robustness of the dissolution method, and 3) isothermal titration calorimetric (ITC) investigation of the dynamic pH change in BDMs.

The NMR and IR analyses of the glyburide APIs are complementary methods that can be used to confirm the results obtained from the previous material characterization outlined in Chapter 3.

In order to establish an IVIVC using *in vitro* dissolution tests, the dissolution conditions have to be investigated. Many research groups have reported that the hydrodynamic properties (agitation force) might be an important factor in simulating the *in vivo* conditions in the GI tract. The focus of such research was on Apparatus I and II because of its wide spread use in the pharmaceutical industry (Kamba *et al.* 2003; Qureshi, 2004; Rostami-Hokjegan *et al.* 2002; Wu *et al.* 2004;). Different agitation speeds were applied in order to investigate the dissolution behaviors of the dosage forms.

Isothermal Titration Calorimetry (ITC) was used to investigate if the pH change of the dynamic dissolution protocol might change the micelle formation as outlined in Chapter 4. ITC measures the relative heat flow of a reaction compared to a reference material. In this case, we used a titration cell and observed the mixing of sodium hydroxide solution (0.02 M) with dissolution media like FaSSIF. ITC is highly sensitive and determines any change in enthalpy accurately (Ababou and Ladbury, 2006). ITC has been used in the past to investigate the critical micelle concentration of micelle system(CMC). It has also been used to investigate the partition equilibrium between a monomeric surfactant and a lipid membrane; the membrane solubilization of surfactant and membrane formation upon dilution of mixed lipid-surfactant micelles (Heerklotz and Seelig, 2000). ITC is also

a standard method for measuring ligand binding to receptors in membranes (Heerklotz, 2004). Isothermal microcalorimetry (IMC) without titration system can be used to evaluate the stability of APIs in the solid state (Brodka-Pfeiffer *et al.* 2003; Liu *et al.* 2002; Otsuka *et al.* 2002; Urakami, 2005). For example, the conversion of the APIs from amorphous forms to crystal forms can be detected by IMC due to its high sensitivity (Otsuka *et al.* 2002). IMC was used to investigate the stability of the glyburide APIs. For both techniques, the heat flow was recorded as a function of time, and therefore, the resulting ITC or IMC curves should derive a mathematical model for the thermodynamic processes measured.

## **A.2. Materials and Methods**

### **A.2.1. Materials**

Five glyburide active pharmaceutical ingredients (APIs) were obtained from several sources: two from a German manufacturer (API-1: Lot 094; API-2: Lot 149, Hoechst AG, Frankfurt, Germany), two from South Africa (API-3: Lot IK2; API-4: Lot IK1, Comment: API-3 was milled from API-4) and API-5 (USP grade raw material: Lot RR302528/0, Fundação para o Remédio Popular (FURP), São Paulo State, Brazil). Two 3.5 mg glyburide tablets were used as follows: Euglucon N<sup>®</sup> 3.5 mg tablets as reference product (GR) (Lot# 01N400, Boehringer Mannheim/Hoechs, Germany) and Glukovital<sup>®</sup> 3.5 mg tablet as test product (GT) (Lot#09601, Dr. August Wolff Arzneimittel, Bielefeld, Germany). Two glyburide tablets (5 mg dose) were from South Africa (ST 1: Lot AB 341; ST 2: Lot AA 541). Potassium bromide, (methyl sulfoxide)-d<sub>6</sub> (DMSO-d<sub>6</sub>) was purchased from Sigma-Aldrich (St. Louis, Missouri, USA). All other chemicals were mentioned in previous sections.

<sup>1</sup>H NMR spectra were recorded on a Bruker<sup>™</sup> AM-300 spectrometer (Bruker BioSpin Corporation, Billerica, Massachusetts, USA), retrofitted with Tecmag<sup>™</sup> MacSpect 3 signal processor (Tecmag, Inc., Houston, Texas, USA). The Infrared spectra (IR) were recorded on a 550 series II MAGNA-IR spectrometer (Nicolet Instrument Corporation, Madison, Wisconsin, USA). All other materials, equipment and methods have been described in detail in the previous chapters.

### **A.2.2. Dissolution Test**

Dissolution tests were performed as described in Chapter 4. Only the rotation speed was changed from 75 to 50 or 100 rpm.

### **A.2.3. Isothermal Titration Calorimetry (ITC) and Isothermal Microcalorimetry (IMC)**

Titration Isothermal Microcalorimetry (ITC) tests were performed using a Thermal Activity Monitor (TAM 2277, Thermometric AB, Järsälla, Sweden) and a microtitration system (2250-series Micro Reaction System, Thermometric AB, Järsälla, Sweden). A WinDaq data acquisition system (WinDaq Di-710 series, DATAQ Instruments Inc. Akron, Ohio, USA) was used to collect the resulting data. A syringe pump (model: 341B, Sage instruments Inc. Freedom, California, USA) was used for the injection of the titration solution. The pH of the test solution was monitored by a pH meter (Orion 520A, Orion Research Incorporated, Boston, Massachusetts, USA). All test solutions were adjusted to pH 5.0 using 1 N hydrochloric acid (HCl). FaSSIF or Blank FaSSIF (2.0 mL, test solutions) were added into a titration ampoule (4 mL) with or without 15 mg glyburide. The same test solution (2.5 mL) was added to the reference ampoule (4 mL). The sample and reference ampoules were equilibrated at 37°C. ITC recorded the output signals when 450  $\mu$ L (0.02N NaOH) was injected at an injection rate of 0.1 mL/h and a 50 rpm agitation was applied to the sample ampoule. Preliminary studies showed that adding 450  $\mu$ L (0.02N NaOH) could adjust the pH of a 2.0 mL testing solution with or without 15 mg glyburide API from pH 5.0 to pH 8.5.

The stability of glyburide APIs was investigated by IMC. Silica powder (1 g) and API powder (1 g) were added into 2 mL reference and sample vials, respectively. The sample and reference vials were equilibrated and kept in the IMC at 37°C over 24 h.

For both ITC and IMC measurements, the heat flow signal ( $dQ/dt$  in  $\mu$ W) was monitored as a function of time and collected by the data acquisition system.

### A.3. Results and Discussion

#### A.3.1. IR and NMR of the Glyburide APIs

The IR and NMR spectra of the API-2 are shown in Fig. A.1 and A.2, respectively. The spectra of the other APIs are superimposable on the API-2's spectrum. This indicates that the APIs have the same chemical structures. The results here confirm the previous conclusion that the APIs are similar in terms of chemical and crystalline. However the surface area, particle size and size distribution are different as discussed in Chapter 3.

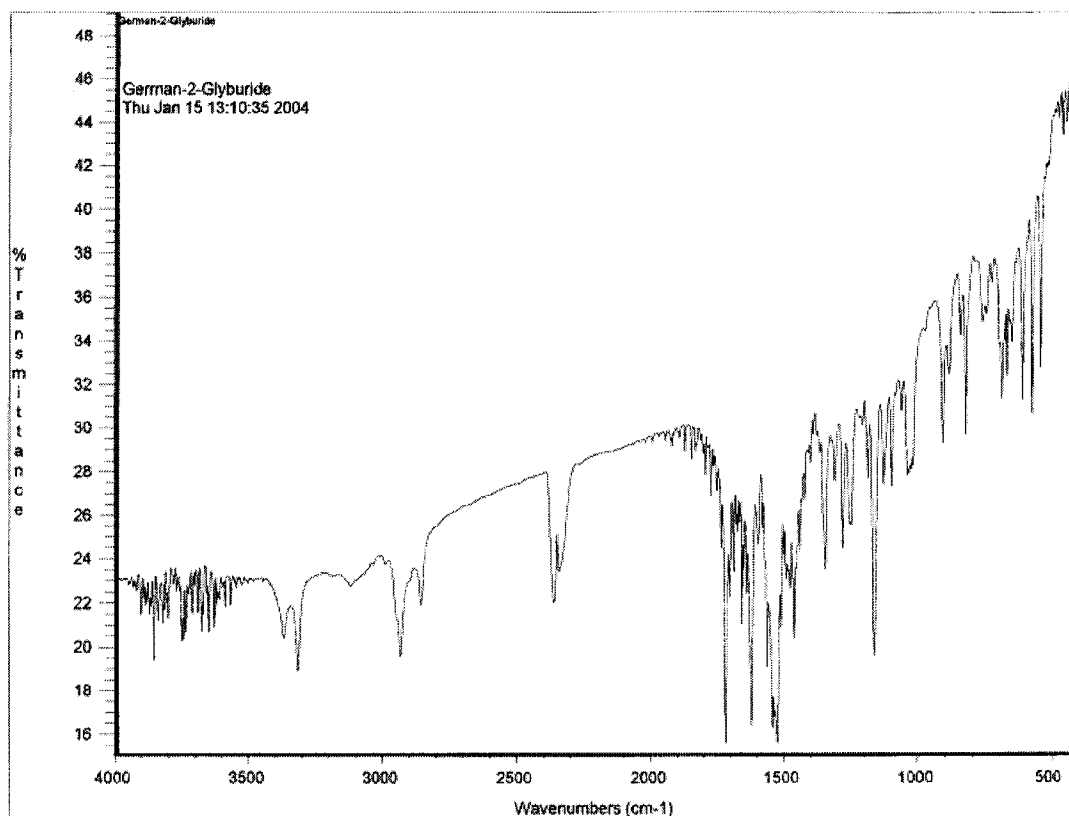


**Figure A.1.** IR spectrum of the glyburide API-2





### **A.3.2. Isothermal Titration Calorimetry (ITC) and Isothermal Microcalorimetry (IMC)**

The ITC results in Fig. A.3 show that the heat flow vs. time curves of the blank-, HQ- and LQ-FaSSIF are superimposable. The heat flow vs. time curves of the dissolution profiles of glyburide powders using blank-, HQ and LQ-FaSSIF are superimposable, too (Fig. A.4). Both resulting curves are similar and have the same trends.

Lecithin and bile salts can form different shapes of micelles by themselves. When both of them associate together, the mixed micelles and vesicles can be formed (Leng *et al.* 2003). The micelle formation process and the shapes of the micelles or vesicles are highly sensitive to environmental changes such as pH. The neutralization reaction between an acid and NaOH is an exothermic reaction. It was expected that ITC will pick up such changes by measuring the heat flow (Martin, 1993). It was expected that FaSSIF and blank-FaSSIF titration curves would be different due to the micelle formation in FaSSIF. The titrations are shown in Fig. A.3 and A.4. The shape of the heat flow curves might be attributed to neutralization reaction only. The heat change during the micelle formation process might be too small to be measured under the chosen experimental conditions. For the stability study of the APIs using IMC, there was no difference between the APIs. The results confirm that no transition from amorphous form and any polymorphic conversion occurred. IMC confirmed that the APIs are stable powders due to very low heat flows.

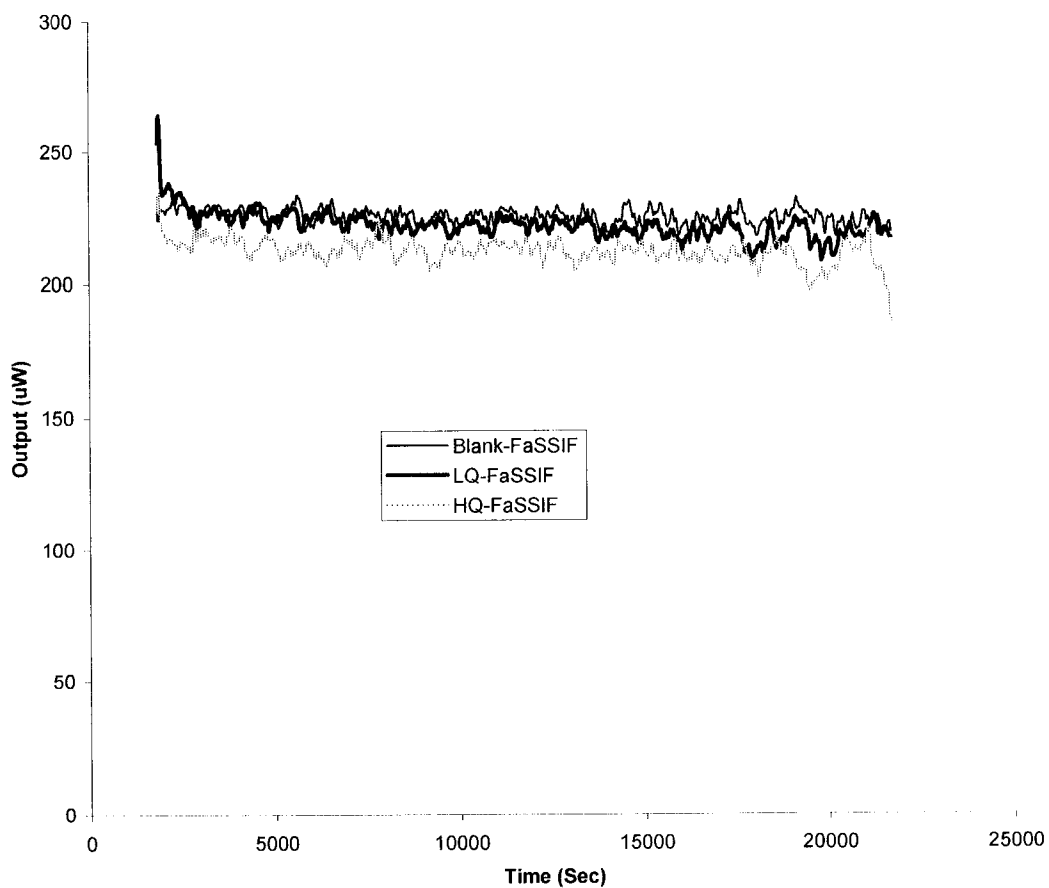


**Figure A.3.** ITC of FaSSIF media without glyburide (titrated from pH 5.0 to pH 8.5; Blank-FaSSIF: FaSSIF buffer without bile salts and lecithin)

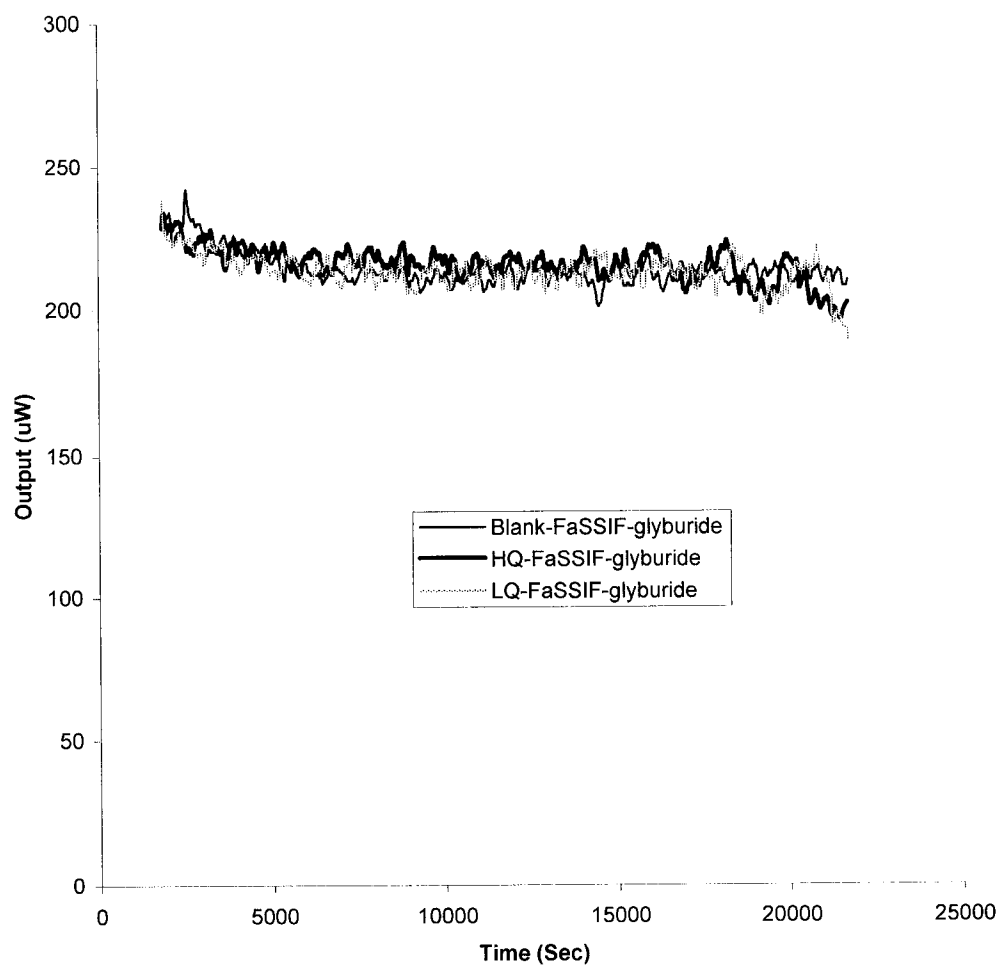


**Figure A.4.** ITC of FaSSIF media with 15 mg glyburide (titrated from pH 5.0 to pH 8.5; Blank-FaSSIF: FaSSIF buffer without bile salts and lecithin)

### **A.3.3. *In Vitro* Dissolution Tests**

#### **A.3.3.1. *In Vitro* Dissolution Tests of the South Africa Products ST 1 and ST 2**

The dynamic dissolution tests of the two South African glyburide products (5 mg dose) are shown in Fig. A.5. The drug release profiles of the two products were similar. The drug release of the formulations increased gradually during the entire testing period. After 3.5 hours the drug release reached its highest point. This can be attributed to the solubility of glyburide at different pH values that is pH-dependent. The drug releases of the formulations (ST 1 and ST 2) at 210 min were 48% and 46%, respectively, when the pH was changed to 7.5. When the pH of the LQ-FaSSIF was changed from 7.5 to 5.0, the drug releases of the formulations (ST 1 and ST 2) dropped to 42% and 39%, respectively, after 1 hour. These results were different from the previous results obtained from the two German products (Chapter 4). The dynamic dissolution tests of the two German products obtained showed that the drug concentration in LQ-FaSSIF remained constant for at least 1 hour after the pH was changed from 7.5 to 5.0. The difference in these two studies might be due to the different batches of the bile salts. Sigma-Aldrich Inc. confirmed that the bile salts used in both studies were provided by different manufacturers. The actual composition of each batch is not known due to the complex composition of the crude material.

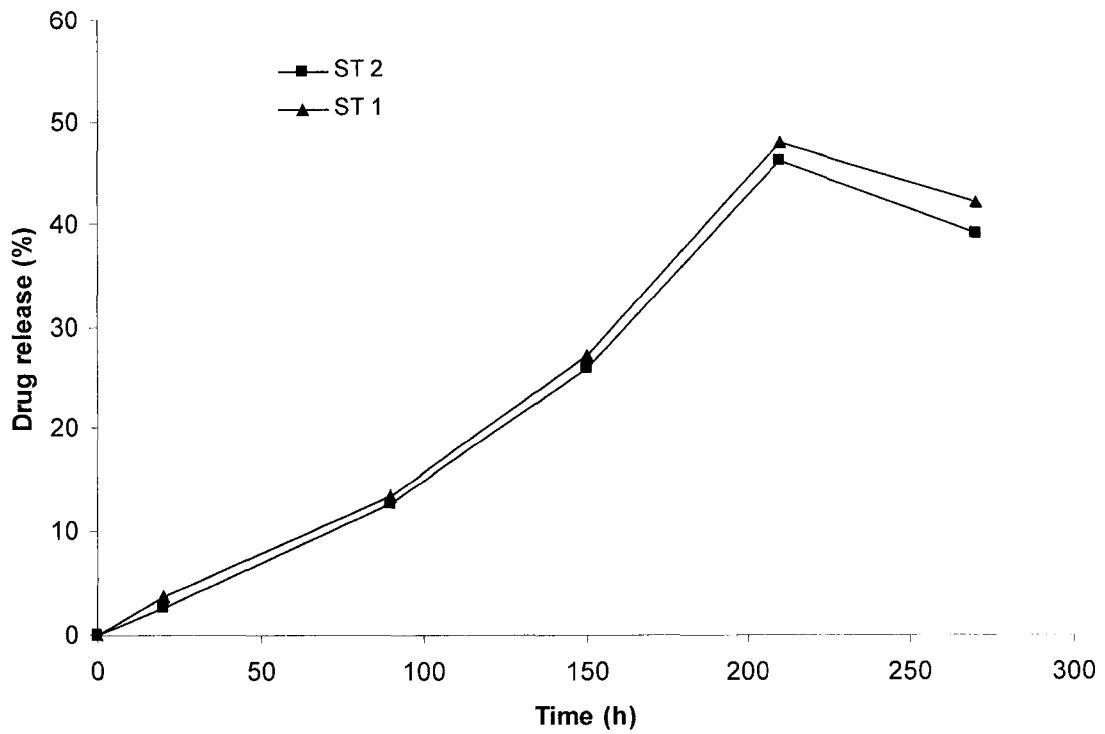


**Figure A.5.** Comparison of the *in vitro* dissolution profiles between South African (ST 1 and ST 2) products using a dynamic pH change dissolution protocol in LQ-FaSSIF (mean, n=2)

### A.3.3.2. *In Vitro* Dissolution Tests of Two German Products at Different Agitation Speeds

Fig. A.6 shows the drug releases of the two German products (GR and GT) obtained at different agitation speeds (50, 75 and 100 rpm) using the dynamic pH change protocol in the LQ-FaSSIF. In order to investigate the impact of the agitation speeds on the release profiles, the difference factors ( $f_1$ ) and similarity factors ( $f_2$ ) were calculated using the equation previously cited (Chapter 4) and are summarized in Table A.1. A higher  $f_1$  value above 15 corresponds to dissimilarity while an  $f_2$  value below 50 indicates differences between the two dissolution profiles (Costa and Lobo, 2001; FDA 1997). The results in Table A.1 show that the drug release profiles between 50 and 75 rpm tend to be different for the reference and the test products ( $f_1$ : 31 and 24;  $f_2$ : 42 and 52, respectively). Although the  $f_1$  and  $f_2$  factors showed differences in the dissolution profiles, the values of the  $f_2$  factors were close to the critical value 50 that divides similarity and dissimilarity (Costa and Lobo, 2001). The other comparison of the drug release profiles obtained from different agitation speeds such as between 50 rpm and 100 rpm or 75 rpm and 100 rpm, did not show dissimilarity. The different agitation speeds might potentially provide more information about the hydrodynamic properties *in vivo* (Kamba *et al.* 2003).

**Table A.1.**  $f_1$  and  $f_2$  factors of the dissolution profiles between different agitation speeds (50, 75 and 100 rpm) of two German products using dynamic pH change in LQ-FaSSIF

	Reference			Test		
	50-75 rpm	50-100 rpm	75-100 rpm	50-75 rpm	50-100 rpm	75-100 rpm
$f_1$	31	14	14	24	13	9
$f_2$	42	56	54	52	64	65

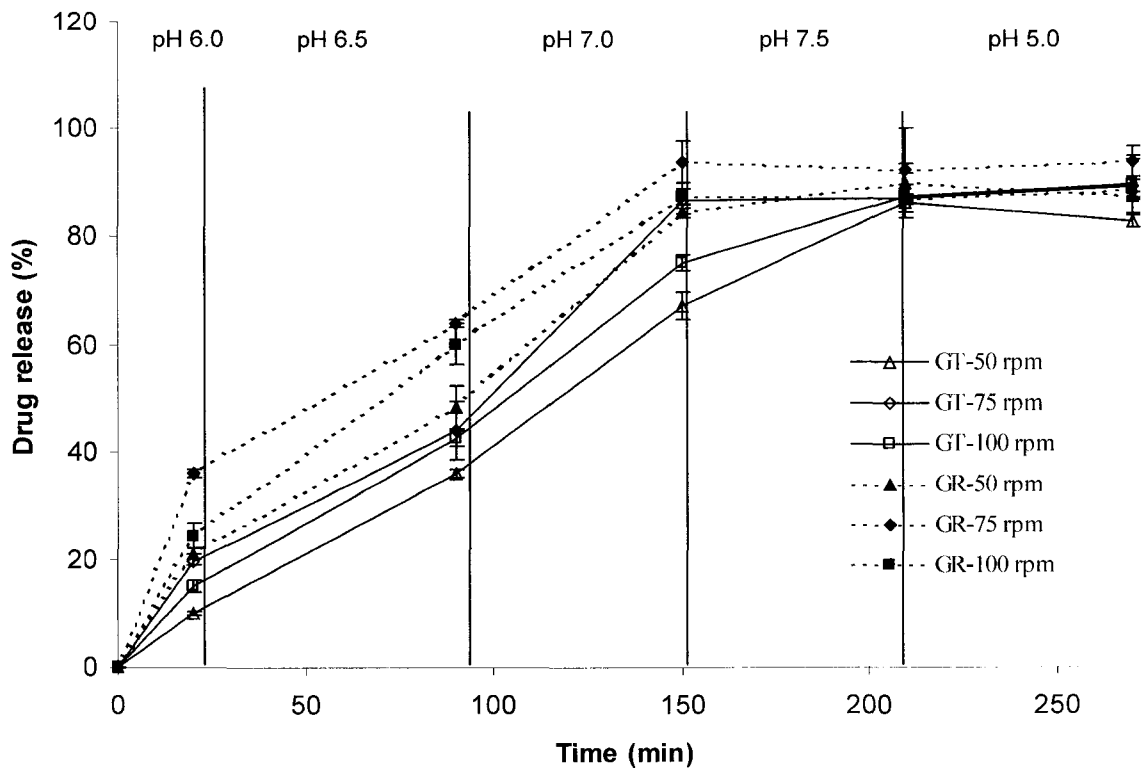


**Figure A.6.** Comparison of *in vitro* dissolution profiles of two German products (GR and GT) at different agitation speeds using a dynamic pH change protocol in LQ-FaSSIF (n=3)

#### A.4. Conclusion

The experiments in this chapter were designed to potentially provide more comprehensive information about certain details observed in the studies reported in Chapter 2, 3, 4, and 5. The material characterizations using IR, NMR and IMC confirm the previous results. However, the results obtained from ITC did not match the expectations. There were no significant differences between FaSSIF and blank-FaSSIF using ITC. The dissolution tests using different agitation speeds potentially simulate the hydrodynamic properties *in vivo*. The results confirm FDA's dissolution guideline that apparatus II using 75 rpm is suitable for the immediate release dosage forms when BDMs were used.

#### A.5. References

Abobou, A. and Ladbury, J. E. Survey of the year 2004: literature on applications of isothermal titration calorimetry. *J. Mol. Recognit.* 19, 79-89, 2006.

Brodka-Pfeiffer, K., Langguth, P., Graß, P. and Häusler, H. Influence of mechanical activation on the physical stability of salbutamol sulphate. *Eur. J. Pharm. Biopharm.* 56, 393-400, 2003.

Costa, P. and Lobo, J. M. S. Modeling and comparison of dissolution profiles. *Eur. J. Pharm. Sci.* 13, 123-133, 2001.

FDA, Guidance for industry: dissolution testing of immediate release solid oral dosage forms. U.S. Department of Health, Food and Drug Administration, Center for Drug Evaluation and Research (CDER) BP, August 1997.

Heerklotz, H. The microcalorimetry of lipid membranes. *J. Phys. Condens. Matter.* 16, R441-R467, 2004.

Heerklotz, H. and Seelig, J. Titration calorimetry of surfactant-membrane partitioning and membrane solubilization. *Biochimica et Biophysica Acta.* 1508, 69-85, 2000.



Kamba, M., Seta, Y., Takeda, N., Hamaura, T., Kusai, A., Nakane, H. and Nishimura, K. Measurement of agitation force in dissolution test and mechanical destructive force in disintegration test. *Int. J. Pharm.* 250, 99-109, 2003.

Leng, J., Egelhaaf, S. U. and Cates, M. E. Kinetics of the micelle-to-vesicle transition: aqueous lecithin-bile salt mixtures. *Biophysical J.* 85, 1624-1646, 2003.

Liu, J., Rigsbee, D. R., Stotz, C. and Pikal, M. Dynamics of pharmaceutical amorphous solids: the study of enthalpy relaxation by isothermal microcalorimetry. *J. Pharm. Sci.* 91 (8), 1853-1862, 2002.

Martin A. Physical pharmacy. 4<sup>th</sup> edition, Williams & Wilkins, Baltimore, Maryland, USA, 1993.

Otsuka, M., Kato, F. and Matsuda, Y. Physicochemical stability of cimetidin amorphous forms estimated by isothermal microcalorimetry. *AAPS Pharm. Sci. Tech.* 3 (4), article 30, 2002.

Qureshi, S. A. Choice of rotation speed (rpm) for bio-relevant drug dissolution testing using a crescent-shaped spindle. *Eur. J. Pharm. Sci.* 23, 271-275, 2004.

Rostami-Hodjegan, A., Shiran, M. R., Tucker, G. T., Conway, B. R., Irwin, W. J., Shaw, L. R. and Grattan, T. J. A new rapidly absorbed paracetamol tablet containing sodium bicarbonate. II. Dissolution studies and in vitro/in vivo correlation. *Drug Dev. Ind. Pharm.* 28 (5), 533-543, 2002.

Urakami, K. Characterization of pharmaceutical polymorphs by isothermal calorimetry. *Current Pharm. Biotech.* 6, 193-203, 2005.

Wu, Y., Kildsig, D. O. and Ghaly, E. S. Effect of hydrodynamic environment on tablets dissolution rate. *Pharm. Dev. Tech.* 9 (1), 25-37, 2004.

## APENDIX B

### DEMONSTRATION OF THE USE OF GASTROPLUS™

#### B.1. Background of GastroPlus™ (modified from GastroPlus™ Manual, 2006)

The original compartmental absorption and transit (CAT) model was developed by Dr. Gordon Amidon at the University of Michigan. It was published in 1996 (Yu *et al.* 1996). The basic theory and equations have been described in Chapter 1. The CAT model does not account many factors such as dissolution, the pH dependent of solubility of drugs, absorption in stomach or colon, gut metabolism, etc, which influence the drug absorption in the GI tract. Simulation Plus Inc. developed the Advanced Compartmental Absorption and Transit (ACAT) model and tried to include all the physiological factors such as absorption in stomach or colon, which influence the oral absorption characteristics of a drug. GastroPlus™ is commercially available program based on the ACAT model. Fig. B.1 shows the model of the ACAT. As described in Fig. B.1, the GI tract is divided into nine compartments and each of them contains four subcompartments: unreleased, undissolved, dissolved, and enterocyte (Drug is considered absorbed by GastroPlus™ when it enters enterocytes). Each arrow in Fig. B.1 represents a process, which influences the drug absorption and each process is described by a specific equation. The simulation process involves the numerical integration of all the equations describing the oral absorption processes such as dissolution, carrier-mediated transport in the gut, gut metabolism, etc for the particular drug.

This project focused on the development of biorelevant *in vitro* methods such as physicochemical analysis, biorelevant *in vitro* dissolution testing and *in vitro* permeability measurements. The obtained *in vitro* data was input into GastroPlus™ as input functions to predict the oral absorption characteristics of the model drug. However, the metabolism of the drug in gut or liver was not included in this study. The modules for metabolism in the gut or the liver in GastroPlus™ were not available in our version (no license).

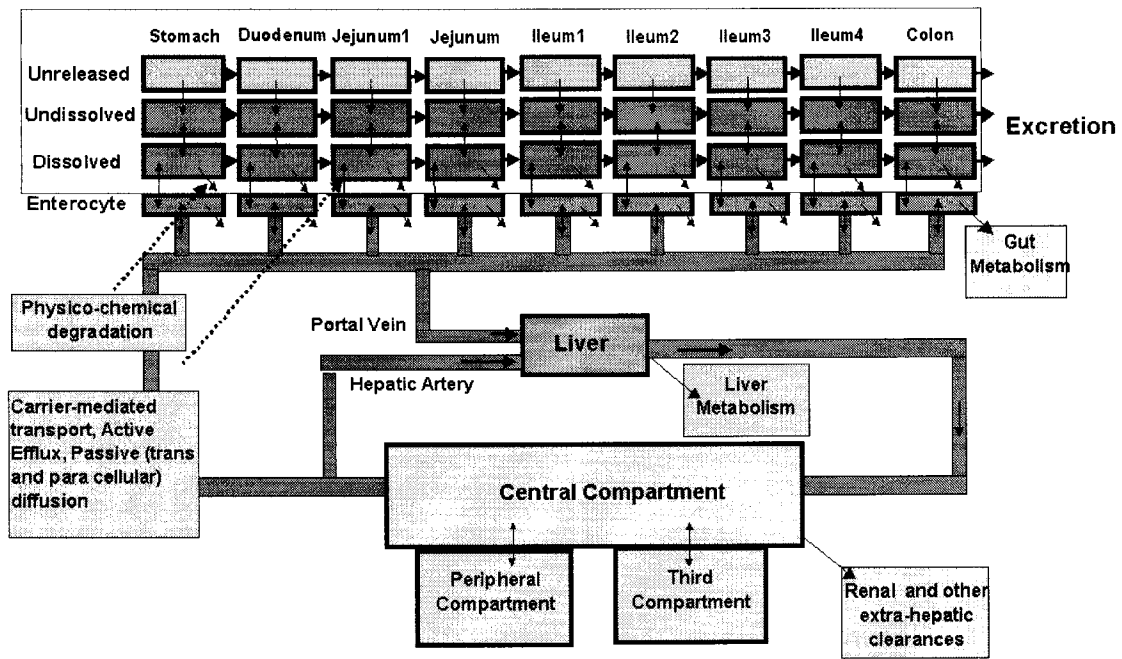


**Figure B.1.** ACAT model compartments (modified from GastroPlus™ Manual, 2006)

## B.2. Running GastroPlus™ Simulations

There are minimum inputs required by GastroPlus™ to perform simulations. These input functions include physicochemical parameters, dose, dosage form for each drug, physiological parameters describing the GI tract of the selected species, and available pharmacokinetic parameters.

## B.2.1. Compound Tab

**Figure B.2.** Compound Tab showing the physicochemical properties of the drug

When GastroPlus<sup>TM</sup> is started, a drug database should be created or opened. Fig. B.2 shows the compound tab. In this sheet, the physicochemical properties of a drug substance can be put into the software. These include molecular weight, pK<sub>a</sub> and logD at a specific pH, dose, dosage form, dose volume, solubility, mean precipitation time, diffusion coefficient, particle density, particle size and size distribution and the available human permeability. The *in vitro* permeability obtained from Caco-2 model can be converted to human permeability based on the database of GastroPlus<sup>TM</sup>. As shown experimental data such as *in vitro* dissolution, pH-solubility, oral plasma concentration vs. time profiles etc. can be loaded from specific data files (A). The dose (1), absorption (2) and dissolution (3) numbers are automatically calculated by the program based on the input parameters.

## B.2.2. Physiology Tab

Propranolol HCl

Compartment Data					Enzyme and Transporter Regional Distributions
Compartment	Peff	ASF	pH	Transit Time (h)	
Stomach	0	0.0	1.30	0.25	
Duodenum	0	1.194	6.00	0.26	
Jejunum 1	0	1.293	6.20	0.95	
Jejunum 2	0	1.474	6.40	0.76	
Ileum 1	0	1.707	6.60	0.59	
Ileum 2	0	2.059	6.90	0.43	
Ileum 3	0	2.587	7.40	0.31	
Caecum	0	0.133	6.40	4.50	
Asc Colon	0	0.240	6.80	13.50	

C1-C4: 0.18148 1.0944 0.0734 0.31836 Qh (L/min): 1.5

Physiology: Human - Physiological - Fasted

ASF Model: Human - Physiological - Fasted

Percent Fluid in Comp Volume: 100

**Figure B.3.** Physiology Tab

After the physicochemical properties of a drug substance have been defined in the compound tab, the physiological conditions can be defined. Fig. B.3 shows the physiology Tab. There is a list of ACAT models such as Human Physiological Fasted and Human Physiological Fed models. Several absorption scale factor models are available as described in Chapter 5 and can be selected. Once the physiological and absorption scale factor models are selected, the pH values, transit time and geometric parameters (lengths, radii, volumes) of the intestine are automatically changed to the physiologically accurate values (default). The default values such as the pH, transit time in each physiological model and the default logD absorption scale factor model were developed and validated through correlation with experimental database. The resulting default values and models

are more appropriate to be used with mean observed data. It is difficult to modify the default value without experimental data for any other cases.

### B.2.3. Pharmacokinetics Tab

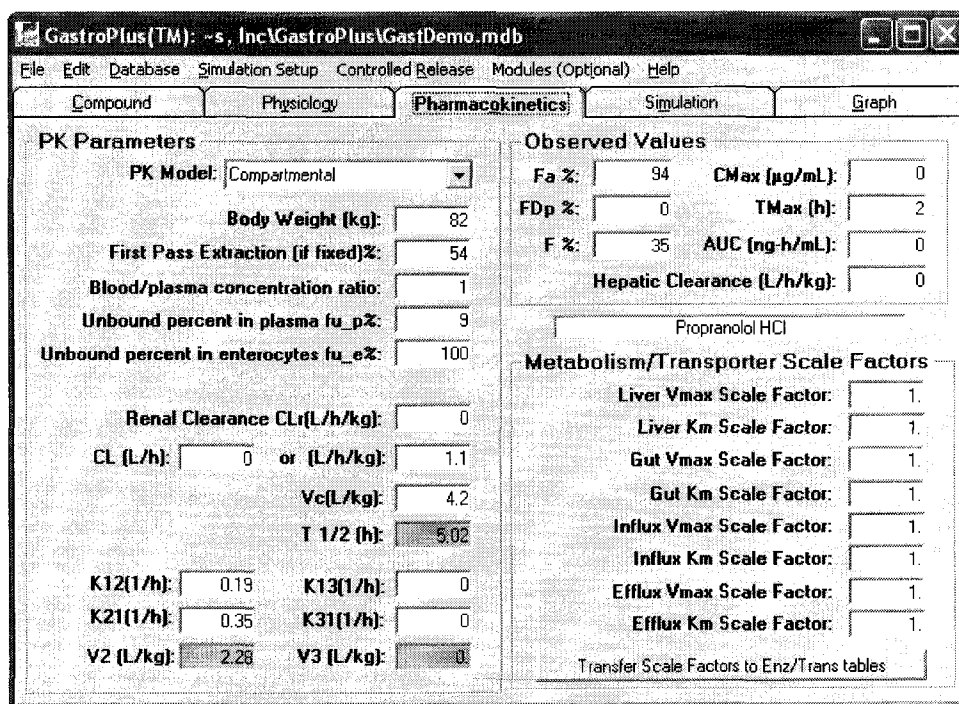


Figure B.4. Physiology Tab

Fig. B.4 shows the pharmacokinetics tab. To simulate the plasma concentration vs. time profiles, the observed pharmacokinetic parameters are needed. The simulated plasma concentration vs. time curves are based on compartmental pharmacokinetic models. It is very important to perform accurately compartmental model fitting, otherwise the simulation will fail due to the wrong model fitting. The pharmacokinetic parameters can be calculated by other commercially available programs such as Kinetica<sup>®</sup> or Winonlin<sup>®</sup>. The minimum parameters include clearance, volume of central compartment, micro-constant rate. The other parameters can be set as default values, which were estimated by the experimental database of GastroPlus<sup>™</sup>.

## B.2.4. Simulation Tab

Once the physicochemical data, physiological models and pharmacokinetic parameters are selected or input, the simulation can be performed in simulation tab (Fig. B.5). The simulation length (h) depends on the expected time period (default 24 h). The outputs in simulation tab sheet (Fig. B.5) include the fraction dose absorbed,  $C_{max}$ , AUC and  $T_{max}$ . In output sheet (Fig. B. 6 and B. 7), the simulated plasma concentration vs. time curve and the fraction dose absorbed in each compartment are presented. The data can be transferred to excel spreadsheets for the convenience of graphical presentation. If no pharmacokinetic parameters are defined, the software will only calculate the fraction dose absorbed in each compartment as shown in Fig. B. 7.

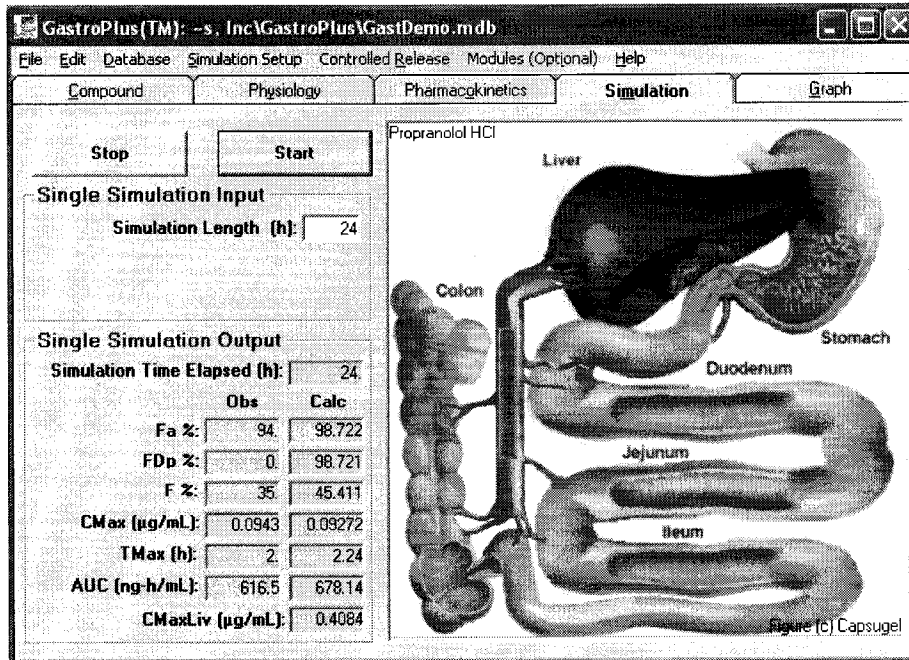


Figure B.5. Simulation Tab

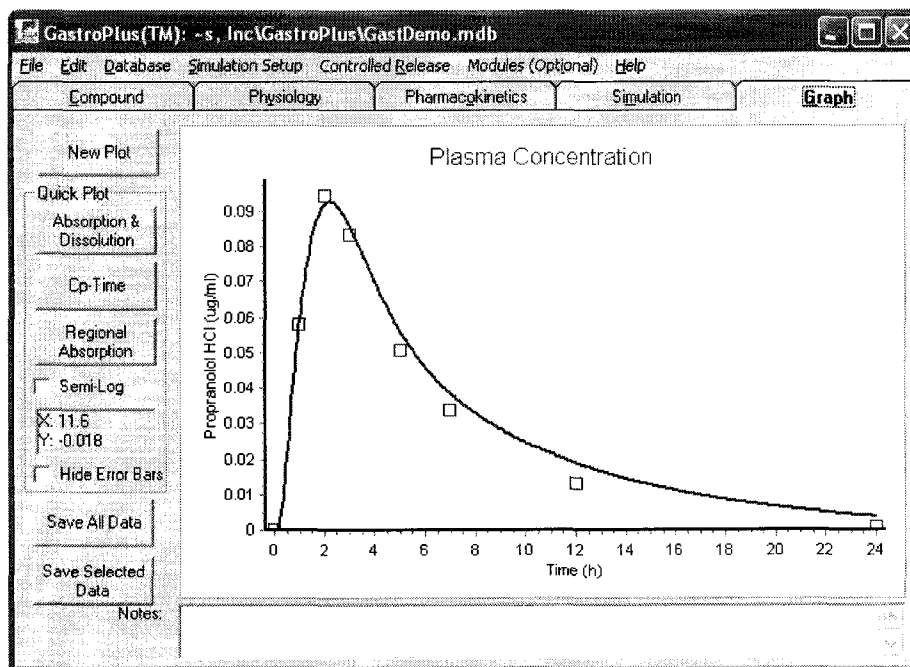


Figure B.6. Simulation output (simulated plasma concentration vs. time curve)

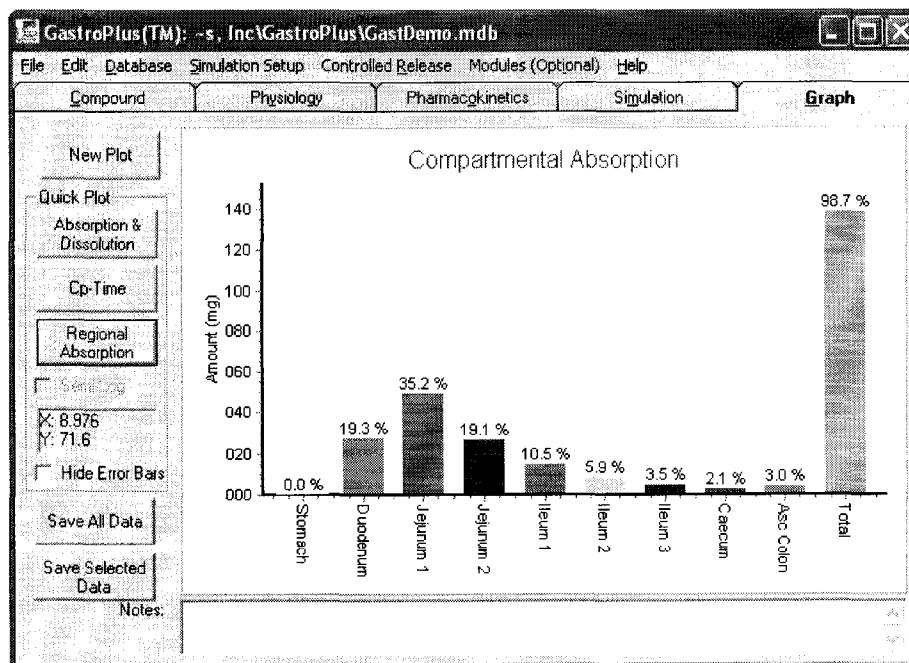


Figure B.7. Simulation output (Fraction dose absorbed in each compartment)



## **B.2.5. Calculation of Pharmacokinetic Parameters**

### **B.2.5.1. Mean and Individual Observed Data**

As mentioned previously, the default values and models in GastroPlus™ were obtained through correlation with the experimental database of the software (GastroPlus™ Manual, 2006). They are more suitable for general cases such as mean observed data. There are some unsuccessful simulations of individual volunteers using their individually pharmacokinetic parameters (calculated by Micro Extravascular model fitting in Kinetica® 4.4.1; Table B.1). Fig. B. 8 and 9 shows the simulation results for two individuals in the German reference and test products' study using physicochemical data (German reference volunteer number 1: GR 1 and German test volunteer number 2: GT 2). Table B. 2 summarizes the prediction errors of  $C_{max}$  and AUC for both cases.

The simulated plasma concentration vs. time curves did not match the observed curves well for both cases (Fig B.8 and 9). The predicted errors of  $C_{max}$  and AUC are up to 34 and 24%, respectively. The unsuccessful simulation might be due to the variability of the observed data resulting in inaccurate calculations and simulations of the parameters, which then influence the drug absorption characteristics. Optimization of each model for the individual case might be not possible without individual information of each of the volunteers.

**Table B.1.** Pharmacokinetic parameters (calculated using Micro Extravascular model fitting in Kinetica® 4.4.1) for two individual volunteers (German reference volunteer number 1: GR 1 and German test volunteer number 2: GT 2)

	$C_{max}$ (ng/mL)	$AUC_{0-n}^*$ (ng/mL*h)	Clearance (L/h)	$V_c$ (L)	$K_{12}$ ( $h^{-1}$ )	$K_{21}$ ( $h^{-1}$ )
GR 1	132	531	5.96	14.47	0.423	0.230
GT 2	298	3530	0.66	6.84	0.216	0.204

\* n : GR 1: 24 h; GT 2: 24 h

**Table B.2.** Simulation results of two individual cases (observed German reference volunteer number 1 (GR 1):  $C_{max}$ : 132 ng/mL;  $AUC_{0-24}$ : 531 ng/mL\*h; German test volunteer number 2 (GT 2):  $C_{max}$ : 298 ng/mL;  $AUC_{0-24}$ : 3530 ng/mL\*h)

Simulated				Prediction Error (%)			
GR 1		GT 2		GR 1		GT 2	
$C_{max}$	AUC	$C_{max}$	AUC	$C_{max}$	AUC	$C_{max}$	AUC
87	496	193	2692	34	7	35	24

$C_{max}$ : ng/mL; AUC: ng/mL\*h

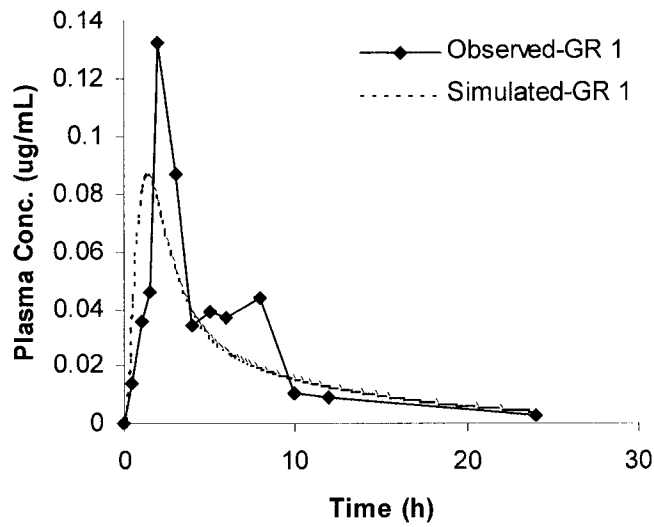


**Figure B. 8.** Simulation of an individual case (German reference volunteer number 1: GR 1)

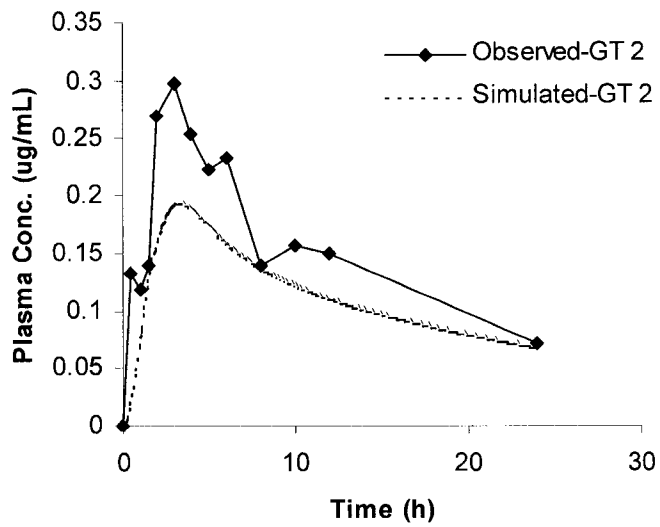


**Figure B. 9.** Simulation of an individual case (German test volunteer number 2: GT 2)

### B.2.5.2. Comparison of the Simulation Using Different Version Programs

The previous results used a volume of central compartment ( $V_c$ ) of only 1.83 L for the mean German reference product (15 volunteers; average body weight 65 kg). This value is smaller than the plasma volume (4.5% body weight: 2.93 L). This set of pharmacokinetic parameters was calculated by Kinetica<sup>®</sup> 3.0. The new version Kinetica<sup>®</sup> 4.4.1 was used to repeat the calculation. Table B.3 summarizes the calculation results using the micro extravascular model fitting in Kinetica<sup>®</sup> 3.0 or Kinetica<sup>®</sup> 4.4.1.

The  $V_c$  calculated by Kinetica<sup>®</sup> (Version 4.4.1) is 4.68 L. It is different from the value (1.83 L) calculated by Kinetica<sup>®</sup> 3.0. In order to evaluate the influence of the different model fitting results on the simulation, the newest GastroPlus<sup>™</sup> (Version 5.1.0033) was used. The method of computer simulation using physicochemical data has been described in Chapter 5. For these two cases, the different pharmacokinetic parameters were used as input and the rest of the settings were kept constant. Fig B.10 and Table B.4 summarize the simulation results. The simulated plasma concentration vs. time curves for both cases match the observed curve well. The two simulated curves are almost superimposable. The sums of squares are 0.011 and 0.002 for using Kinetica<sup>®</sup> 3.0 and using Kinetica<sup>®</sup> 4.4.1, respectively. The prediction errors of  $C_{max}$  and AUC for using Kinetica<sup>®</sup> 3.0 and using Kinetica<sup>®</sup> 4.4.1 are 7% and 4%, and 8% and 1%, respectively. The difference in the simulations is due to the different input pharmacokinetic parameters obtained from different Kinetica<sup>®</sup> versions. However, both sets of parameters gave relatively similar simulation results.

**Table B.3.** Comparison of pharmacokinetic parameters (mean German reference GR; 15 volunteers; average body weight 65 kg) using the micro extravascular model fitting in Kinetica<sup>®</sup> 3.0 or Kinetica<sup>®</sup> 4.4.1

	Clearance (L/h)	$V_c$ (L)	$K_{12}$ ( $h^{-1}$ )	$K_{21}$ ( $h^{-1}$ )
Kinetica <sup>®</sup> 3.0	2.47	1.83	0.409	0.100
Kinetica <sup>®</sup> 4.4.1	2.17	4.68	0.379	0.103

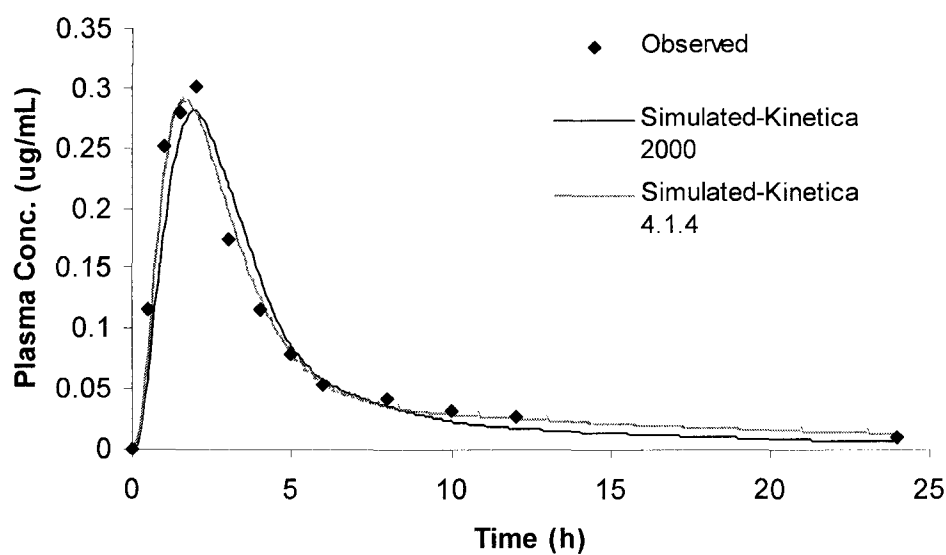


**Figure B.10.** Comparison of the simulations between the pharmacokinetic parameters calculated by Kinetica<sup>®</sup> 3.0 and Kinetica<sup>®</sup> 3.0 (Mean German reference GR)

**Table B.4.** Summary of the simulations using the pharmacokinetic parameters calculated by Kinetica<sup>®</sup> 3.0 and Kinetica<sup>®</sup> 4.4.1 (Mean German reference GR; Observed:  $C_{max}$ : 301 ng/mL;  $AUC_{0-24}$ : 1359.6 ng/mL\*h)

	Simulated		Prediction Error (%)		
	$C_{max}$	AUC	$C_{max}$	AUC	SS
Kinetica <sup>®</sup> 3.0	281	1257.1	7	8	0.011
Kinetica <sup>®</sup> 4.4.1	289	1373.4	4	1	0.002

SS: Sum of Squares  $(Y_{obs} - Y_{pred})^2$

### B.2.6. Influence of the Absorption Patterns on the Terminal Phase Fitting

In Chapter 5 (Chapter 5, Fig 5.7), the terminal phase of the simulated plasma concentration vs. time curves using *in vitro* dissolution data did not fit the observed data well. However, the physicochemical data gave much better fitting at the terminal phase of the curves (Chapter 5, Fig. 5.2). This might be due to the different absorption patterns between using physicochemical data and using dissolution data. Fig. B.11 was modified from Fig. 5.8 (Chapter 5). It clearly shows that the fractions dose absorbed using *in vitro* dissolution data are higher than using physicochemical data in early four compartments. The fractions dose absorbed in last three compartments using *in vitro* dissolution data are lower compared to physicochemical data, especially in colon compartment. The fractions dose absorbed of *in vitro* dissolution data and physicochemical data in the colon compartment are 1.9% and 10.1%, respectively. This might be the reason for the differences in the predicted values between 8 and 24 h. The dissolution data seem to provide too much drug for absorption in the early compartments and nearly no drug dose (1.9%) was available in the colon compared to the physicochemical model where 10.1% of the dose was still available for absorption.

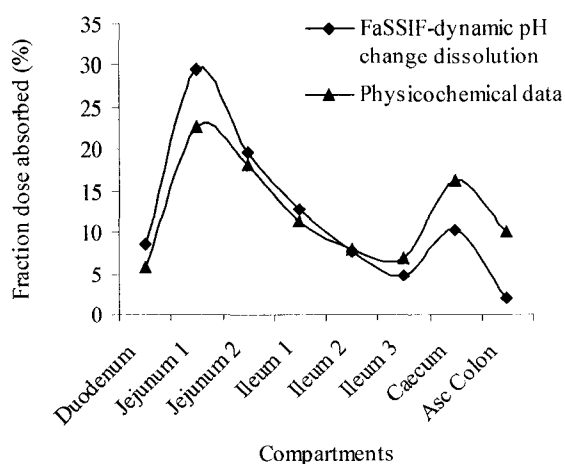


**Figure B.11.** Comparison of the predicted absorption patterns using physicochemical data and using dissolution profiles at dynamic pH changes (modified from Fig. 5.8, Chapter 5)

### B.3. Discussion

GastroPlus™ is based on the ACAT model. It is a complex program. It tries to describe all absorption influencing processes by mathematic equations. The derived equations (models) were developed and validated by correlation with an experimental database. The models in the program are more suitable for mean observed data (GastroPlus™ Manual, 2006). As mentioned above, the irregular individual observed data might result in inaccurate pharmacokinetic model fitting and consequently wrong simulations. The observed individual data in Fig. B.8 and B.9 shows that the irregular observed data results in double or triple peaks in the plasma concentration vs. time curves. This causes inaccurate model fitting using Kinetica®. Also, GastroPlus™ can only simulate observed data that are well fitted. Further investigation of the individual case is valuable for the development of a universal *in silico* method. However, the mean observed data (plasma concentration vs. time) was used through the entire project due to the large variability of the individual data.

Computer modeling and simulation rely on the scientifically validated experimental database. Further development and validation of the software programs such as GastroPlus™ and Kinetica® is necessary. However, different results might be obtained from different versions of programs due to small modification of the models. The comparison of Kinetica® 3.0 and 4.4.1 model fitting was performed using GastroPlus™ (section B.2.5.2). The simulation results are similar. For the terminal phase fitting, the simulation using pharmacokinetic parameters obtained from Kinetica® 4.4.1 is relatively better than from Kinetica® 3.0 as shown in Fig. B.10. This confirms the successful modification of the program.

The terminal phase of the simulated plasma concentration vs. time curves using *in vitro* dissolution data did not fit the observed data well (Fig. 5.7). However, the physicochemical data gave much better fitting at the terminal phase of the curves (Fig. 5.2). This might be due to the different absorption patterns when using physicochemical data or using dissolution data. The dosage dissolution model in GastroPlus™ might over estimate the drug release and absorption in the early four compartments. On the other hand, the numerical integration of all the equations (models) in GastroPlus™ using

physicochemical data is more successful than using *in vitro* dissolution data, which has been confirmed by the previous results (Chapter 6). *In vitro* dissolution data only partially fulfill the hypothesis.

#### **B.4. Conclusion**

GastroPlus™ is more suitable to predict mean observed data. To be able to predict each individual pharmacokinetic profile, modifications of the default models in GastroPlus™ is desirable. However, the adjustment of the default model is highly dependent on the individual. Due to the constant improvements in the software, the version of the programs should be identified. Further investigations and improvements for individual case are needed. The development of suitable *in vitro* dissolution models is also necessary.

#### **B.4. References**

Brocks, D. Advanced pharmacokinetics (Pharm 615 class notes), Faculty of Pharmacy and Pharmaceutical Sciences, University of Alberta, Edmonton, Alberta, Canada, 2002.

GastroPlus Manual, version 5.1. Simulation Plus Inc. Lancaster. USA. 2006.

Yu, L. X., Crison, J. R. and Amidon, G. L. Compartmental transit and dispersion model analysis of small intestinal transit flow in humans. *Int. J. Pharm.* 140, 111-118 1996.



## APPENDIX C

### DEMONSTRATION OF KINETICA<sup>®</sup>

#### C.1. Introduction

Kinetica<sup>®</sup> is a pharmacokinetic and pharmacodynamic software. It is used to study the pharmacokinetic parameters of observed data. The resulting pharmacokinetic parameters are used by GastroPlus<sup>™</sup> to further develop an IVIVC.

There are two bioequivalence studies (German and South African) described in Chapter 3. Fig. C. 1 and C. 2 show the observed individual data for the German reference and the test products. There was a large variability among the individual observed data. Many individual plasma concentration vs. time curves have irregular shapes. Fig. C. 3 and C. 4 show the mean observed data for German and South African studies. The plasma concentration vs. time curves show regular shapes. Therefore, mean observed data were investigated instead of individual data due to the potentially inaccurate model fittings and simulations in this project (also mentioned in Appendix B).

In section C.2, six sets of pharmacokinetic parameters are appended which were calculated by Kinetica<sup>®</sup> 4.4.1 using micro extravascular model fitting. The observed plasma concentration vs. time data were simply input into the software's datasheet and were automatically calculated by the software. The six sets of data are presented as the output of the software. Only important information, which contains the required parameters for GastroPlus<sup>™</sup> are presented. These data sets include mean German referenc (GR) and test (GT), mean South African test 1 (ST 1) and test 2 (ST 2), and two individual volunteers described in Appendix B (GR 1 and GT 2).

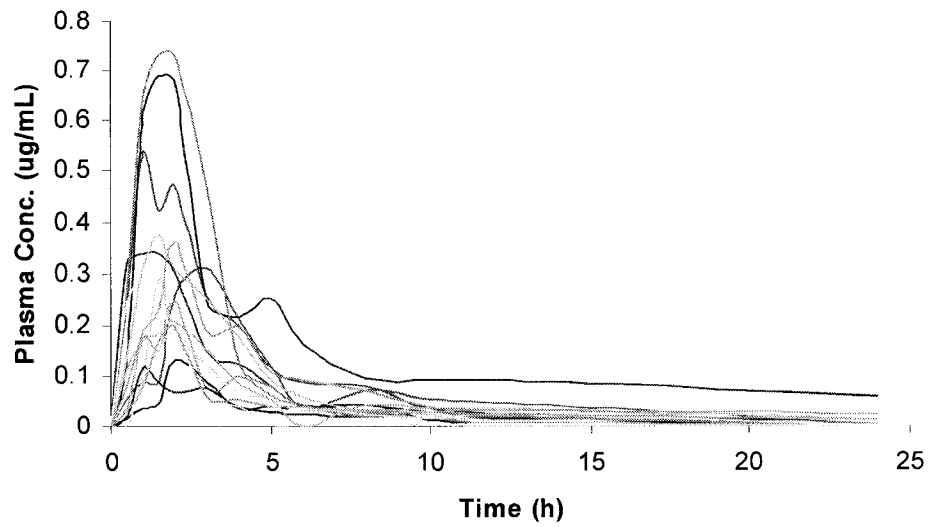


**Figure C.1.** Individual observed data of 15 volunteers for German reference product

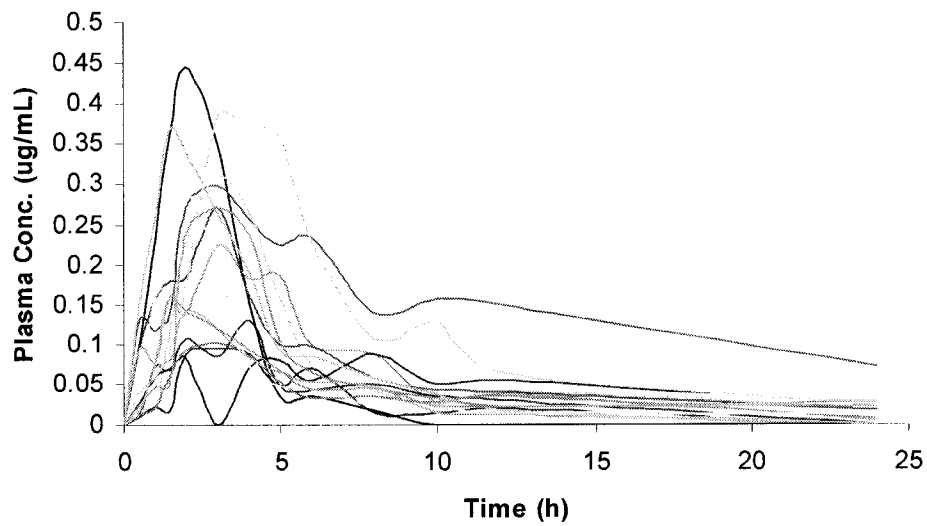


**Figure C.2.** Individual observed data of 15 volunteers for German test product

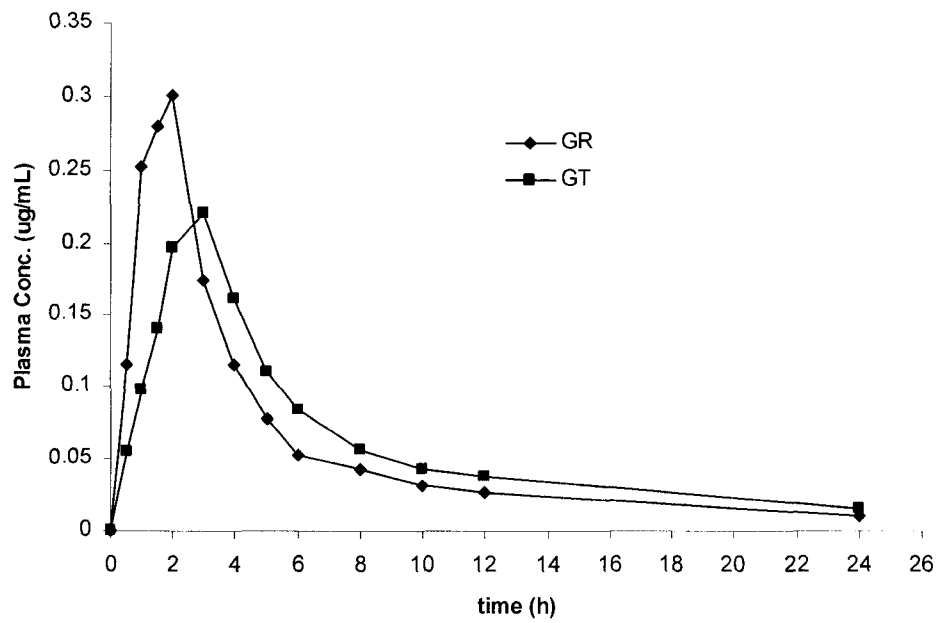


**Figure C.3.** Mean observed data for German reference (GR) and test (GT) products

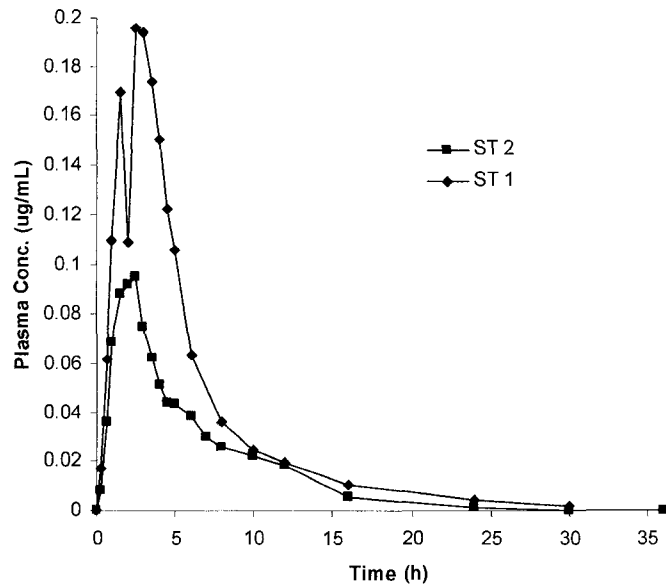


**Figure C.4.** Mean observed data for South African test 1 (ST 1) and test 2 (ST 2) products

## C.2. Data Sets

Kinetica Version 4.4.1

Dataset name: Mean German reference

Model FitMicroExtravascular

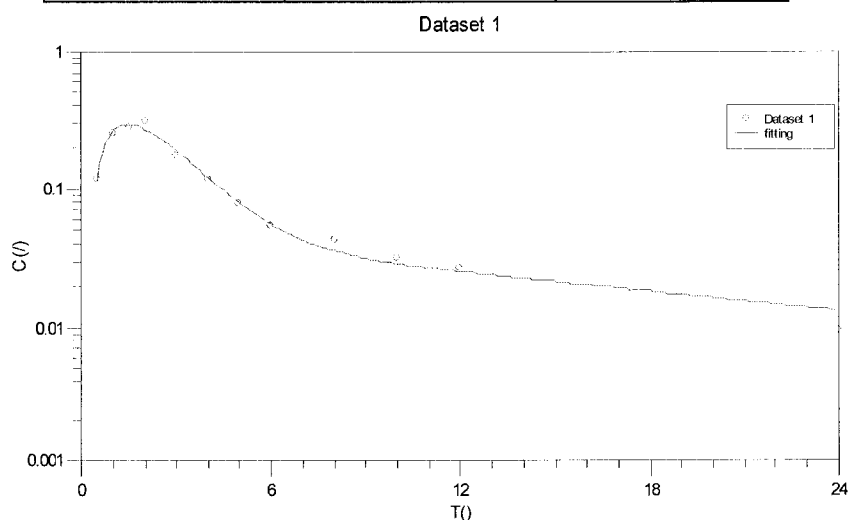
Objective function: 0.0015115

Akaike criteria: -65.9359

Schwartz criteria: -70.4811

T	C	Ycalc	Residuals	Weighted Res.
0.5	0.11537	0.111236	0.00413426	0.00413426
1	0.25165	0.26082	-0.0091699	-0.0091699
1.5	0.28006	0.291456	-0.0113958	-0.0113958
2	0.30134	0.27	0.0313398	0.0313398
3	0.17425	0.188477	-0.0142268	-0.0142268
4	0.11553	0.120685	-0.00515531	-0.00515531
5	0.07791	0.0786628	-0.000752767	-0.000752767
6	0.05327	0.0551902	-0.00192019	-0.00192019
8	0.0421	0.0355374	0.00656258	0.00656258
10	0.03157	0.0287769	0.00279313	0.00279313
12	0.02643	0.0252054	0.00122455	0.00122455
24	0.00962	0.0131791	-0.00355913	-0.00355913

	Without weights	With weights
Sum	-0.000125517	-0.000125517
Mean	-1.04597e-005	-1.04597e-005
SumOfSquares	0.0015115	0.0015115
Std. dev.	0.0117221	0.0117221



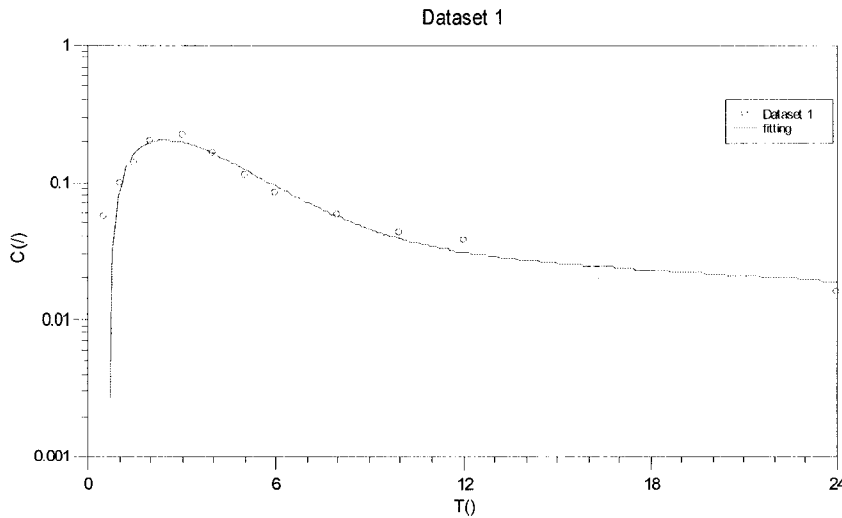
Text Field Name	Data Field
Concentration unit	ug/mL

Numerical Field Name	Units	Data Field
Dose	ug	3500
Ka	h <sup>-1</sup>	0.928808
Lag	h	0.310506
Volume	mL	4683.37
Kel	h <sup>-1</sup>	0.463449
K12	h <sup>-1</sup>	0.379322
K21	h <sup>-1</sup>	0.102858
K13		
K31		
AUC	ug.h/mL	1.61253
AUMC	ug.h <sup>2</sup> /mL	18.0469
MRT	h	9.80453
Lz	h <sup>-1</sup>	0.0534293
Cmax calc	ug/mL	0.291554
Tmax calc	h	1.46907
A	ug/mL	0.703284
Alpha	h <sup>-1</sup>	0.8922
B	ug/mL	0.0440402
Beta	h <sup>-1</sup>	0.0534293
C		
Gamma		
Thalf_Ka	h	0.746276
Tab <sub>s</sub>	h	3.73138
Thalf_alpha	h	0.776896
Thalf_beta	h	12.9732
Thalf_gamma		
Thalf_Lz	h	12.9732
Thalf_Kel	h	1.49563
Vz	mL	40623.8
Cl	mL/h	2170.5

Kinetica Version 4.4.1  
 Dataset name: Mean German test  
 Model FitMicroExtravascular  
 Objective function: 0.0047014  
 Akaike criteria: -52.3187  
 Schwartz criteria: -56.864

T	C	Ycalc	Residuals	Weighted Res.
0.5	0.05488	0	0.05488	0.05488
1	0.09805	0.0864379	0.0116121	0.0116121
1.5	0.14005	0.164145	-0.0240952	-0.0240952
2	0.19747	0.197291	0.000179033	0.000179033
3	0.22094	0.195696	0.0252438	0.0252438
4	0.16133	0.161131	0.00019872	0.00019872
5	0.11096	0.123878	-0.0129184	-0.0129184
6	0.08363	0.0934149	-0.00978486	-0.00978486
8	0.05703	0.0556841	0.00134587	0.00134587
10	0.04252	0.0384072	0.00411281	0.00411281
12	0.03741	0.0306399	0.00677008	0.00677008
24	0.01543	0.0185377	-0.00310767	-0.00310767

	Without weights	With weights
Sum	0.0544363	0.0544363
Mean	0.00453636	0.00453636
SumOfSquares	0.0047014	0.0047014
Std. dev.	0.0201234	0.0201234



Text Field Name	Data Field
Concentration unit	ug/mL

Numerical Field Name	Units	Data Field
Dose	ug	3500
Ka	h <sup>-1</sup>	0.588129
Lag	h	0.676598
Volume	mL	6363.53
Kel	h <sup>-1</sup>	0.280756
K12	h <sup>-1</sup>	0.313904
K21	h <sup>-1</sup>	0.0730677
K13		
K31		
AUC	ug.h/mL	1.95903
AUMC	ug.h <sup>2</sup> /mL	40.2854
MRT	h	18.187
Lz	h <sup>-1</sup>	0.0322832
Cmax calc	ug/mL	0.20411
Tmax calc	h	2.42382
A	ug/mL	0.512819
Alpha	h <sup>-1</sup>	0.635444
B	ug/mL	0.0371905
Beta	h <sup>-1</sup>	0.0322832
C		
Gamma		
Thalf_Ka	h	1.17856
Tabs	h	5.89281
Thalf_alpha	h	1.09081
Thalf_beta	h	21.4708
Thalf_gamma		
Thalf_Lz	h	21.4708
Thalf_Kel	h	2.46886
Vz	mL	55341.4
Cl	mL/h	1786.6

Kinetica Version 4.4.1

Dataset name: Mean South African test 1

Model FitMicroExtravascular

Objective function: 0.00650254

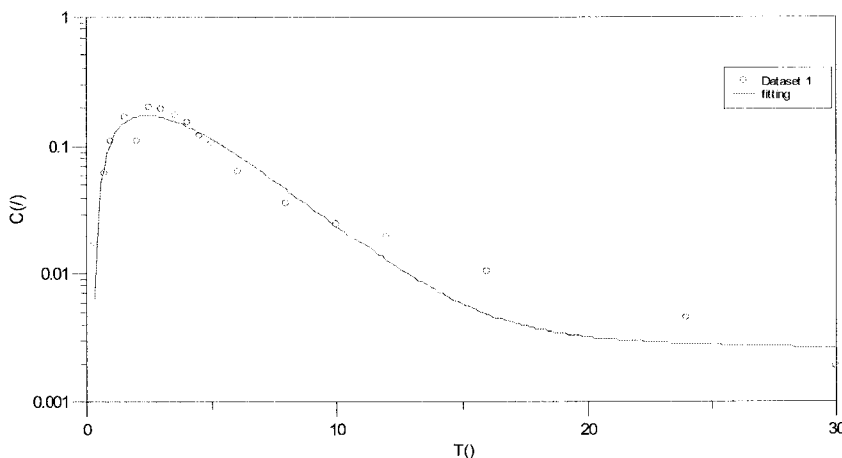
Akaike criteria: -78.6401

Schwartz criteria: -81.969

T	C	Ycalc	Residuals	Weighted Res.
0.33	0.01687	0.00626379	0.0106062	0.0106062
0.68	0.06164	0.0712019	-0.00956186	-0.00956186
1	0.10922	0.112756	-0.00353639	-0.00353639
1.5	0.16942	0.152277	0.0171427	0.0171427
2	0.10907	0.169871	-0.0608009	-0.0608009
2.5	0.19559	0.173112	0.0224779	0.0224779
3	0.19383	0.167338	0.0264922	0.0264922
3.5	0.17372	0.156258	0.0174623	0.0174623
4	0.1504	0.142407	0.00799325	0.00799325
4.5	0.12202	0.127478	-0.0054577	-0.0054577
5	0.10605	0.112566	-0.0065157	-0.0065157
6	0.06339	0.0852058	-0.0218158	-0.0218158
8	0.03614	0.0455208	-0.00938079	-0.00938079
10	0.02465	0.0235363	0.00111366	0.00111366
12	0.01968	0.0125118	0.00716823	0.00716823
16	0.01012	0.00486062	0.00525938	0.00525938
24	0.00446	0.00285349	0.00160651	0.00160651
30	0.0019	0.00263383	-0.000733829	-0.000733829

	Without weights	With weights
Sum	-0.000480756	-0.000480756
Mean	-2.67087e-005	-2.67087e-005
SumOfSquares	0.00650254	0.00650254
Std. dev.	0.0195577	0.0195577

Dataset 1





Text Field Name	Data Field
Concentration unit	ug/mL

Numerical Field Name	Units	Data Field
dose	ug	5000
Ka	h <sup>-1</sup>	0.485368
lag	h	0.301878
Volume	mL	10749.6
Kel	h <sup>-1</sup>	0.35538
K12	h <sup>-1</sup>	0.11907
K21	h <sup>-1</sup>	0.0136494
K13		
K31		
AUC	ug.h/mL	1.30884
AUMC	ug.h <sup>2</sup> /mL	38.5074
MRT	h	27.0588
Lz	h <sup>-1</sup>	0.010149
Cmax calc	ug/mL	0.17333
Tmax calc	h	2.39304
A	ug/mL	0.461655
Alpha	h <sup>-1</sup>	0.477951
B	ug/mL	0.0034804 5
Beta	h <sup>-1</sup>	0.010149
C		
Gamma		
Thalf_Ka	h	1.42809
Tab	h	7.14044
Thalf_alpha	h	1.45025
Thalf_beta	h	68.2969
Thalf_gamma		
Thalf_Lz	h	68.2969
Thalf_Kel	h	1.95044
Vz	mL	376408
Cl	mL/h	3820.18

Kinetica Version 4.4.1

Dataset name: Mean South African test 2

Model FitMicroExtravascular

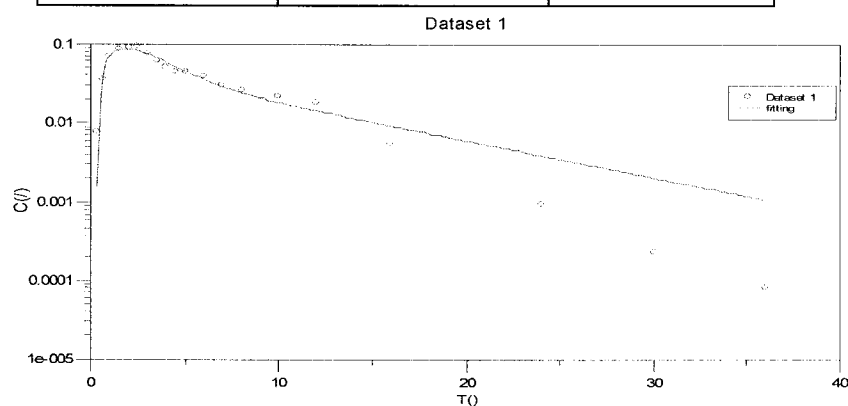
Objective function: 0.000482798

Akaike criteria: -140.718

Schwartz criteria: -143.731

T	C	Ycalc	Residuals	Weighted Res.
0.33	0.007891	0.00158103	0.00630997	0.00630997
0.68	0.03582	0.046485	-0.010665	-0.010665
1	0.06859	0.0702316	-0.0016416	-0.0016416
1.5	0.08834	0.0865168	0.00182319	0.00182319
2	0.09178	0.0882922	0.00348779	0.00348779
2.5	0.0945	0.0830668	0.0114332	0.0114332
3	0.07468	0.0750178	-0.000337778	-0.000337778
3.5	0.06233	0.0663607	-0.00403071	-0.00403071
4	0.05156	0.0581811	-0.0066211	-0.0066211
4.5	0.04409	0.0509335	-0.00684348	-0.00684348
5	0.04338	0.0447358	-0.00135576	-0.00135576
6	0.03826	0.0352229	0.00303706	0.00303706
7	0.0299	0.0286739	0.00122612	0.00122612
8	0.02558	0.0240811	0.00149892	0.00149892
10	0.02198	0.0181259	0.00385408	0.00385408
12	0.01832	0.0142691	0.00405094	0.00405094
16	0.00539	0.00919282	-0.00380282	-0.00380282
24	0.00098	0.00389274	-0.00291274	-0.00291274
30	0.00023	0.00204505	-0.00181505	-0.00181505
36	8e-005	0.00107437	-0.000994373	-0.000994373

	Without weights	With weights
Sum	-0.00429908	-0.00429908
Mean	-0.000214954	-0.000214954
SumOfSquares	0.000482798	0.000482798
Std. dev.	0.00503605	0.00503605



Text Field Name	Data Field
Concentration unit	ug/mL

Numerical Field Name	Units	Data Field
dose	ug	5000
Ka	h <sup>-1</sup>	0.802986
lag	h	0.320461
Volume	mL	24059.3
Kel	h <sup>-1</sup>	0.337544
K12	h <sup>-1</sup>	0.288751
K21	h <sup>-1</sup>	0.241811
K13		
K31		
AUC	ug.h/mL	0.615682
AUMC	ug.h <sup>2</sup> /mL	4.76883
MRT	h	6.17979
Lz	h <sup>-1</sup>	0.107281
Cmax calc	ug/mL	0.0887639
Tmax calc	h	1.82899
A	ug/mL	0.165041
Alpha	h <sup>-1</sup>	0.760825
B	ug/mL	0.0427791
Beta	h <sup>-1</sup>	0.107281
C		
Gamma		
Thalf_Ka	h	0.863212
Tab	h	4.31606
Thalf_alpha	h	0.911047
Thalf_beta	h	6.46107
Thalf_gamma		
Thalf_Lz	h	6.46107
Thalf_Kel	h	2.0535
Vz	mL	75699.4
Cl	mL/h	8121.08

Kinetica Version 4.4.1

Dataset name: German reference volunteer 1

Model FitMicroExtravascular

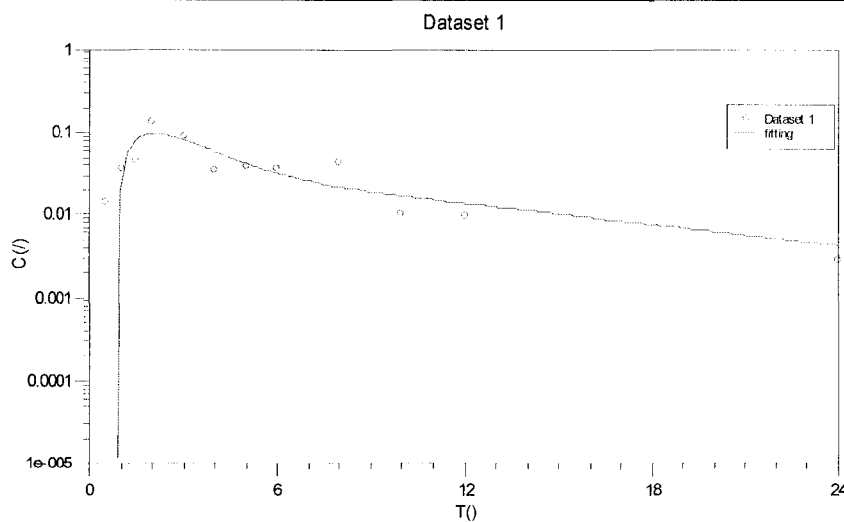
Objective function: 0.00405637

Akaike criteria: -54.0896

Schwartz criteria: -58.6349

T	C	Ycalc	Residuals	Weighted Res.
0.5	0.0141	0	0.0141	0.0141
1	0.0358	0.0262714	0.00952862	0.00952862
1.5	0.0462	0.0823397	-0.0361397	-0.0361397
2	0.132	0.0966067	0.0353933	0.0353933
3	0.0872	0.0816555	0.00554448	0.00554448
4	0.0342	0.0586155	-0.0244155	-0.0244155
5	0.039	0.0421264	-0.00312642	-0.00312642
6	0.0366	0.0319848	0.00461517	0.00461517
8	0.0438	0.0219229	0.0218771	0.0218771
10	0.0101	0.0170746	-0.00697459	-0.00697459
12	0.00928	0.0138473	-0.0045673	-0.0045673
24	0.00285	0.00424718	-0.00139718	-0.00139718

	Without weights	With weights
Sum	0.0144379	0.0144379
Mean	0.00120316	0.00120316
SumOfSquares	0.00405637	0.00405637
Std. dev.	0.019162	0.019162



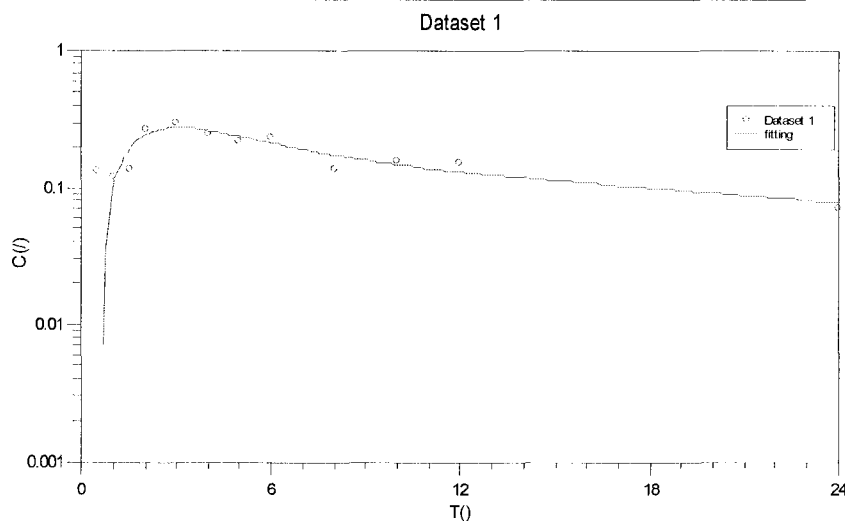
Text Field Name	Data Field
Concentration unit	ug/mL

Numerical Field Name	Units	Data Field
Dose	ug	3500
Ka	h <sup>-1</sup>	0.937269
Lag	h	0.870025
Volume	mL	14468.2
Kel	h <sup>-1</sup>	0.411999
K12	h <sup>-1</sup>	0.423011
K21	h <sup>-1</sup>	0.230495
K13		
K31		
AUC	ug.h/mL	0.587163
AUMC	ug.h <sup>2</sup> /mL	4.66711
MRT	h	6.01161
Lz	h <sup>-1</sup>	0.0981705
Cmax calc	ug/mL	0.0967773
Tmax calc	h	2.07306
A	ug/mL	0.205081
Alpha	h <sup>-1</sup>	0.967334
B	ug/mL	0.0368293
Beta	h <sup>-1</sup>	0.0981705
C		
Gamma		
Thalf_Ka	h	0.739539
Tab	h	3.6977
Thalf_alpha	h	0.716554
Thalf_beta	h	7.06065
Thalf_gamma		
Thalf_Lz	h	7.06065
Thalf_Kel	h	1.6824
Vz	mL	60719.6
Cl	mL/h	5960.87

Kinetica Version 4.4.1  
 Dataset name: German test volunteer 2  
 Model FitMicroExtravascular  
 Objective function: 0.0243678  
 Akaike criteria: -32.5739  
 Schwartz criteria: -37.1192

T	C	Ycalc	Residuals	Weighted Res.
0.5	0.133	0	0.133	0.133
1	0.118	0.0979756	0.0200244	0.0200244
1.5	0.14	0.192328	-0.0523276	-0.0523276
2	0.27	0.244028	0.025972	0.025972
3	0.298	0.275624	0.0223758	0.0223758
4	0.255	0.263807	-0.00880715	-0.00880715
5	0.223	0.239212	-0.0162117	-0.0162117
6	0.234	0.213974	0.0200255	0.0200255
8	0.14	0.174318	-0.0343184	-0.0343184
10	0.157	0.148689	0.00831089	0.00831089
12	0.15	0.131509	0.0184908	0.0184908
24	0.0713	0.0771566	-0.00585665	-0.00585665

	Without weights	With weights
Sum	0.130678	0.130678
Mean	0.0108898	0.0108898
SumOfSquares	0.0243678	0.0243678
Std. dev.	0.0456715	0.0456715



Text Field Name	Data Field
Concentration unit	ug/mL

Numerical Field Name	Units	Data Field
Dose	ug	3500
Ka	h <sup>-1</sup>	0.672469
Lag	h	0.664855
Volume	mL	6835.03
Kel	h <sup>-1</sup>	0.097223
K12	h <sup>-1</sup>	0.216193
K21	h <sup>-1</sup>	0.203606
K13		
K31		
AUC	ug.h/mL	5.26694
AUMC	ug.h <sup>2</sup> /mL	119.529
MRT	h	20.5423
Lz	h <sup>-1</sup>	0.0416407
Cmax calc	ug/mL	0.275699
Tmax calc	h	3.06219
A	ug/mL	0.320854
Alpha	h <sup>-1</sup>	0.475382
B	ug/mL	0.191214
Beta	h <sup>-1</sup>	0.0416407
C		
Gamma		
Thalf_Ka	h	1.03075
Tabs	h	5.15375
Thalf_alpha	h	1.45808
Thalf_beta	h	16.6459
Thalf_gamma		
Thalf_Lz	h	16.6459
Thalf_Kel	h	7.12946
Vz	mL	15958.5
Cl	mL/h	664.522